Elucidation of the complex mode-of-resistance of the natural topoisomerase type IIA inhibitors cystobactamids

Dissertation

zur Erlangung des Grades

des Doktors der Naturwissenschaften

der Naturwissenschaftlich-Technischen Fakultät

der Universität des Saarlandes

von

Katarina Cirnski

Saarbrücken

2021

Die vorliegende Arbeit wurde von November 2016 bis November 2020 unter Anleitung von Herrn Prof. Dr. Rolf Müller an Helmholtz-Institut für Pharmazeutische Forschung Saarland (HIPS) angefertigt.

Danksagung

In erster Linie möchte ich meinem Doktorvater Prof. Dr. Rolf Müller meinen besonderen Dank dafür aussprechen, dass er mich in seine Forschungsgruppe aufgenommen hat. Seine Anleitungen und Ratschläge und die wissenschaftlichen Diskussionen mit Ihm waren während meiner Promotion von entscheidender Bedeutung.

Zweitens möchte ich mich bei Prof. Dr. Andriy Luzhetskyy für die wissenschaftliche Begleitung und die Übernahme der Zweitkorrektur der Dissertation danken.

Ein großes Dankeschön geht an Dr. Jennifer Herrmann, meine unmittelbare Vorgesetzte. Vielen Dank für den Austausch Ihres Wissens, Ihrer Erfahrungen und Ideen sowie für die vielen Diskussionen, die wir im Laufe der Jahre geführt haben. Vielen Dank für die Unterstützung und konstruktive Kritik meiner wissenschaftlichen Arbeiten. Sie verbessern weiterhin meine wissenschaftlichen Instinkte und machen mich zu einer besseren Wissenschaftlerin.

Ich möchte mich auch bei Viktoria George, Yumi Park, Janetta Coetzee, Asfandyar Sikandar, Sari Rasheed, Anastasia Andreas, Timo Risch, Felix Deschner, Alexandra Amann, Stefanie Schmidt, Dr. Susanne Kirsch-Dahmen, Christina Decker, Ellen Merckel und Verena und Besnik Qallaku für die guten und lustigen Zeiten bedanken, die wir zusammen verbracht haben. Vielen Dank für eure Unterstützung und Freundschaft.

Mein Dank gilt auch den aktuellen und ehemaligen Mitarbeitern der Abteilung MINS.

Zu guter Letzt möchte ich mich bei meinen Freunden und meiner Familie bedanken. Vielen Dank, dass ihr mich nicht nur unterstützt, sondern auch ermutigt habt, dieses Abenteuer in Deutschland zu beginnen.

Zusammenfassung

Cystobactamide sind neuartige Topoisomerase IIa Inhibitoren mit antibakterieller Breitbandaktivität, die möglicherweise dazu beitragen können, die trockene Antibiotika-Pipeline zu füllen. Diese Arbeit beschreibt die umfassende Charakterisierung der antibakteriellen Aktivität von Cystobactamiden und die assoziierten Resistenzmechanismen in verschiedenen Bakterienspezies. In *Escherichia coli* und *Pseudomonas aeruginosa* wurden neue Mechanismen der Resistenzbildung entdeckt, die auf spezifischen Mutationen in regulatorischen Zweikomponentensystemen beruhen. Mutationen im QseBC-System von *E. coli* führen letztlich zu Modifikationen von Lipid A der äußeren Membran. Der Resistenzmechanismus in *P. aeruginosa* beruht auf Mutationen im CpxSR-Zweikomponentensystem, welche zu komplexen Downstream-Effekten führen; Die Bakterien werden resistent gegenüber Cystobactamiden durch Modifikation ihrer Zellhülle, und deren Export über Multidrug-Effluxpumpen. Der Resistenzmechanismus in *Klebsiella pneumoniae* bedarf weiterer Studien, aber es konnte gezeigt werden, dass das hochaffine Bindeprotein AlbA maßgeblich an der Resistenz gegenüber Cystobactamiden beteiligt ist. In *Acinetobacter baumannii* und *Staphylococcus aureus* wurden Mutationen in den Targetenzymen Gyrase und Topoisomerase IV gefunden, die zum Teil durch Mutationen begleitet waren, die zur Modifikationen der äußeren Membran von *A. baumannii* oder der Hochregulation von Multidrug-Effluxpumpen in *S. aureus* führen.

Summary

Cystobactamids are novel topoisomerase IIa inhibitors with broad-spectrum antibacterial activity that could help to fill the dry antibiotic pipeline. This thesis describes the extensive evaluation of the antibacterial activity of cystobactamids and the characterization of associated resistance mechanisms in different bacterial species. In *Escherichia coli* and *Pseudomonas aeruginosa*, new modes of resistance were uncovered relying on specific mutations in regulatory two-component systems. Mutations in the QseBC system in cystobactamid-resistant *E. coli* lead to modifications of lipid A of the outer membrane. The mode of resistance in *P. aeruginosa* relies on mutations in the CpxSR two-component system, triggering a complex response and the bacteria become resistant to cystobactamids though cell envelope modifications and export via multidrug efflux pumps. The mode of resistance in *Klebsiella pneumoniae* needs further investigation but it was found that the high-affinity binding protein AlbA plays a major role in cystobactamid resistance. Mutations in the target enzymes gyrase and topoisomerase IV were found in *Acinetobacter baumannii* and *Staphylococcus aureus*, which were partly accompanied by mutations leading to outer membrane modifications in *A. baumannii* and the upregulation of multidrug efflux pumps in *S. aureus*.

Vorveröffentlichungen der Dissertation

Teile dieser Arbeit wurden vorab mit Genehmigung der Naturwissenschaftlich-Technischen Fakultät, vertreten durch den Mentor der Arbeit, in folgenden Beiträgen veröffentlicht oder sind derzeit in Vorbereitung zur Veröffentlichung:

Publikationen:

Cirnski K*, Coetzee J*, Herrmann J, Müller R. Metabolic Profiling to Determine Bactericidal or Bacteriostatic Effects of New Natural Products using Isothermal Microcalorimetry. J Vis Exp. 2020 Oct 29; (164). doi: 10.3791/61703.

Elgaher WAM, Hamed MM, Baumann S, Herrmann J, Siebenbürger L, Krull J, **Cirnski K**, Kirschning A, Brönstrup M, Müller R, Hartmann RW. Cystobactamid 507: Concise Synthesis, Mode of Action, and Optimization toward More Potent Antibiotics. Chemistry. 2020 Jun 5; 26(32):7219-7225. doi: 10.1002/chem.202000117.

Planke T, **Cirnski** K, Herrmann J, Müller R, Kirschning A. Synthetic and Biological Studies on New Urea and Triazole Containing Cystobactamid Derivatives. Chemistry. 2020 Apr 1; 26(19):4289-4296. doi: 10.1002/chem.201904073

Testolin T, **Cirnski K**, Rox K, Prochnow H, Fetz V, Grandclaudon C, Mollner T, Baiyoumy A, Ritter A, Leitner C, Krull J, van den Heuvel J, Vassort A, Sordello S, Hamed MM, Elagher WAM, Herrmann J, Hartmann RW, Müller R, Brönstrup M. Synthetic studies of cystobactamids as antibiotics and bacterial imaging carriers lead to compounds with high *in vivo* efficacy. Chemical Science. 2019 Dec 11:1316-1334. doi: 10.1039/C9SC04769G

Moeller M, Norris MD, Planke T, **Cirnski K**, Herrmann J, Müller R, Kirschning A. Scalable Syntheses of Methoxyaspartate and Preparation of the Antibiotic Cystobactamid 861-2 and Highly Potent Derivatives. Org Lett. 2019 Oct 18; 21(20):8369-8372. doi: 10.1021/acs.orglett.9b03143

Sikandar A, **Cirnski K**, Testolin G, Volz C, Brönstrup M, Kalinina OV, Müller R, Koehnke J. Adaptation of a Bacterial Multidrug Resistance System Revealed by the Structure and Function of AlbA. J Am Chem Soc. 2018 Dec 5;140(48):16641-16649. doi: 10.1021/jacs.8b08895

Publikationen, die nicht Teil dieser Arbeit sind

Abdel-Aziz SA, **Cirnski K**, Herrmann J, Abdel-Aal MAA, Salem OIA. Novel fluoroquinolone hybrids: A dual targeting approach for developing potent antibacterial agents that inhibit DNA gyrase and urease. *Manuscript submitted to Pharmacological Reports* (2021).

Režen T, Zmrzljak UP, Bensa T, Tomaš TC, **Cirnski K**, Stojan J, Rozman D. Novel insights into biological roles of inducible cAMP early repressor ICER. Biochem Biophys Res Commun. 2020 Sep 17; 530(2):396-401. doi: 10.1016/j.bbrc.2020.05.017

Anversa Dimer F, de Souza Carvalho-Wodarz C, Goes A, **Cirnski K**, Herrmann J, Schmitt V, Pätzold L, Abed N, De Rossi C, Bischoff M, Couvreur P, Müller R, Lehr CM. PLGA nanocapsules improve the delivery of clarithromycin to kill intracellular Staphylococcus aureus and Mycobacterium abscessus. Nanomedicine. 2020 Feb; 24:102125. doi: 10.1016/j.nano.2019.102125.

Hug JJ, Bader CD, Remškar M, **Cirnski K**, Müller R. Concepts and Methods to Access Novel Antibiotics from Actinomycetes. Antibiotics (Basel). 2018 May 22; 7(2):44. doi: 10.3390/antibiotics7020044.

*: Authors contributed equally to the manuscript

Table of Contents

<center>

Chapter 1

</center>

1 Introduction

1.1 Antimicrobial resistance

According to the World Health Organization (WHO), antimicrobial resistance (AMR) is defined as lack of response from microorganisms, such as bacteria, fungi, parasites and viruses, to medicines designed to inhibit or kill them [1]. Herein, AMR refers to antibiotic resistance of bacterial pathogens.

Antimicrobial resistance is not a recent development as bacteria have evolved over time to protect themselves. Bacteria represent the biggest production reservoir of antimicrobials, therefore antimicrobial resistance as a natural defense is as old as the biosynthetic clusters encoding these compounds [2], and predates the use of antibiotics [3, 4]. E.g., 30,000-year-old Canadian High North permafrost [5] and 5,000-year-old Siberian permafrost [6] microbiome samples revealed the presence of genes encoding resistance to β-lactams, tetracycline, glycopeptides and vancomycin. Furthermore, several resistance-conferring genes were found in gut microbiome of a pre-Columbian Andean mummy [7] and oral microbiome of human skeletons from a medieval monastery [8], confirming the presence of resistance gene in both human commensals and human pathogens in the absence of selective pressure. Centuries later, the targeted exposure to antibiotics, when treating infections, presents a selective pressure bacteria need to overcome in order to survive [9-11]. Bacteria typically develop these resistance mechanisms rapidly after a certain antibiotic has been introduced to the clinics, and consequently render the antibiotic useless (Fig 1).

Antibiotic enters market

Antimicrobial resistance development
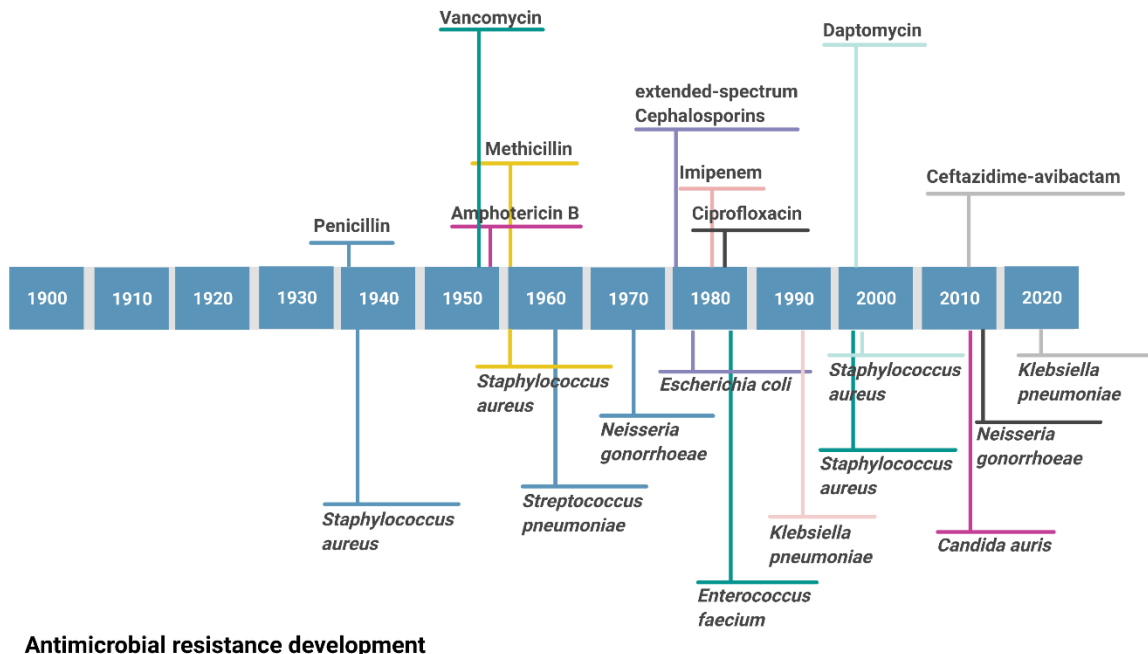
Fig. 1. Timeline of antibiotic introduction (above timeline) to market and detected antibiotic resistance (below timeline) [12, 13].
Colored lines connect the antibiotic with a resistant bacterial species. Only a few examples shown.

Therefore, AMR not only poses a great risk for the health system, but also consequently exerts substantial economic burden [14]. According to the Organization for Economic Co-operation and Development (OECD) a patient infected with resistant bacteria requires an extended hospital stay, and a more intensive and expensive medical care, resulting in additional treatment cost of US$10,000 to US$40,000 per capita [15]. Center for Disease Control and Prevention (CDC) estimates 23,000 deaths yearly in the USA due to AMR, and a total of US$20 billion in healthcare costs. Moreover, AMR negatively affects labor supply, resulting in additional loss of US$35 billion [14]. Furthermore, The World Bank estimates, due to AMR, a loss of gross domestic product (GDP) exceeding US$1 trillion annually after 2030, and reaching US$2 trillion annually by 2050. In the worst-case scenario GDP losses are estimated to reach US$3.4 trillion annually by 2030, and rising to US$6.1 trillion annually by 2050 [16].

1.1.1 Causes of AMR:

AMR is a worldwide, multifaceted problem, facilitated by the following factors (Fig 2):

- Biological factors:

Biological factors include intrinsic resistance and acquired resistance. Intrinsic resistance is described as a set of genes shared within a species, and it is not a consequence of horizontal gene transfer (HGT) or prior exposure to antibiotics [17]. E.g., *Escherichia coli* is intrinsically resistant to macrolides, due to the presence of the *erm* gene, an erythromycin ribosomal methyltransferase that methylates the 23S ribosomal RNA [18]. The presence of sulfhydryl reagent variable (SHV) β-lactamase [19], fosfomycin resistance protein A [20] and OqxAB efflux pump [21] in *Klebsiella pneumoniae*, make this pathogen intrinsically resistant to penicillins, fosfomycin and quinolones.

Acquired resistance in bacteria happens via mutation of the chromosomal DNA or via HGT. Three mechanisms of HGT exist: transformation, conjugation and transduction. Transformation, the uptake of genetic material from environment facilitated by a genetically encoded natural competence present in over 80 bacterial species, both Gram-negative and Gram-positive [22, 23]. Conjugation is a direct transfer of genetic material between bacteria and transduction is transfer of genetic material through bacteriophages [24]. HGT is facilitated in high cell density environments and it is induced at the onset of the stationary phase, upon antibiotic stress, DNA damage and starvation [23]. Predominant mechanism of AMR dissemination in hospital settings is conjugation; e.g. extended-spectrum β-lactamase (ESBL) and carbapenemase, commonly located on plasmids, are disseminated via inter- and intraspecies conjugation in the *Pseudomonas*, *Acinetobacter* and *Enterobacteriaceae* [25]. In contrast, mutations of the bacterial chromosome are often accompanied by a fitness cost for the bacteria. Thus, such mutations are only maintained if needed, i.e. in case of continuous

antibiotic pressure or if the potential fitness cost can be compensated, e.g. through mutations in other genes [10]. High-level resistance to rifampicin is mediated through mutations in *rpoB* gene, encoding the β-subunit of RNA polymerase. Most rifampicin-resistant *M. tuberculosis* mutants have significantly reduced fitness; however, secondary mutations in other genes, such as *rpoA* and *rpoC*, reduced the initial fitness loss [26, 27].

Another form of surviving the antibiotic pressure is persistence, also known as antibiotic tolerance. Upon exposure to antibiotic, less than 1% of bacterial population transitions into dormancy, a state of metabolic inactivity and diminished growth rate [28]. Persistence does not equal resistance, as it is characterized as a transient phenotypic trait of a bacterial subpopulation, even though it results in survival when exposed to stress [29-31]. E.g., dormancy enables survival of bacteria when exposed to β-lactams [32].Furthermore, persistence is commonly associated with persistent or chronic infections, such as pacemaker infections [33], and endocarditis [34], as they are often linked to treatment failure [35].

- Human use of antibiotics:

In developing countries, the lack of AMR surveillance combined with poor quality of antibiotics available, unregulated access to antibiotics, and their misuse are the strongest factors driving AMR. E.g., a recent study showed that, especially in developing countries, despite good theoretical knowledge on antibiotics and AMR, only a third of physicians requested microbiological tests and even rarely (in up to 25% cases) used results as a guide to establish a correct diagnosis and treatment regime. In some cases, this was due to inadequate microbiological services and resources. The study also revealed a lack of knowledge on local antibiotic resistance patterns and prescribing guidelines, lack of recent training on antibiotic use, and overconfidence in antibiotic prescribing [36, 37]. A study performed in Nigeria, where no quality assurance methods are in place to ensure high quality of medicine, revealed that up to 40% of ampicillin/cloxacillin formulations were substandard [38]. Furthermore, the use of

expired antibiotics, either due to improper storage or their use past their shelf live, for treatment of infantile diarrhea, not only resulted in adverse drug reactions, but also led to 6-fold increase in resistance rates [39]. Counterfeit drugs containing either excessive- or insufficient amounts of active ingredient and dangerous contaminants can directly cause death in humans and promote AMR. In Nigeria 47 children died because paracetamol syrup they ingested was adulterated with diethylene glycol, an industrial solvent [40]. Similarly, presence of diethylene glycol in glycerine and sulfanilamide caused several deaths in Bombay [41] and USA [42], respectively. Unregulated retail of medicine, especially antibiotics, in Asia, Africa and Latin America, where antibiotics can be bought in local pharmacies, drugstores, grocery stores and roadside stalls, resulting in self-medication and overconsumption, is the strongest driver of AMR [43]. A survey performed in rural Bangladesh revealed that only 8% of all purchased antibiotics was prescribed by physicians [44].

In developed countries, AMR is mainly driven by prophylactic use of antibiotics for common procedures, such as caesarian section, organ transplants, chemotherapy, and for prevention of numerous urinary tract infections, recurrent cellulitis, meningococcal disease, etc. [43, 45]. Furthermore, intra- and intercontinental migration of humans, livestock animals and migratory birds affects both the rate and extent of AMR in developed countries. Analysis of toilet waste from airplanes flying into Copenhagen from South Asia revealed an influx of *Salmonella enterica* and genes critical to resistance spread, such as bla_{CTX-M} (an ESBL) [46]. Broiler birds imported into Sweden, positive for nalidixic acid resistant *E. coli*, were identified as cause for rapid increase in quinolone resistant *E. coli* despite the absence of the selective pressure [47]. Furthermore, ESBL-producing *Enterobacteriaceae* were detected in chicken meat in Egypt [48], dairy in China [49] and Algeria [50], and in companion animals in Europe [51]. Although erroneous prescription of antibiotic remains a problem also in developed countries, patient incompliance and self-medication are more problematic [43]. A survey performed in the

suburban emergency department in the USA revealed that 22% of participants received prescriptions for antibiotics for treatment of cold symptoms, and 17% of participants regularly took leftover medication (oral antibiotics), without prior consultation with a physician, for treatment of cold symptoms and sore throat [52]. Furthermore, a large survey done across the countries in the European Union (EU) found that 3-41% of participants reported consumption of leftover medicine from previous prescriptions [53]. The use of leftover medicine was more common in the southern, western and northern countries of the EU [54].

- <u>Use in industrial agriculture:</u>

The prophylactic use of antibiotics to advance production of farm animals, i.e. improved growth rate, feed utilization [55, 56], conception rate [57], lean-meat production [55, 58], etc., in addition to use of antibiotics to treat sick animals, is the leading cause of AMR in humans [59]. Prophylactic use happens by addition of antibiotics to water and feed, resulting in uncontrolled and varying amounts of antibiotics consumed by individual animals [60]. Ingestion of antibiotics not only leads to increased selective pressure of gastrointestinal microbiome, but also results in accumulation in animal tissue; this is especially problematic because of direct human consumption and their adverse effects, such as allergic hypersensitivity, phototoxic skin reactions, tendon rupture, teratogenicity during the first trimester of pregnancy, nephrotoxicity, hepatotoxicity, etc. [61, 62]. In Cameroon, edible chicken tissues and eggs were reported to contain chloramphenicol and tetracycline residues above the maximum residue limit recommended by the EU [63]. Similarly, higher ciprofloxacin concentrations were detected in egg whites in Bangladesh, and oxytetracycline in edible beef tissues in Nigeria [64]. Furthermore, proper handling, storage and disposal of antibiotics by farmers is also a non-negligible contributing factor to AMR dissemination. Exposure of animals to continuous sub-lethal doses due to improper storage, promotes resistance development of gastrointestinal microbes [65]. Additionally, farmers tend to dispose of antibiotics by dumping them directly

into drains, refuse dumps or onto bare ground [66] instead of disposing them through the local supplier, waste disposal contractor or consult local authority [67]. Moreover, farm waste streams, manure and illegal runoffs release not only resistant bacteria directly into the soil and groundwater but also antibiotics. Released antibiotics exert selective pressure on sensitive bacteria in environment, thereby expediting resistance development and dissemination [60, 65]. The biggest threat currently is the use of colistin, a last-line antibiotic for treatment of multi-drug resistant (MDR) bacteria, for prevention of post weaning diarrhea in pigs, and the dissemination of plasmid-mediated *mcr-1* resistance from *E. coli* [68].

- Environmental dissemination:

Not only antimicrobials, but also pesticides and heavy metals released into the environment from pharmaceutical industry, industrial agriculture, hospital and urban sewage results in substantial amounts of antibiotics present in the environment. In turn, this exerts a selective pressure on microorganisms and facilitates the development of AMR and its dissemination [60]. This has already been described for several antibiotic classes such as tetracyclines, sulfonamides, quinolones, aminoglycosides and macrolides. Pathogenic bacteria that became resistant in their natural environment reach humans through water (irrigation with wastewater, contamination of water sources), soil (manure containing antibiotics), and air, and they can cause complicated infections with limited treatment options [69]. Contamination of groundwater with *Vibrio cholera* in India caused an outbreak of cholera [70], and contamination of well water with *Shigella flexneri* 2b caused and outbreak of shigellosis in China [71], both due to the resistance development in response to presence of multiple antimicrobial agents previously used for treatment of cholera and shigellosis, poor hygiene and overcrowding. Contamination of drinking water in Uganda with MDR *Citrobacter* sp., *Enterobacter* spp., *Klebsiella* sp., *Proteus* spp., *Pseudomonas* sp., and *Sallmonella* sp., due to unregulated use of antibiotic, agriculture and medical practices, caused a variety of nosocomial infections [72].
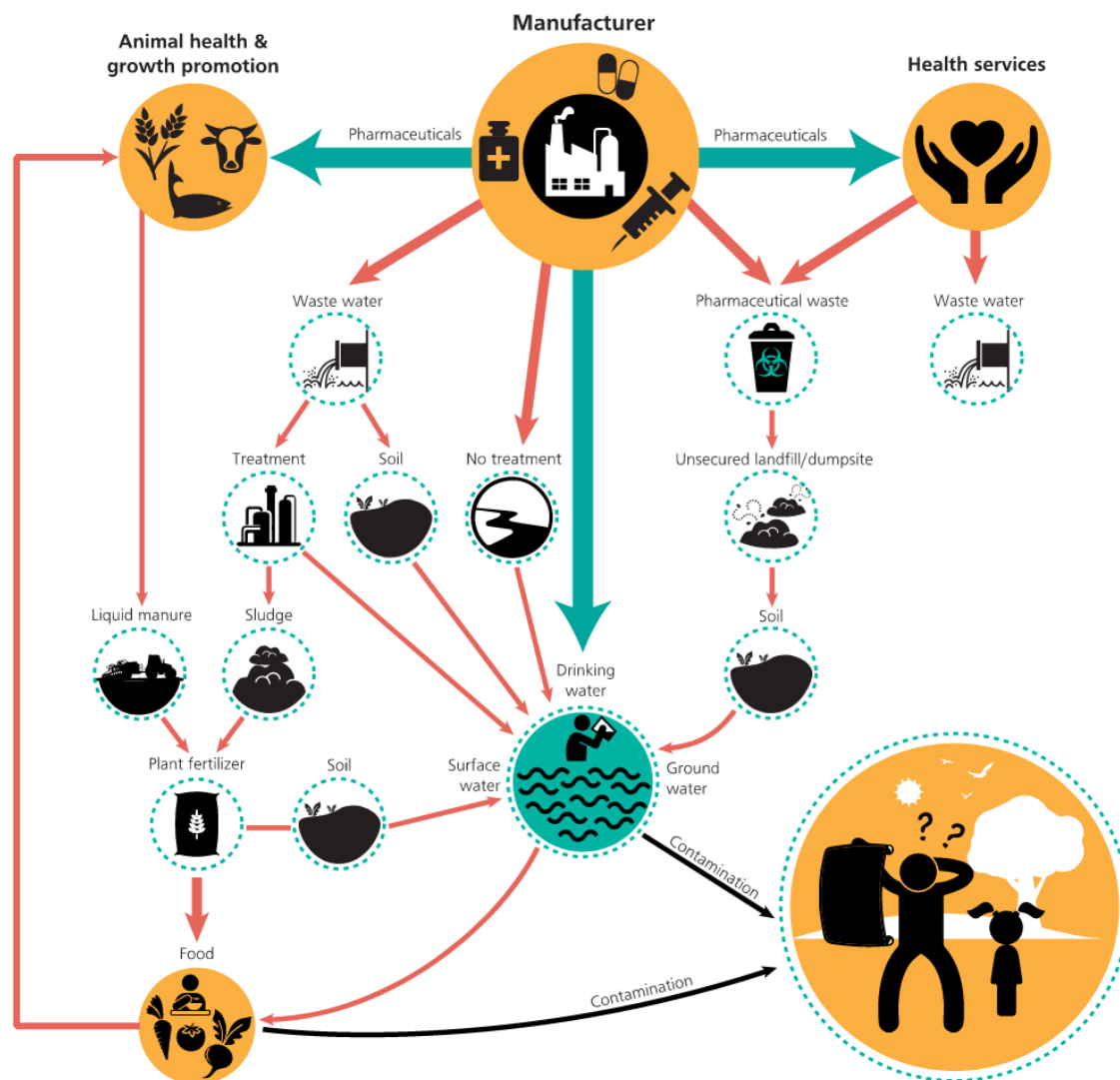
Fig. 2. Emergence and spread of AMR (schematic representation taken from [73]).

1.1.2   Solutions to combat AMR:

A recent article in Nature Reviews Microbiology highlighted the need to reach four interconnected goals to successfully overcome AMR; (i) antibiotic discovery has to become affordable, (ii) we need to produce antibiotics that will meet the currently unmet clinical needs, (iii) unnecessary antibiotic use needs to be limited, and (iv) a worldwide access to effective treatment options has to be ensured [74]. Since AMR is a worldwide problem, we need a well-coordinated action approach. WHO launched a One Health holistic approach within the global action plan (GAP) on antimicrobial resistance, bringing together representatives from all

sectors to design and implement different programs, policies and legislation with the objective to improve the outcome of public health [1]. They outlined five objectives to achieve this goal:

- improving the awareness and knowledge of AMR (communication, education, training),

- surveillance and research (incidence, prevalence, development and spread of infection, basic research and translational studies),

- reduction of infections (sanitation, hygiene, infection prevention),

- optimized use of antimicrobials (over-prescription, over-the-counter and internet sales), and

- increase investment in new medicines, diagnostic tools, vaccines and other interventions [75].

However, to ensure its success, countries have to develop and implement national action plans within the guidelines and objectives of GAP. Additionally, WHO holds yearly the World Antimicrobial Awareness Week (WAAW) to increase awareness on AMR and encourage best practices among all sectors to slow the development and spread of AMR. Moreover, in 2015 WHO launched a Global Antimicrobial Resistance and Use Surveillance System (GLASS) to fill in the knowledge gaps and help with strategy development on how to develop and implement AMR surveillance systems. The establishment of a priority pathogen list in 2017 by the WHO was instrumental in refocusing research and development (R&D) of new antimicrobials, vaccines and diagnostic tools. Furthermore, a public-private partnership, Global Antibiotic Research and Development Partnership (GARDP), is set to deliver five new treatment options targeting life-threatening drug-resistant bacteria found on the WHO priority pathogen list [1]. However, in order to achieve these goals, human behavior needs to change. Many recent publications highlight the undervalued contributions of social and behavioral sciences on a sustainable change in antimicrobial prescription and the reasonable use of antibiotics in conjunction with improved antimicrobial stewardship [76-78].

1.2 Antibiotic pipeline

Due to increasing AMR and lack of new antibiotics in the pipeline we have effectively reached the so-called post-antibiotic era, where no effective treatment options are available to treat infections that were once treatable [79]. Since the mid-1980s the approval of new antibiotics has decreased by 90% [80] as a consequence of scientific, economic and regulatory hurdles [79]. Large pharmaceutical companies continue to exit the R&D programs. However, public and philanthropic investment increased over the years, mainly due to the efforts of several agencies and initiatives providing funding and guidance for antibiotic development: Biomedical Advanced Research and Development Authority (BARDA), Combating Antibiotic Resistant Bacteria Biopharmaceutical Accelerator (CARB-X), GARDP, Innovative Medicines Institute (IMI), Joint Programming Initiative on Antimicrobial Resistance (JPIAMR), and the Replenishing and Enabling the Pipeline for Anti-Infective Resistance (REPAIR) Impact Fund. Currently, small companies and not big pharmaceutical companies submit 95% of all compounds in the antibiotic pipeline [81]. Since July 2017, eight new antibiotics were approved. However, these new antibiotics are mostly derivatives of known classes, including Pretomanid, a nitroimidazole, for the treatment of extremely drug-resistant tuberculosis (XDR TB) [82]. Most are also active against carbapenem-resistant *Enterobacteriaceae*, however, none of the antibiotics shows activity against carbapenem-resistant *Acinetobacter baumannii* (CRAB) or carbapenem-resistant *Pseudomonas aeruginosa* (CRPA), emphasizing the gap between approved antibiotics and the WHO priority pathogens list. Since September 2019, there are 50 antibiotics and combinations, and 10 biologicals in the clinical pipeline. Over half of them (32) target WHO priority pathogens, twelve are active against at least one Gram-negative pathogen, twelve target TB, and six are active against *Clostridium difficile*. From the antibiotics in clinical development, only Taniborbactam (boronate-β-lactamase inhibitor (BLI)), Zoliflodacin and Gepotidacin (both novel topoisomerase inhibitors), Afabicin (FabI inhibitor),

TXA-709 (FtsZ inhibitor), and VNRX-7145 (BLI) fulfill at least one innovation criterion, however, only two are active against critical MDR Gram-negative pathogens. The majority of the antibiotics in the pipeline are β-lactams and BLI combinations. Furthermore, there is a continued lack of antibiotics targeting CRAB and CRPA. Based on the statistics, current pipeline could yield eleven new approved antibiotics in the next 5 years [83]. WHO´s publicly available database on preclinical development of antibacterials shows 252 molecules being developed in 145 institutions worldwide, targeting the pathogens on the WHO priority pathogen list. Of these, 43% are single agents and 36% are nontraditional products, 40% target a single pathogen and almost 33% target cell wall synthesis or act on the membrane [84]. WHO emphasizes that to successfully tackle AMR, innovation in R&D of new antibacterials together with reinvested funding in R&D, and improved cost efficiency of clinical trials is paramount [83].

1.3 Mode of Resistance

There are four main mechanisms described that that enable bacteria to become resistant to antibiotics: (i) limited drug uptake, (ii) modification of the drug target, (iii) inactivation of the drug, and (iv) active drug efflux [10, 11, 17, 85]. These types of resistance mechanisms are found in all bacteria but some differences exist between how Gram-negative and Gram-positive bacteria preferably react. These dissimilarities are mainly due to the difference in their cell wall composition. Among many other distinctions, Gram-negative bacteria possess an outer membrane that is not present in Gram-positive bacteria. While Gram-negative bacteria use all four of the above mentioned mechanisms to achieve resistance, Gram-positive bacteria less frequently employ active drug efflux and limited drug uptake [17]. Another way of drug uptake limitation is persistence [35] and biofilm formation, where cells are incased in a thick matrix with exopolysaccharide, eDNA, and extracellular proteins [86], resulting in diminished or reduced compound penetration.

The outer membrane (OM) acts as a checkpoint for the entry of antibiotics and changes in the OM structure of Gram-negative bacteria hinder the uptake of various antibiotic classes by direct modification of either OM lipopolysaccharides (LPS) or porin channels. Changes leading to reduced number of porins, and mutations leading to changed specificity of porins, hinder their activity by preventing them to reach their cytoplasmic target [17]. Reduced number of porins present in the OM of *Enterobacteriaceae* spp. and *Neisseria gonorrhoeae* leads to carbapenem resistance [87, 88], and resistance to β-lactams and tetracycline [89], respectively. Modifications of the LPS in the outer membrane happen via reduction of the negative charge, by adding positively charged residues, and leads to resistance to cationic antimicrobial peptides, such as polymyxins [90].

Modification of the drug target is the most common resistance mechanism. E.g., several mutations in both gyrase and topoisomerase IV conferring varying degrees of resistance against fluoroquinolones [91-93] are known. Resistance to glycopeptides like vancomycin is enabled via HGT of *van* genes, resulting in modified peptidoglycan precursors [94] rendering vancomycin ineffective. Single nucleotide polymorphism (SNP) mutations in *rpoB* gene, encoding the β subunit of RNA polymerase, the target of rifampicin, result in resistance to rifampicin [95, 96].

Inactivation of a drug can happen in several ways. Antibiotics can be degraded by hydrolases, chemically modified or sequestered. Chemical modification happens by addition of acetyl, phosphoryl or adenyl group to the antibiotic [17, 85, 97]. E.g., β-lactams are inactivated by β-lactamase that hydrolyze a specific site in the β-lactam ring causing it to open [98]. Aminoglycosides are large molecules with exposed hydroxyl and amide groups, are especially susceptible to chemical modification [85]. Another way of drug inactivation is sequestration of the drug by resistance proteins. Sequestration of the albicidin by AlbA, and its subsequent

modification was shown to be the mechanism of resistance against albicidin in *K. pneumoniae* [99, 100].

Active drug efflux is chromosomally encoded and is either constitutively or inducibly expressed or overexpressed. Generally, several families of efflux pumps are found in bacteria and they transport a wide variety of substances. Multidrug and toxic compound extrusion (MATE), small multidrug resistance (SMR), major facilitator superfamily (MFS) and ATP-binding cassette (ABC) efflux pumps are located in the cell membrane and are present in both Gram-negative and Gram-positive bacteria. Members of MATE and MFS families are found on chromosome of Gram-positive bacteria and can lead to intrinsic resistance to fluoroquinolones [101]. However, the resistance-nodulation-cell division (RND) family of efflux pumps, exclusively present in the Gram-negative species, is probably clinically the most important as it spans through the entire cell envelope and confers resistance to several antibiotics [102].

1.4 Cystobactamids

Cystobactamids are non-ribosomally synthesized linear peptides, produced by myxobacteria belonging to the *Cystobacterinae* suborder [103]. They possess a unique chemical structure and are composed of a *para*-nitrobenzoic acid unit (PNBA), two *para*-aminobenzoic acid units (PABA), two PABA units with different substitution patterns and a central β-methoxyasparagine linker [103-105]. Cystobactamids are topoisomerase IIa poisons, and interfere with DNA replication by stabilizing the cleavage complex, leading to double-stranded DNA breaks. Cystobactamids display activity against Gram-negative, Gram-positive including *Enterobacteriaceae* spp., non-fermenters and MDR isolates, and exhibit limited cross-resistance with fluoroquinolones [103]. The native producer strain is difficult to genetically manipulate and produces only low titers of natural cystobactamids. Therefore, heterologous expression in *Myxococcus xanthus* DK1622 has been established [106] with the aim to increase productivity and to fully exploit the structural diversity encoded in the biosynthetic gene cluster.

In parallel, several synthetic routes to cystobactamids were described in the course of this work [104, 105, 107-110]. Chemical syntheses also enabled the generation of numerous non-natural cystobactamid derivatives [105, 107-109] to explore structure-activity and structure-property-relationships (SAR and SPR). New derivatives were designed with the goals to improve solubility, physiochemical properties, potency and spectrum coverage. The *in vivo* activity of cystobactamids could be already demonstrated. The synthetic derivative CN-DM-861 efficiently reduced the bacterial load in muscle, lung and kidney after intravenous administration in a mouse model of *E. coli* thigh infection [105]. Cystobactamids present a novel antibiotic class with broad-spectrum activity with the potential to be the lead structure in our fight against AMR.

Chapter 2

Cystobactamids efficiently kill multi-drug resistant uropathogenic *Escherichia coli* and reveal QseBC regulated LPS modifications in resistance development

K. Cirnski[1,2], T. Risch[1,2], A. Jousset[9], N. Zaburannyi[1,2], D. Kohnhäuser[2,3], G. Testolin[2,3,#], D. Hörömpöli[8], Leonhard Knegendorf[12], Patrick Chhatwal[12], M. Rohde[10], M. Loose[4], T. Chakraborty[5], A. Vassort[11], F. Wagenlehner[6], M. Rima[9], T. Naas[9], H. Brötz-Österhelt[8], Dirk Schlüter12, M. Bischoff[7], M. Brönstrup[2,3], J. Herrmann[1,2], R. Müller[1,2,*]

(manuscript in preparation)

[1] Department Microbial Natural Products, Helmholtz Institute for Pharmaceutical Research Saarland (HIPS), Helmholtz Centre for Infection Research and Pharmaceutical Biotechnology, Saarland University, Saarbrücken, Germany

[2] German Centre for Infection Research (DZIF), partner site Hannover-Braunschweig

[3] Department Chemical Biology, Helmholtz Centre for Infection Research, Braunschweig, Germany

[4] Clinic for Urology, Paediatric Urology and Andrology, Justus-Liebig University of Giessen, Giessen, Germany

[5] Institute of Medical Microbiology, German Centre for Infection Research, Justus-Liebig-University, Giessen, Germany

[6] Clinic for Urology, Pediatric Urology and Andrology, Justus-Liebig University of Giessen, Giessen, Germany

[7] Institute of Medical Microbiology and Hygiene, Saarland University, Homburg/Saar, Germany

[8] Department of Microbial Bioactive Compounds, University of Tübingen, Tübingen, Germany

[9] Institut Pasteur, Assistance Publique Hôpitaux de Paris, Université Paris-Sud, Paris; Bacteriology-Hygiene Unit

[10] Central Facility for Microscopy, Helmholtz Centre for Infection Research, Braunschweig, Germany

[11] Evotec ID, 1541 Avenue Marcel Merieux, 69289 Marcy l´Etoile, France

[12] Institute of Medical Microbiology and Hospital Epidemiology, Hannover Medical School, Hannover, Germany

* Corresponding author

E-mail: rolf.mueller@helmholtz-hips.de

#Present Address: Department of Chemistry and Chemical Biology, Harvard University, Cambridge, MA 02138, US

Short Title: QseBC confers resistance to Cystobactamids via LPS modification

2 Cystobactamids efficiently kill multi-drug resistant uropathogenic *Escherichia coli* and reveal QseBC regulated LPS modifications in resistance development

2.1 Abstract

Due to steadily increasing antimicrobial resistance and the shortage of novel antimicrobials reaching the market, the need to evaluate develop new antibacterial agents is higher than ever. In the present study, we undertook an extensive microbiological and mechanistic evaluation of a novel natural compound class, the cystobactamids, acting as potent inhibitors of bacterial gyrase and topoisomerase IV with IC_{50} values in the sub-µM and µM range, respectively. We focused our research on *Escherichia coli*, an important nosocomial pathogen, and could demonstrate that cystobactamids efficiently kill multi-drug resistant *E. coli* with high potency. *In vitro* studies revealed a bactericidal mechanism with a rapid onset of action. Based on their mode of action cystobactamid-resistant *E. coli* mutants developed at a low frequency of resistance, 10^{-8}-$< 10^{-10}$. Intriguingly, no mutations were found in *gyrA* or *parC* target genes and instead all mutations were observed in QseBC, a virulence-regulating, quorum-sensing *E. coli* two-component system. Resistance to cystobactamids did not induce a fitness cost in the *E. coli* mutants, however, isothermal microcalorimetry revealed a significant change of heat release during metabolic processes. RT-qPCR showed that exposing wildtype *E. coli* to cystobactamid did not result in a significant change in *qseBC* and *pmrAB* transcript levels. However, transcriptome analyses of resistant mutants revealed that the two-component systems QseBC and PmrAB are strongly interconnected and together they initiate a cascade of events leading to lipopolysaccharide (LPS) modifications. In case of cystobactamids, we observed two major lipid A modifications connected to the *arn* operon: addition of either one or two 4-amino-4-deoxy-L-arabinose units.

2.2 Author Summary

Escherichia coli is an important nosocomial pathogen. Due to multi-drug resistant (MDR) phenotypes that emerge at an alarming rate and limited treatment options, we present a natural product scaffold with the potential to become a new drug for the treatment of patients suffering from severe infections caused by *E. coli*, such as complicated urinary tract infections (cUTI). In addition to assessing the potency of cystobactamids on ESKAPE pathogens (*Enterococcus faecium*, *Staphylococcus aureus*, *Klebsiella pneumoniae*, *Acinetobacter baumannii*, *Pseudomonas aeruginosa*, and *Enterobacter* spp.), we focused our study on MDR *E. coli* clinical isolates resistant to e.g. third-generation cephalosporins, fluoroquinolones, and polymyxins. Having demonstrated that cystobactamids efficiently kill MDR *E. coli* we studied resistance rates and the underlying mechanisms in more detail. We found that cystobactamids at low frequency elicit a novel mode of resistance through mutations in the quorum-sensing *E. coli* two-component system QseBC. QseBC interacts with the PmrAB two-component system, leading to significantly increased transcript levels of *arnT*, *eptA*, *cptA* and *waaH* genes. These mutations lead to LPS and lipid A modifications and, in turn, an increase in net positive charge of the outer membrane. A similar resistance mechanism is known for polypeptide antibiotics, however, cystobactamid-resistant *E. coli* mutants are sensitive to colistin treatment and we did not detect cross-resistance with other antibiotic classes used for treatment of infections caused by Gram-negative bacteria. In conclusion, we describe the potent activity of cystobactamids against Gram-negative pathogens and elucidate their mechanism of resistance in *E. coli* mutants that developed at a low frequency. Our work has a significant impact on the further pre-clinical development of cystobactamids and it contributes to a deeper understanding of antimicrobial resistance.

2.3 Introduction

Salvarsan, penicillin and streptomycin sparked the golden era of antibiotics, which was followed by the most prolific period of antibiotic development between 1950 and 1960; over half of all antibiotics discovered in that period are still in use today [111, 112]. By now, the antibiotic pipeline is running dry, and in particular, new antibiotics to treat multi-drug resistant Gram-negative bacteria are rare, due to a broken economic model, stringent regulation, and the innovation gap in research and development [113, 114]. Additionally, once a new antibiotic is brought to the market and introduced into clinical settings antimicrobial resistance (AMR) will almost certainly develop. Consequently, and according to WHO [115], AMR has become one of the top global threats humanity is currently facing. Although it occurs naturally, misuse of antimicrobials to treat humans and animals is accelerating this process, leading to increased medical costs and higher mortality rates [1]. Combined misuse of antimicrobials [1], dwindling numbers of new antimicrobials discovered and approved for use [81], and horizontal gene transfer [116-118] resulted in the emergence of multi-drug resistant (MDR), extensively-drug resistant (XDR) and even pan-drug resistant (PDR) bacteria [119]. This has effectively put us on the doorstep of the post-antibiotic era, where there are almost no effective treatment options available to combat these infections. Although alternative approaches to antibiotics are being investigated, such as phage therapy, bacteriocins, predatory bacteria, etc., antibiotics will remain an invaluable tool to combat and control infectious diseases [120].

Bacteria belonging to the family *Enterobacteriaceae*, such as *Escherichia coli*, *Enterobacter* spp. and *Klebsiella* spp. are the predominant cause of various nosocomial infections. In particular, *E. coli* causes numerous infectious diseases, including diarrhea, urinary tract infections (UTIs), urosepsis, sepsis and several other conditions. In total, pathogenic *E. coli* causes up to 30% of all nosocomial infections and up to 80% of community-acquired UTIs (CAUTI) [121-124]. However, due to chromosomal mutations, exchange of mobile genetic

elements and plasmids carrying resistance genes, infections caused by *E. coli* are becoming increasingly difficult to treat. Rising numbers of isolates are becoming resistant to β-lactam antibiotics via mobile genetic elements encoding for β-lactamases, to aminoglycosides via mobile genetic elements encoding aminoglycoside modifying enzymes and plasmid-mediated 16S rRNA methyltransferases, and to carbapenems by expressing carbapenemases, overexpression of efflux pumps and modifications of porins. Transposons carrying genes for resistance to carbapenems usually simultaneously carry genes conferring resistance to fluoroquinolones (FQs), trimethoprim-sulfamethoxazole and aminoglycosides [125]. Most worrying in the clinical setting is resistance to the most important β-lactams, third-generation cephalosporins (3GCs), carbapenems, and to β-lactam/β-lactamase inhibitor combinations. High-level resistance to quinolones is often mediated by target mutations in the so-called quinolone resistance-determining region (QRDR) of DNA gyrase and topoisomerase IV, whereas low-level resistance is conferred via plasmids carrying *qnr* genes encoding pentapeptide proteins protecting the target enzymes. Various efflux pumps can also cause resistance towards FQs, whereas upregulation of the AcrAB-TolC efflux pump is the major cause of efflux-mediated FQ resistance in *E. coli* [126].

FQs and 3GCs are the first line of defense when treating UTIs [127-129]. Carbapenems, colistin and tigecyline are our last line of defense [125], however resistance to colistin, due to *mcr* genes encoding a transferase enzyme that inactivates colistin, has already been observed worldwide [130, 131]. Furthermore, tigecycline non-susceptible strains have already been isolated from humans and animals. Resistance to tigecycline is due to efflux, ribosome protection or Tet(X) enzymes that inactivate tetracycline and tetracycline derivatives by modifying them [132-137]. Resistance of *Enterobacteriaceae* to last resort antibiotics in conjunction with high all-cause mortality and the high healthcare and community burden, is therefore highly problematic. This has led the US Center for Disease Control (CDC) and World Health Organization (WHO) to

place carbapenem-resistant, ESBL-producing Enterobacteriaceae as priority 1 pathogens (critical) for the research and development of new antibiotics targeting MDR and XDR Gram-negative bacteria without co-/cross-resistance to existing antibiotic classes [115, 138].

Cystobactamids were first isolated from the myxobacterium *Cystobacter* sp. Cbv34. Their unique chemical scaffold comprises a *para*-nitrobenzoic acid unit (PNBA), two *para*-aminobenzoic acid units (PABA), two PABA units with different substitution patterns and a central β-methoxyasparagine linker (Fig. 1) [103, 104]. Albicidin [139] and cystobactamids are not only structurally highly similar but they also share the same target. They target bacterial type IIa topoisomerase and efficiently kill both Gram-negative and Gram-positive bacteria by stabilizing the DNA cleavage complex. Cystobactamids display excellent activity (nM to µM range) in particular against *E. coli*, including FQ-resistant and MDR isolates. Cystobactamids therefore present a viable option for development of treatment options for cUTI indications as replacement for FQs, which has been shown to have considerable side effects and their use results in MDR development, resulting in sever restriction or suspension of FQ use [140]. Due to low yields from the natural producer strain(s) cystobactamid heterologous expression was established [106], strengthened by a total synthesis program, which enabled the generation of structurally diverse synthetic cystobactamid derivatives on multi-mg scale. Structure-activity relationship studies yielded improved cystobactamid derivatives with broad-spectrum antibacterial activity [105, 107-109]. Currently, the most potent natural derivative is Cys861-2 that served as inspiration for synthesis of the initial synthetic frontrunner CN-DM-861. Using an *in vivo E. coli* infection model, we have shown that intravenous application of CN-DM-861 effectively reduced bacterial load in thigh, kidney and lung [105]. In the present study, we have shown that cystobactamids effectively killed MDR *E. coli* and they retained activity on FQ-resistant *E. coli* strains with high potency. We have also shown that resistance towards cystobactamids is not due to FQ or albicidin cross-resistance but rather due to a novel mode of

resistance involving quorum-sensing *E. coli* (qse) two-component system. Observed mutations in the *qseBC* lead to upregulation of the *arn* and *qse* operon, as well as *eptA*, *cptA* and *waaH* genes resulting in LPS modifications.

A
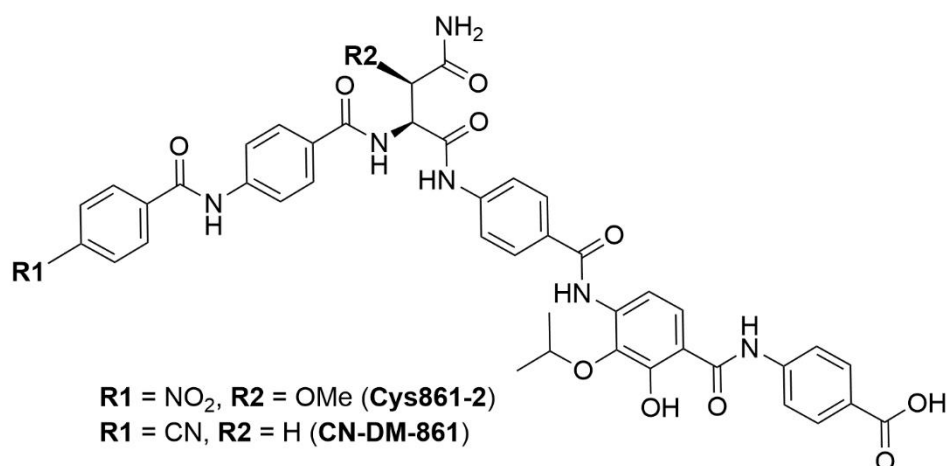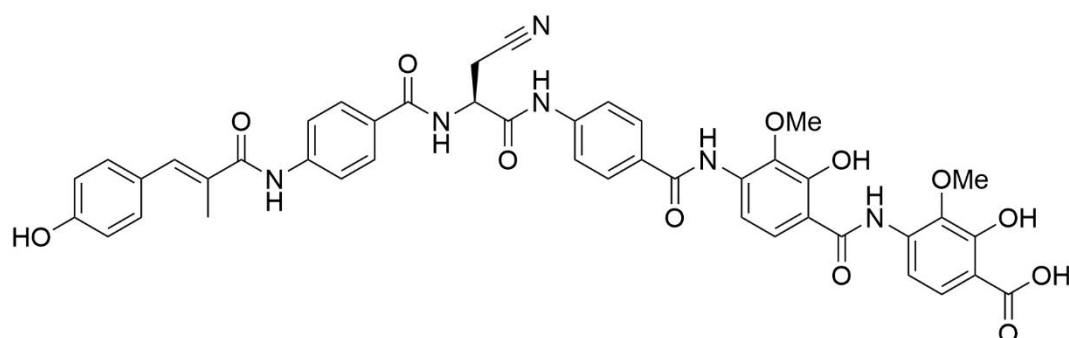
R1 = NO₂, R2 = OMe (**Cys861-2**)
R1 = CN, R2 = H (**CN-DM-861**)

B

Fig. 1. Chemical structures of cystobactamids and albicidin.
(A) Cystobactamids Cys861-2 and CN-DM-861. (B) Albicidin.

2.4 Results

2.4.1 FQ resistance in *E. coli*

Cystobactamids display a similar mode of action as FQs. Thus, in order to explore potential cross-resistance of cystobactamids and FQs, the activity of natural Cys861-2, its synthetic derivative CN-DM-861, and ciprofloxacin (CIP) were assessed using a panel of *E. coli* indicator strains known to be FQ resistant (Table 1). Both, Cys861-2 and CN-DM-861 are very potent,

with MICs (minimum inhibitory concentrations) ranging from 0.005 µg/mL to 1 µg/mL. The synthetic derivative CN-DM-861 exhibited stronger activity against *E. coli* than the natural derivative and it was equipotent to CIP. The potency of cystobactamids was further increased in *E. coli* strains that are efflux-deficient. Deletion of *acrB* or *tolC* of the AcrAB-TolC efflux pump had only marginal effects on the MICs of Cys861-2 but we found up to 10-fold decreased MICs for CN-DM-861. In contrast, overexpression of the pump by disruption of the gene encoding the regulator MarR did not affect CN-DM-861 activity but we observed 10-fold higher MIC for Cys861-2 when comparing the mutant to the wildtype strain (0.64 vs. 0.06 µg/mL). This effect was even more pronounced when both regulators *acrR* and *marR* were deleted (*E. coli* LM367) where the MIC of Cys861-2 increased to 4 µg/mL while the activity of CN-DM-861 remained unaffected. In conclusion, both cystobactamid derivatives seem to be substrates of the AcrAB-TolC efflux pump with Cys861-2 being more affected than CN-DM-861. For the latter, overexpression of the efflux pump has no effect and inactivation of AcrAB-TolC in *E. coli* makes the mutant strains hypersusceptible to cystobactamid treatment. The biggest effect was observed using an *hldE* deletion mutant, with a 1000-fold and 240-fold increase in activity for Cys861-2 and CN-DM-861, respectively. HldE is involved in the biosynthesis of the heptose precursors in the inner core of LPS, and mutations in this gene lead to formation of truncated LPS [141]. We observed no effect on activity of CN-DM-861 in strains harboring the major known FQ related GyrA and ParC mutations, however, approx. 10-fold drop in activity was observed for Cys861-2. Combined increased efflux and target mutations additionally hampered the activity of Cys-861-2, whereas no effect was observed for CN-DM-861. *E coli* strains CH418, CH448, CH440, and CH460 carrying major GyrA and ParC mutations in combination with different plasmid-mediated FQ resistance mechanisms, namely Qnr proteins, aminoglycoside acetyltransferase (*aac(6´)-lb-cr*), and Qnr efflux proteins (QepA), were fully resistant to CIP with MIC > 6.4 µg/mL. However, all remain highly susceptible to both Cys861-2 and CN-DM-861, with CN-DM-861 being 6.3-fold, 25-fold, 2-

fold and 20.8-fold more potent, respectively. The same observations were made for *E. coli* Swiss 9, carrying the *mcr-1* gene conferring colistin resistance, and *E. coli* G38, carrying a *kpc-2* gene encoding a carbapenemase. Both remain highly susceptible to both cystobactamids and are fully resistant to CIP. The activity of Cys861-2 and CN-DM-861 is in the same range for *E. coli* Swiss 9, with MIC values of 0.25 and 0.125 µg/mL, respectively. In contrast, CN-DM-861 is 6.3-fold more potent than Cys861-2 in the carbapenemase-producing strain, with MIC values of 0.016 and 0.1 µg/mL, respectively. *E coli* G487, expressing a β-lactamase, remained CIP and cystobactamid sensitive. MIC values of CN-DM-861 and CIP are in the same range (0.016 and 0.025 µg/mL, respectively) whereas Cys861-2 was 7.8-fold less potent than CN-DM-861 with MIC of 0.125 µg/mL.

Table 1. MIC profile of cystobactamids Cys861-2, CN-DM-861 and CIP on selected *E. coli* strains.

Strain	MIC [µg/mL]		
	Cys861-2	CN-DM-861	CIP
E. coli MG1655/K12[a]	0.064	0.01	0.01
E. coli MG1655/K12 Δ*acrB*	0.08	0.004	0.004
E. coli BW25113[a]	0.25	0.05	0.01
E. coli DSM-1116[a]	0.05	0.01	0.01
E. coli ATCC-25922[a]	1	0.06	0.01
E. coli ATCC-25922 Δ*hldE*	0.001	0.00025	0.004
E. coli ATCC-25922 Δ*tolC*	0.0025	0.0025	0.002
E. coli WT[a]	0.06	0.06	0.025
E. coli WT-III [*marR* (Δ74bp)]	0.64	0.06	0.05
E. coli WT-3 [*gyrA* (S83L, D87G)]	0.64	0.06	0.32
E. coli LM693 [*gyrA* (S83L, D87N), *parC* (S80I)]	1	0.02	> 6.4
E. coli LM367 (Δ*marR*, Δ*acrR*)	4	0.06	0.1
E. coli LM705 [*gyrA* (S83L, D87N), *parC* (S80I), Δ*marR*, Δ*acrR*]	4	0.125	> 6.4
E. coli CH460 [*gyrA* (S83L, D87N), *parC* (S80I, E84V), QepA]	0.125	0.02	> 6.4
E. coli CH440 [*gyrA* (S83L, D87N), *parC* (S80I, E84V), *aac(6´)-lb-cr*]	0.5	0.02	> 6.4

E. coli CH448 [*gyrA* (S83L), QnrS]	0.25	0.125	> 6.4
E. coli CH418 [*gyrA* (S83L, D87N), *parC* (S80I, E84G), QnrA]	0.125	0.006	> 6.4
E. coli Swiss 9 (*mcr-1*+)	0.25	0.125	> 6.4
E. coli G38 (KPC-2)	0.1	0.016	> 6.4
E. coli G487 (OXA-48)	0.125	0.016	0.025

Qnr, pentapeptide repeat protein; *mcr-1*+, colistin resistant; KPC-2, *K. pneumoniae* carbapenemase-2; OXA-48, carbapenemase.

[a], wildtype.

2.4.2 Cystobactamids are active against clinical isolates of ESKAPE pathogens and MDR uropathogens

To further assess the potent activity that was observed on *E. coli* strains (Table 1), we extended our profiling to clinical ESKAPE pathogens (Table 2) and most relevant uropathogens (Table 3). Furthermore, the activity of Cys861-2 against pathogenic *E. coli* strains was assessed in artificial urine (Table 4). Cys861-2 displayed very good activity against Gram-positive *Staphylococcus* spp. and *Enterococcus* spp., with median MICs of 0.13 µg/mL and 0.2-0.4 µg/mL, respectively. Importantly, the tested isolates of *Staphylococcus* spp. and *Enterococcus* spp. were less susceptible to CIP treatment with median MICs of 0.2-0.4 µg/mL and > 6.4 µg/mL, respectively. With respect to the Gram-negative ESKAPE species, Cys861-2 was most potent on *Enterobacter* spp. and *Acinetobacter baumannii* with median MICs of 0.5-2 µg/mL and 1 µg/mL, respectively. Highest MICs were observed for *Klebsiella* spp. (2-8 µg/mL) and *Pseudomonas aeruginosa* (4 µg/mL). In general, Cys861-2 was active on all ESKAPE pathogens with median MICs in the sub- to one-digit µg/mL range, and its activity on Gram-positive bacteria outcompetes the activity of CIP. For Gram-negative bacteria, CIP was on average by one order of magnitude more potent than Cys861-2.

Table 2. Activity of natural derivative Cys861-2 and CIP on clinical ESKAPE pathogens.

		Cys861-2	CIP
		median MIC	
species	n	[µg/mL]	
Enterobacter spp.	4	0.5-2	0.03
Staphylococcus spp.	10	0.13	0.2-0.4
Klebsiella spp.	12	2-8	0.03
A. baumannii	9	1	0.4
P. aeruginosa	11	4	0.2
Enterococcus spp.	8	1-2	> 6.4

Next, we extended the activity profiling of Cys861-2 to recent isolates of important uropathogens (Table 3), where we also included MDR bacteria. MICs determined on uropathogens are in line with ESKAPE panel testing results, the only discrepancy was observed for *Enterococcus* spp. where the median MIC of Cys861-2 was 4-fold lower. *E. coli* was the most sensitive species and *Proteus* spp. was non-sensitive. Cys861-2 outcompeted CIP and remained active on ESBL-producing and colistin resistant *E. coli*. Median minimal bactericidal concentration (MBC) was only 2-4-fold higher than median MIC, indicating a bactericidal mode of action.

Table 3. Median MIC and MBC values of cystobactamid Cys861-2 and CIP on uropathogens.

		Cys861-2	CIP	Cys861-2	CIP
		median MIC		median MBC	
Species	n	[µg/mL]		[µg/mL]	
P. aeruginosa	10	4-8	0.125	32-64	0.25
Klebsiella spp.	11[a]	8	8	16	2
Enterobacter spp.	8[b]	2	≤ 0.06-1	4	≤ 0.06-4

Proteus spp.	9	> 64	≤ 0.06	> 64	≤ 0.06
Enterococcus spp.	25	2	1	8	2
E. coli	37[c]	0.5	≤ 0.06	1	≤ 0.06
E. coli (sensitive)	15	0.5	≤ 0.06	0.5	≤ 0.06
E. coli (ESBL)	7	1	> 64	1	> 64
E. coli (SSBL)	8	1	≤ 0.06	1	≤ 0.06
E. coli (*mcr-1*[+])	5	0.5	16	1	32
E. coli (CR)	2	2	1-2	2-4	1-2

ESBL, extended spectrum β-lactamase; SSBL, small spectrum β-lactamase; CR, carbapenem resistant; *mcr-1*[+], colistin resistant isolate.
[a], contains 2 ESBL and 2 CR isolates.
[b], contains 1 CR isolate.
[c], contains 7 ESBL, 8 SSBL, 2 CR, and 5 *mcr-1+* isolates.

Due to the excellent activity of Cys861-2 against *E. coli* uropathogenic isolates, we investigated whether its activity was retained in artificial urine and at various physiologically relevant pH values (Table 4-5). We observed that MIC in artificial urine is on average 2-4-fold lower than in standard Müller-Hinton broth (MHB) for all tested *E. coli* isolates (sensitive, ESBL, SSBL and colistin resistant). However, MBC is on average 2-4-fold higher in artificial urine. When determining the MIC at various pH, we discovered that with the exception of pH 5.5 where MIC of Cys861-2 was ≤ 0.06 µg/mL, MIC values were stable at pH 6.5 to pH 8.5 (0.13-0.25 µg/mL). Low pH conditions had no impact on MBC and values were stable at 0.25-1 µg/mL at pH 5.5 to pH 8.5.

Table 4. MIC and MBC determination of Cys861-2 in MHB and artificial urine for selected clinical isolates of *E. coli*.

	MIC [µg/mL]		MBC [µg/mL]	
Isolate	MHB	AU	MHB	AU
E. coli 38[a]	1	0.5	1	1
E. coli 51	0.5	0.25	0.5	1
E. coli 54[b]	0.5	0.25	0.5	2

E. coli 57[a]	0.5	0.25	1	0.5
E. coli 61	0.5	0.13	0.5	0.5
E. coli 83[b]	0.5	0.13	1	0.5
E. coli Af48[c]	0.5	0.25	0.5	2
median MIC/MBC	0.5	0.25	0.5	1

ESBL, extended spectrum β-lactamase; SSBL, small spectrum β-lactamase; *mcr-1+*, colistin resistant isolate; AU, artificial urine.
[a], ESBL.
[b], SSBL.
[c], *mcr-1+*.

Table 5. MIC and MBC determination of Cys861-2 using *E. coli* 51 in artificial urine at various pH values.

pH	5.5	6.5	7.5	8.5
MIC [µg/mL]	≤ 0.06	0.25	0.13	0.25
MBC [µg/mL]	0.5	1	0.25	0.5

Based on the observed activities, we aimed to assess whether the potent antibacterial activity is also observed on recent, relevant clinical *E. coli* strains isolated from mid-flow urine samples and urocatheters at Medical School Hannover (MHH), Germany. We tested a large number of isolates (n = 50) with varying resistance profiles using the improved synthetic derivative CN-DM-861, and we used CIP and cefotaxim as controls (Table 6). The determined MIC_{50} values of CN-DM-861, CIP and cefotaxim were all in the same range (0.06 µg/mL, 0.03 µg/mL, and 0.13 µg/mL, respectively). However, only cystobactamid CN-DM-861 was able to kill also the more challenging and MDR *E. coli* subpopulations and MIC_{90} was 0.5 µg/mL. In comparison, MIC_{90} values of CIP and cefotaxim were > 6.4 µg/mL and > 64 µg/mL, respectively. No cross-

resistance with 3GC and FQ was observed. Furthermore, CN-DM-861, CIP and cefotaxim all exhibit a broad MIC distribution (Fig. 2).

Table 6. MIC$_{50}$ and MIC$_{90}$ determination of CN-DM-861, CIP and cefotaxim on a large panel of *E. coli* clinical isolates.

Strain	n	MIC$_{50}$ [µg/mL]			MIC$_{90}$ [µg/mL]		
		CN-DM-861	CIP	CTX	CN-DM-861	CIP	CTX
E. coli[a]	50	0.06	0.03	0.13	0.5	> 6.4	> 64
Ec CIP^{Rb}	12	0.13	> 6.4	0.25	1	> 6.4	> 64
Ec CAZ^{Rb}	7	0.13	> 6.4	> 64	0.5	> 6.4	> 64
Ec AMP^{Rb}	28	0.25	0.1	0.125	1	> 6.4	> 64
Ec TMP-SMX^{Rb}	17	0.25	3.2	0.125	2	> 6.4	> 64

CTX, cefotaxim; CAZ, ceftazidime; AMP, ampicillin; TMP-SMX, trimethroprim-sulfamethoxazole; Ec, *E. coli*.
[a], recent clinical isolates.
[b], subset of *E. coli*.
[R], resistant.
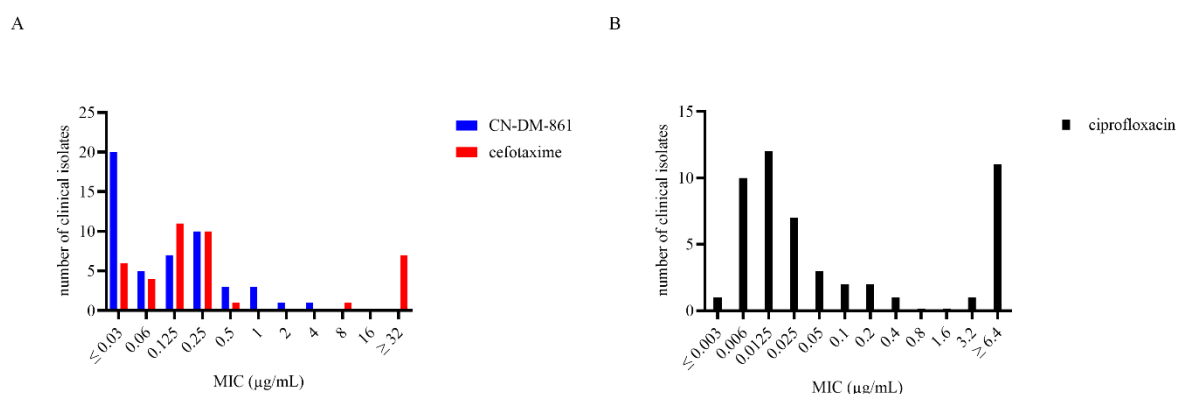
Fig. 2. MIC distribution of *E. coli* clinical isolates.
(A) MIC distribution for cefotaxime and CN-DM-861. (B) MIC distribution of ciprofloxacin. N = 50.

Both, the natural product Cys861-2 and the synthetic derivative CN-DM-861 were subjected to *in vitro* profiling to determine time-kill kinetics (Fig. 3). For both compounds, we observed a fast bactericidal effect, as we reached 3-log10 reduction of the initial bacterial load in approximately 2 hours after exposure. The bacterial load continued to decline until 4 hours post exposure, reaching the limit of detection. Until 6 hours post exposure, both compounds had the

same kinetics. However, for Cys861-2, we observed regrowth to occur at 1x MIC and 2x MIC at 8 hours post exposure and complete regrowth after 24 hours. Minimal regrowth was observed for 4x MIC and no regrowth was observed for 8x MIC. Contrarily, CN-DM-861 tested at 1x MIC and 2x MIC showed significantly less pronounced regrowth compared to Cys861-2 at 8 hours post exposure. No regrowth was observed for CN-DM-861 at 4x MIC and 8x MIC after 24 hours. Both compounds act fast bactericidal, with CN-DM-861 exhibiting an improved profile compared to Cys861-2.
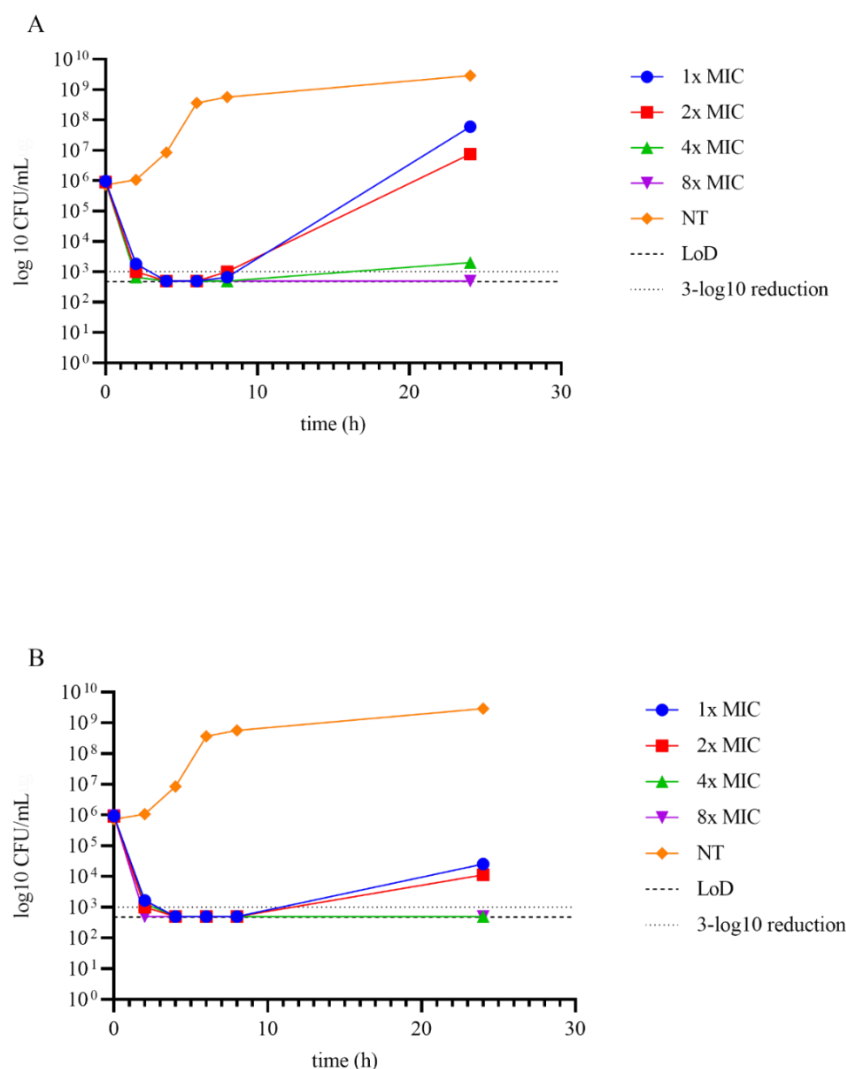
Fig. 3. Time-kill kinetics for Cys861-2 and CN-DM-861.
Time-kill curves determined on *E. coli* ATCC-25922 at 1x MIC, 2x MIC, 4x MIC and 8x MIC including a non-treated control (NT). LoD, limit of detection. (A) Cystobactamid Cys861-2. (B) Cystobactamid CN-DM-861.

We also assessed *in vitro* on-target activities for Cys861-2 and CN-DM-861 and compared their potency with that of CIP (Table 7). Half-inhibitory concentrations (IC_{50}) on wildtype *E. coli* DNA gyrase were in the same range for Cys861-2, CN-DM-861 and CIP (0.42 µM, 0.26 µM, and 0.59 µM, respectively). However, CIP lost activity on *E. coli* gyrase carrying the S83L mutation in *gyrA*, which is part of the quinolone resistance-determining region (QRDR) [142] with $IC_{50} > 50$ µM. Intriguingly, both Cys861-2 and CN-DM-861 remained active in the low, single-digit µM range (IC_{50} of 1.7 and 0.8 µM, respectively). Loss of inhibitory effect of CIP was significantly lower when tested on *E. coli* gyrase carrying the D426N mutation (*gyrB* subunit, QDRD [142]) with IC_{50} of 7.3 µM. Cystobactamids Cys861-2 and CN-DM-861 remained more active in comparison, with IC_{50} of 2.1 µM and 2.9 µM, respectively. These results indicate that there is possibly a partial overlap of gyrase binding sites of FQs and cystobactamids. However, cystobactamids remain active (IC_{50} in low µM range) on S83L and D462N mutant enzymes, whereas these mutations significantly impact the activity of CIP.

Table 7. IC_{50} values determined for Cys861-2, CN-DM-861 and CIP on *E. coli* DNA gyrase wildtype and mutant enzymes.

Compound	*E. coli* DNA gyrase supercoiling assay, IC_{50} [µM]		
	WT	S83L[a]	D426N[b]
Cys861-2	0.42	1.70	2.1
CN-DM-861	0.26	0.80	2.9
CIP	0.59	> 50	7.3

IC_{50}, half-inhibitory concentration; WT, wildtype.
[a], mutation in GyrA QRDR, confers approximately 100-fold resistance to FQs.
[b], mutation in GyrB QRDR, confers approximately 10-fold resistance to FQs.

2.4.3   Cystobactamid resistance is not mediated by common importers

Using *E. coli* mutant strains and mutated DNA gyrase enzymes, we detected only minor cross-resistance of cystobactamids with FQs although both classes target bacterial type IIa

topoisomerases. Apart from target mutations (*gyrA*, *parC*) and target protection (Qnr proteins) that confer FQ resistance, we also excluded high-level cystobactamid resistance through upregulation of the AcrAB-TolC efflux pump in *E. coli*. Furthermore, the observed partial cross-resistance of FQs with Cys861-2 could be overcome by the improved synthetic derivative CN-DM-861.

Albicidin is another natural product topoisomerase inhibitor that is structurally similar to cystobactamids [100]. Several resistance mechanisms towards albicidin have been reported to date, namely through AlbA [100, 143], AlbB [144] and AlbD [145], however, none of these enzymes are present in *E. coli*. Importantly, albicidin resistance can also be conferred by inactivation mutations of Tsx, a nucleoside-specific, channel-forming protein that serves as an importer for deoxynucleosides and albicidin. Tsx also serves as a receptor for bacteriophages and colicins [146, 147]. We tested Cys861-2 and CN-DM-861 using an *E. coli tsx* deletion strain and compared cystobactamid activity to that of CIP and albicidin (Table 8). Albicidin and Cys861-2 were active in the same range on the wildtype strains with MIC values of 0.4 µg/mL and 0.2-0.4 µg/mL, respectively. The improved synthetic derivative CN-DM-861 was 8-fold more potent than natural Cys861-2. As expected, albicidin lost its activity when *tsx* was deleted (MIC > 6.4 µg/mL) and the reference drug CIP remained active. Despite the structural similarity of albicidin and cystobactamids, both Cys861-2 and CN-DM-861 were still active on *E. coli* Δ*tsx* and we observed only a marginally shifted MIC (2-fold compared to the parent wildtype *E. coli*). Thus, we concluded that cystobactamids reach their intracellular target in Gram-negative *E. coli* through another importer system, and in contrast to albicidin they are not imported through Tsx.

Table 8. MIC values of Cys861-2, CN-DM-861, albicidin and CIP on wildtype *E. coli* and a *tsx* deletion mutant.

	MIC [μg/mL]	
	E. coli	
Compound	WT	Δ*tsx*
Cys861-2	0.2-0.4	0.8
CN-DM-861	0.05	0.1
Albicidin	0.4	> 6.4
CIP	0.006	0.0125

WT, wildtype.

Although cystobactamids exhibit a rather high molecular weight (> 850 Da), are highly unpolar, and have numerous rotatable bonds [105], we hypothesized that their elongated structure possibly enables entry via porins. The main porins OmpF and OmpC have been described as responsible for antibiotic translocation in *E. coli* [148-150]. We tested both Cys861-2 and CN-DM-861 against strains lacking one or more porins, and cefoxitin was used as a positive control (Table S1). No effects were observed for either Cys861-2 or CN-DM-861-2 for any of the porins deleted. Furthermore, cystobactamids contain aromatic systems; it is therefore possible that pore-like structure form due to the π-stacking, enabling its entry without affecting its structure and functional effects [151-153]. Lastly, due to presence of carboxylic acid, isopropoxy-, hydroxyl-, nitro- and methoxy group, latter two not present in CN-DM-861, it is possible that under the experimental conditions the net charge of the compound is affected and cystobactamids translocate into the cells via passive diffusion. Thus, it remained unclear at this stage how cystobactamids can translocate across the Gram-negative cell envelope.

2.4.4 Cystobactamid-resistant mutants develop at a low frequency and carry mutations in the bacterial quorum-sensing two-component system QseBC

Based on our findings, FQ- and albicidin-related resistance mechanisms do not play a major role in cystobactamid resistance. Thus, we assessed the level of spontaneous resistance development and endeavored to isolate and characterize cystobactamid-resistant *E. coli* mutants. We performed spontaneous resistance development experiments with several *E. coli* strains using the synthetic derivative CN-DM-861. We also included an efflux-deficient strain (*tolC* deletion) and a more challenging FQ resistant clinical isolate (*E. coli* CH448), carrying both the major gyrase A mutation (S83L) and the QnrS protein. When treated with 4x MIC of CN-DM-861 we were able to isolate resistant clones from all strains except for *E. coli* ATCC-25922 and the frequency of resistance (FoR) was highly variable with values between 10^{-7} and $< 10^{-10}$ (Table 9). FoR determined at 4x MIC was 2-3 orders of magnitude higher than that of CIP for all tested strains. However, at 8x MIC the FoR was very low for both CIP and CN-DM-861 ($< 10^{-10}$). The efflux-deficient strain displayed a lower FoR for CN-DM-861 than its isogenic parent strain; this was not the case for CIP. The FQ resistant strain had the highest FoR at 4x MIC of all strains (1×10^{-7}), however, at 8x MIC FoR was significantly lower ($< 4 \times 10^{-10}$). Next, resistant mutants were characterized and subjected to whole genome sequencing (WGS) (Table 9 and Table S2). Additional characterization of resistant mutants revealed a MIC shift in a rather large range for *E. coli* AG100/K12 mutants and a smaller MIC shift range for *E. coli* ATCC-25922 *ΔtolC* mutants, 50-3200-fold and < 12-200-fold respectively (Table S3). However, all resistant mutants were still sensitive to CN-DM-861 in a sub- to low micromolar range. No co-/cross-resistance was observed for *E. coli* ATCC-25922 *ΔtolC* with CIP, whereas minor co-/cross-resistance was observed for *E. coli* AG100/K12 (0.5-4 fold). We extended co-resistance testing to clinically relevant antibiotics, namely ceftazidime, aztreonam, gentamicin, colistin and meropenem. We found no co-resistance with any of the tested antibiotics (Table

S4). Resistant mutants did not revert to a sensitive phenotype after 10 passages under non-selective conditions (Table S5). Importantly, none of the isolated cystobactamid-resistant mutants displayed significant cross-resistance with CIP and other relevant antibiotics. WGS revealed that mutations causing resistance to cystobactamids cluster in a quorum-sensing two-component system, QseBC (Fig. 4), with QseC, a sensor histidine kinase, being the preferred target for accumulation of mutations. Mapping of mutations to functional domains of QseC revealed the dimerization and histidine phosphotransfer domains, and a catalytic ATP-binding domain as the mutation hotspots indicating that the ability to autophosphorylate and phosphorylate/dephosphorylate QseB is impaired in the *E. coli* mutants. Mutations were found in QseB as well, however, with a much lower occurrence. The mutational hotspot in QseB was the active site of the protein, which indicates that activation of QseB via phosphorylation might be hampered.
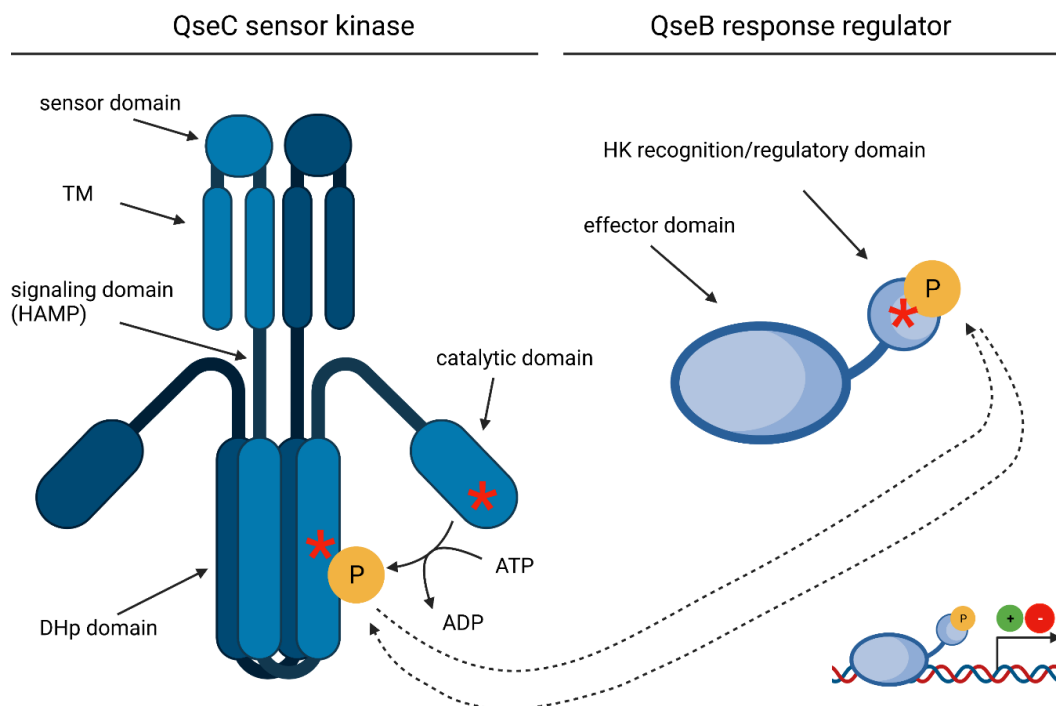
Fig. 4. QseBC TCS signaling pathway and mutational hotspots in cystobactamid-resistant *E. coli*.
QseBC TCS consists of QseC, a sensor (histidine) kinase and QseB, a response regulator. Upon signal recognition and binding in the periplasmic space, conformational changes in HAMP signaling domain lead to QseC autophosphorylation in an ATP-depended manner. Activated QseC transfers the phosphoryl group to QseB.

Activated QseB binds to promoter regions of genes under its control, and activates (green) or represses (red) their transcription. QseC can also dephosphorylate QseB.

TM, transmembrane domain; HAMP, histidine kinase, adenylyl cyclases, methyl-binding proteins, and phosphatases; DHp, dimerization and histidine phosphotransfer domain; HK, histidine kinase. P, phosphoryl group. Red asterix, mutational hotspot.

Created in BioRender.com.

Table 9. Frequency of resistance, characterization of resistant mutants and whole genome sequencing results.

Frequency of Resistance				
	CN-DM-861		CIP	
strain	4x MIC	8x MIC	4x MIC	8x MIC
E. coli DSM-1116[a,b]	$2 \times 10^{-7*}$	nd	1×10^{-9}	nd
E. coli AG100/K12 [a]	4×10^{-8}	nd	2×10^{-10}	nd
E. coli ATCC-25922	$< 3 \times 10^{-10}$	$< 3 \times 10^{-10}$	4×10^{-9}	$< 3 \times 10^{-10}$
E. coli ATCC-25922 Δ*tolC* [a]	4×10^{-8}	nd	4×10^{-10}	nd
E. coli CH448 (S83L, QnrS)	1×10^{-7}	$< 4 \times 10^{-10}$	$< 4 \times 10^{-10}$	$< 4 \times 10^{-10}$

CN-DM-861[R] mutant characterization				
	mutation in	MIC shift[c] (CN-DM-861, parent vs. Cys[R] mutant)	co-/cross-resistance with CIP[c] (CIP, parent vs. Cys[R] mutant)	co-/cross-resistance with crAB[d]	reversibility of resistance[e]
E. coli AG100/K12		50-3200	0.5-4		
E. coli ATCC-25922 Δ*tolC*	QseBC	< 12-200	1-2	no	non-reversible

WGS results							
		MIC CN-DM-861 [µg/mL]	*qseC*	*qseB*	*ftsW*	*fhdD*	*ssuB*
E. coli AG100/K12	WT	0.0025	na	na	na	na	na
E. coli AG100/K12 CN-DM-861[R]	#1	0.125	357In				
	#2	0.25	362Fs				
	#3	2	362Fs				
	#4	2	357In		I139F		

Strain	Mutant	MIC					
	#5	0.125	E125**				N48K
	#6	0.25	440In				
	#7	8	346Fs				
	#8	0.5	440In				
	#9	0.25		G15C			
E. coli ATCC-25922 *ΔtolC*	WT	0.0025	na	na	na	na	na
	#1	0.125	P251S				
	#2	0.5	259In				
	#3	< 0.03		A80V			
	#4	0.25	P251S				
E. coli ATCC-25922 *ΔtolC* CN-DM-861[R]	#5	0.5	259In				Q87L
	#6	0.5	441Fs				
	#7	0.125	V257E				
	#8	0.25	441Fs				
	#9	0.25	441Fs				

nd, not determined; WGS, whole genome sequencing; crAB, clinically relevant antibiotics; In, insertion; Fs, frameshift; WT, wildtype; Cys[R], cystobactamid resistant.

[*], determined for Cys861-2.

[**], STOP codon.

[a], obtained resistant mutants selected for WGS.

[b], WGS results can be found in Table S2.

[c], results can be found in Table S3.

[d], results can be found in Table S4.

[e], results can be found in Table S5.

[R], resistant.

na, not applicable.

A subset of resistant mutants of *E. coli* ATCC-25922 Δ*tolC* was selected and investigated using isothermal microcalorimetry (IMC) in comparison with standard OD_{600} measurements. ICM measures total heat released over time. Recorded heat curves represent sum of all metabolic processes, exothermal and endothermal, and not just heat released due to biomass formation. While standard OD_{600} measurements did not reveal any differences in growth kinetics of selected resistant mutants (Fig. 5A), ICM revealed differences on the metabolic level (Fig. 5B).

We observed significant differences in metabolic heat profiles when comparing resistant mutants to sensitive wildtype. Standard *E. coli* heat curve recorded in cation-adjusted Müller-Hinton broth (caMHB) has two peaks. The first peak corresponds to biomass formation until early exponential phase and it is comparable to increasing values from OD_{600} measurements; the second peak represents the metabolic activity during stationary phase, where heat emission due to growth is minimal. When we examine the first peak approximately 2.5 hours from start of experiment, a slightly lower heat flow for mutant #4 (*qseC*, P251S) and mutant #9 (*qseC*, 441Fs) is observed, whereas heat flow for mutant #3 (*qseB*, A80V) was equal to that of sensitive wildtype. The observed difference was relatively small and this could be the reason why we did not detect differences in growth kinetics using the standard OD_{600} method. At 4 hours after experiment start, equaling late exponential phase, we observed varying degrees of metabolic activity. The heat flow of *E. coli* wildtype remained constant, i.e. the level of metabolic activity did not change significantly. At approximately 17 hours, heat flow suddenly dropped to 0 µW, which can be attributed to cell death. Resistant mutant #3 had the same heat flow profile as *E. coli* wildtype, however, metabolic activity lasted 2 hours longer, before it dropped down to 0 µW. Mutant #4 had the lowest level of metabolic activity during the stationary phase. It reached its peak at 15 hours and then gradually declined to reach net heat emission of 0 µW at 24 hours. Contrarily, mutant #9 exhibited a very metabolically active stationary phase, emitting 100 µW of heat at its peak activity, 2-3-fold higher than mutants #3, #4 and wildtype. However, the sudden drop of metabolic activity was detected sooner, at approximately 11 hours. Metabolic exertion together with the lack of oxygen ultimately leads to cell death and lysis, with endothermal processes being more pronounced than exothermal processes, thus, resulting in negative net heat emission. Next, detailed analysis of thermograms was performed. Analysis of lag phase duration (Fig. 6A) revealed statistically significantly shorter lag phase for mutants #4 and #9, and no differences in lag phase duration for mutant #3. Analysis of maximum growth rate (Fig. 6B) revealed that only mutant #4 had significantly lower maximum growth rate

compared to wildtype. No statistically significant difference was observed when analyzing total emitted heat (Fig. 6C) of resistant mutants compared to the wildtype.
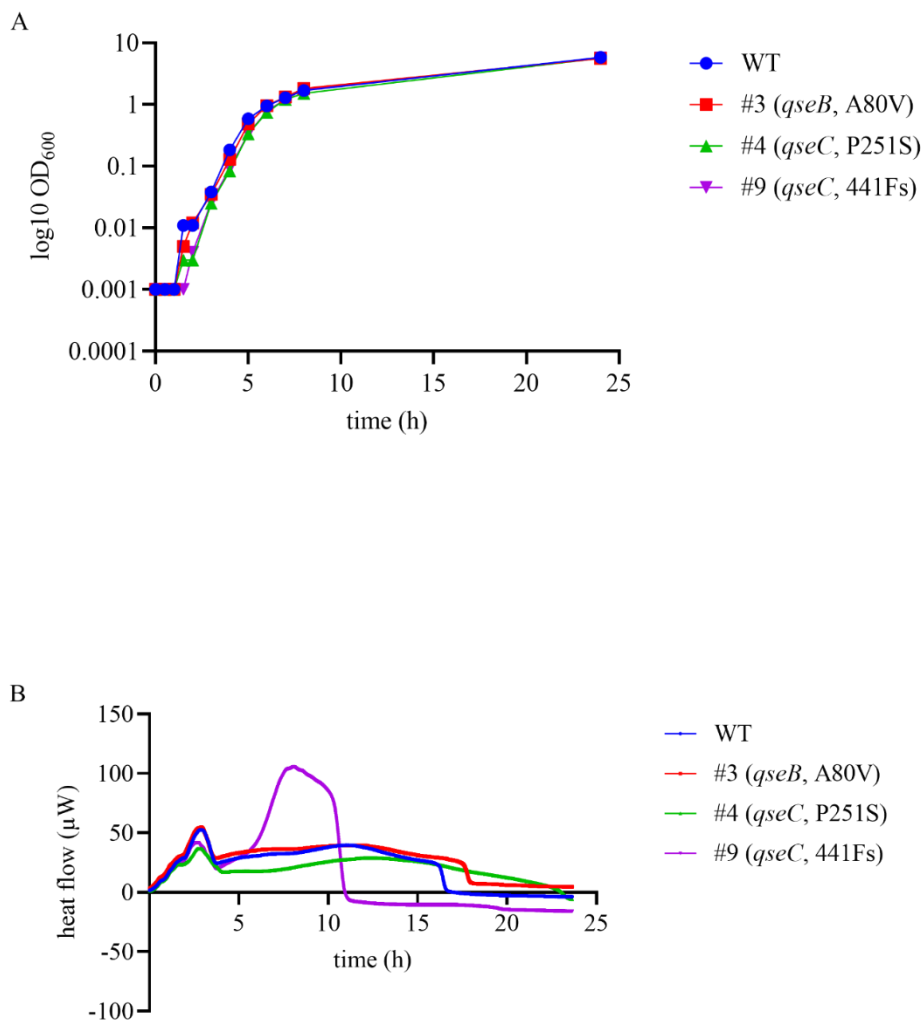
Fig. 5. Growth and heat flow curves for selected *E. coli* ATCC25922 Δ*tolC* CN-DM-861 resistant mutants and wildtype.
(A) Growth curves. (B) Heat flow.
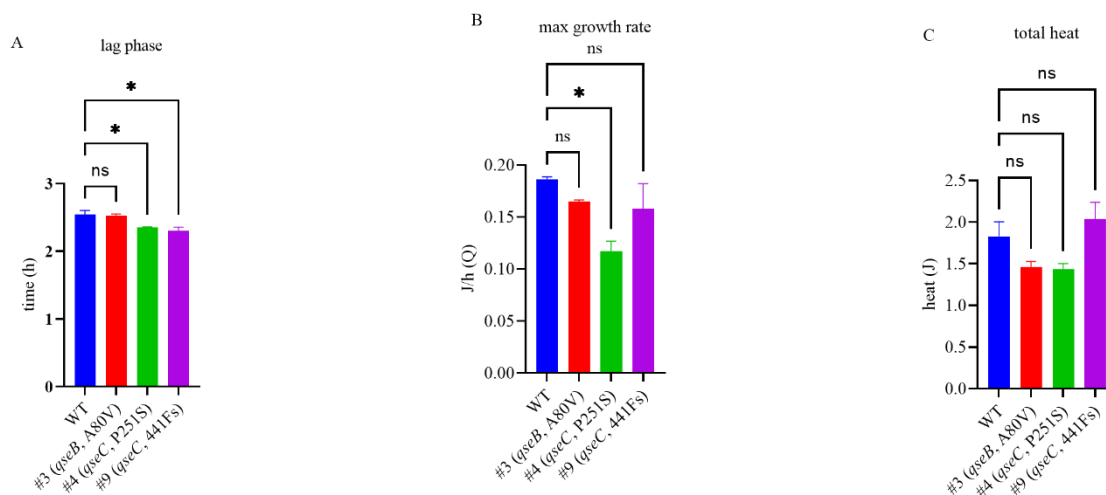
Fig. 6. Analyzed heat flow parameters recorded for selected cystobactamid CN-DM-861 resistant mutants of *E. coli* ATCC-25922 Δ*tolC*.
(A) Lag phase duration. (B) Maximum growth rate. (C) Total heat emitted. Ordinary one-way ANOVA was used to analyze the results. ns, not significant; * $p < 0.05$.

2.4.5   SNPs in *qseB* or *qseC* lead to a resistant phenotype

Because the only common mutations observed in cystobactamid-resistant *E. coli* mutants were found in QseBC, we investigated whether deletion of *qseB* or *qseC* confers resistance to cystobactamids (Table 10). However, deletion of *qseB* or *qseC* did not result in any resistance to cystobactamids. Moreover, when exchanging proline for alanine at position 251 in QseC using seamless mutagenesis [154], the same level of resistance is observed as with resistant mutants obtained during spontaneous resistance development (Table 11). Furthermore, we tried to rescue the sensitive phenotype by complementing resistant mutants carrying *qseC* mutations (Table 12). Transcription regulation of *qseBC* is both *qseBC*-dependent (autoregulation) and *qseBC*-independent (constitutive). Autoregulated promoter of *qseBC* has two binding sites, a low-affinity biding site (-360 bp to -500 bp) and a high-affinity binding site (-120 bp to +130 bp). A high concentration of phosphorylated QseB first binds to the high-affinity binding site followed by binding to the low-affinity site, and binding to the low-affinity site enables fine-tuned transcription autoregulation [155]. Because low-affinity binding site overlaps with *ygiW* gene divergently co-transcribed with *qseBC* operon, we cloned a wildtype copy of *qseC*

together with the truncated native promoter (containing only the high-affinity binding site) on a BAC (mimicking the wildtype situation – only one copy of *qseC* on *E. coli* chromosome) in order to avoid unexpected experimental results. Furthermore, Juárez-Rodríguez et al. observed that complementation of a *qseC* deletion mutant with a *qseC* on a multicopy plasmid resulted in biomass and biofilm levels greater than the wildtype [156]. Complemented *E. coli* ATCC-25922 Δ*tolC* CN-DM-861^R #4 (*qseC*, P251S) mutant retained the same MIC for Cys861-2 as its respective resistant mutant, meaning the sensitive phenotype was not restored or alleviated. However, we observed a 8- and 4-fold decrease in MIC for Cys861-2 and CN-DM-861, respectively, when we complemented *E. coli* DSM-1116 Cys861-2 resistant mutant #1, but not for mutant #3.

Table 10. MIC values of Cys861-2, CN-DM-861 and CIP determined on *E. coli* MG1655 with deletion of *qseB* or *qseC*.

	MIC [µg/mL]		
Strain	Cys861-2	CN-DM-861	CIP
E. coli MG1655	0.25	0.05	0.01
E. coli MG1655 Δ*qseB*	0.25	0.05	0.01
E. coli MG1655 Δ*qseC*	0.25	0.05	0.01

Table 11. MIC values determined on *E. coli* ATCC-25922 Δ*tolC, qseC* (P251A) in comparison to MIC values of resistant mutants obtained during spontaneous resistance development.

	MIC [µg/mL]	
Strain	CN-DM-861	CIP
E. coli ATCC-25922 Δ*tolC*	0.0025	0.0025
E. coli ATCC-25922 Δ*tolC* CN-DM-861^R #4 (*qseC*, P251S)[a]	0.25	0.0025
E. coli ATCC-25922 Δ*tolC* CN-DM-861^R #7 (*qseC,* V257E)[a]	0.125	0.0025
E. coli ATCC-25922 Δ*tolC* (*qseC*, P251A)[b]	0.25	0.0025

[a] obtained during spontaneous resistance development.
[b] obtained using seamless mutagenesis.
[R] resistant.

Table 12. MIC values of complemented resistant mutants.

Strain	MIC [µg/mL]		
	Cys861-2	CN-DM-861	CIP
E. coli DSM-1116	0.05	0.01	0.01
E. coli DSM-1116 Cys861-2[R] #1	4	4	0.006
E. coli DSM-1116 Cys861-2[R] #1/pBeloBAC-P$_{qseBC}$*qseC*	1	0.5	0.01
E. coli DSM-1116 Cys861-2[R] #3	2	0.5	0.006
E. coli DSM-1116 Cys861-2[R] #3/pBeloBAC-P$_{qseBC}$*qseC*	1	0.25	0.001
E. coli ATCC-25922 Δ*tolC*	0.0025	0.0025	0.0025
E. coli ATCC-25922 Δ*tolC* CN-DM-861[R] #4	0.125	0.25	0.0025
E. coli ATCC-25922 Δ*tolC* CN-DM-861[R] #4/pBeloBAC-P$_{qseBC}$*qseC*	0.125	0.125	0.0025

[R], resistant.

2.4.6 Cystobactamid resistant mutants exhibit attenuated virulence *in vitro*

QseBC is involved in regulation of several virulence factors, in particular type 1 pili, curli and flagella. [157, 158]. Based on MIC assessment of *E. coli* Δ*qseB*, Δ*qseC* and cystobactamid-resistant mutants, mutations do not equal inactivations. We hypothesized, based on where these mutations are located in *qseBC* that observed mutations resulted in altered autokinase and kinase and/or phosphatase activity of QseC, and the diminished activation of QseB. Hypothesized effects would therefore result in changed transcription levels of genes under the transcriptional control of QseB, and resulted in changes in motility and biofilm formation. Swimming motility was assessed for each mutant type present in resistant mutants of *E. coli* ATCC-25922 Δ*tolC* (Fig. 7A, 7B). We observed that all mutants carrying *qseC* mutations were significantly less motile (swimming motility). Resistant mutants #3 (*qseB*, A80V), and #4 (*qseC*, P251S) were also assessed for their biofilm forming capacity (Fig. 7C). Biofilm forming capacity was assessed with crystal violet assay using growth-normalized biofilm accumulation

known as specific biofilm formation index (SBF [159]). Both mutants displayed significantly reduced biofilm forming potential, with SBF measured as 0.47, 0.59, respectively. Despite the significant loss of virulence, all mutants remained partially motile and were able to form biofilm. Basal activity of the *qseBC*-independent constitutive promoter could explain the observed residual activity of virulence genes.
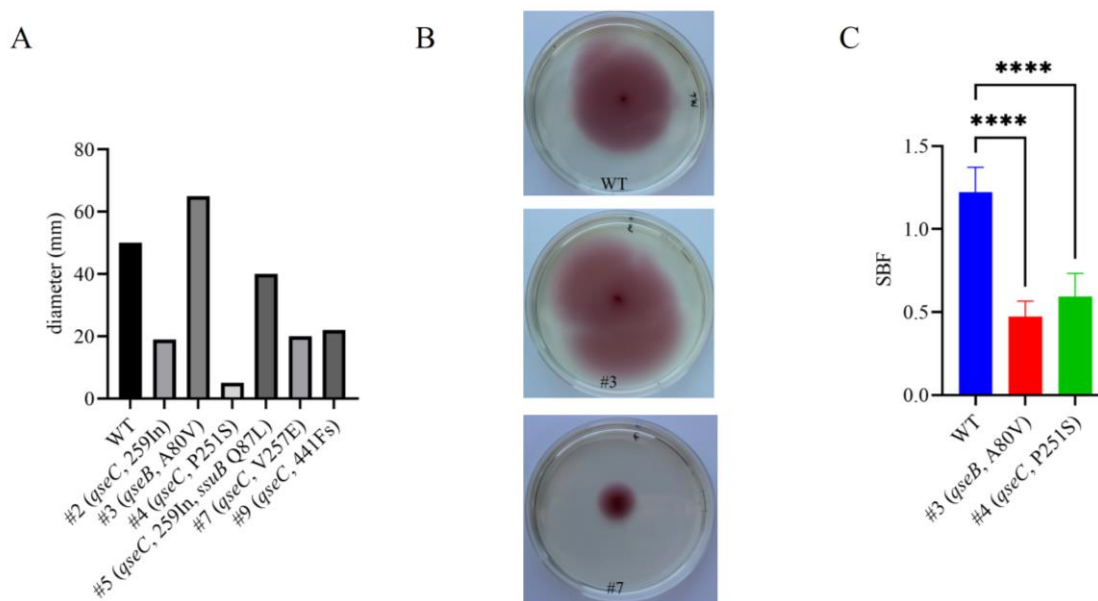
Fig. 7. Virulence assessment on selected cystobactamid CN-DM-861 resistant mutants of *E. coli* ATCC-25922 Δ*tolC*.
(A) Swimming motility of mutants carrying *qseB*, and *qseC* mutations. (B) Swimming motility on agar plates with TTC. (C) SBF comparison of mutants carrying *qseB*, and *qseC* mutations determined in LB. Ordinary one-way ANOVA was used to analyze the results. ns, not significant; *, $p < 0.05$; ****, $p < 0.001$.

2.4.7 Cystobactamids do not induce the transcription of *qseBC*, *pmrAB*, *pmrD* or *marR*

Literature search revealed links between QseBC and PmrAB [160], and MarR [161]. We therefore investigated whether addition of cystobactamid CN-DM-861 affects the transcription levels of *qseB*, *qseC*, *pmrA*, *pmrB*, *pmrD*, *marA* and *marR* in *E. coli* wildtype (Fig. 8A). No effect on transcription was observed for any of the investigated genes following treatment with CN-DM-861. However, when we compared the transcription levels of selected genes in resistant mutants vs. wildtype, we observed different levels of gene expression. In resistant mutant #3 (*qseB*, A80V), both *qseB* and *qseC* transcript levels were increased by approximately

20-fold and 15-fold, respectively (Fig. 8B). The same observations were made for resistant mutant #4 (*qseC*, P251S) where 3-4-fold higher transcript levels of *qseB* and *qseC* were observed compared to mutant #3, a 72-fold and 61-fold increase was observed, respectively, when comparing *qseB* and *qseC* expression in mutant #4 vs. wildtype *E. coli* (Fig. 8C). As expected, in both mutants *qseB* had higher fold change than *qseC*. Mutant #3, but not mutant #4, also displayed reduced transcript levels of *pmrB* and *marR*, -2.3-fold and -3.1-fold, respectively. Mutations in *pmrAB* and *marR* are described to confer resistance to several antibiotic classes. However, we did not observe cross-resistance in the QseBC mutants with either colistin, cefotaxime, gentamicin, tobramycin, or tetracycline although transcript levels of *pmrB* and *marR* were decreased in mutant #3 (Table S6).
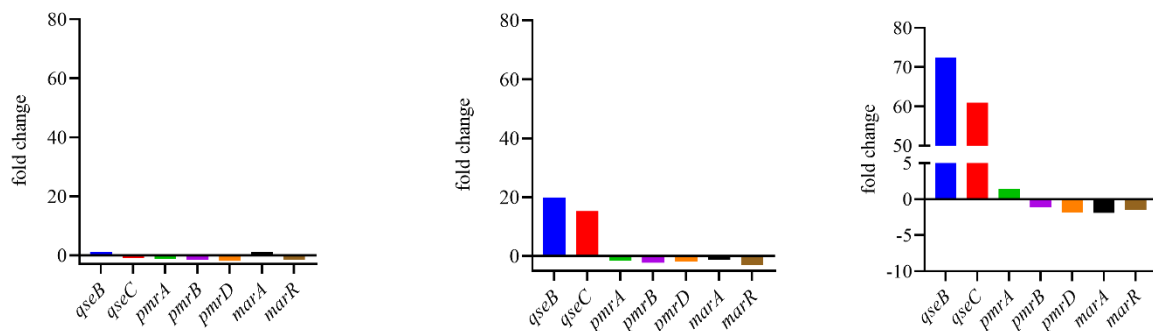
Fig. 8. RT-qPCR results for *qseB*, *qseC*, *pmrA*, *pmrB*, *pmrD*, *marA* and *marR* assessed on *E. coli* ATCC-25922 Δ*tolC* wildtype and CN-DM-861 resistant mutants #3 and #4.
(A) Wildtype exposed to 0.5x MIC CN-DM-861 and compared to non-treated wildtype. (B) Resistant mutant #3 (*qseB*, A80V) *vs.* wildtype. (C) Resistant mutant #4 (*qseC*, P251S) *vs.* wildtype.

2.4.8 Transcriptomics reveals upregulation of genes responsible for LPS modification and downregulation of virulence genes

Deletion of *qseC* was reported to result in abnormal bacterial morphology, i.e. causing bacterial cells to be longer and wider [162]. Thus, we investigated whether similar morphological changes can be observed for cystobactamid-resistant *E. coli* mutants carrying SNPs in *qseB* and *qseC*. Scanning electron microscopy did not reveal any obvious changes of the bacterial surface (Fig. 9A). However, cells of resistant mutant #4, carrying a *qseC* P251S mutation, were

significantly longer, wider, and had a larger diameter than wildtype cells. No statistically significant changes in cell dimensions were detected for cells of resistant mutant #3 carrying the *qseB* A80V mutation (Fig. 9B). Transmission electron microscopy did not reveal obvious morphological changes of the outer membrane or plasma membrane (Fig. 9C).
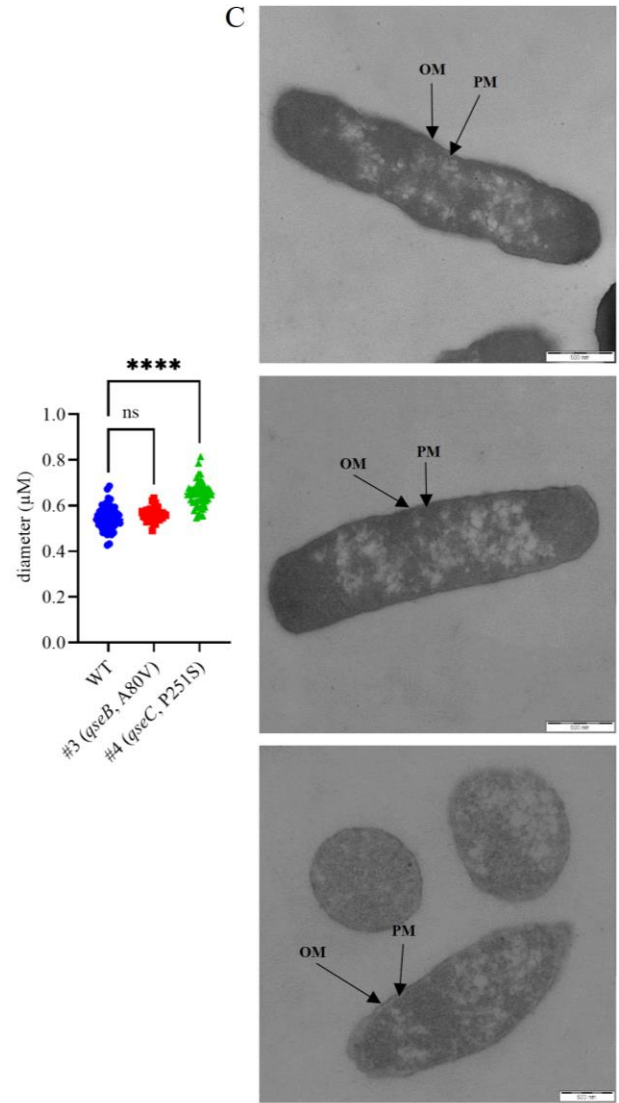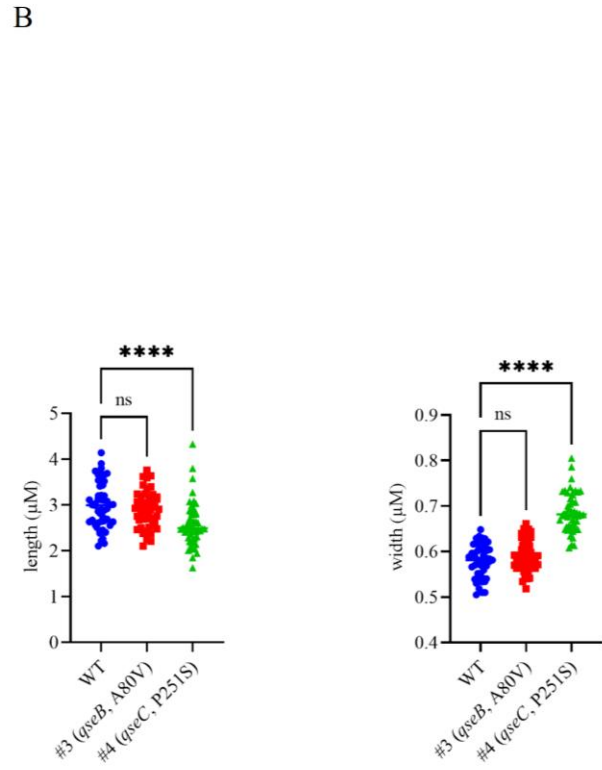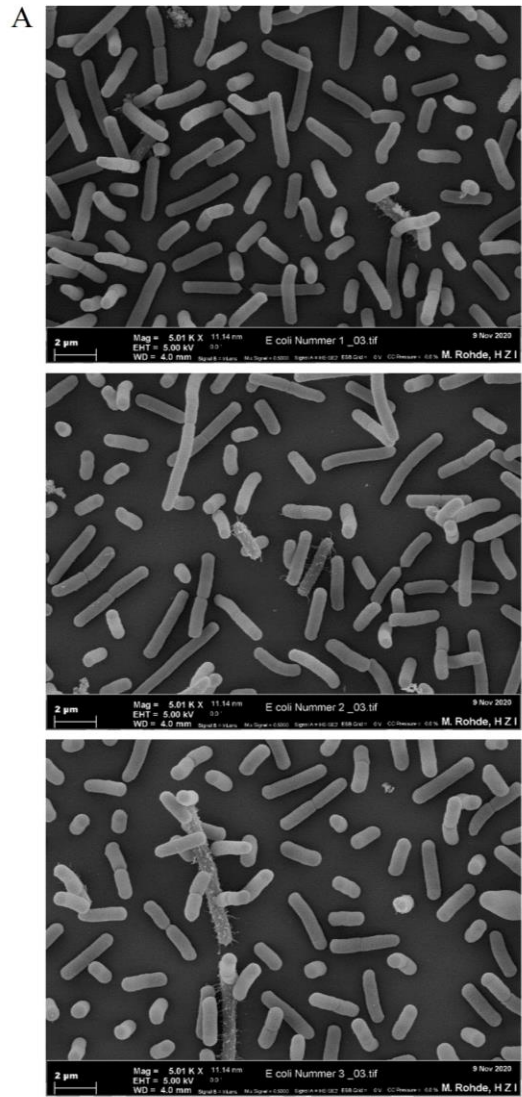
Fig. 9. Cell morphology and dimensions assessment on selected cystobactamid CN-DM-861 resistant mutants of *E. coli* ATCC-25922 Δ*tolC* and wildtype.
(A) Electron microscopy images for wildtype (top), *qseB* mutant #3 (middle) and *qseC* mutant #4 (bottom). (B) Length (left), width (middle) and diameter (right) of wildtype, *qseB* mutant #3 and *qseC* mutant #4. (C) Transmission electron microscopy images for wildtype (top), *qseB* mutant #3 (middle) and *qseC* mutant #4 (bottom). Ordinary one-way ANOVA was used to analyze the results. ns, not significant; ****, $p < 0.001$; OM, outer membrane; PM periplasmic membrane.

The results from RT-PCR experiments gave first hints on *qseBC* interacting with *pmrAB* and the *mar* operon, both already linked to antibiotic resistance in the literature. However, changes in transcript levels of *pmrB* and *marR* in the cystobactamid-resistant *E. coli* mutant #3 (*qseB*, A80V) and #4 (*qseC*, P251S) mutation were not associated with cross-resistance to other antibiotic classes. Thus, the exact mechanism of resistance of cystobactamids in *E. coli* remained unclear, and we thought to study the global transcriptome changes of selected *E. coli* mutants. The transcriptomes of several *E. coli* mutants that were obtained by selecting for resistance against cystobactamids [#1 (*qseC*, P251S), #2 (*qseC*, 259In), #6 (*qseC*, 441Fs), #7 (*qseC*, V257E)] and the *qseC* P251A mutant that was generated in a targeted approach were compared to wildtype *E. coli*. In summary, the mutants had 35 upregulated and 58 downregulated genes in common (Fig. 10), and the full list of significantly up- or downregulated genes and operons can be found Table S7. Most prominently, we found the following genes or operons significantly upregulated: The *arn* and *qse* operons responsible for synthesis and translocation of 4-amino-4-deoxy-L-arabinose (L-Ara4N) onto lipid A [163] and quorum-sensing, respectively [157]; *waaH* (implicated in incorporation of glucuronic acid to the LPS [164]), *ygiW* (implicated in stress response, co-transcribed with *qseBC* [165]), *eptA* and *cptA* (connected to the addition of phosphoethanolamine (pEtN) to lipid A and the core region of LPS, respectively [166]), and *ygiS* (implicated in stress response [167]). The most significantly downregulated genes or operons included the *flg*, *fli* and *flh* operons, responsible for flagellar assembly [168], and the genes *motB* (flagellar assembly [168]), *yhjB* (putative response regulator [169]), and *yrbL* (Pho-regulatory network protein [170]). Based on the described functions of the upregulated genes, we concluded that cystobactamid resistance is

likely caused by specific LPS modifications in a manner similar to colistin resistance (Fig. 11-12). The downregulation of genes related to motility and virulence in *E. coli*, is fully in accordance with literature-described [171-173] QseBC functions and our findings from *in vitro* motility and biofilm assessments.
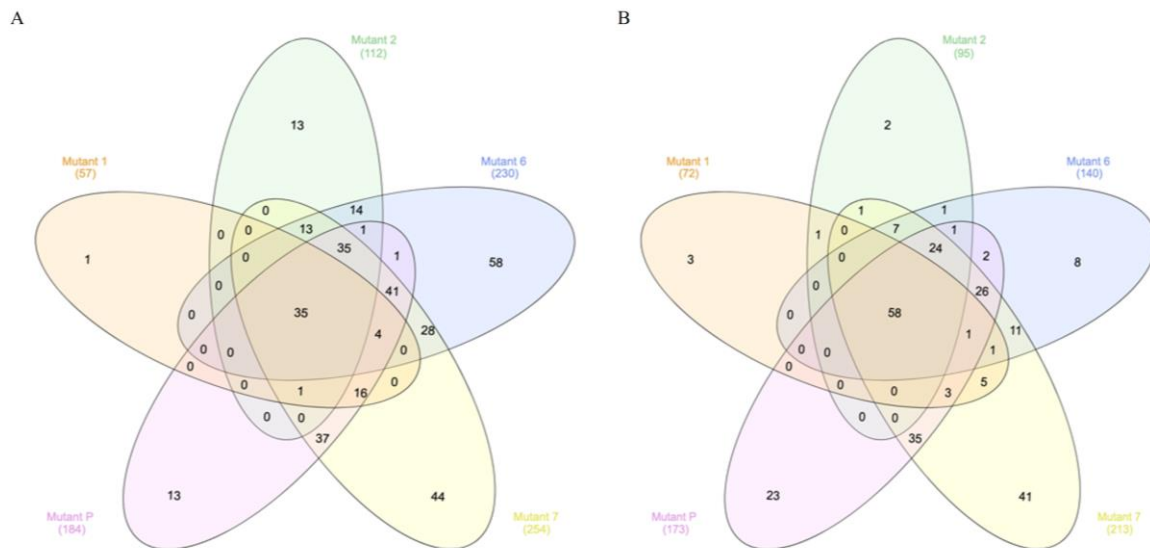
Fig. 10. Venn diagram of upregulated and downregulated genes.
(A) Upregulated genes, FC > 2. (B) Downregulated genes, FC < 0.5. Adjusted p-value < 0.05.
mutant 1: *qseC* (P251S); mutant 2: *qseC* (259In); mutant 6: *qseC* (441Fs); mutant 7: *qsec* (V257E); mutant P: *qseC* (P251A). Mutants 1, 2, 6, and 7 were obtained during spontaneous resistance development, mutant P was achieved using seamless mutagenesis. In, insertion; Fs, frameshift.
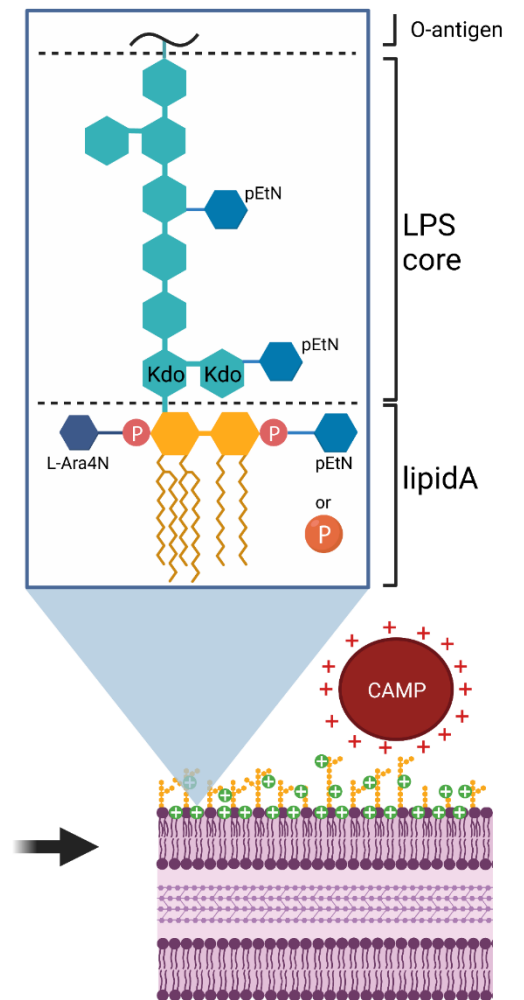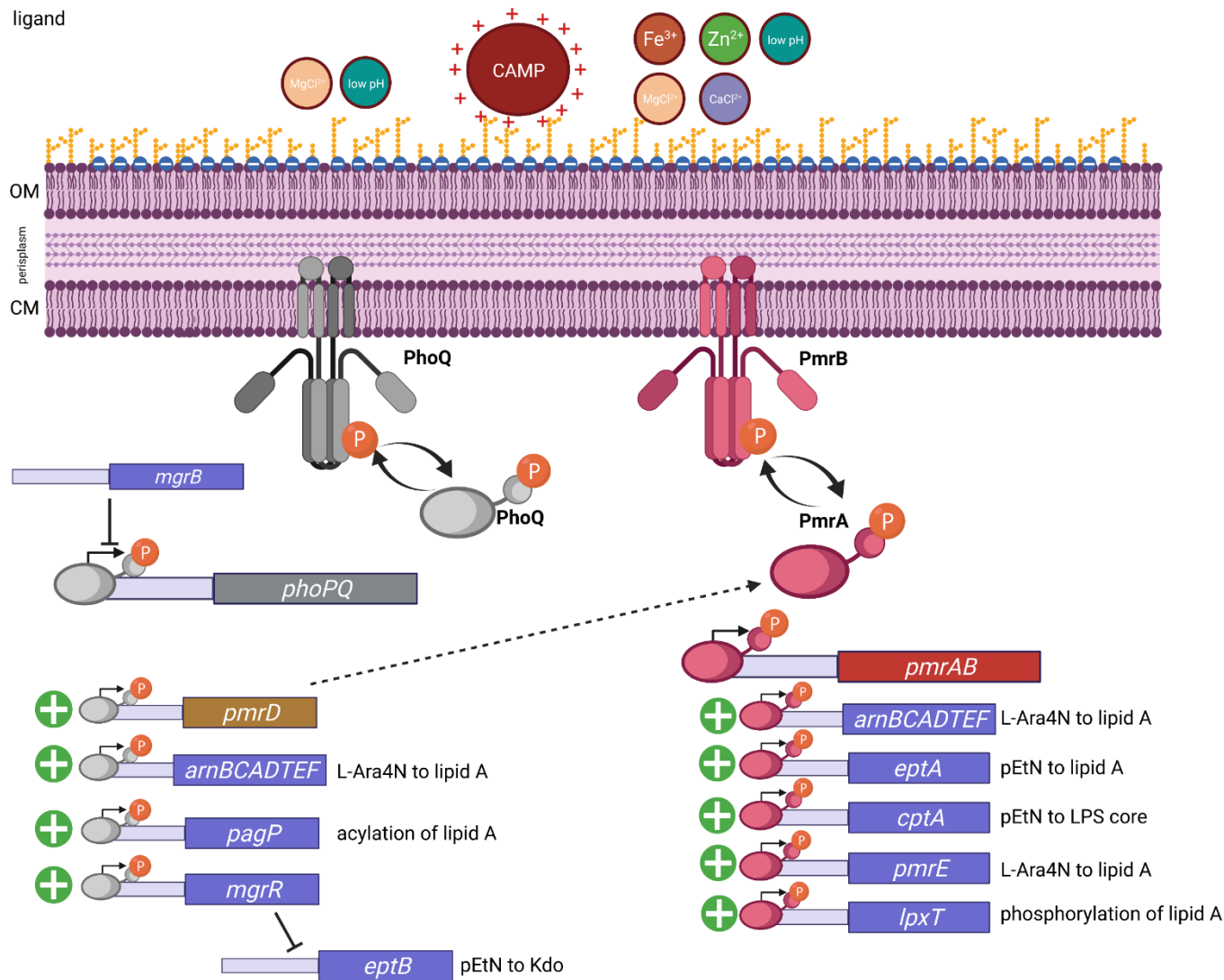
Fig. 11. Chromosomally encoded colistin mode of resistance in *E. coli* (schematic representation).
Upon signal recognition (ligand) by sensor kinase PhoP and PmrB, both undergo autophosphorylation, and transfer the phosphoryl group to their respective cognate response regulators PhoQ and PmrA. Activated PhoP positively regulates its own trancription, and transcription of *pmrD* (binds to PmrA and keeps it in the activated state), *arn* operon (encodes proteins responsible for synthesis and addition of L-Ara4N to lipid A), *pagP* (acylation of lipid A), and *mgrR* that acts as a repressor of *eptB* (addition of pEtN to 3-deoxy-D-*manno*-oct-2-ulosonic acid (Kdo) units of the LPS core). MgrB acts as a repressor of *phoPQ* transcription. Similarly, activated PmrA acts as an activator of *arn* operon, *eptA* and *pmrE* (addition of pEtN to lipid A), *cptA* (addition of pEtN to LPS core), and *lptX* (phosphorylation of lipid A) genes. Addition of L-Ara4N and pEtN to LPS results in increased positive net charge of the OM and decreased affinity of colistin for OM, thus resulting in resistance to colistin.
Created with BioRender.com.
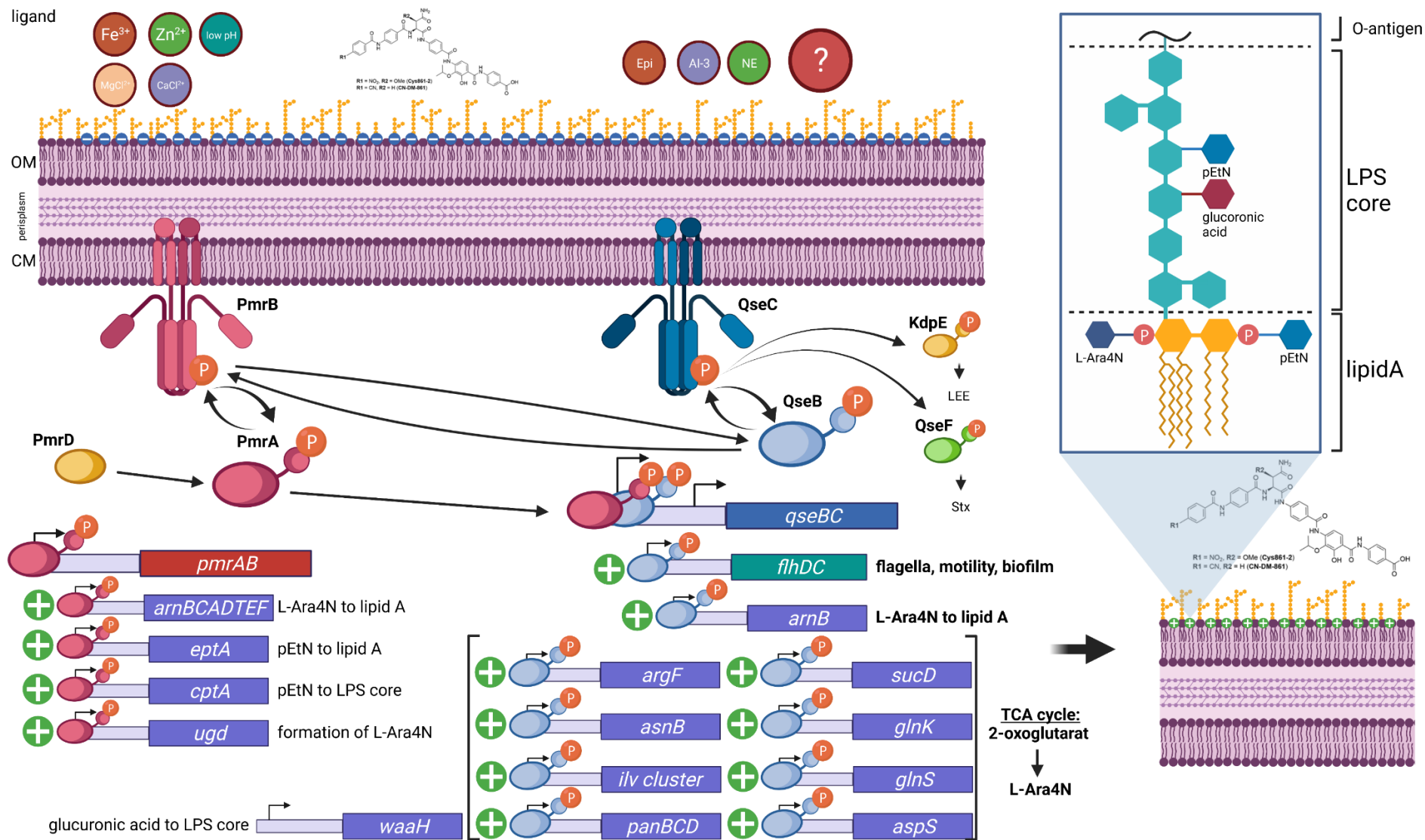
Fig. 12. Cystobactamid mode of resistance in *E. coli* (schematic representation).
Upon signal recognition, histidine kinase PmrB autophosphorylates and in turn activates both its cognate response regulator PmrA, and its non-cognate response regulator QseB, thereby activating the transcription of genes under their control. In cystobactamid-resistant mutants, activated PmrA binds to promoter regions of *eptA*, *cptA* and *arn* operon, resulting in addition of pEtN to lipid A and LPS core, and addition of L-Ara4N to lipid A, respectively. QseB is activated by its cognate histidine kinase QseC in response to environmental signals. Activated QseB positively regulates expression of *qseBC* and *flhDC* operon, master regulator of flagella, motility and biofilm. Undecaprenyl-glucuronic acid (*ugd* gene, under control of PmrA) serves as a starter unit for *arn* operon to form L-Ara4N in a 2-oxoglutarate-dependent manner, a tricarboxylic acid cycle (TCA) metabolite; QseB binds to *arnB* promoter and activates its transcription. ArnB is responsible for transamination of undecaprenyl-4-keto-pyranose to L-Ara4N. Consumption of 2-oxoglutarate leads to formation of glutamate. Glutamate in turn is shuffled back into the TCA cycle via acetyl coenzyme A (Co-A), succinate and fumarate intermediates, regulated by *argF*, *asnB*, *ilv* cluster, *panBCD*, *sucD*, *glnK*, *glnS*, and genes, to offset the loss of 2-oxoglutarate consumed for LPS modifications. QseB binds to promoter regions of these genes and activates their transcription. Furthermore, not only can PmrB phosphorylate QseB and initiate the regulatory cascade, but phosphorylated PmrA can bind to the *qseBC* promoter and activate its transcription, resulting in PmrAB-QseBC cross-talk that upregulates transcription of genes under QseB control. *waaH* gene is not under control of either PmrAB or QseBC TCS, but was found significantly upregulated in cystobactamid-resistant mutants, and is responsible for addition of glucuronic acid to LPS core. QseC can also phosphorylate non-cognate response regulators KdpE and QseF; KdpE regulates the transcripton of the locus of enterocyte effacement (LEE) and formation of attaching and effacing (AE) lesions and type three secretion system (T3SS) and QseF regulates transcription and expression of Shiga toxin (Stx). Created with BioRender.com.

2.4.9 Lipid A is modified in *qseC* (P251S) mutant

The *arn* operon is responsible for the synthesis, translocation and addition of L-Ara4N onto phosphate groups of lipid A. [174, 175]. The *arn* operon was highly upregulated in all studied cystobactamid-resistant *E. coli* mutants carrying *qseC* mutations. Thus, we compared isolated lipid A from sensitive wildtype *E. coli* ATCC-25922 Δ*tolC* to lipid A from *E. coli* ATCC-25922 Δ*tolC* CN-DM-861[R] #3 (*qseB*, A80V) and #4 (*qseC*, P251S) (Fig. 13). Following isolation of lipid A from these strains and analysis by MALDI-TOF/TOF we could indeed confirm the presence of modified lipid A in *qseC* mutant #4, but not in *qseB* mutant #3. The *qseC* mutant #4 had two different and modified species present in the outer membrane: lipid A with addition of one L-Ara4N moiety and lipid A with addition of two L-Ara4N moieties.

2.5 Discussion

The most successful antibiotics target vital cellular functions, among others DNA replication [176]. Quinolones are to date the most successful topoisomerase inhibitors [142], however, due to their toxicity issues [177] and global rise of AMR, other non-quinolone scaffolds, such as novobiocin [178], cyclothialidine [179, 180], gepotidacin [181], and zoliflodacin [182], with novel chemical scaffolds, and novel mode of action and/or resistance are gaining importance [142]. In this study, we present a comprehensive evaluation of novel topoisomerase type IIa inhibitors, cystobactamids. Extensive microbiological evaluation of cystobactamids revealed potent antibacterial activity against important ESKAPE pathogens. Similar to zoliflodacin [182] and gepotidacin [181], both novel bacterial topoisomerase inhibitors (NBTI), cystobactamids displayed broad-spectrum activity and importantly their activity against Gram-positive pathogens is even superior to that of the clinically used and highly potent drug ciprofloxacin. In particular, MICs of cystobactamids on *S. aureus* and vancomycin-resistant *Enterococcus* spp. (VRE) were throughout low, whereas VRE isolates were completely resistant to ciprofloxacin. However, the activity of cystobactamids against *K. pneumoniae* and *P. aeruginosa* was moderate. We then focused our study on *E. coli* and other important uropathogens. The activity of cystobactamids against *E. coli* was excellent and we only found *Proteus* spp. as a gap in the antibacterial spectrum. The tested strains included MDR strains, namely ESBL-producing, carbapenem-resistant *K. pneumoniae*, carbapenem-resistant *Enterobacter* spp., and ESBL/SSBL, carbapenem- and colistin-resistant *E. coli*. Furthermore, we could further confirm that cystobactamids display superior activity against recent clinical isolates of *E. coli*, including strains resistant to third-generation cephalosporins, ciprofloxacin,

ampicillin, and trimethroprim-sulfamethoxazole. The novel topoisomerase inhibitors also retained their activity in artificial urine and at various physiologically relevant pH values. We could also show that cystobactamids act very rapidly through a bactericidal mechanism. Taken together, cystobactamids are promising new candidates for the development of drugs for the treatment of UTI.

Due to their common targets, we carefully evaluated potential cross-resistance of cystobactamids with FQs and albicidin. We only detected minimal co-/cross-resistance for the natural product cystobactamid Cys861-2 with FQs. Encouragingly, the optimized synthetic CN-DM-861 did not show FQ cross-resistance. Cystobactamids like fluoroquinolones are subjected to expulsion from bacterial cells by efflux pumps, however, it was shown that antibiotic scaffold derivatization can overcome this issue [183, 184]. Cystobactamid derivatization also decreased the effect of efflux and increased the overall antibacterial potency. Despite the lack of cross-resistance in FQ-resistant *E. coli* mutant strains, we could also demonstrate that cystobactamids also inhibit gyrase supercoiling activity using mutant enzymes. Whereas ciprofloxacin was inactive on a GyrA S83L mutant enzyme and less effective against a GyrB D426N mutant enzyme, cystobactamids remained highly active with a minimally reduced inhibitory potential compared to IC_{50} values on the wildtype *E. coli* gyrase, indicating a possible partial overlap of binding sites of FQs and cystobactamids, and also arguing for a slightly different mode of action than that of FQ. Importantly, cystobactamids remain active on ciprofloxacin-resistant strains regardless of the type of resistance (*qnr* proteins, target mutations, efflux).

Another possible resistance mechanisms was impaired uptake through specific importers, such as OmpF and OmpC porins in *E. coli* [185, 186] for fluoroquinolones, and Tsx for albicidin [146, 147]. However, we could exclude Tsx, as described for albicidin, and we could also exclude major porins to be responsible for the uptake of cystobactamids into *E. coli*. In conclusion, we excluded albicidin and FQ-related modes of resistance as a cause for resistance

development in *E. coli* against cystobactamids. Thus, cystobactamids present a novel resistance-breaking compound family with a unique chemical structure and superior antimicrobial activity. In order to forward cystobactamids as potential leads for the treatment of UTIs into (pre-)clinical phases, extensive absorption, distribution, metabolism, excretion and toxicity (ADMET) and pharmacokinetic/pharmacodynamics (PK/PD) profiling is required and currently on its way. Nevertheless, based on their biological activity profile cystobactamids appear to be excellent candidates for antibiotic development.

To understand how resistance towards cystobactamids develops, we performed *in vitro* resistance development experiments with several *E. coli* strains. The obtained mutants developed at a low frequency (10^{-8}-10^{-10}), which was comparable to ciprofloxacin (10^{-9}-10^{-10}). FQ [91, 93, 187] and NBTI [188] resistance is mostly caused by target mutations. Surprisingly, we found, almost exclusively, mutations in a quorum-sensing QseBC two-component system evolving in parallel to cystobactamid resistance. However and interestingly, the mutations observed did not lead to a phenotype equivalent to *qseBC* deletions, which were found susceptible to cystobactamid. Only the point mutations observed or introduced which result in single amino acid substations were shown to be responsible for cystobactamid resistance. Observed MIC discrepancy between *qseB*, *qseC* deletion strains and point mutants is puzzling. No observed MIC changes in *qseB* and *qseC* deletion background are, however, in line with results obtained by Li and co-workers, where deletion of *qseBC* in an *E. coli* strain isolated from a dairy cow with mastitis, resulted in no observed change in MIC of ciprofloxacin, gentamicin, penicillin, ofloxacin, kanamycin, oxacillin, neomycin, tetracycline and sulfamethoxazole [161]. There is no literature data available on effects of point mutations present in DHp and catalytic domain of QseC and regulatory domain of QseB on the MIC of antimicrobials. However, numerous point mutations present in these domains have been described for both PmrAB and PhoPQ TCS for several Gram-negative species, and resulted in

significant MIC shift and clinical resistance and cross-resistance [189-194], which is partially in contrast with our findings. Obtained cystobactamids-resistant mutants displayed a relatively high MIC shift compared to the corresponding parent strains; however, they remained sensitive to cystobactamids with MIC in the sub- to low µg/mL range and displayed no co-/cross-resistance to clinically relevant antibiotic classes. All described mutations in *E. coli* PmrAB and PhoPQ are gain-in-function mutations leading to increased antimicrobial resistance to several antibiotics, namely CAMP [189, 190, 192, 194]. Sequencing of resistant mutants obtained in this study, revealed numerous single nucleotide polymorphisms, predominantly in the *qseC* gene with only a few mutants carrying mutations in *qseB* gene. Within QseC, we found two mutational hotspots. First, within the histidine kinase domain, responsible for dimerization and autophosphorylation of QseC, and phosphorylation/dephosphorylation of QseB. Mutations in the histidine kinase domain, namely P251S, 259In and V257E, are situated very close to a conserved H246 residue responsible for phosphotransfer [195]. Replacement of proline with serine, and valine with glutamic acid might prevent dimerization of QseC needed for autoactivation [196]. We hypothesized that the observed mutations probably decrease the autokinase, and kinase and/or phosphatase activity of QseC, if not completely abolish it. The most prominent mutation we observed was exchange of prolin to other amino acids (serine or alanine) at position 251 in QseC. This residue is adjacent to conserved H246 residue crucial for its kinase activity. Exchange of H246 for alanine, leucine, and aspartate revealed that QseC could only dephosphorylate QseB in presence of H246 [195]. Therefore, we exchanged a proline to alanine on position 251 in a clean genetic background and we observed the same level of resistance towards cystobactamids as that of mutants obtained during resistance development. These experiments indicated that QseB and QseC need to be present, activated and that their role in cystobactamid resistance is probably linked to complex regulatory processes. Furthermore, we complemented several *qseC* mutants with a wildtype copy of *qseC* under control of a truncated native promoter. Complementation only had an effect in *E. coli*

DSM-1116 resistant mutants harboring numerous mutations in their genome, including *qseC* mutations. Contrarily, complementation of a resistant *E. coli* ATCC-25922 Δ*tolC* mutant only carrying a *qseC* mutation had no effect, leading us to believe that some genes mutated in *E. coli* DSM-1116 background could be controlled by QseBC or complementation with a high copy plasmid, and/or stronger promoter, or full length native promoter would successfully complement the *qseC* SNP mutant. The second mutational hotspot was the ATP-binding domain, where the terminal phosphate in ATP is transferred to the histidine residue leading to autophosphorylation [197]. This indicates that the observed frameshift mutation at position 441, at the very end of ATPase-binding domain, possibly results in impaired autokinase function. Only two mutations were observed in *qseB*, G15C and A80V. Both are close to a conserved D51 residue, which is the receiver of a phosphoryl group from QseC and PmrB [160, 195, 198], leading us to conclude that either phosphorylation and/or dephosphorylation of QseB by QseC and/or PmrB was hindered. Positions of point mutations could also explain the MIC discrepancy between *qseB* and *qseC* deletion mutants and point mutations in comparison to their respective wildtype and the observed mutant phenotypes. We therefore speculate that point mutations present in QseBC will have a similar activating effect on genes under the control of QseBC. With the exception of MIC, the obtained cystobactamid-resistant mutants displayed similar phenotypic characteristics as literature described *qseB* and *qseC* deletion mutants, exhibiting decreased *in vitro* virulence (biofilm, motility) [157, 160, 171], change (increase) in bacterial cell dimensions [162] that was more pronounced for *qseC* mutants than *qseB* mutant, and no fitness loss [190]. This was further supported by IMC enabling detection of differing metabolic profiles of mutant strains versus wildtype. We were able to link those differences to the genotype of mutants. We linked the QseC P251S mutation to low metabolic activity during mid- to late exponential phase that was maintained for a long period before it slowly tapered off. A very sudden and intense metabolic burst in the stationary phase was linked to *qseC* 441Fs

mutation and the QseB A80V mutant displayed an almost identical heat flow profile as the wildtype.

The QseBC regulatory network has been studied and it has been shown to be involved in resistance mainly towards cationic antibiotics, where cross-talk between PmrAB and QseBC mediates regulation of expression of genes involved in LPS modification and resistance to CAMP [157, 160, 171, 195, 198, 199]. Resistance to colistin is conferred by chromosomally encoded determinants responsible for limiting the uptake of colistin by modifying lipid A (L-Ara4N [90], and pEtN encoding genes [200]), efflux of colistin (KpnEF [201], AcrAB, Sap proteins [202]) or inactivation (colistinase [203]). In 2011 mobile, plasmid-mediated resistance to colistin emerged [202, 204]. To date 9 *mcr* gene variants (pEtN transferase) have been reported [205], with *mcr-1* and *mcr-3* being the most frequent [202]. Furthermore, first plasmid conferring resistance to colistin encoding a pEtN transferase (*mcr-9* gene) together with *qseBC*, was recently isolated from *E. coli* [206] and XDR, NDM-1-producing *Klebsiella quasipneumoniae* [207]. Kieffer and co-workers and Faccone and co-workers showed that *mcr-9* on its own resulted in reduced susceptibility to colistin, but not in colistin resistance. Subinhibitory concentrations of colistin led to expression of *mcr-9*, and inducible expression of *mcr-9* was linked to *qseB* and *qseC*, situated directly downstream of *mcr-9*. Only in presence of QseBC together with *mcr-9* strains obtained resistance against colistin. [206, 207]. To the best of our knowledge, cystobactamids are the only antibiotic compounds to date to elicit mutations in QseBC, and directly implicate QseBC in resistance towards antibiotics.

To better understand the role of PmrAB-QseBC cross-talk and help elucidate the mode of resistance of cystobactamids in *E. coli*, we performed transcriptomic experiments and compared several *qseC* mutants (P251S, 259In, V257E, and 441Fs) to wildtype *E. coli*. All displayed significantly upregulated *arn* and *qse* operons, *ygiW*, *waaH*, *cptA* and *eptA* genes. Additionally, using RT-qpCR we showed in both mutant types, A80V *qseB* mutant and P251S *qseC* mutant,

71

only *qseB* and *qseC* were significantly upregulated, but not *pmrA*, *pmrB*, *pmrD*. Upregulation of the *qseBC* operon could be due to loss of phosphatase activity of QseC mutants or signal-mediated activation of QseC, ending in increased amounts of phosphorylated QseB, which in turn binds to its own promotor, and activates the transcription. Secondly, PmrA can bind to QseBC promoter and induce its transcription [199]. Since we did not observe an increase of *pmrA* and *pmrB* transcripts in our RT-qPCR experiments, we concluded that PmrAB-mediated activation of QseB is not occurring. However, transcriptomics result showed that all *qseC* mutants had 2-6-fold increase in *pmrA* transcript levels. This discrepancy could be due to the methodology used, experimental differences and analysis of results, as the observed fold changes are not directly comparable. To further confirm this, we compared the levels of *qseB* and *qseC* transcript, in our cystobactamid-resistant *qseC* mutants, obtained with RT-qPCR and transcriptomics. We could show that using RT-qPCR we observed approx. 70- and 65-fold upregulation of *qseB* and *qseC*, respectively, whereas transcriptomics analysis revealed approx. 122- and 18-fold upregulation, respectively. Synthesis and addition of 4-amino-4-deoxy-L-arabinose to phosphate group of lipid A is encoded by the *arn* operon [174], and addition of phosphoethanolamine on lipid A and inner core of LPS is encoded by *eptA* and *cptA* [166, 208], respectively, both under regulation of PmrA. Lastly, the *waaH* gene is responsible for the incorporation of glucuronic acid to the third heptose of the inner core oligosaccharide of the LPS [209]. In turn, cystobactamid-resistance is mediated through LPS modifications, in particular, lipid A carrying additional L-Ara4N and pEtN moieties, and pEtN addition and glucuronation of inner core oligosaccharides. These modifications of LPS would lead to an increased net positive charge of the outer membrane resulting in repelling forces, as was shown for colistin [90, 202, 210]. The significantly up-regulated *ygiW* gene is co-transcribed with *qseB*, and it was found to be a stress reducing protein in *E. coli*, protecting bacterial cells against hydrogen peroxide, cadmium and acid stress [165], in our case it most probably protects the bacterial cells against cystobactamids´ antibiotic effect. QseC SNP mutants exhibit decreased

in vitro virulence, confirmed by transcriptomics results where *flg*, *fli*, *flh* operons involved in flagellar assembly and biofilm formation, were found to be significantly downregulated. Additionally *yhjH* and *yrbL* genes were also significantly downregulated. The YhyH protein is controlled by FlhDC/FliA and plays a role in curli expression. Pesavento and co-workers showed that absence of YhyH in *E. coli* abolished motility [211] resulting in decreased virulence. YrbL, a protein under control of PhoPQ, SocSR, and PmrAB, with unknown function, was shown to be involved in n-butanol tolerance [170, 212]. Since the role of YrbL is currently unknown, it is difficult to predict how exactly it protects the bacterial cells against cystobactamids. However, since transcription of *yrbL* is under the control of TCSs involved with OM modifications, we presume it helps with stabilization of the outer layer of the OM or is involved in increasing the positive charge of LPS. Contrary to our transcriptomics results, where point mutations in QseC lead to upregulation of genes directly involved in LPS modification and are under the transcriptional regulation of both PmrAB and QseBC, Hadjifrangiskou and co-workers reported that microarray analyses of *qseC* deletion mutants in *E. coli* revealed several virulence genes to be dysregulated, including genes responsible for the formation of type 1 and S pili. However, the majority of genes with altered expression were part of metabolism, membrane transport, stress response, DNA and RNA processing [158]. Additionally, Hurst and co-workers reported that *qseB* deletion mutant in *E. coli* had significantly upregulated genes involved in upregulating three anaplerotic pathways that feed acetyl Co-A, succinate and fumarate into the TCA cycle to supply enough 2-oxoglutarate needed for lipid A modifications [213]. Observed differences between our transcriptomics study and the studies performed by Hadjifrangiskou and co-workers, and Hurst and co-workers could explain the role of point mutations in QseBC and cystobactamid resistance.

We were also interested in whether exposure of wildtype *E. coli* to cystobactamid would affect the transcription levels of *qseB, qseC*, *pmrA*, *pmrB*, *pmrD*. Addition of sub-MIC amounts of

cystobactamid did not affect the gene transcription levels significantly in wildtype, which indicates that cystobactamid is not directly recognized as a signal for either QseBC or PmrAB two-component systems (TCS). However, this could be because we might not have reached the threshold concentration needed to activate/repress the TCS. It was recently reported that QseBC decreased antibiotic susceptibility in *E. coli* by upregulating multidrug efflux pump associated genes, namely *marA* [161]. Additionally, the *mar* locus was identified as a determinant contributing to resistance to all major antibiotic classes, not only quinolones but also tetracyclines and β-lactams [214]. We did not observe significant up- or downregulation or either *marA* or its repressor gene *marR* in wildtype *E. coli* exposed to cystobactamid or in *qseB* and *qseC* cystobactamid-resistant mutants. In addition, MIC values determined for ciprofloxacin, colistin, cefotaxime, gentamicin, tobramycin and tetracycline did not differ significantly between the two mutants and the wildtype.

We were able to confirm the presence of modified lipid A species in *qseC* mutants but not in *qseB* mutants, thus concluding that passive transport of cystobactamids through the outer membrane is hindered. The compounds may get trapped because of the increased positive charge. Assessment of various cystobactamid derivatives with different substitution patterns and functional groups, will help to elucidate how lipid A modifications confer resistance to cystobactamids, especially since the phenol at ring D and the terminal carboxylic acid would be negatively charged at physiological pH. However, cystobactamids are highly lipophilic and can probably overcome the charged nature of the lipid bilayer. Furthermore, cystobactamids have very few rotatable bonds making them very rigid. It is possible that their rigidity enables penetration of the OM and charge plays a secondary role. Additionally, determining the amount of cystobactamids in the cytosol of sensitive and lipid A-modified resistant *E. coli* mutants, will help us to confirm that cystobactamid resistance indeed relies on hindered cellular uptake through outer membrane modifications.

In summary, cystobactamids represent a new chemical scaffold with potent broad-spectrum antibacterial activity, including excellent activity against MDR strains. Interestingly, their mode of resistance in *E. coli* does not rely on already described mechanisms and cystobactamids do not show cross-resistance with other antibiotic classes. To the best of our knowledge, cystobactamids are the first antibiotics for which resistance is mediated through mutations in the QseBC two-component regulatory system of *E. coli*. To date, little is known about the role of point mutations within this system and their effect on autophosphorylation and kinase/phosphatase activity of QseC and QseB. In addition, the effect on cross-talk with PmrAB will need to be investigated in more detail. However, we were able to elucidate a decisive part of the mode-of-resistance of cystobactamids in *E. coli*, where mutations in QseBC trigger a cascade of events ultimately leading to LPS modifications likely to reduce compound uptake.

2.5 Materials and Methods

2.5.1 MIC and MBC determination

MIC values were determined using broth microdilution method, with colony suspension method as previously described [215]. MBC was determined as previously described [216]. For determination of MIC and MBC in artificial urine, medium was substituted with artificial urine. Artificial urine was prepared as previously described [217].

2.5.2 Antibacterial susceptibility testing using disc diffusion method

Antibiotic discs were purchased from Becton, Dickinson and Co. (Franklin Lakes, USA). Assay was performed following manufacturer´s protocol.

2.5.3 Time-kill kinetics

Assay was performed in caMHB. Compounds were dissolved in DMSO to achieve a 100 times stock concentrations. Final concentration of DMSO in assay did not exceed 1%. Tested concentrations equaled 1x MIC, 2x MIC, 4x MIC and 8x MIC. Control sample was run in caMHB in presence of 1% DMSO. Starting bacterial count equaled 1×10^6 CFU/mL. Samples were run in triplicates. In short, overnight culture was diluted 1:10 in fresh broth to determine OD_{600}. This value was used to calculate the amount of overnight culture needed to achieve the starting bacterial count. Compounds or pure DMSO were added to appropriate test tubes to achieve desired final concentrations. Samples were placed on a shaking incubator at 37 °C and 180 rpm, and sampling occurred at 0, 2, 4, 6, 8 and 24 hours. After sampling serial dilutions in 96-well plate were performed, followed by Miles and Misra total viable count where we plated 20 µL spots of dilutions on CASO agar plates. Plates were left to dry in the sterile bench before they were transferred to a 37 °C static incubator. Colonies on plates were counted after 18 hours of incubation.

2.5.4 Cystobactamid sensitivity of *E. coli* porin mutants

Assay was performed as previously described [218].

2.5.5 Supercoiling assay

All *E. coli* DNA Gyrases were purchased from Inspiralis, Norwick, UK. Assays were performed as previously described [103] with one modification. Final DMSO concentration was 1% not 5%.

2.5.6 *In vitro* resistance development

Strain glycerol stock was streaked out on a CASO agar plate and incubated overnight in a static incubator at 37 °C. Following day, a single colony was picked up and used to inoculate fresh Mueller-Hinton broth (MHB). Liquid culture was incubated at 37 °C at 180 rpm for approximately 16-18 hours. OD_{600} of overnight culture was determined and used to calculate the volume of culture needed to plate 5 x 10^9 CFU/plate. Bacterial load was confluently spread over the surface of the agar plate until it was completely soaked in. Plates were incubated in a static incubator for 24 hours at 37 °C. Frequency of resistance was determined at four times and eight times the MIC value. Total viable count was determined by serial dilutions of the overnight culture and plating it on non-selective CASO agar plates. Frequency of resistance was determined as ratio between the number of bacteria growing on selective plates and the number of bacteria in the inoculum. Obtained resistant clones were assessed to determine the MIC shift.

2.5.7 Fitness cost

Glycerol stocks of sensitive wildtype strain and its resistant clones were streaked out on CASO agar plates and incubated overnight in a static incubator at 37 °C. Next, liquid overnight cultures in caMHB were prepared, without selective pressure for the resistant clones or the sensitive wildtype. Liquid cultures were incubated at 37 °C and 180 rpm for approximately 16-18 hours. Next OD_{600} was determined and adjusted to 0.01 in fresh caMHB medium (0.001 if ran in

parallel with isothermal microcalorimetry assay). Cultures were incubated at 37 °C at 180 rpm for 24 hours. Sampling of cultures occurred at predetermined time points to determine the OD_{600}.

2.5.8 Isothermal microcalorimetry

Sample preparation, assay execution and analysis was performed as previously described [219]. Strains were grown overnight in MHB at 180 rpm and 37 °C. No compound was added to assay as metabolic profiles between wildtype and mutant were being compared.

2.5.9 Reversibility of resistant phenotype

Sensitive wildtype strain and its resistant clones were streaked out on CASO agar plates and incubated overnight in a static incubator at 37 °C. The following day overnight cultures were prepared by inoculating a single colony in MHB without selective pressure. Cultures were grown overnight at 180 rpm and 37 °C. Next ten consecutive days we performed subcultivations where fresh MHB was inoculated with the previous overnight culture in a 1:10 000 ratio. At predetermined subcultivations, the cultures were used to perform MIC determination.

2.5.10 Swimming motility

Swimming potential of sensitive wildtype and resistant clones was assessed using Luria-Bertani (LB) containing 3 g/L agar and 0.5 g/L triphenyltetrazolium chloride (TTC). Overnight cultures were grown at 180 rpm and 37 °C. Next, one µL of the overnight culture was spotted in the center of the agar plate, on top of the agar. Plates were incubated in a static incubator at 37 °C for 24 hours. Diameter of the swimming zone was measured to compare swimming potential of resistant mutants compared to the wildtype.

2.5.11 Biofilm formation

Assay was performed as described elsewhere [159]. We performed a one-step assay using LB and MHB. Microtiter plates were incubated at 37 °C. Compounds, to assess effect on biofilm formation, were added at the beginning of the experiment. Compounds were solubilized in DMSO. Final DMSO concentration did not exceed 1%. Proper controls were used.

2.5.12 Seamless mutagenesis

Seamless mutagenesis imploring recombineering and *ccdB* counterselection was used to generate *E. coli* ATCC-25922 *ΔtolC* P251A mutant. Protocols and plasmids used were identical as described elsewhere [154]. PCR reactions were done using Phusion polymerase and following the manufacturer´s protocol. PCR reactions were ran on a 0.8% agarose gel, bands with correct size were excised and cleaned using Gel and PCR Clean-up kit (Macherey and Nagel). Primers used in construction of the *qseC* P251A mutant can be found in Table S8.

2.5.13 Complementation assay

To join *qseBC* high-affinity promoter together with *qseC* and ampicillin resistance gene, overlap extension PCR was used. We followed the protocol described in dx.xoi.org/10.17504/protocols.io.psndnde using a Phusion polymerase. PCR reactions were ran on a 0.8% agarose gel, bands with correct size were excised and cleaned using Gel and PCR Clean-up kit (Macherey and Nagel). Primers used in construction of pBeloBAC-P$_{qseBC}qseC$ can be found in Table S9. Final overlap PCR product had two homology regions with pBeloBAC plasmid. Homology regions were used to integrate the PCR product into the plasmid backbone using *E. coli* GBO5 with Red/ET genes encoded in genomic DNA. Protocol was as follows: overnight cultures of *E. coli* GBO5 containing pBeloBAC were grown in LB in presence of a selection marker at 30°C. Next day fresh 1.4 mL Eppendorf tubes, containing LB medium and a selection marker, were prepared and inoculated with 30 µL of the overnight culture. Cells were grown on an orbital shaker at 600 rpm until they reached OD_{600} 0.2 when 40 µL of 10 %

L-arabinose was added to induce Red/ET genes. Cells were then grown until they reached OD_{600} 0.35-0.4. Next cells were spun down in a precooled centrifuge at 15 000 rpm for 1 minute. Supernatant was decanted and bacterial pellet was resuspended in ice-cold sterile water. This step was repeated twice. In the last step a bit of supernatant was left in the Eppendorf tube and was used to resuspend the cells. Resuspended cells were kept on ice. Next, we electroporated 500 ng of PCR product into prepared *E. coli* cells at 1350 V, 10 PF and 600 Ohms, using a 1 mm cuvette. Electroporated cells were resuspended in 1 mL LB (no selection pressure present) and returned to Eppendorf tubes and incubated at 37°C for 75 minutes for recovery. Next, cells were spun down, and plated on a LB agar plate containing 100 µg/mL ampicillin. Plates were incubated 24-48 hours in a static 30°C incubator. Obtained clones were used for isolation of plasmids. Correct plasmid, checked by sequencing and restriction digest, was electroporated into desired recipient *E. coli* strains using the same cell preparation and electroporation procedures as described above. Throughout the cloning process appropriate controls were used.

2.5.14 RNA isolation and RT-qPCR

Overnight cultures were diluted 1:100 in fresh medium and incubated at 37°C and 180 rpm until they reached OD_{600} 0.5. Next, cultures that were not induced were directly subjected to RNA isolation. Induction was performed at OD_{600} 0.5 and cultures were left on the shaker until they reached OD_{600} 0.8-0.9. Exposure to CN-DM-861 was done at 0.5x MIC values. RNA isolation and cDNA synthesis was performed as described before [99]. Purity and concentration of RNA samples was determined using a Nanodrop spectrometer. Peqstar 96Q (Peqlab, Erlangen, Germany) cycler was used to assess gene expression levels. cDNA was diluted 1:10 and primer pairs in Table S10 were used. qPCR was ran in 10 µL reactions using GoTaq Master Mix (Promega, Madison, WI, USA) in triplicates. Comparative threshold cycle (ΔΔCt) method [220] was used to determine relative mRNA quantity with *ifhB* normalization.

2.5.15 Transcriptomics

RNA isolation and purification:

Overnight cultures of *E. coli* were diluted 100-fold in fresh MHB and allowed to grow to an OD_{600} of 0.5. 2 ml of each culture were taken and mixed with RNA protect according to the manufacturer's recommendations. Cells were immediately pelleted by a 10 min centrifugation at 5000 g. Biological triplicates were performed. RNA was extracted using GeneJet RNA extraction kit. DNAse treatment was performed with the dsDNAse kit according to the manufacturer's protocol. RNA concentration was measured using Qubit RNA BR assay kit, and RNA quality was evaluated using the Agilent 2100 Bioanalyzer RNA 6000 Nano Kit. RIN > 9 were obtained for all the RNA samples.

RNA library and sequencing:

A total of 250 ng of total RNA for each sample was used for the preparation of cDNA libraries. Illumina Stranded Total RNA Prep Ligation with Ribo-Zero Plus was used according to the manufacturer's instructions (Illumina, San Diego, CA, USA). The quality of the cDNA was validated using the Agilent 2100 Bioanalyzer DNA1000 kit (Agilent Technologies) and quantity was determined with the Qubit dsDNA BR Assay (ThermoFisher Scientific). Equimolar pool of RNA-Seq libraries was made to a final molarity of 2 nM, and 1.4 pM were loaded in the sequencer. Sequencing of the libraries was performed with an Illumina NextSeq 500 in single-read mode with 75 cycles, with 1% of PhiX intern control sequences.

RNASeq data analysis and differential expression analysis:

Raw sequencing data were demultiplexed and quality control was done using the Aozan tool [221]. An average of 23.4 M ± 4.8 M reads per sample was obtained, with a Q30 of 92.6%. PhiX sequences account for 1.85% of total reads, close to what was expected. Ribodepletion efficiency was assessed with FastQ Screen and was below 2% on average [222]. Reads generated from strand-specific RNA-seq experiments were aligned to the genome of *E. coli*

ATCC-25922 genome (NZ_CP009072.1) by using the software Bowtie (version 0.12.7) [223]. Reads that mapped in more than four different positions on the genome were discarded i. e. reads corresponding to rRNA. RNA-seq data were analysed as described [224] by using Rsamtools (version 1.26.2), GenomicAlignments (version 1.10.1). GenomicFeatures (version 1.26.4) and DESeq2 (version 1.14.1) and SARTools [225] in R 3.3.1. Only adjusted p-values were used and were obtained using the Benjamini-Hochberg correction for false discovery rate [226]. Read count data were visually assessed using the Artemis genome viewer [227]. Venn diagrams were drawn using InteractiVenn [228].

2.5.16 Electron microscopy

Overnight cultures of wildtype and resistant clones was back-diluted 100-fold in fresh MHB and grown at 37 °C and 180 rpm until it reached OD_{600} 0.6. Next, glutaraldehyde solution Grade I, 25% in H2O (Sigma Aldrich), specially purified for use as an electron microscopy was added to a final concentration of 3%.

For scanning electron microscopy (SEM) sample preparation, the cells were washed twice in TE buffer (20 mM TRIS, 1 mM EDTA, and pH 6.9) and incubated on a round, Poly-L-Lysine pretreated coverslip for 10 minutes at room temperature. Afterwards, the coverslips were transferred to TE buffer including 1% glutaraldehyde, incubated for 10 minutes at room temperature, and washed twice in TE buffer. The samples were dehydrated on ice with a graded series of acetone (10%, 30%, 50%, 70%, and 90%) for 10 min each, followed by two steps in 100% acetone at room temperature before critical-point drying with liquid CO2 in a CPD300 (Leica). The coverslips were mounted onto aluminum stubs with carbon adhesive discs and covered with a gold palladium film by sputter coating for 55 seconds at 45 mA with a SCD 500 (Bal-Tec). Examination was performed with the field emission scanning electron microscope Merlin (Zeiss) using the Everhart Thornley HESE2 detector and the inlens SE detector in a 25:75 ratio with an acceleration voltage of 5 kV.

For transmission electron microscopy (TEM), the samples were washed twice with EM Hepes buffer (0.1 M HEPES, 0.09 M sucrose, 10 mM CaCl2, 10 mM MgCl2, and pH 6.9) before treatment with 1% OSO4 for 1 hour at room temperature. Afterwards, the samples were washed twice with EM Hepes buffer and the pellets resupended in 2% noble agar before dehydration with ethanol (10%, 30%, 50%, 70%, 90%, 2*100%) for 30 minutes each and embedding in LR White (LRW) in a stepwise manner (EtOH:LRW -> 1:1 (14 h); 1:2 (24 h); 2x 100% LRW (24 h)). After addition of the starter, samples polymerized at 50° C for 2 days. Ultrathin sections of approx. 80 nm were generated with an UltracutS Ultramicrotome (Reichert / Leica) and post-treated with 4% uranylacetate for 3 minutes to increase contrast. Examination was performed with a TEM 910 (Zeiss) at 80 kV and with various magnifications.

2.5.17 Isolation and chemical characterization of Lipid A

Isolation of lipid A was done as previously described [229].

Matrix-Assisted Laser Desorption Ionization Time-of-flight/Time-of-flight Mass Spectrometry (MALDI-TOF/TOF MS): The isolated lipid A samples were prepared as described above. The lyophilized samples were reconstituted using a chloroform:methanol 4:1 (v/v) mixture with a target concentration of 5 mg/mL. Before use, each sample was centrifuged (15 000 g, 10 min) to exclude precipitates. For matrix preparation, saturated 6-aza-2-thiothymine solution (Thermo Fisher Scientific) in 50% acetonitrile was mixed with saturated aqueous tribasic ammonium citrate solution (20:1, v/v). For deposition, 2 µL of sample was mixed with 2 µL of ATT matrix in an Eppendorf head. Afterwards, 0.5 µL of this mixture was spotted on the MALDI-plate and allowed to crystallize. Calibrant mixture was added near to the sample spots. Potential structure modifications of lipid A was analysed by using UltraFlex (Bruker Daltonic GmbH, Bremen) MALDI-TOF/TOF mass spectrometer with felxControl software (version 3.4). MS data were received using negative reflection mode with settings as follows; mass range: 1000-2500 m/z,

shots: 4000, frequency: 200 Hz, laser intensity: 90%. The data were analyzed using flexAnalysis (version 3.4).

2.5.18 Whole genome sequencing

Total DNA of selected resistant clones and wildtype control samples were subjected to whole-genome sequencing on Illumina MiSeq platform at the Helmholtz Centre for Infection Research (Braunschweig, Germany). Libraries were constructed according to paired-end protocol and subsequently sequenced to a total read length of 2 x 300bp. Samples yielded 0.54-0.97 Gbp of data, which resulted in an estimated 110x-198x mean genome coverage. The raw data was then mapped to a reference sequence of *E. coli* DSM-1116, GenBank accession number NC_017635. Geneious version 8.1.5 with default settings was used for reference-guided sequence assembly, subsequent variant calling and data analysis.

2.5.19 Acknowledgments

2.6 Supporting Information

A

B
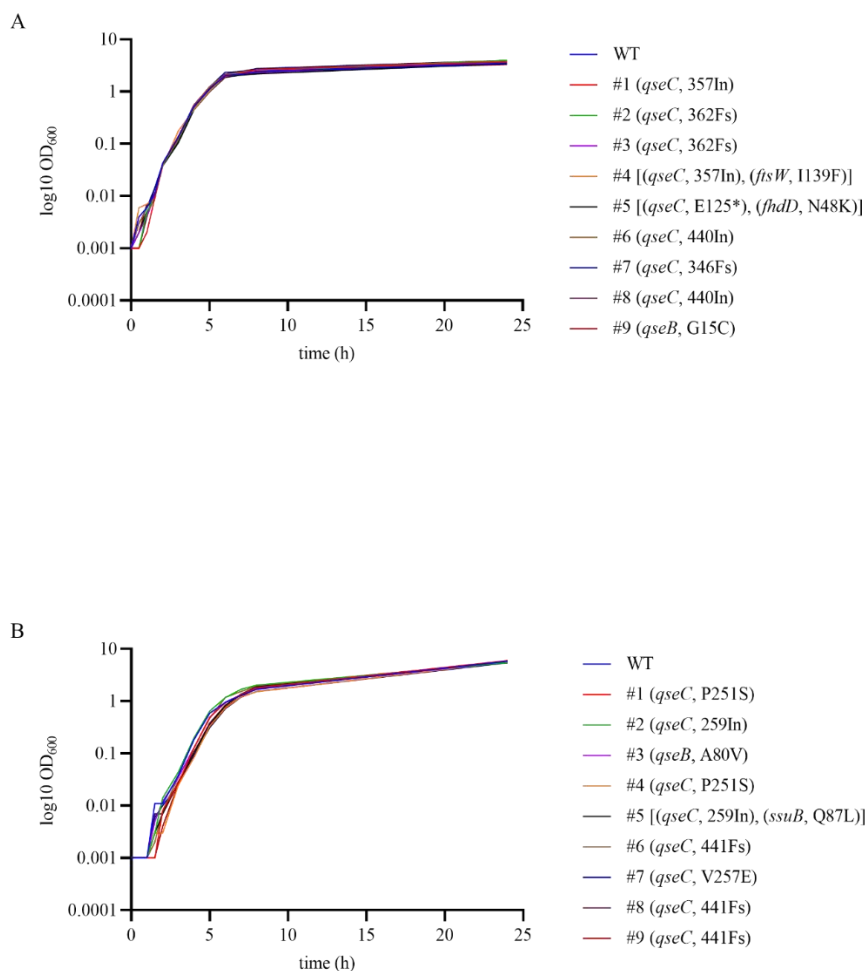
S1 Fig. Growth curves for *E. coli* CN-DM-861 resistant mutants.
(A) E. coli AG100/K12. (B) E. coli ATCC-25922 ΔtolC.
WT, wildtype; Fs, frameshift; In, insertion; *, STOP codon.

S1 Table. MIC values for Cys861-2, CN-DM-861 and cefoxitin determined on *E. coli* lacking one or more porins.

E. coli	MIC [µg/mL]		
	Cys861-2	CN-DM-861	cefoxitin
WT	0.25	0.125	8
ΔompF	0.25	0.0625	16
ΔompC	0.25	0.0625	8
ΔompA	0.25	0.0312	4

Δ*ompF* Δ*ompC*	0.25	0.0156	64
Δ*ompF* Δ*ompA*	0.25	0.0312	8
Δ*ompC* Δ*ompA*	0.125	0.0312	4
ΔEFCNBYA	0.25	0.0312	64

WT, wildtype.

S2 Table. WGS results of *E. coli* DSM-1116 clones resistant to Cys861-2 and CIP.

Locus	Description	WT		Cys861-2^R					CIP^R				
		1	2	1	2	3	4	5	1	2	3	4	5
ECW_RS00500 (Protein translocase subunit SecA)	AA residue #811 Phe -> Leu				X								
ECW_RS00500 (Protein translocase subunit SecA)	AA residue #879 Val -> Glu			X									
ECW_RS01120 (type VI secretion protein IcmF)	AA residue #773 Thr -> Pro	X											
ECW_RS01330 (flagellar M-ring protein FliF)	AA residue #493 Lys -> Ile											X (77%)		
ECW_RS01680 (flagellar basal body L-ring protein)	AA residue #83 Lys -> Ile		X											
ECW_RS02340 (pyrroline-5-carboxylate reductase)	AA residue #192 Leu -> Leu											X (65%)		
ECW_RS02400 (nuclease SbcCD subunit D)	AA residue #12 Gly -> Asp				X									
ECW_RS03145 V ECW_RS03150 (Intergenic region)	Base 653,621 changed from C to G		X											
ECW_RS03425 (apo-citrate lyase phosphoribosyl-dephospho-CoA transferase)	AA residue #39 Pro -> Pro		X											
ECW_RS03470 (cold shock-like protein CspE)	AA residue #60 Gly -> Asp	X												
ECW_RS03785 (phosphoglucomutase)	AA residue #236 Leu -> Leu							X						
ECW_RS03795 (ornithine decarboxylase)	AA residue #708 Gly -> Asp				X									

Gene	Mutation										
ECW_RS03975 (succinate dehydrogenase iron-sulfur subunit)	AA residue #16 Asp -> His		X								
ECW_RS04295 (cyclic pyranopterin monophosphate synthase accessory protein)	AA residue #70 Trp -> Cys			X							
ECW_RS04675 (hypothetical protein)	AA residue #74 Arg -> Gln	X			X			X			X
ECW_RS05270 (chromosome partition protein MukB)	AA residue #251 Val -> Val								X		
ECW_RS05880 (curli production assembly/transport component CsgE)	AA residue #10 Ala -> Val							X			
ECW_RS06720 (sodium:proton antiporter)	AA residue #295 Val -> Leu				X						
ECW_RS07760 (hypothetical protein)	AA residue #869 Cys -> STOP							X			
ECW_RS08740 (terminase)	AA residue #526 Tyr -> Ser						X		X	X	X
ECW_RS08975 (dimethyl sulfoxide reductase subunit A)	AA residue #441 Ala -> Asp		X								
ECW_RS09605 (cyclic di-GMP regulator CdgR)	AA residue #170 Gln -> His								X		
ECW_RS09920 (hypothetical protein)	Start codon TTG -> GTG						X				
ECW_RS10285 (RNA chaperone ProQ)	AA residue #219 Ser -> Leu							X			
ECW_RS10675 (tyrosine transporter TyrP)	AA residue #155 Ile -> Thr							X			
ECW_RS11060 (hypothetical protein)	AA residue #449 Lys -> Asn							X			
ECW_RS11295 (polymerase)	AA residue #294 Met -> Ile					X					
ECW_RS11295 (polymerase)	AA residue #52 Ile -> Lys							X			

Gene	Mutation	1	2	3	4	5	6	7	8	9	10	11	12
ECW_RS11845 (fimbrial assembly chaperone protein StcB)	AA residue #211 Thr -> Ile										X		
ECW_RS12465 (DNA gyrase subunit A)	AA residue #83 Ser -> Trp								X		X	X	X
ECW_RS13865 (hydrolase)	AA residue #59 Asn -> Ile							X					
ECW_RS14770 (glycine betaine/L-proline transport ATP-binding protein ProV)	AA residue #88 Asp -> Glu										X		
ECW_RS15370 (signal transduction histidine-protein kinase BarA)	AA residue #720 Gln -> STOP		X	X		X	X	X	X		X	X	X
ECW_RS15775 (membrane protein)	AA residue #27 Ile -> Ile			X									
ECW_RS16565 (type II secretion system protein)	AA residue #74 Ala -> Ala			X									
ECW_RS16880 V ECW_RS16885 (Intergenic region)	Base 3,383,328 changed from C to A			X									
ECW_RS16895 (sensor protein QseC)	AA residue #55 Leu -> STOP							X					
ECW_RS16895 (sensor protein QseC)	AA residue #96 Arg -> STOP						X						
ECW_RS16895 (sensor protein QseC)	AA residue #175 Leu -> STOP					X							
ECW_RS16895 (sensor protein QseC)	Deletion of 9 bp: 3,385,187-3,385,195				X								
ECW_RS16895 (sensor protein QseC)	AA residue #286 Ala -> Pro			X									
ECW_RS17000 (hypothetical protein)	AA residue #198 Ile -> Leu			X									
ECW_RS17250 (fimbrial usher protein)	AA residue #492 Arg -> Cys	X											
ECW_RS17365 (threonine/serine transporter TdcC)	AA residue #23 Thr -> Thr					X							

Gene	Mutation									
ECW_RS17735 (sugar fermentation stimulation protein B)	AA residue #39 Ala -> Val		X							
ECW_RS18220 (ribosomal RNA small subunit methyltransferase B)	AA residue #298 Thr -> Asn						X	X	X	X
ECW_RS18965 (gamma-glutamyltranspeptidase)	AA residue #182 Ile -> Thr							X		
ECW_RS19020 (high-affinity branched-chain amino acid transport system permease protein LivH)	AA residue #102 Ser -> Phe							X		
ECW_RS19175 (membrane protein)	AA residue #157 Arg -> Ser			X						
ECW_RS19350 (glutamate decarboxylase alpha)	AA residue #191 Pro -> Arg	X								
ECW_RS19375 (membrane protein)	AA residue #184 Arg -> His			X						
ECW_RS20360 (inner membrane protein YidH)	AA residue #37 Val -> Gly			X	X	X				
ECW_RS20475 (DNA gyrase subunit B)	AA residue #464 Ser -> Tyr						X			X
ECW_RS21155 (uridine phosphorylase)	AA residue #78 Val -> Val	X								
ECW_RS23040 V ECW_RS23045 (Intergenic region)	Base 4,630,644 changed from A to T						X			

Nucleotide coordinates shown for the forward DNA strand. Amino acid coordinates shown relative to the start of the respective protein. Percentages indicate percentage of reads harboring the mutation, that is either non-clonal population, or sequencing errors.

V, in-between; AA, amino acid; ECW, *E. coli* WT.

[R], resistant.

S3 Table. MIC and MIC shift values of *E. coli* AG100/K12 and *E. coli* ATCC-25922 Δ*tolC* clones resistant to CN-DM-861.

	MIC [µg/mL]		MIC shift	
Strain	CN-DM-861	CIP	CN-DM-861	CIP
E. coli ATCC-25922 Δ*tolC*	0.0025	0.0025	na	na
E. coli ATCC-25922 Δ*tolC* CN-DM-861[R] #1	0.125	0.0025	50	1

Strain			
E. coli ATCC-25922 Δ*tolC* CN-DM-861^R #2	0.5	0.0025	200	1
E. coli ATCC-25922 Δ*tolC* CN-DM-861^R #3	< 0.03	0.0025	<12	1
E. coli ATCC-25922 Δ*tolC* CN-DM-861^R #4	0.25	0.0025	100	1
E. coli ATCC-25922 Δ*tolC* CN-DM-861^R #5	0.5	0.0025	200	1
E. coli ATCC-25922 Δ*tolC* CN-DM-861^R #6	0.5	0.0025	200	1
E. coli ATCC-25922 Δ*tolC* CN-DM-861^R #7	0.125	0.0025	50	1
E. coli ATCC-25922 Δ*tolC* CN-DM-861^R #8	0.25	0.0025	100	1
E. coli ATCC-25922 Δ*tolC* CN-DM-861^R #9	0.25	0.0025	100	1
E. coli AG100/K12	0.0025	0.0025	na	na
E. coli AG100/K12 CN-DM-861^R #1	0.125	0.0025	50	1
E. coli AG100/K12 CN-DM-861^R #2	0.25	0.005	100	2
E. coli AG100/K12 CN-DM-861^R #3	2	0.0025	800	1
E. coli AG100/K12 CN-DM-861^R #4	2	0.005	800	2
E. coli AG100/K12 CN-DM-861^R #5	0.125	0.0025	50	1
E. coli AG100/K12 CN-DM-861^R #6	0.25	0.0025	100	1
E. coli AG100/K12 CN-DM-861^R #7	8	0.01	3200	4
E. coli AG100/K12 CN-DM-861^R #8	0.5	0.0025	200	1
E. coli AG100/K12 CN-DM-861^R #9	0.25	0.0025	100	1

na, not applicable.

S4 Table. Co-/cross-resistance of *E. coli* AG100/K12 and *E. coli* ATCC-25922 Δ*tolC* resistant to CN-DM-861 with relevant clinical antibiotics as determined in a filter disc assay.

		diameter of inhibition zone [mm]					
	antibiotic	ciprofloxacin	ceftazidime	aztreonam	gentamicin	colistin	meropenem
Strain	disc potency (µg)	5	30	30	10	10	10
E. coli AG100/K12	wt	44	36	41	21	13	41
	CN-DM-861^R #1	40	35	40	20	12	43
	CN-DM-861^R #2	40	35	40	21	12	42
	CN-DM-861^R #3	38	34	38	21	12	40

	CN-DM-861[R] #4	38	36	40	21	12	42
	CN-DM-861[R] #5	38	32	36	19	12	40
	CN-DM-861[R] #6	38	30	35	21	12	39
	CN-DM-861[R] #7	37	33	37	20	12	38
	CN-DM-861[R] #8	37	32	37	19	12	39
	CN-DM-861[R] #9	32	29	33	20	12	37
E. coli ATCC-25922 Δ*tolC*	wt	35	26	29	20	10	31
	CN-DM-861[R] #1	35	29	33	20	10	31
	CN-DM-861[R] #2	36	29	30	19	11	32
	CN-DM-861[R] #3	34	28	30	19	10	32
	CN-DM-861[R] #4	35	27	30	19	10	31
	CN-DM-861[R] #5	35	28	29	20	10	32
	CN-DM-861[R] #6	36	30	31	21	11	33
	CN-DM-861[R] #7	35	28	30	18	9	32
	CN-DM-861[R] #8	33	29	30	18	10	30
	CN-DM-861[R] #9	35	27	30	20	10	30

In green sensitive phenotype, in yellow intermediate resistant phenotype.

S5 Table. Reversibility of resistance determined for selected *E. coli* clones obtained in resistance development to CN-DM-861.

	MIC [µg/mL]					
	starting point		passage 3		passage 10	
strain	CN-DM-861	CIP	CN-DM-861	CIP	CN-DM-861	CIP
E. coli ATCC-25922 Δ*tolC*	0.0025	0.0025	0.0025	0.0025	0.0025	0.0025
E. coli ATCC-25922 Δ*tolC* CN-DM-861[R] #5	0.5	0.0025	1	0.0025	0.25	0.0025
E. coli AG100/K12	0.0025	0.0025	0.0025	0.0025	0.0025	0.0025
E. coli AG100/K12 CN-DM-861[R] #6	0.25	0.0025	0.25	0.0025	0.25	0.0025
E. coli AG100/K12 CN-DM-861[R] #7	8	0.01	8	0.01	8	0.01

S6 Table. MIC values of several antibiotic classes and cystobactamids determined on *E. coli* ATCC-25922 Δ*tolC* wildtype and CN-DM-861 resistant mutants #3 and #4.

	E. coli ATCC-25922 Δ*tolC*							
	MIC [µg/mL]							
Strain	Cys861-2	CN-DM-861	CIP	colistin	cefotaxime	gentamicin	tobramycin	tetracycline
WT	0.0125	0.0012	0.0025	0.5	0.025	1	0.5	1.6
RM #3 (*qseB*, A80V)	0.25	0.06	0.0025	2	0.025	1	1	0.5
RM #4 (*qseC*, P251S)	0.125	0.25	0.0025	0.5	0.025	1	0.25	1

WT, wildtype; RM, resistant mutant (resistant to CN-DM-861).

S7 Table. Full list of upregulated and downregulated genes common to all mutants.

Gene	Product	Mutant 1	Mutant 2	Mutant 6	Mutant 7	Mutant P
	hypothetical protein	13.6	5.1	5	16.8	9.3
	hypothetical protein	30	14.6	18.5	56.9	55.1
	histidine phosphatase super family protein	100.7	36.8	44.3	134	127.7
arnB	UDP-4-amino-4-deoxy-L-arabinose--oxoglutarate aminotransferase	67.6	22.4	22.8	57	52
arnC	undecaprenyl-phosphate 4-deoxy-4-formamido-L-arabinose transferase	71.5	23	24	60.9	57.9
arnA	bifunctional polymyxin resistance protein ArnA	81	25.1	26.5	67	62.2
arnD	putative 4-deoxy-4-formamido-L-arabinose-phosphoundecaprenol deformylase ArnD	53.2	20.3	22.1	52.3	47.6
arnT	undecaprenyl phosphate-alpha-4-amino-4-deoxy-L-arabinose arabinosyl transferase	51.4	20.5	21.7	48.8	47.2
arnE	putative 4-amino-4-deoxy-L-arabinose-phosphoundecaprenol flippase subunit ArnE	32	16.7	17.8	38	33.9
arnF	putative 4-amino-4-deoxy-L-arabinose-phosphoundecaprenol flippase subunit ArnF	34.5	14.6	16	33.6	34.2
cptA	phosphoethanolamine transferase CptA	8.9	8.5	9	9.3	8.6
waaH	glycosyltransferase like 2 family protein	695.3	66	74.3	708.2	492.6
	flavodoxin-like fold family protein	4.8	2	2.3	10	8.1
	PTS system%2C mannose/fructose/sorbose%2C IIC component family protein	7.7	2.7	3.4	12.2	5.9
	fimbrial family protein	20.1	3.4	3.9	19.7	10.6
qseC	sensor protein qseC	107.5	51.6	100.2	110.4	120.9

Gene	Protein					
qseB	response regulator	121.6	93.7	95.6	100	109.1
ygiW	protein YgiW	456	334	297.6	283.4	301.2
	gyrI-like small molecule binding domain protein	351.9	413.8	421.8	432.4	435.1
ygiS	putative binding protein YgiS	34.8	37.2	41.1	43	47.7
	putative membrane protein	40.5	20.5	18.2	26	29.3
pmrA	transcriptional regulatory protein PmrA	5.9	2.8	2.7	4.8	4.1
eptA	phosphoethanolamine transferase EptA	13.3	5.4	5.2	10.8	8.9
	major Facilitator Superfamily protein	91.6	92.2	88.9	105.1	111.6
	esterase-like activity of phytase family protein	370.5	266.9	247.1	283.9	301.7
	methyltransferase domain protein	48.9	8.5	6.7	46.1	27.7
	methyl-accepting chemotaxis (MCP) signaling domain protein	5.5	3.9	4.2	7.6	8.7
	hypothetical protein	18.5	10.7	11.9	23	25
	prokaryotic cytochrome b561 family protein	51	27.3	28.8	53.1	58.3
	hypothetical protein	81.9	65.6	54.8	53.2	48.6
	hypothetical protein	17.7	16.1	15.7	15.5	13.2
	hypothetical protein	11.7	10.1	9.5	10.5	9.6
ybjG	putative undecaprenyl-diphosphatase YbjG	12.6	5.4	5.5	11.3	11
phoE	outer membrane pore protein E	55	5.3	5.5	61.4	24.3

ugd	UDP-glucose 6-dehydrogenase	10.3	2.8	3.4	13	9.4
ibpA	small heat shock protein IbpA	0.47	0.22	0.2	0.17	0.26
ibpB	small heat shock protein IbpB	0.43	0.23	0.211	0.19	0.21
yhjH	cyclic di-GMP phosphodiesterase YhjH	0.07	0.08	0.07	0.07	0.06
	asmA family protein	0.41	0.41	0.41	0.38	0.36
yrbL	phoP regulatory network YrbL family protein	0.04	0.03	0.03	0.02	0.02
aer	aerotaxis receptor	0.27	0.28	0.23	0.26	0.24
soxS	regulatory protein SoxS	0.47	0.35	0.29	0.23	0.26
	hypothetical protein	0.46	0.35	0.32	0.24	0.33
tsr	methyl-accepting chemotaxis protein I	0.22	0.26	0.24	0.23	0.23
fliR	flagellar biosynthetic protein FliR	0.26	0.24	0.29	0.21	0.34
fliQ	flagellar biosynthetic protein FliQ	0.09	0.21	0.30	0.20	0.17
fliP	flagellar biosynthetic protein FliP	0.14	0.20	0.18	0.16	0.18
fliO	flagellar biosynthetic protein FliO	0.13	0.17	0.15	0.13	0.15
fliN	flagellar motor switch protein FliN	0.08	0.13	0.14	0.13	0.14
fliM	flagellar motor switch protein FliM	0.13	0.14	0.15	0.14	0.17
fliL	flagellar basal body-associated FliL family protein	0.10	0.10	0.11	0.11	0.15
fliK	flagellar hook-length control FliK family protein	0.13	0.13	0.11	0.11	0.14

fliJ	flagellar export protein FliJ	0.15	0.15	0.12	0.14	0.14
fliI	flagellar protein export ATPase FliI	0.12	0.15	0.18	0.19	0.16
fliH	flagellar assembly FliH family protein	0.18	0.22	0.20	0.27	0.19
fliG	flagellar motor switch protein FliG	0.16	0.16	0.19	0.17	0.19
fliF	flagellar M-ring protein FliF	0.08	0.12	0.17	0.11	0.18
fliE	flagellar hook-basal body complex protein FliE	0.10	0.25	0.21	0.17	0.20
fliT	flagellar FliT family protein	0.13	0.12	0.12	0.11	0.13
fliS	flagellar protein FliS	0.13	0.11	0.08	0.10	0.10
fliD	flagellar hook-associated protein 2	0.06	0.06	0.05	0.04	0.04
	hypothetical protein	0.06	0.05	0.04	0.04	0.04
fliA	RNA polymerase sigma factor for flagellar operon	0.05	0.08	0.08	0.07	0.06
fliZ	flagellar regulatory protein FliZ	0.21	0.19	0.16	0.12	0.17
	yecR-like lipofamily protein	0.30	0.34	0.29	0.37	0.33
motB	motility protein B	0.17	0.24	0.26	0.26	0.30
cheA	chemotaxis protein CheA	0.18	0.17	0.19	0.19	0.18
cheW	CheW-like domain protein	0.17	0.16	0.17	0.15	0.15
tar	methyl-accepting chemotaxis protein II	0.10	0.12	0.10	0.09	0.10
	hypothetical protein	0.08	0.08	0.07	0.111	0.05

cheR	chemotaxis protein methyltransferase	0.20	0.17	0.17	0.164	0.16
	cheB methylesterase family protein	0.21	0.17	0.16	0.151	0.13
cheY	chemotaxis protein CheY	0.26	0.20	0.20	0.19	0.21
cheZ	protein phosphatase CheZ	0.26	0.26	0.24	0.238	0.24
flhB	flagellar biosynthetic protein FlhB	0.26	0.26	0.26	0.252	0.28
cfa	cyclopropane-fatty-acyl-phospholipid synthase	0.37	0.5	0.38	0.265	0.27
ycgR	flagellar brake protein YcgR	0.19	0.13	0.11	0.185	0.14
flgL	flagellar hook-associated protein 3	0.20	0.22	0.21	0.215	0.22
flgK	flagellar hook-associated protein FlgK	0.21	0.22	0.21	0.213	0.21
flgJ	flagellar rod assembly protein/muramidase FlgJ	0.28	0.27	0.27	0.288	0.33
	flagellar P-ring family protein	0.33	0.34	0.33	0.299	0.34
	flagellar L-ring family protein	0.21	0.19	0.18	0.176	0.23
flgG	flagellar basal-body rod protein FlgG	0.13	0.12	0.11	0.099	0.11
	flagellar hook-basal body family protein	0.10	0.11	0.10	0.094	0.12
flgE	flagellar hook protein FlgE	0.10	0.09	0.09	0.077	0.10
flgD	basal-body rod modification protein flgD	0.06	0.07	0.06	0.057	0.08
flgC	flagellar basal-body rod protein FlgC	0.05	0.07	0.06	0.048	0.07
flgB	flagellar basal-body rod protein FlgB	0.06	0.06	0.06	0.042	0.07

flgA	flagella basal body P-ring formation protein FlgA	0.24	0.26	0.28	0.246	0.23
flgM	flagellar biosynthesis anti-sigma factor FlgM	0.34	0.37	0.34	0.359	0.42
flgN	FlgN family protein	0.32	0.33	0.32	0.406	0.38
sfaA	S-fimbrial protein subunit SfaA	0.36	0.45	0.36	0.11	0.35
phoH	protein PhoH	0.38	0.23	0.16	0.14	0.23

mutant 1: *qseC* (P251S); mutant 2: *qseC* (259In); mutant 6: *qseC* (441Fs); mutant 7: *qseC* (V257E); mutant P: *qseC* (P251A). Mutants 1, 2, 6, and 7 were obtained during spontaneous resistance development, mutant P was achieved using seamless mutagenesis. In, insertion; Fs, frameshift. Upregulated FC > 2, downregulated FC < 0.5, adjusted p-value < 0.05.

S8 Table. Primers used in construction of *E. coli* ATCC-25922 Δ*tolC qseC* P251A.

primer name	Sequence (5´→3´)
qseC_amp-ccdB_FW	TGGTTCGTGAACGACGCTTTACCTCCGACGCAGCTCACGAACTACGTAGCTTTGT TTATTTTTCTAAATACATT
qseC_amp-ccdB_RW	TCGTCAGAAAGCTGCGCAACTTCGGTTTGCACTTTCAGCGCCGTTAACGCTTATAT TCCCCAGAACAT
qseC_P251A_FW_long	TCCGTTGGTTGAGTCGCTAAATCAACTGTTCGCCCGCACACATGCGATGATGGTT CGTGAACGACGCTTTACCTCCGACGCAGCTCACGAACTACGTAGC
qseC_P251A_RW_long	CGATCCCGTAATGTAATTGAAGCAGCGCTTTTTTCCGCGCTTGCGGATCATCGTCA GAAAGCTGCGCAACTTCGGTTTGCACTTTCAGCGCCGTTAACGC

S9 Table. Primers used in overlap extension PCR for construction of pBeloBAC-P*qseBCqseC*.

primer name	Sequence (5´→3´)
H1_p_RBS_FW	TCCTGTGCGACGGTTACGCCGCTCCATGAGCTTATCGCGAATAAAGTTTATTACT CCCTTTAATGTCTGT
p_RBS_qseC_RW	GACTAAGACGTTGGGTAAATTTCATTTTTTCATCCCTGCGATAACCG
p_RBS_qseC_FW	CGGTTATCGCAGGGATGAAAAAATGAAATTTACCCAACGTCTTAGTC
qseC_pamp_RW	GAATGTATTTAGAAAAATAAACAAATTACCAGCTTACCTTCGCCTC
qseC_pamp_FW	GAGGCGAAGGTAAGCTGGTAATTTGTTTATTTTTCTAAATACATTC
pamp_H2_RW	TTCAGGCGTAGCAACCAGGCGTTTAAGGGCACCAATAACTGCCTTTTACCAATG CTTAATCAGTGA
H1_FW	TCCTGTGCGACGGTTACGCC
H2_RW	TTCAGGCGTAGCAACCAGGC

S10 Table. Primers used in qPCR.

gene	primer name	Sequence (5´→3´)
ihfB	ihfB_FW	GCCAAGACGGTTGAAGATGC
	ihfB_RW	GAGAAACTGCCGAAACCGC
qseB	qseB_FW2	GTTTACACAAGGTCGTCAGG
	qseB_RW2	GCCATTCGCGCAAAATATC
qseC	qseC_FW1	TCAACGAAATCAACGCGG
	qseC_RW1	GTGGGTAAAGATGGCAAAGG
pmrA	pmrA_FW	TGCTACGACGCCATAATAATC
	pmrA_RW	AGTTCTTCTCCGCTCATCC
pmrB	pmrB_FW2	ACCAGCACGCTCGATAATG
	pmrB_RW2	TTTTCGCCAGCAGTTCCAG
pmrD	pmrD_FW	GGGATTTACTCTCGCCTTTG
	pmrD_RW	TTTACACTGCCGTTCCCAC
marR	marR_FW2	TCTCCGCTGGATATTACCG
	marR_RW2	CGACCGACAACACTTTTTTC
marA	marA_FW3	ACGCAATACTGACGCTATTACC
	marA_RW3	TAACCCGAACGCTCTGACAC

Chapter 3

3 Mutations in CpxSR two-component system confer resistance to Cystobactamids in *Pseudomonas aeruginosa*

3.1 Introduction

Pseudomonas aeruginosa is a Gram-negative, opportunistic human pathogen [230, 231] causing community-acquired [232-236] and hospital-acquired and ventilator-associated infections [231, 237-242] such as pneumonia and bacteremia. *P. aeruginosa* does not pose a high threat to healthy individuals but it readily infects immunocompromised patients, e.g. human immunodeficiency virus (HIV) infected patients [243-245] and patients with cystic fibrosis (CF) [246-248]. In infected CF patients it was found that *P. aeruginosa* displays highly upregulated expression of virulence factors, i.e. pyocyanin, pyoverdine, LasA and LasB elastase, lectin A, rhamnolipids, endotoxin A, and several others. The expression of virulence factors and genes involved in biofilm formation and motility, antimicrobial resistance, and stress response are regulated by quorum sensing regulators such as LasRI and RhlI, which play a crucial role in colonization during pathogenesis leading to less effective treatments [249, 250].

In 2017, *P. aeruginosa* was found causing infections in 32 000 hospitalized patients, resulting in 2 700 deaths and estimated 767 million dollars of healthcare cost in the USA alone according to the Center for Disease Control (CDC) [138]. In EU /EEA, *P. aeruginosa* accounted for 5.6% of all bacterial infections in the period 2015-2019. Approximately 32% of isolates were resistant to at least one antibiotic group under surveillance, with FQ resistance being the most frequent, found in approximately 19% of isolates, followed by piperacillin-tazobactam resistance (16.9%), carbapeneme resistance (16.5%), ceftazidime resistance (14.3%), and resistance to

aminoglycosides (11.5%). Resistance to two or more antibiotic groups was observed in approximately 18% of isolates. [251]. A ten-years observational study in a German hospital with patients suffering from pneumonia caused by *P. aeruginosa*, revealed increasing resistance among *P. aeruginosa* isolates to various antibiotics, including ciprofloxacin, levofloxacin, ceftazidime and fosfomycin, with only few isolates susceptible to colistin [252]. Surveillance of carbapenemase-producing *P. aeruginosa* (CPPA) in several medical centers in Cologne, Germany, revealed a high incidence of CPPAs of which the majority were hospital-acquired, predominantly in intensive care units [253]. *P. aeruginosa* is intrinsically resistant to β-lactam antibiotics. It has chromosomally encoded β-lactamases; the AmpC cephalosporinase and OXA enzymes, both being inducibly expressed. In addition, the inducible expression of the MexXY efflux pump leads to resistance to aminoglycosides. In addition to intrinsic and inducible resistance, *P. aeruginosa* readily mutates chromosomal determinants in order to obtain resistance; several mutations resulting in the hyperproduction of efflux pumps and lipopolysaccharide modifications, mainly leading to resistance to fluoroquinolones and polymyxins, are known [254]. The generally low outer membrane permeability of *P. aeruginosa* additionally hampers the activity of antibiotics. Moreover, *P. aeruginosa* readily acquires ESBL and carbapenemase via horizontal gene transfer. Among transferrable aminoglycoside resistance determinants, acquisition of 16S rRNA methyltransferase is the most problematic as it confers resistance to all aminoglycosides, including the next-generation aminoglycoside plazomicin, which was introduced in 2018 for the treatment of urinary tract infections [255]. Rising numbers of MDR and XDR isolates [256-259] coupled with *P. aeruginosa*´s intrinsic resistance to antibiotics is resulting in very limited treatment options.

3.2 Results

3.2.1 Activity of cystobactamids against *P. aeruginosa* strains

Both, the natural derivative Cys861-2 and its semi-synthetic derivative CN-DM-861 were inactive on wildtype *P. aeruginosa* PAO1 (Table 1). Cys861-2 was also inactive on wildtype *P. aeruginosa* PA14, whereas CN-DM-861 showed a weak to medium activity with varying MICs per single experiment, whereas determined MICs of CN-DM-861 with *P. aeruginosa* PA14 ranged from 4-32 µg/mL. The MIC of ciprofloxacin on both wildtype strains was considerably lower than that of cystobactamids, 0.2 µg/mL (PAO1) and 0.125 µg/mL (PA14), respectively. The activity of both, Cys861-2 and CN-DM-861, was significantly improved for the efflux-deficient strains *P. aeruginosa* PAO750 and *P. aeruginosa* PA14Δ*mexAB* with MICs in the low µg/mL range. Cystobactamids were not active against *P. aeruginosa* NCTC13437, a VIM-10 and VEB-1 type ESBL producing strain, and *P. aeruginosa* DSM46316, an ESBL producing strain. Activity assessment using clinical isolates CIP107309, CIP105381, and R1541, revealed in general a higher potency of the natural derivative Cys861-2 compared to its semi-synthetic derivative CN-DM-861. Taken together, efflux seems to be the major cause of cystobactamid resistance in *P. aeruginosa*, and importantly, there was no direct correlation to other resistance phenotypes, including fluoroquinolone resistance.

Table 1: MIC values of Cys861-2, CN-DM-861 and ciprofloxacin on selected *P. aeruginosa* strains.

Strain	MIC [µg/mL]		
	Cys861-2	CN-DM-861	CIP
P. aeruginosa PAO1	> 64	> 64	0.2
P. aeruginosa PAO750 (Δ*mexAB-oprM*, Δ*mexCD-oprJ*, Δ*mexEF-oprN*, Δ*mexJK*, Δ*mexXY*)	8	1	0.006
P. aeruginosa PA14	> 64	4-32	0.125
P. aeruginosa PA14Δ*mexAB*	0.5	0.5	0.0125
P. aeruginosa NCTC13437[a]	> 64	> 64	> 6.4

P. aeruginosa DSM24600 (CRE)	> 64	> 64	3.2
P. aeruginosa DSM46316 (ESBL)	> 64	> 64	0.4
P. aeruginosa CIP107309[b]	16	4	0.2
P. aeruginosa CIP105381[b]	16	> 64	0.4
P. aeruginosa R1541[b]	8	> 64	> 6.4

CRE, carbapenem-resistant *Enterobacteriaceae*; ESBL, extended-spectrum β-lactamase; VIM, Verona Integron-encoded Metallo- β-lactamase; VEB, Vietnamese extended-spectrum β-lactamase.
[a] producing VIM-10 and VEB-1 type ESBL.
[b] clinical isolate.

We further assessed the activity of Cys861-2 and CN-DM-861 on a larger panel of clinical isolates provided by the Institute of Medical Microbiology and Hygiene of Saarland University with varying susceptibility towards ciprofloxacin (Table 2). Despite the relatively high MICs on the small panel of *P. aeruginosa* strains (Table 1), the median MICs for Cys861-2 and CN-DM-861 were as low as 4 µg/mL on the clinical isolate panel. Both cystobactamids were equipotent, except for the activity against the ciprofloxacin resistant strain P57, where MIC of Cys861-2 and CN-DM-861 were 8 µg/mL and > 64 µg/mL, respectively. The median MIC of ciprofloxacin in this panel of clinical isolates was 0.125 µg/mL. Next, we determined MBCs of Cys861-2 and ciprofloxacin in a subset if strains (Table 2). Compared to median MICs the MBCs increased 8- to 16-fold for Cys861-2 (32-64 µg/mL) and only 2-fold for ciprofloxacin (0.25 µg/mL).

Table 2: MIC and MBC values of Cys861-2, CN-DM-861 and ciprofloxacin on selected clinical isolates of *P. aeruginosa*.

	MIC [µg/mL]			MBC [µg/mL]	
strain	Cys861-2	CN-DM-861	CIP	Cys861-2	CIP
P. aeruginosa 27	16	nd	0.125	> 64	0.25
P. aeruginosa 107	4	nd	0.25	8	0.25
P. aeruginosa 111	> 64	nd	64	> 64	64
P. aeruginosa 134	4	nd	0.125	32	0.25
P. aeruginosa 160	8	nd	0.125	16	0.5
P. aeruginosa 228	2	nd	0.125	4	0.25

P. aeruginosa 260	> 64	nd	≤ 0.06	> 64	0.25
P. aeruginosa 590	4	nd	0.125	64	0.5
P. aeruginosa 813	8	nd	0.125	> 64	0.25
P. aeruginosa P51	> 64	> 64	0.4	nd	nd
P. aeruginosa P52	4	4	0.1	nd	nd
P. aeruginosa P53	8	8	0.2	nd	nd
P. aeruginosa P54	4	4	0.8	nd	nd
P. aeruginosa P55	4	4	0.1	nd	nd
P. aeruginosa P56	4	4	0.8	nd	nd
P. aeruginosa P57	8	> 64	> 6.4	nd	nd
P. aeruginosa P58	8	8	0.8	nd	nd
P. aeruginosa P59	4	4	0.2	nd	nd
P. aeruginosa PT16	4	4	0.1	nd	nd
P. aeruginosa PT17	4	4	0.1	nd	nd
P. aeruginosa ATCC27853[a]	2	nd	0.125	8	0.125
Median	4	4	0.125	32-64	0.25

nd, not determined.
[a] quality control strain.

Biofilm is a complex community of sessile bacterial cells and it enables bacterial persistence under unfavorable conditions, like exposure to antibiotics. The major component of biofilms is the extracellular polymeric substance (EPS) matrix, composed of polysaccharides, proteins, lipids and extracellular DNA (eDNA) [260]. Therefore, we tested whether cystobactamids could reduce the biofilm forming ability of *P. aeruginosa*. Both Cys861-2 and CN-DM-861 significantly reduced biofilm formation in both PA14Δ*mexAB* and PAO750 background (Fig. 1). In PA14Δ*mexAB* background we observed a dose depended effect on inhibition of biofilm formation for Cys861-2, as exposure to 2x MIC had a greater effect than exposure to 0.5x MIC, whereas addition of CN-DM-861 gave comparable results at both 0.5x and 2x MIC concentrations. In PAO750 background both Cys861-2 and CN-DM-861 gave comparable results at 0.5x and 2x MIC concentrations and significantly reduced biofilm formation. Ciprofloxacin significantly reduced biofilm formation in both *P. aeruginosa* strains, however,

in PAO750 it was less effective than cystobactamids. This was further substantiated by severely decreased eDNA content (Fig 1C) in presence of sub-inhibitory levels of CN-DM-861; the same effect was observed for CIP.
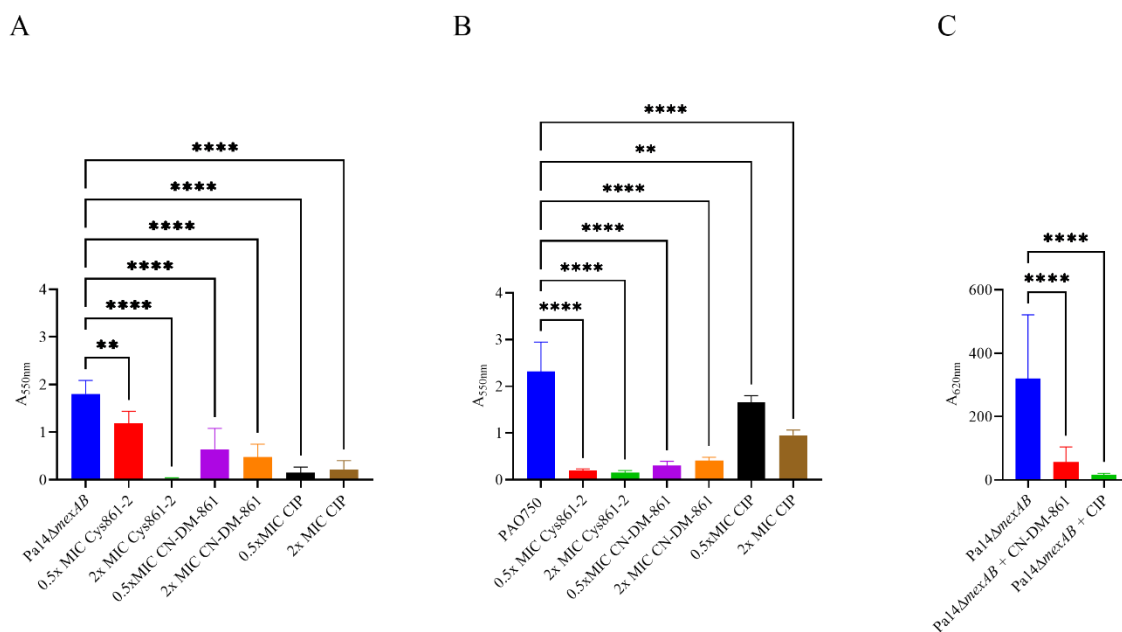
Fig 1. Inhibitory effect of cystobactamid Cys861-2, CN-DM-861 and ciprofloxacin on biofilm formation and eDNA content.
Inhibitory effect on biofilm formation was tested at 0.5x MIC and 2x MIC. (A) *P. aeruginosa* PA14Δ*mexAB* wildtype (B) PAO750 wildtype. (C) Effect of sub-inhibitory concentration of CN-DM-861 and ciprofloxacin on eDNA content in *P. aeruginosa* PA14Δ*mexAB*. Ordinary one-way ANOVA were used to analyze the data; **, $p < 0.01$; ****, $p < 0.001$.

3.2.2 Bactericidal activity of cystobactamids

Time-kill kinetics were assessed using the efflux-deficient strain *P. aeruginosa* PA14Δ*mexAB*. Bacteria were treated with 4x, 8x and 16x MIC of Cys861-2 and bacterial killing was determined using standard testing (plating and counting of colony-forming units, CFU) and isothermal calorimetry (Fig. 2). Using the standard method of recording CFU/mL over time, we found that all three tested concentrations had the same effect. Already at 4x MIC we observed a pronounced bactericidal effect with approximately 3-log reduction of CFUs in the first 8 hours. However, higher concentrations of Cys861-2 (8x and 16x MIC) did not further enhance the killing effect. For all tested concentrations regrowth was observed, and after 24

105

hours, CFU/mL reached the initial inoculum of approximately 10^6 viable cells per mL. This bacterial population growing after treatment with 4x to 16x MIC could explain the relatively high shift between MIC and MBC (Table 2) observed with clinical isolates. Interestingly, isothermal microcalorimetry revealed different results. We could observe a steady increase in net metabolic activity at 4x MIC, reaching approximately 20 µW at the end of the experiment; these results are in line with standard time-kill assay results. However, at 8x and 16x MIC, no metabolic activity was observed throughout the duration of the experiment, recorded heat flow was 0 µW. These results are contradictory to standard time-kill assay results, where regrowth was observed after 24 hours, and could be due to differences in experimental conditions during the experimental run.
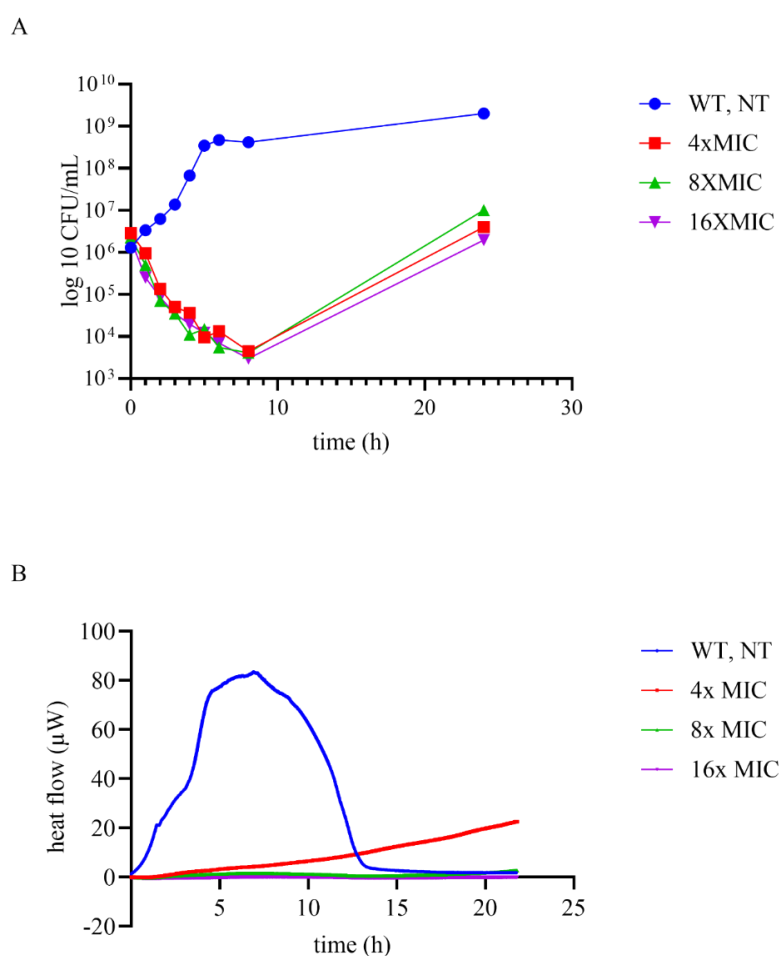
Fig 2. Time-kill curves of cystobactamid Cys861-2 on *P. aeruginosa* PA14Δ*mexAB* tested at 4x, 8x, and 16x MIC.
(A) Using standard method, CFU/mL over time. (B) Using isothermal microcalorimetry, µW over time. NT, non-treated. WT, wildtype.

3.2.3 Frequency of resistance and mutant characterization

We assessed the frequency of cystobactamid-resistant mutant development in several *P. aeruginosa* strains and performed a detailed evaluation of the obtained resistant mutants (Table 3). FoR for *P. aeruginosa* PA14Δ*mexAB* was 6 x 10^{-7} and 2.4 x 10^{-7} at 4x and 8x MIC of Cys861-2, respectively. For CN-DM-861, the FoR at 4x MIX was slightly lower (1 x 10^{-8}) and comparable to the FoR of ciprofloxacin at 4x MIC (2x 10^{-8}). The semi-synthetic derivative CN-DM-861 was also used to determine FoR on additional *P. aeruginosa* strains. At 4x MIC, spontaneous mutants developed at a frequency of 6.6 x 10^{-9} and 8 x 10^{-8} in the *P. aeruginosa* strains PAO750 and CIP107309, respectively. Taken together, the FoR of cystobactamids in *P. aeruginosa* is on average in the range of 10^{-8}. In comparison, ciprofloxacin-resistant mutants developed on average at lower frequencies and with larger variation between *P. aeruginosa* strains (10^{-11} to 10^{-8}). Next, the level of resistance of selected mutants was determined. The *P. aeruginosa* PA14Δ*mexAB* mutants selected with 4- and 8x MIC of Cys861-2 displayed high-level resistance with MICs being > 64 µg/mL, which corresponds to a shift in MIC of > 264-fold for the mutants in comparison to the parent strain. The same was observed for *P. aeruginosa* PA14Δ*mexAB* mutants selected with 4x MIC of CN-DM-861, where high-level resistance was found, however, two out of nine mutants displayed lower level resistance with MICs of 16 and 32 µg/mL, respectively. Interestingly, CN-DM-861 resistant mutants of *P. aeruginosa* PAO750, which developed at relatively low frequency showed a less pronounced shift in MIC (8- to >32-fold) (S1 Table). We did not observe co-/cross-resistance with any of the tested clinically relevant antibiotics (S2 Table). However, a 40-80-fold increase in ciprofloxacin MIC was detected in cystobactamid-resistant mutants of PA14Δ*mexAB*, however, this was only observed for mutants selected with CN-DM-861 and not with the mutants selected with Cys861-2 (S1 Table). In CN-DM-861-resistant mutants of PAO750 the resistance level to ciprofloxacin was varying between 0.5- and 16-fold. We also assessed whether the induced cystobactamid-resistant phenotype of *P. aeruginosa* is reversible; however, the level of

resistance remained unchanged after ten passages in non-selective medium as determined by MIC (S3 Table). In order to study underlying mechanisms of cystobactamid-resistance and partial ciprofloxacin-resistance in the generated mutant strains we analyzed mutations by WGS. We found mutations in the CpxSR two-component system for all resistant mutants, whereas point mutations in *cpxS* were more frequent (in 19 out of 23 resistant mutants) than point mutations in *cpxR* (in 4 out of 23 resistant mutants). We observed a limited number of point mutations in *cpxS*, with S236P and I279T being the most frequent ones. Only one point mutation was detected in *cpxR*, L16R, and it was always in presence of a Y563N mutation in PA14_RS04500 (putative peptide synthetase).

Table 3. Frequency of resistance in *P. aeruginosa*, resistant mutant characterization, and whole genome sequencing results

Frequency of Resistance					
Cys861-2		CN-DM-861		CIP	
4x MIC	8x MIC	4x MIC	8x MIC	4x MIC	8x MIC
strain					
P. aeruginosa PA14Δ*mexAB*[a]	6×10^{-7}	2.4×10^{-7}	1×10^{-8}	nd	2×10^{-8}	nd
P. aeruginosa PAO750[a]	nd	nd	6.6×10^{-9}	nd	1×10^{-11}	nd
P. aeruginosa CIP107309	nd	nd	8×10^{-8}	3×10^{-8}	2×10^{-8}	$< 9 \times 10^{-11}$

Resistant mutant characterization					
strain	resistant to	mutation in	MIC shift[b] (Cys861 or CN-DM-861, parent vs. Cys[R] mutant)	co-/cross-resistance with CIP[b] (CIP, parent vs. Cys[R] mutant)	co-/cross-resistance with crAB[c]	reversibility of resistance[d]
P. aeruginosa PA14Δ*mexAB*	Cys861-2		> 256	no	nd	
P. aeruginosa PA14Δ*mexAB*	CN-DM-861	CpxSR	> 256	40-80	no	no

P. aeruginosa PAO750		8-> 32	0.5-16			

WGS results						
Strain	mutant number	MIC [µg/mL]	*cpxS*	*cpxR*	PA14_RS04500	*tamB*
P. aeruginosa PA14Δ*mexAB*	WT	0.25	-	-	-	-
P. aeruginosa PA14Δ*mexAB* Cys861-2^R	#1	> 64	S236P			
	#2	> 64	S236P			
	#3	> 64	S236P			
	#4	> 64	S236P			
	#5	> 64	S236P			
P. aeruginosa PA14Δ*mexAB*	WT	0.25	-	-	-	-
P. aeruginosa PA14Δ*mexAB* CN-MD-861^R	#1	> 64	L252Q			
	#2	> 64	287In			
	#3	> 64		L16R	Y563N	
	#4	> 64		L16R	Y563N	
	#5	> 64	S236P		Y563N	
	#6	> 64	T163P			
	#7	> 64	S227R		Y563N	
	#8	> 64		L16R	Y563N	V855G
	#9	> 64		L16R	Y563N	
P. aeruginosa PAO750	WT	2	-	-	-	-
P. aeruginosa PAO750 CN-DM-861^R	#1	32	I279T			
	#2	16	I279T			
	#3	16	I279T			
	#4	16	I279T			
	#5	16	I279T			

#6	32	A251P
#7	> 64	A251P
#8	> 64	I279T
#9	> 64	I279T

Cys[R], cystobactamid-resistant; nd, not determined; WGS, whole genome sequencing; crAB, clinically relevant antibiotics; In, insertion.

[a] obtained resistant mutants selected for WGS.

[b] results can be found in S1 Table.

[c] results can be found in S2 Table.

[d] results can be found in S3 Table.

[R] resistant.

Having found predominantly mutations in *cpxRS* of cystobactamid-resistant mutants of *P. aeruginosa*, we assessed whether these point mutations lead to a fitness cost. For this, standard growth curves based on absorbance measurements (OD_{600}) were determined and we did not detect any apparent difference between the parent strains PA14Δ*mexAB* and PAO750 and corresponding cystobactamid-resistant clones. The results for all resistant clones are shown in Figure S1. We selected the same set of mutants and *P. aeruginosa* parent strains and studied potential differences on the level of metabolic activity using isothermal microcalorimetry, which might not be obvious in simple OD_{600} readings (Fig. 3-4, S2-3). Most apparently, we observed significant differences of heat profiles of the parent strains *P. aeruginosa* PA14Δ*mexAB* and PAO750. However, when comparing the heat profiles of the wildtype strains with the heat profiles of corresponding mutants we observed only very subtle changes. Only the Cys861-2-resistant mutant #3 (*cpxS*, S236P) of *P. aeruginosa* PA14Δ*mexAB* displayed significant differences compared to its corresponding parent strain. The main differences were recorded 7 hours post experimental start (hpes), when the resistant mutant reaches a higher heat flow than the wildtype. At around 14 hpes, the recorded heat flow for the mutant suddenly dropped to zero µW and remained at zero. In contrast, the heat flow of wildtype started slowly declining at around 13 hpse and reached zero µW at 20 hpse. Analysis of the thermograms revealed significant differences in time to activity and maximum decay velocity between the

wildtype and resistant mutants. Observed differences were linked directly to the mutations present in the genome of cystobactamid-resistant mutants, namely *cpxS* and *cpxR*. These mutations lead to increased metabolic activity in the stationary growth phase and result in faster depletion of available nutrients and oxygen leading to sudden cessation of metabolism. Metabolic burden of these mutations is decoupled from biomass formation and was therefore not detected in standard fitness cost assays.
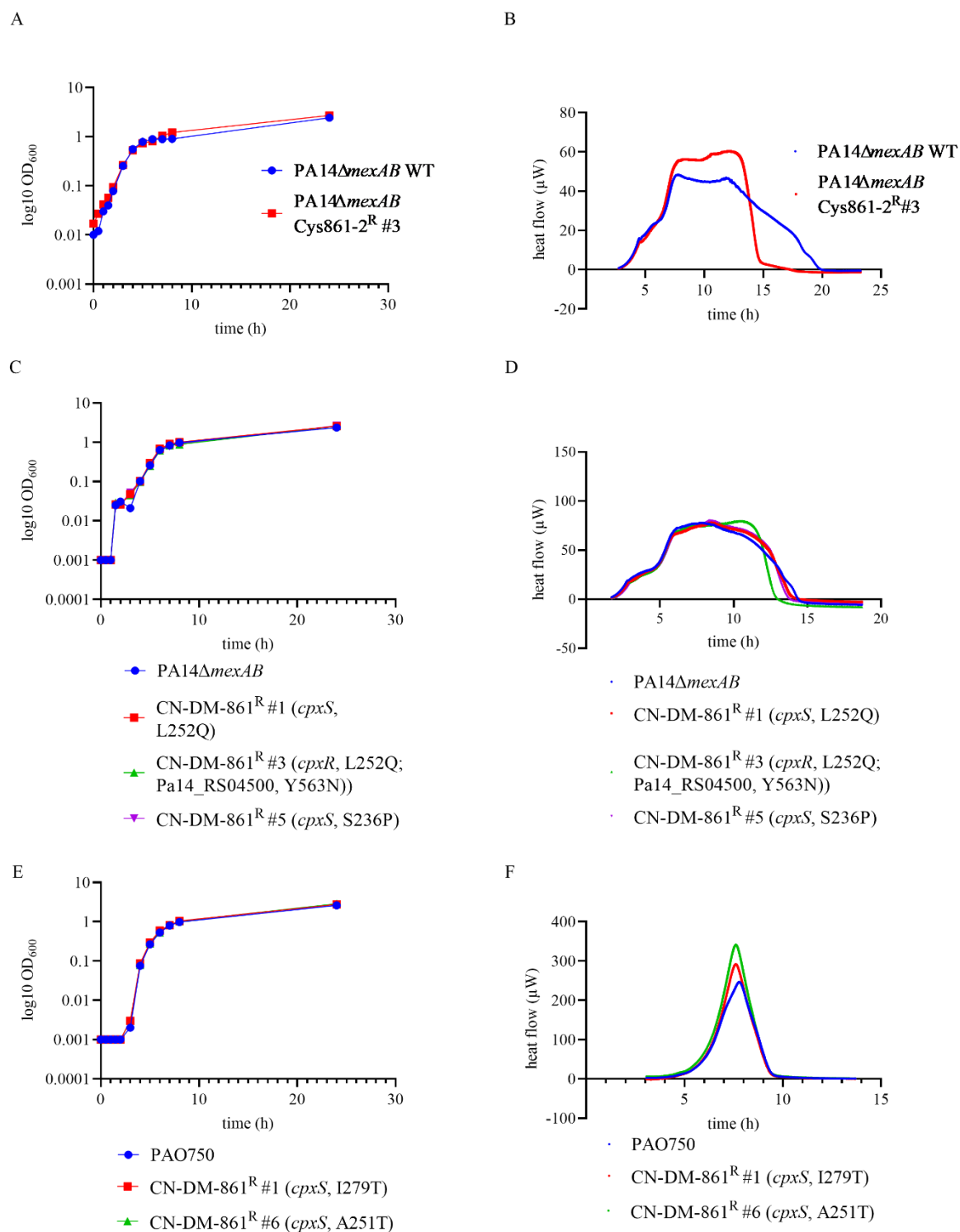
Fig 3. Growth kinetics and metabolic profiles of selected cystobactamid-resistant mutants of *P. aeruginosa* PA14Δ*mexAB* (Cys861-2 and CN-DM-861) and PAO750 (CN-DM-861).
(A) OD_{600} over time, *P. aeruginosa* PA14Δ*mexAB*, Cys861-2[R]. (B) ICM, *P. aeruginosa* PA14Δ*mexAB*, Cys861-2[R]. (C) OD_{600} over time, *P. aeruginosa* PA14Δ*mexAB*, CN-DM-861[R]. (D) ICM, *P. aeruginosa* PA14Δ*mexAB*, CN-DM-861[R]. (E) OD_{600} over time, PAO750, CN-DM-861[R]. (F) ICM, PAO750, CN-DM-861[R]. [R], resistant.
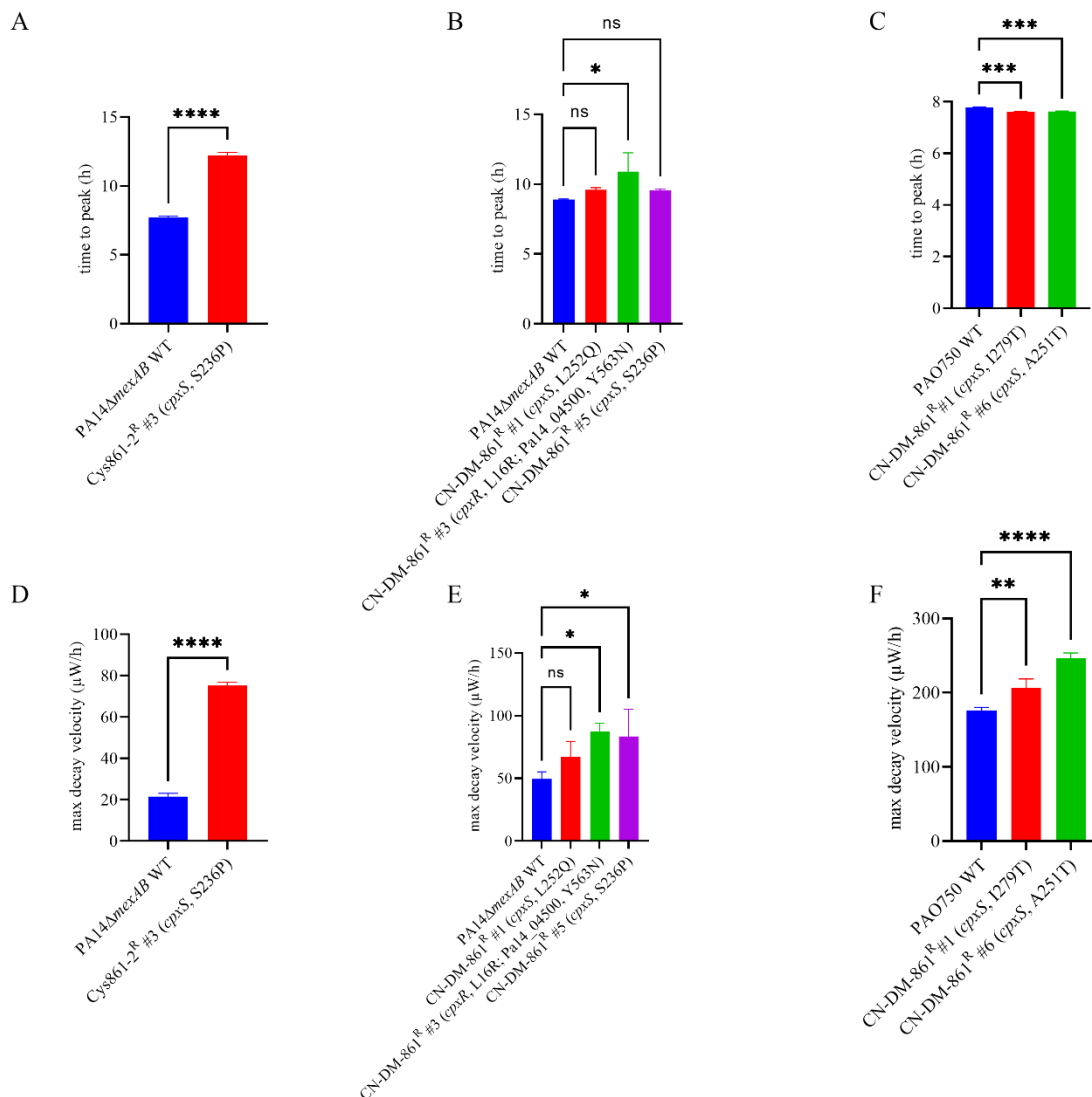
Fig 4. Time to peak and max decay velocity assessed for selected *P. aeruginosa* PA14Δ*mexAB* (Cys861-2 and CN-DM-861) and PAO750 (CN-DM-861) resistant mutants.
(A) Time to peak, *P. aeruginosa* PA14Δ*mexAB*, Cys861-2[R]. (B) Time to peak, *P. aeruginosa* PA14Δ*mexAB*, CN-DM-861[R]. (C) Time to peak, PAO750 CN-DM-861[R]. (D) Max decay velocity, *P. aeruginosa* PA14Δ*mexAB*, Cys861-2[R]. (E) Max decay velocity, *P. aeruginosa* PA14Δ*mexAB*, CN-DM-861[R]. (F) Max decay velocity, PAO750 CN-DM-861[R]. [R], resistant; Unpaired t-test and ordinary one-way ANOVA were used to analyze the data; ns, not significant; *, $p < 0.05$; **, $p < 0.01$; ***, $p < 0.005$; ****, $p < 0.001$.

3.2.2 *In vitro* virulence of cystobactamid-resistant *P. aeruginosa* mutants

When we first generated cystobactamid-resistant *P. aeruginosa* mutants and analyzed their genome, we noticed similarities between the *P. aeruginosa* and *E. coli* WGS results (Chapter 2). Resistant mutants generated in both *E. coli* and *P. aeruginosa* background exclusively

carried mutations in two-component systems, QseBC TCS and an unannotated TCS, respectively. Therefore, we initially suspected that TCS in *P. aeruginosa*, only recently annotated CpxSR, could also play a role in quorum sensing and virulence regulation. We therefore assessed the level of biofilm formation (Fig. S4), and motility (Table S4) of *P. aeruginosa* mutants strains, and checked their cell size and morphology (Fig. S5-6) and assessed their virulence *in vivo* (Fig. S7). At the time when these studies were conducted it was not clear whether the observed *cpxRS* mutations in cystobactamid-resistant *P. aeruginosa* would activate or inactivate the two-component system. Thus, we tested transposon mutants of *cpxS* (Pa14_22730, 3206-1, and 3206-2) and *cpxR* (3204) in *P. aeruginosa* PA14 and PAO1 along with the mutants selected with CN-DM-861 and Cys861-2 that showed point mutations in *cpxS* and/or *cpxR*. Transposon mutants result in a nonsense protein and were used to determine if the point mutations in *cpxS* and *cpxR* in cystobactamid-resistant mutants are gain-in- or loss-of function mutations. We did observe changes in motility of *P. aeruginosa* cystobactamid-resistant mutants, their ability to form biofilms, changes in their cell dimensions and decreased virulence *in vivo*, however, no clear link to genotype could be found, unlike in *E. coli* mutants.

3.2.3 Transcriptome analysis

In order to understand how mutations in CpxSR confer resistance to cystobactamid and how *P. aeruginosa* reacts when exposed to sub-lethal concentrations of cystobactamids, we performed transcriptome analyses of PA14Δ*mexAB* Cys861-2^R mutant #3 (*cpxS*, S236P) compared to its wildtype, and transcriptome analysis of wildtype exposed to CN-DM-861.

3.2.4.1 Wildtype vs. mutant

The *P. aeruginosa* PA14Δ*mexAB* Cys861-2^R mutant #3, carrying a S236P mutation in CpxS, displayed 63 upregulated and 19 downregulated genes compared to the parent strain

PA14Δ*mexAB*, after applying cut-off values of p < 0.001 and minimum log fold change in expression <-2 or >2. The complete table of up- and down-regulated genes can be found in Table S5. Here, we focused on the top 20 differentially expressed genes (DEG) (Table 4). The highest upregulated genes encode for YeiH family protein, alpha/beta hydrolase, Spy/CpxP family refolding chaperone, YgiW/YdeI family stress tolerance oligonucleotide/oligosaccharide binding (OB) fold protein, multidrug efflux RND MuxABC transporter, cation-efflux transporter FieF, multidrug efflux RND transporter OpmB, chaperones and PchB involved in the incorporation of salicylate into the siderophore pyochelin. Down-regulated genes include several genes encoding putative or uncharacterized proteins (transcriptional regulators, hydrolase, transferase, isomerase), peptide synthase PvdL protein, nitrat/nitrite transporter and xylulose kinase.

Table 4. Differentially expressed genes found in transcriptome analysis of *P. aeruginosa* PA14Δ*mexAB* Cys861-2[R] mutant #3 (*cpxS*, S236P) compared to its respective wildtype.

locus tag	Product	FC
PA14_RS28950	YeiH family protein	12.17
PA14_RS28955	alpha/beta hydrolase	11.37
PA14_RS09225	Spy/CpxP family protein refolding chaperone	8.64
PA14_RS05075	hypothetical protein	8.37
PA14_RS01705	YgiW/YdeI family stress tolerance OB fold protein	7.58
PA14_RS05080	CDF family cation-efflux transporter FieF	7.37
PA14_RS00850	purine permease	6.94
PA14_RS09220	HAMP domain-containing histidine kinase	6.70
PA14_RS15410	TonB-dependent receptor	6.28
PA14_RS13040	multidrug efflux RND transporter periplasmic adaptor subunit MuxA	5.93

PA14_RS15065	molecular chaperone	5.67
PA14_RS13045	multidrug efflux RND transporter permease subunit MuxB	5.37
PA14_RS03745	isochorismate lyase PchB	5.07
PA14_RS05085	hypothetical protein	5.02
PA14_RS13050	multidrug efflux RND transporter permease subunit MuxC	4.98
PA14_RS13055	multidrug efflux RND transporter outer membrane subunit OpmB	4.86
PA14_RS23880	PepSY domain-containing protein	4.86
PA14_RS03755	pyochelin biosynthesis salicyl-AMP ligase PchD	4.78
PA14_RS01740	YjiK family protein	4.68
PA14_RS12125	PepSY domain-containing protein	4.55
PA14_RS08425	putative isomerase	-2.05
PA14_RS08415	putative acyl carrier protein	-2.06
PA14_RS08410	uncharacterized protein	-2.07
PA14_RS26440	putative transcriptional regulator	-2.37
PA14_RS14505	possible glycosyltransferase	-2.41
PA14_RS10810	putative enoyl-CoA hydratase	-2.72
PA14_RS20330	uncharacterized protein	-3.17
PA14_RS26930	putative transcriptional regulator, GntR family	-3.82
PA14_RS29190	aminotransferase	-4.13
PA14_RS16835	nitrate/nitrite transporter	-4.32
PA14_RS13565	PvdL	-4.55
PA14_RS14005	xylulose kinase (Xylulokinase) (EC 2.7.1.17)	-4.74

PA14_RS13320	probable MFS transporter	-5.11
PA14_RS08045	putative membrane protein	-5.24
PA14_RS00395	uncharacterized protein	-5.31
PA14_RS22000	urease accessory protein	-5.35
PA14_RS04850	possible hydrolase	-5.40
PA14_RS04405	Putative transcriptional regulator, AraC family	-7.02
PA14_RS11815	putative protease	-9.35

FC, fold change.

3.2.4.2 Exposure of *P. aeruginosa* PA14Δ*mexAB* to cystobactamid

In order to further consolidate our findings from the transcriptome analysis of cystobactamid-resistant *P. aeruginosa* PA14Δ*mexAB*, we treated the sensitive parent strain with 0.5x and 2x MIC of CN-DM-861 and investigated changes compared to an untreated control on the transcriptional level by RNA sequencing. In general, the results from *P. aeruginosa* treated with either 0.5x or 2x MIC of CN-DM-861 were very similar. Approximately 50% of DEGs were commonly found under both treatment conditions, predominantly the downregulated genes. After applying the cut-off values of p < 0.001 and log fold change <-2 or >2, we found a rather small number of DEGs both up- and downregulated for both exposure conditions (0.5x, 2x MIC) and across all time points (20, 40, 60 min), and the number of DEGs decreased over time (Table 5). When *P. aeruginosa* PA14Δ*mexAB* was treated at sub-MIC (0.5x) of CN-DM-861 genes involved in glycolysis, gluconeogenesis, TCA cycle, uptake of nutrients and exclusion of deleterious substances (MFS transporters), type VI secretion system (T6SS), osmotic protection and detoxification were found significantly up-regulated at 20 min post exposure (pe). Simultaneously, genes involved in uptake and metabolism of organic acids, LysR transcriptional regulator and TolC secretion were downregulated. At 40 min pe, genes

117

involved in valine catabolism, release of toxins and iron metabolism were upregulated, whereas genes involved in ethanolamine uptake, type III secretion system (T3SS), biosynthesis and transport of alginate across membrane, and development/maintenance/spread of biofilm were downregulated. Finally, at 60 min pe genes involved in ATP synthesis, solute export, utilization of inorganic phosphate and metabolism of lipids, amino acid, carbohydrate and hormones were upregulated, whereas genes involved in valine catabolism, cobalamine synthesis and glycogen formation were downregulated. Only genes involved in valine catabolism and MFS transporters were shared over time. The most drastic difference in expression level was observed for 3-hydroxyisobutyrate dehydrogenase (valine catabolism), that was upregulated 9-fold at 40 min pe and downregulated 4-fold only 20 minutes later at 60 min pe. While downregulated genes were shared between both, sub-inhibitory (0.5x MIC) and excess concentration (2x MIC), upregulated genes were distinctly different between the two tested concentrations. For 2x MIC at 20 min pe, genes involved in L-hydroxyproline metabolism, uptake of sulfur, biosynthesis of coenzyme A and pantothenate were upregulated. At 40 min pe, the only upregulated gene was a gene encoding an AraC family transcriptional regulator positively regulating expression of genes involved in carbon metabolism, stress response, virulence and pathogenesis. At 60 min pe, genes involved in cofactor biosynthesis and a gene encoding a protein with unknown function containing a DUF2868 domain were found.

Table 5. DEGs of *P. aeruginosa* PA14Δ*mexAB* exposed to 0.5x MIC and 2x MIC cystobactamid CN-DM-861 after 20, 40 and 60 min.

	0.5x MIC							
	20 min pe			40 min pe			60 min pe		
locus tag	product	2log FC	locus tag	Product	2log FC	locus tag	product	2log FC
PA14_RS 11760	hypothetical protein	10.1	PA14_RS 22250	3-hydroxyisobutyrate dehydrogenase	8.83	PA14_RS 10570	cytochrome b	11
PA14_RS 26110	dihydrolipoyl dehydrogenase	7.6	PA14_RS 00390	type VI secretion system membrane subunit TssM	5.71	PA14_RS 10680	LysE family translocator	8.21
PA14_RS 12705	relaxase/mobilization nuclease and DUF3363 domain-containing protein	7.11	PA14_RS 11965	ferric enterobactin esterase PfeE	4.93	PA14_RS 12245	PhoX family phosphatase	8
PA14_RS 04395	MFS transporter	6.61	PA14_RS 02835	PHB depolymerase family esterase	4.75	PA14_RS 02570	ComF family protein	7.84
PA14_RS 16130	FecR family protein	6.07	PA14_RS 01835	DUF2868 domain-containing protein	4.1	PA14_RS 04385	SDR family oxidoreductase	6.41
PA14_RS 06085	MFS transporter	5.45	PA14_RS 14015	sn-glycerol-3-phosphate ABC transporter ATP-binding protein UgpC	-2.78	PA14_RS 07800	aliphatic sulfonate ABC transporter substrate-binding protein	5.25
PA14_RS 28975	choline ABC transporter substrate-binding protein	4.53	PA14_RS 11430	PA2778 family cysteine peptidase	-3.84	PA14_RS 21525	CoA transferase	4.8
PA14_RS 14470	FAD-dependent oxidoreductase	3.87	PA14_RS 04775	ethanolamine permease	-4.04	PA14_RS 08565	FUSC family protein	3.86
PA14_RS 02190	chemotaxis signal transduction system protein ChpA	-2.02	PA14_RS 26910	ABC transporter substrate-binding protein	-5.52	PA14_RS 12710	S26 family signal peptidase	3.46
PA14_RS 15735	MFS transporter	-3.24	PA14_RS 31435	hypothetical protein	-5.64	PA14_RS 21810	DUF3892 domain-containing protein	-2.21
PA14_RS 11025	LysR family transcriptional regulator	-5.38	PA14_RS 14050	acyl-CoA/acyl-ACP dehydrogenase	-5.65	PA14_RS 15735	MFS transporter	-3

locus tag	product	2log FC	locus tag	product	2log FC	locus tag	product	2log FC
PA14_RS 13990	SfnB family sulfur acquisition oxidoreductase	-6.18	PA14_RS 15690	short-chain fatty acid transporter	-6.75	PA14_RS 28930	L-serine ammonia-lyase	-3.3
PA14_RS 19590	TolC family protein	-6.61	PA14_RS 03280	hypothetical protein	-7.53	PA14_RS 15685	3-hydroxybutyrate dehydrogenase	-3.78
PA14_RS 21505	TRAP transporter large permease	-7.85	PA14_RS 00455	type VI secretion system ATPase TssH	-7.61	PA14_RS 10725	bifunctional cobalt-precorrin-7 (C(5))-methyltransferase/cobalt-precorrin-6B (C(15))-methyltransferase	-6.89
PA14_RS 15470	hypothetical protein	-8.44	PA14_RS 30640	type III secretion system needle length determinant PscP	-9.73	PA14_RS 14895	4-alpha-glucanotransferase	-10.8
PA14_RS 25145	fimbrial biogenesis outer membrane usher protein	-9.37	PA14_RS 07425	alginate biosynthesis protein Alg44	-10.4			
PA14_RS 00940	ABC transporter ATP-binding protein	-9.72	PA14_RS 07420	alginate biosynthesis TPR repeat lipoprotein AlgK	-11.3			

2x MIC								
20 min pe			40 min pe			60 min pe		
locus tag	product	2log FC	locus tag	Product	2log FC	locus tag	product	2log FC
PA14_RS 19440	D-hydroxyproline dehydrogenase subunit beta LhpB	13.28	PA14_RS 27145	AraC family transcriptional regulator	8.18	PA14_RS 01835	DUF2868 domain-containing protein	9.53
PA14_RS 14185	amino acid adenylation domain-containing protein	6.57	PA14_RS 09935	hypothetical protein	-2.35	PA14_RS 16065	cobaltochelatase subunit CobN	4.48
PA14_RS 13705	non-ribosomal peptide synthetase	5.54	PA14_RS 00955	OprD family porin	-2.38	PA14_RS 14250	hypothetical protein	3.42
PA14_RS 00145	SulP family inorganic anion transporter	5.08	PA14_RS 14015	sn-glycerol-3-phosphate ABC transporter ATP-binding protein UgpC	-2.86	PA14_RS 14245	hypothetical protein	3.2
PA14_RS 27705	acetyl-CoA sensor PanZ family protein	4.38	PA14_RS 18320	urea transporter	-3.59	PA14_RS 15735	MFS transporter	-2.8
PA14_RS 15410	TonB-dependent receptor	2.65	PA14_RS 11430	PA2778 family cysteine peptidase	-3.68	PA14_RS 15685	3-hydroxybutyrate dehydrogenase	-3.58

Gene	Product	FC	Gene	Product	FC	Gene	Product	FC
PA14_RS 02190	chemotaxis signal transduction system protein ChpA	-2.03	PA14_RS 04775	ethanolamine permease	-4	PA14_RS 28930	L-serine ammonia-lyase	-3.87
PA14_RS 19435	4-hydroxyproline epimerase	-2.97	PA14_RS 26910	ABC transporter substrate-binding protein	-5.13	PA14_RS 10725	bifunctional cobalt-precorrin-7 (C(5))-methyltransferase/cobalt-precorrin-6B (C(15))-methyltransferase	-6.71
PA14_RS 15735	MFS transporter	-3.29	PA14_RS 14050	acyl-CoA/acyl-ACP dehydrogenase	-5.57	PA14_RS 14895	4-alpha-glucanotransferase	-10.3
PA14_RS 11025	LysR family transcriptional regulator	-5.69	PA14_RS 31435	hypothetical protein	-6.07			
PA14_RS 13990	SfnB family sulfur acquisition oxidoreductase	-6.37	PA14_RS 15690	short-chain fatty acid transporter	-6.89			
PA14_RS 19590	TolC family protein	-7.01	PA14_RS 03280	hypothetical protein	-7.57			
PA14_RS 21505	TRAP transporter large permease	-7.57	PA14_RS 00455	type VI secretion system ATPase TssH	-7.79			
PA14_RS 15470	hypothetical protein	-8.14	PA14_RS 07425	alginate biosynthesis protein Alg44	-10			
PA14_RS 00940	ABC transporter ATP-binding protein	-8.73	PA14_RS 30640	type III secretion system needle length determinant PscP	-10.2			
PA14_RS 25145	fimbrial biogenesis outer membrane usher protein	-9.4	PA14_RS 07420	alginate biosynthesis TPR repeat lipoprotein AlgK	-10.9			

FC, fold change; pe, post exposure.

3.3 Discussion

Due to the superior activity of cystobactamids against a broad-spectrum of Gram-negative and Gram-positive bacteria, we set out to characterize their activity against the important and hard-to-treat pathogen *P. aeruginosa*. The overall goal was to characterize the *in vitro* potency and antibacterial mechanism of the natural product Cys861-2 and its semi-symnthetic derivative CN-DM-861. Further, the mechanism-of-resistance of cystobactamids in *P. aeruginosa* was studied. Compared to other cystobactamid-sensitive bacterial species, we found only moderate activity against *P. aeruginosa*. The main cause of *P. aeruginosa* being non-susceptible to cystobactamids appears to be efflux through the constitutively expressed *MexAB*-OprM system, both in PA14 and PAO1 strains. The semi-synthetic derivative CN-DM-861 only showed a minimal improvement in activity compared to the natural derivative Cys861-2. Although we did not detect any activity of cystobactamids on ESBL-producing *P. aeruginosa*, we did observe activity on FQ-resistant clinical isolates and MDR strains. Genome analysis of clinical isolates resistant to both cystobactamids and ciprofloxacin, and clinical isolates sensitive to cystobactamid but resistant to ciprofloxacin, could help identifying the determinants responsible for the divergence in sensitivity. Nevertheless, we obtained median MICs of 4 µg/mL for both derivatives across a panel of clinical isolates of *P. aeruginosa*. This prompted us to assess whether cystobactamids can prevent *P. aeruginosa* to form biofilms. Biofilms are especially difficult to treat due to decreased antibiotic penetration and failure to be recognized and cleared by the host immune system as is the case in CF [261]. Furthermore, *P. aeruginosa* readily forms biofilm on catheters and ventilators leading to increased risk of exposure of hospitalized patients to a potentially deadly biofilm infection. We were able to show that cystobactamids effectively reduce biofilm formation already at sub-inhibitory concentrations, additionally confirmed by observed reduction of eDNA detected in the presence of cystobactamids. Cystobactamids could therefore present a new alternative treatment option.

However, more in-depth studies are needed to fully elucidate and evaluate cystobactamids´ potential to inhibit biofilm formation. The observed differences in terms of resistance patterns (MIC shift and cross-resistance with ciprofloxacin) of the cystobactamid-resistant *P. aeruginosa* mutants cannot be fully explained by their corresponding genotypes; they all carry mutations in the same genes, *cpxS* or *cpxR*, and only a few resistant mutants have additional mutations in PA14_RS004500 (putative peptide synthetase) and *tamB* (involved in membrane biogenesis). A study conducted by Lee et al. revealed that 91.7% of the Pa14 genome is present in PAO1, and that 95.8% of the PAO1 genome is present in Pa14 [262]. The observed differences in the resistant mutants could be explained by discrepancies in the two genomic backgrounds, however, larger comprehensive data sets are needed to discern whether genomic background is the cause of this dicrepancy.

P. aeruginosa combats the antibacterial activity of cystobactamids by upregulating genes responsible for nutrient uptake, iron and sulfur uptake, and by activating genes responsible for detoxification, osmotic protection, and stress response. Meylan and co-workers have shown that nutrient uptake of carbon sources stimulated the TCA cycle and affected downstream processes such as drug transport and the electron transport chain i.e. respiratory activity, which resulted in resistance to tobramycin [263], it is therefore possible that the same downstream effects happens upon cystobactamid exposure. Similarly, in *E. coli*, mutations in QseBC result in upregulation of genes responsible for replenishment of TCA cycle upon 2-oxoglutarat depletion for LPS modifications resulting in cystobactamid resistance. Whether upregulation of genes responsible for nutrient uptake could result in LPS modifications in *P. aeruginosa* is currently under investigation. Iron is crucial for energy production, DNA replication, electron transport and virulence, and is scavenged from the environment or from host proteins via pyoverdine and pyochelin siderophores. Furthermore, it was shown to be a contributing factor for pathogenesis of *P. aeruginosa in vivo*, especially in CF patients [264]. Iron uptake genes

were not only upregulated in *P. aeruginosa* exposed to cystobactamid, but they were also upregulated in cystobactamid-resistant *P. aeruginosa* mutant #3 with mutated *cpxS* (S236P). We are currently investigating whether the upregulated nonribosomal peptide synthetase (NRPS) belongs to another iron chelator. Whether CpxSR TCS acts as a transcriptional activator of pyochelin biosynthesis genes is currently unknown. Furthermore combination therapy of cystobactamids and iron chelators, several already approved by the FDA [265], could prove beneficial and could result in potentiated efficacy of cystobactamids against *P. aeruginosa*. Downregulates genes found are involved in ethanolamine uptake, biosynthesis and transport of alginate and glycogen formation. The downregulated genes found were surprising as ethanolamine serves as a carbon and nitrogen source and its utilization presents a growth advantage over organisms unable to grow on ethanolamine [266]. However, *in vitro* sufficient amounts of carbon are provided as rich medium was used, potentially explaining the repression of ethanolamine uptake genes. Additionally, in *E. coli* ethanolamine was found to be consumed for the modification of LPS molecules thereby hindering cystobactamid uptake. Genes involved in biosynthesis of alginate were also downregulated. Alginate is a polysaccharide that encapsulates *P. aeruginosa*, protects it from antibiotics and enables long-term survival as shown in patients with CF [267]. However, it was only found to be expressed in CF lung and not in other environments [268], explaining why these genes were downregulated in vitro upon cystobactamid exposure.

Resistance development experiments revealed that in *P. aeruginosa* lacking *mexAB*, resistance to cystobactamids is conferred via mutations in the two-component system CpxSR. Cpx response is known to mediate stress response and antibiotic resistance in *E. coli*, and it is regulated by the CpxAR two-component system resulting in cell envelope modifications [269]. CpxS in *P. aeruginosa* is presumed to be a homolog of CpxA in *E. coli* [270]. However, CpxSR is a two-component system found in pathogenic and nonpathogenic *P. aeruginosa* and it was

only recently described to play a role in cellular hysteresis. Cellular hysteresis is a change in cellular physiology induced by one antibiotic and sensitizes bacteria to another subsequently administered antibiotic, and cell response to β-lactams in *P. aeruginosa*. While negative cellular hysteresis, a fast acting mechanism, favored mutations in CpxS, with T163P being the most common mutation and resulting in moderate ciprofloxacin resistance [270], we only found one resistant mutant with this mutation, with S236P and I279T mutations being the predominant ones, however it could explain the observed CIP MIC shift in cystobactamid-resistant mutants. Additionally, CpxR was identified as a direct activator of the *MexAB*-OprM and MuxABC-OpmB [271] multidrug efflux pumps, inducing expression beyond basal levels, which is in line with our transcriptomics analysis of Cys861-2 resistant mutant lacking *mexAB* and harboring a *cpxS* S236P mutation. This mutant had strongly upregulated transcription of the *mux-opm* operon, together with upregulation of Spy/CpxP chaperones, known protein folding and degrading factors in *E. coli* under the control of Cpx regulon [272, 273]. Due to direct upregulation of *mex-opr* and *mux-opm* operon, and similarities with *E. coli* results, namely mutations observed in the QseBC TCS, we speculate that mutations in CpxR are also gain-in-function and upregulate expression of CpxP, leading to cell envelope modifications. Additionally, the *mux* operon was confirmed to be an orthologue of *mdtABCD* encoding a RND efflux pump in *E. coli* under the control of the BaeSR two-component system, conferring resistance to novobiocin [274]. Two other genes that were upregulated in the cystobactamid resistant mutant were *pchB* and *pchD*, genes involved in biosynthesis of pyochelin. Pyochelin is a siderophore produced under iron-limiting conditions, to ensure enough Fe^{3+} is available for DNA and RNA synthesis, DNA replication, energy production and electron transport, all essential biological functions [124, 275, 276]. However, to avoid cellular toxicity due to metal accumulation, a cation diffusion facilitator FieF effluxes Fe^{2+} and potentially other metal ions and regulates iron homeostasis in the bacterial cell [277, 278]. Since cystobactamids interfere with DNA replication and induce SOS response, it is likely that these mutations are linked to

compensation of cystobactamid mode of action and rather than to cystobactamid resistance. Furthermore, the other two genes upregulated in *cpxS* S236P cystobactamid-resistant mutant were *ydeI* and *ygiW*. YdeI and YgiW are oligosaccharide/oligonucleotide binding (OB-) fold proteins, both are known to interact with porins, OmpD and OmpF, respectively. YdeI is under RcsBCD, PmrAB and PhoPQ control in *Salmonella enterica*, and is important for resistance against polymyxin B, however, it does not modify the LPS of *Salmonella*. Both YdeI-OmpD and YgiW-OmpF interactions contribute to polymyxin resistance. The exact mechanism of polymixin resistance through the interaction of OB-proteins with porins is unknown in Gram-negatives. Furthemore, OB-fold proteins are made of five antiparallel sheets forming a closed or partially opened barrel that functions as a scaffold for the binding of small polymers, including nucleotides and sugars. However, bacterial OB-fold proteins lack residues needed for nucleotide binding and are of unknown function [279]. No information is available for YdeI and YgiW orthologues in *P. aeruginosa*, we therefore speculate that OB-fold proteins might be able to bind cystobactamids in the periplasmic space, temporarily sequester them, and in the interaction with the respective porin expel them back in the environment or they could contribute to LPS modification in a yet unknown way.

Taken together mutations in CpxSR might confer resistance to cystobactamids in three distinct ways, (i) cell envelope modifications by upregulation of Spy/CpxP expression, (ii) efflux through upregulation of MuxABC-OpmB expression, and (iii) limited uptake (YdeI-OmpF, YgiW-OmpF) or possible LPS modifications.

3.4 Materials and Methods

3.4.1 Minimal Inhibitory Concentration (MIC) and Minimal Bactericidal Concentration (MBC) determination

MIC [215] and MBC [216] values were determined as previously described.

3.4.2 Time-kill kinetics

Assay was performed as previously described in Chapter 1, with one modification. Tested concentrations equaled 4x MIC, 8x MIC and 16x MIC. Starting inoculum was $1\text{-}2\text{x}10^6$ CFU/mL.

3.4.3 Supercoiling assay

P. aeruginosa DNA Gyrase (Inspiralis, Norwick, UK) supercoiling assay was performed as previously described [103].

3.4.4 In vitro resistance development

Assay was performed as described in Chapter 2.

3.4.5 Fitness cost

Assay was performed as described in Chapter 2.

3.4.6 Isothermal microcalorimetry

Sample preparation, assay execution and analysis was performed as previously described [219]. Strains were grown overnight in MHB at 180 rpm and 37 °C. Starting OD_{600} was adjusted to 0.001. To assess fitness of mutants vs. wildtype, no compound was added. To assess the time-kill kinetics, compound dissolved in DMSO was added equaling 4x MIC, 8x MIC and 16x MIC in caMHB. DMSO concentration did not exceed 1%. Controls samples were ran in presence of DMSO.

3.4.7 Reversibility of resistant phenotype

Assay was performed as described in Chapter 2.

3.4.8 Motility

Assay was performed as previously described [280]. *P. aeruginosa* cultures were grown in LB at 180 rpm and 37°C overnight. One µL of overnight culture was spotted in the center of a plate, for swimming and swarming motility, and was incubated for 16 h at 37°C. For assessment of twitching motility we stab inoculated the agar plates at the interface of agar and petri dish, using sterile toothpicks. Twitching plates were incubated 48 h at 37°C. Diameters of motility zones were measured.

3.4.9 Biofilm formation

Assay was performed as previously described [280].

3.4.10 eDNA content

Strains were streaked out on CASO agar plates and incubated overnight at 37°C. Next day, a single colony was picked from the agar plate and used to inoculate 10 mL of LB medium. Liquid culture was incubated at 37°C and 200 rpm for 16 h. Overnight culture was centrifuged for 10 min at 1800 x g. Extracellular matrix was removed by gently shaking the centrifuged culture prior to discarding the supernatant. Culture was washed with 10 mL of PPGAS medium and centrifuged as before. Supernatant was discarded and pellet was resuspended in 5 mL of PPGAS with vortexing to ensure breakdown of bacterial cells. OD_{600} of resuspended culture was measured and adjusted to 0.02 in fresh 15 mL of PPGAS medium. 190 µL of culture was aliquoted to the microtiter plate wells and 10 µL of 1mg/mL propidium iodine was added. Plates were shaken for 60 s at 500 rpm and afterwards placed in a static incubator at 37°C for 24 h. The following day the cell suspension was removed by inverting the plate and brisk shaking followed by light tapping on the paper towel. Wells were washed once with 200 µL of PBS

followed by two washing steps with 200 µL of milliQ water. Finally the wells were filled with 100 µL of milliQ water and fluorescence was measured; excitation at 544 nm, emission at 620 nm. When effect of compounds was investigated we additionally added 2 µL of 100x stock solution to experimental wells; 2 µL of DMSO was added to control wells.

3.4.11 *In vivo* virulence

Embryos/larvae of brass line were used. All experiments performed ended at ≤120 hpf, and are, according to EU Directive 2010/63/EU, not considered animal experiments. Embryos/larvae were were anaesthetized through immersion in tricaine at a final concentration 170 µg/mL and injected into yolk sack with 50 CFU/larvae. Per condition, 30-50 larvae were used. Larvae were incubated in 0.3x Danieau´s solution at 28°C and under a 14 h/10 h light/dark cycle and regularly monitored.

3.4.12 Transcriptomics

<u>Sample preparation:</u>

For comparison of *P. aeruginosa* PA14Δ*mexAB* vs. PA14Δ*mexAB* Cys861-2R #3 transcriptome the strains were streaked out on a CASO agar plate and grown overnight at 37°C in a static incubator. Next day, a single colony was picked and used to inoculate 5 mL of MHB medium. Cultures were incubated for 18 h at 37°C and 200 rpm. Next, cultures were centrifuged at 15 000 rpm for 10 min, supernatant was discarded and pellets were frozen in liquid nitrogen and stored at - 80°C. To ascertain the effect of cystobactamid exposure on *P.aeruginosa* transcriptome, the culture was prepared as described above. However, liquid overnight culture was back diluted 100x, split in three parts and exposed to 0.5x MIC, 2x MIC and the third part was left untreated. After 20, 40 and 60 min the cultures were collected and centrifuged at 15 000 rpm for 10 min. Supernatant was discarded, pellets were frozen in liquid nitrogen and stored at - 80°C. All samples were done in triplicates.

<u>RNA extraction and cDNA library preparation:</u> For total RNA isolation, cell pellets were resuspended in 600 µL of lysis buffer (0.5 mg/mL lysozyme, TE pH 8.0). Next, 60 µL 10% w/v SDS was added and tubes were inverted. The mixtures were heated for 2 min to 64°C in a water bath, prior to the addition of 66 µL 3M NaOAc, pH 5.2, 1 M EDTA and mixed by inversion. Next, 750 µL phenol (Roti-Aqua phenol) was added, the tubes were inverted, and incubated for 6 min in the 64°C water bath. Afterwards, samples were put on ice, centrifuged 15 min, 13,000 rpm, 4°C, and the aqueous phases was transferred to 2 mL PLG tubes. After addition of 750 µL of chloroform, tubes were mixed vigorously for 20 s, centrifuged 12 min, 13,000 rpm, 4°C, and the aqueous layers were transferred to new 2 mL tubes. After the addition of 1.4 mL of 30:1 mix EtOH:3M NaOac, pH 6.5, RNA was precipitated at -20°C overnight, the pellets were washed once in 75% v/v ethanol, air-dried, and resuspended in 50 µL pre-warmed (65°C) water. To remove genomic DNA, RNA samples were incubated with 0.25 U of DNase I (Fermentas) per 1 µg of RNA for 45 min at 37°C and efficient removal was confirmed by control PCR. cDNA libraries were generated at Vertis Biotechnologie AG (Freising-Weihenstephan, Germany) – deliberately omitting an rRNA depletion step – as follows. Total RNA was sheared via ultrasound sonication, four 30-s pulses at 4°C, to generate on average 200- to 400-nt fragments. Fragments of <20 nt were removed using the Agencourt RNAClean XP kit (Beckman Coulter Genomics) and the Illumina TruSeq adapter was ligated to the 3' ends of the remaining fragments. First-strand cDNA synthesis was performed using M-MLV reverse transcriptase (NEB) wherein the 3' adapter served as a primer. The first-strand cDNA was purified, and the 5' Illumina TruSeq sequencing adapter ligated to the 3' end of the antisense cDNA. The resulting cDNA was PCR amplified to about 10 to 20 ng/µL using a high-fidelity DNA polymerase. The TruSeq barcode sequences were part of the 5' and 3' TruSeq sequencing adapters. The cDNA library was purified using the Agencourt AMPure XP kit (Beckman Coulter Genomics) and analyzed by capillary electrophoresis (Shimadzu MultiNA microchip).

Prepared Sequencing libraries were sequenced on a NextSeq 500 platform in single-read mode with a read length of 75 bp.

Computational analysis of RNA-Seq data: Illumina reads were initially quality trimmed with a Phred quality score cut-off of 20 and afterwards the adapter sequences were removed. Both trimming steps were done by cutadapt version 1.17 [281]. For size filtering and mapping the RNA-seq analysis tool READemption version 0.4.3 [282], which integrates the short read mapper segemehl [283], was used. All reads that had a length shorter than 20 nucleotides were discarded. The remaining reads were mapped, using segemehl's split align feature, to the *P. aeruginosa* genome (NCBI RefSeq accession number: ASWV00000000). Reads with an accuracy equal or greater than 95% were kept for further analysis. Gene quantification was carried out by READemption [282] and differential gene expression analysis was performed using DESeq2 version 1.20.0 [284].

3.4.13 Electron microscopy

Assay was performed as described in Chapter 2.

3.4.14 Whole genome sequencing

WGS was performed as described before in Chapter 2. Samples yielded 0.47-0.58 Gbp of data, which resulted in an estimated 71x-88x mean genome coverage. The raw data was then mapped to a reference sequence of *P. aeruginosa* Pa14, GenBank accession number ASWV00000000.

3.5 Supporting information

A

B

C

D
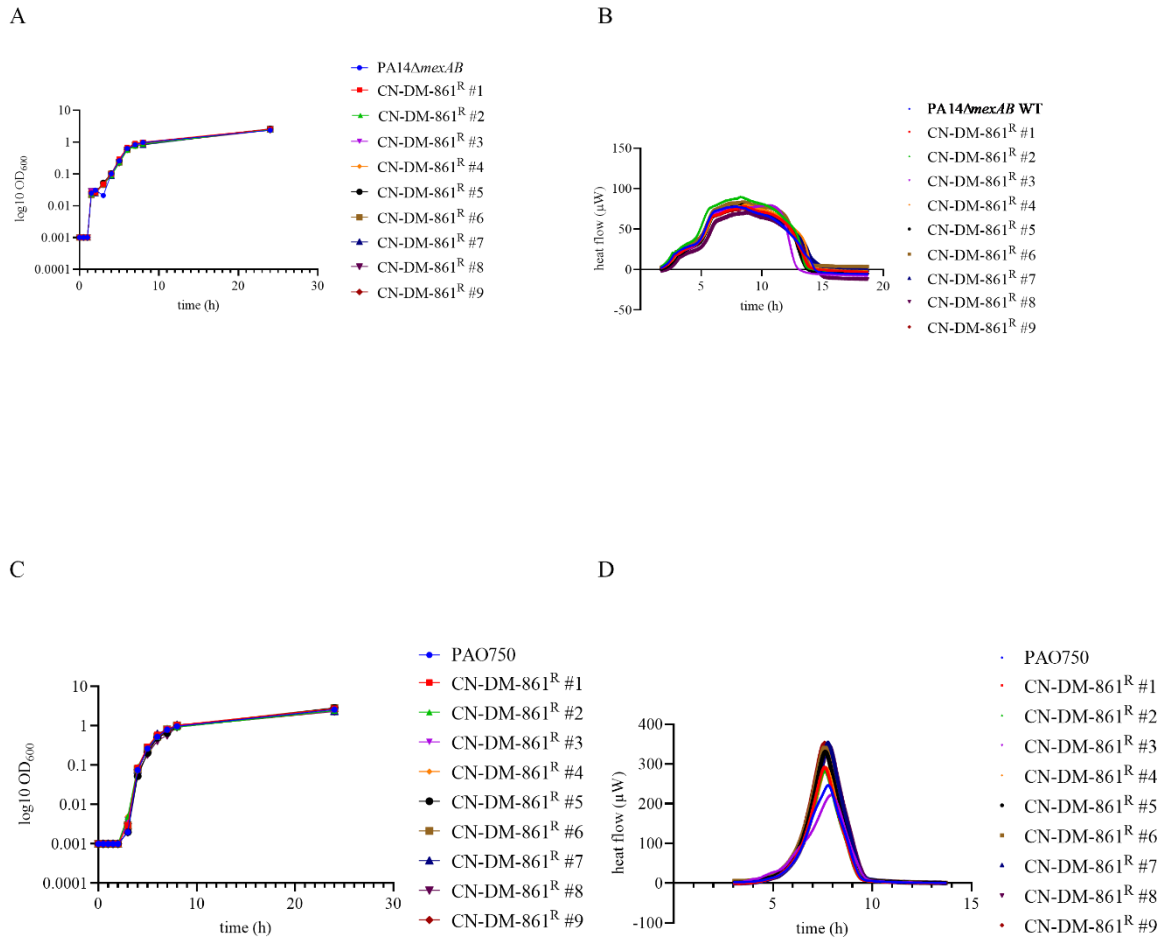
S1 Fig. Fitness assessed for *P. aeruginosa* PA14Δ*mexAB* and PAO750 CN-DM-861 resistant mutants.
(A) OD_{600} over time, *P. aeruginosa* PA14Δ*mexAB*. (B) ICM, *P. aeruginosa* PA14Δ*mexAB*. (C) OD_{600} over time, PAO750. (D) ICM, PAO750. [R], resistant.
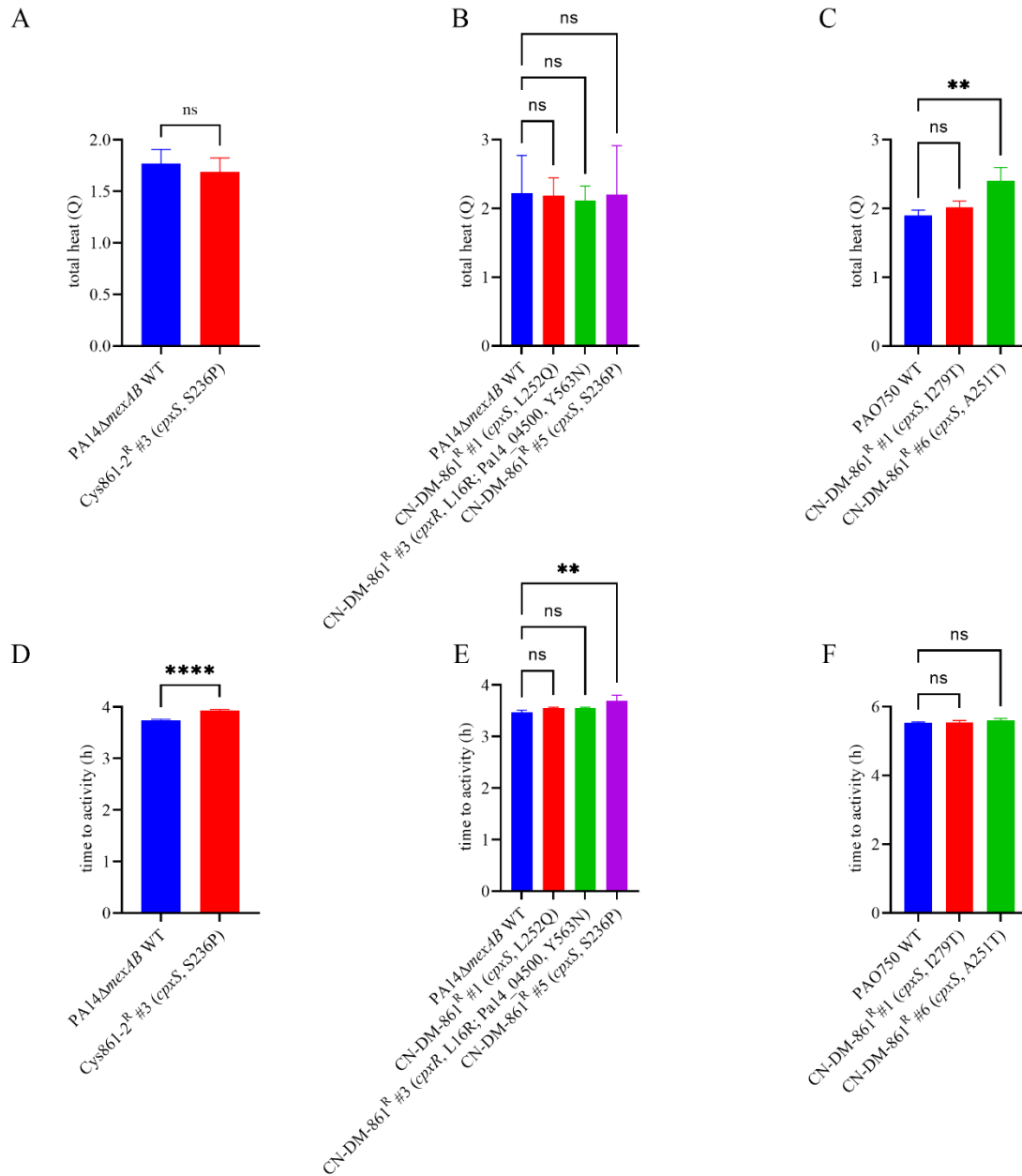
S2 Fig. Total heat and time to activity assessed for selected *P. aeruginosa* PA14Δ*mexAB* (Cys861-2 and CN-DM-861) and PAO750 (CN-DM-861) resistant mutants.
(A) Max metabolic velocity, *P. aeruginosa* PA14Δ*mexAB*, Cys861-2[R]. (B) Max metabolic velocity, *P. aeruginosa* PA14Δ*mexAB*, CN-DM-861[R]. (C) Max metabolic velocity, PAO750 CN-DM-861[R]. (D) Metabolic rate, *P. aeruginosa* PA14Δ*mexAB*, Cys861-2[R]. (E) Metabolic rate, *P. aeruginosa* PA14Δ*mexAB*, CN-DM-861[R]. (F) Metabolic rate, PAO750 CN-DM-861[R]. [R], resistant; Unpaired t-test and ordinary one-way ANOVA were used to analyze the data; ns, not significant; **, $p < 0.01$; ****, $p < 0.001$.
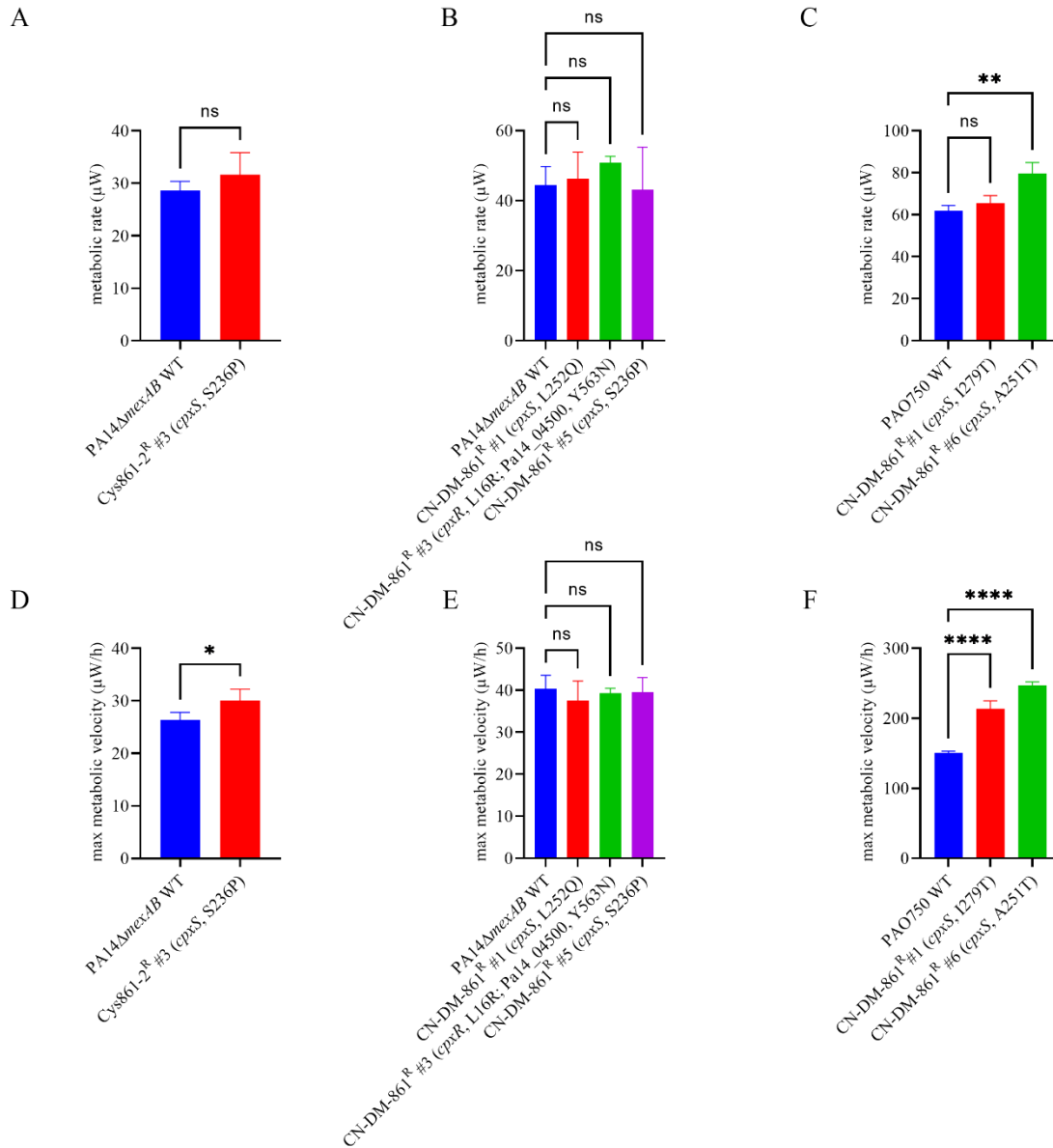
S3 Fig. Metabolic rate and max metabolic velocity assessed for selected *P. aeruginosa* PA14Δ*mexAB* (Cys861-2 and CN-DM-861) and PAO750 (CN-DM-861) resistant mutants.
(A) Metabolic rate, *P. aeruginosa* PA14Δ*mexAB*, Cys861-2[R]. (B) Metabolic rate, *P. aeruginosa* PA14Δ*mexAB*, CN-DM-861[R]. (C) Metabolic rate, PAO750 CN-DM-861[R]. (D) Max metabolic velocity, *P. aeruginosa* PA14Δ*mexAB*, Cys861-2[R]. (E) Max metabolic velocity, *P. aeruginosa* PA14Δ*mexAB*, CN-DM-861[R]. (F) Max metabolic velocity, PAO750 CN-DM-861[R]. [R], resistant; Unpaired t-test and ordinary one-way ANOVA were used to analyze the data; ns, not significant; *, $p < 0.05$; **, $p < 0.01$; ****, $p < 0.001$.
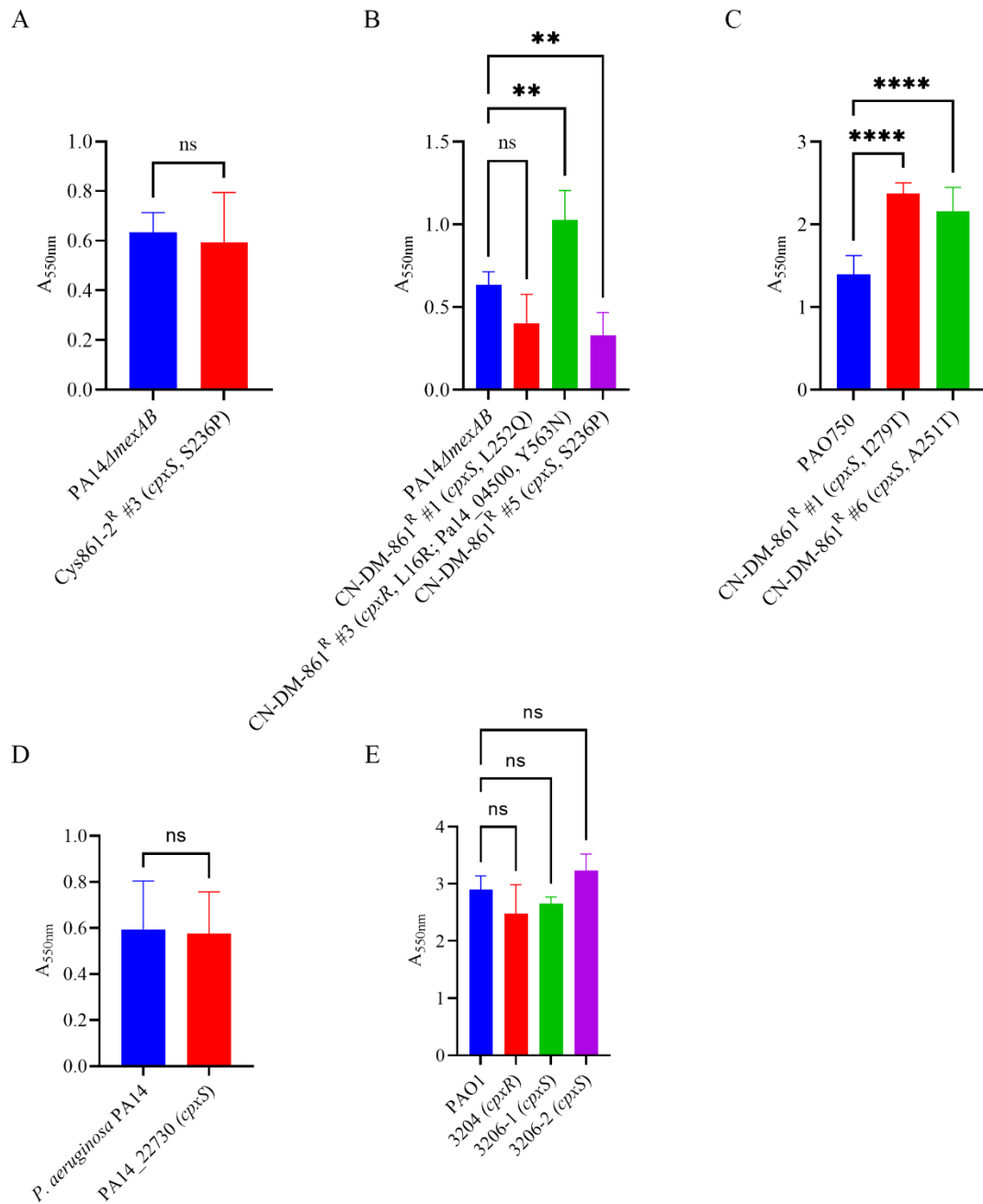
S4 Fig. Determination of biofilm formation for several wild-type strains, *P. aeruginosa* PA14, PA14Δ*mexAB*, PAO750 and PAO1, cystobactamid-resistant mutants and transposon mutants.
(A) *P. aeruginosa* PA14Δ*mexAB* wildtype and Cys861-2[R]. (B) *P. aeruginosa* PA14Δ*mexAB* wildtype and CN-DM-861[R]. (C) PAO750 wildtype and CN-DM-861[R]. (D) *P. aeruginosa* PA14 wildtype and *cpxS* transposon mutant. (E) PAO1 wildtype and *cpxR* (3204) and *cpxS* (3206-1, 3206-2) transposon mutants. [R], resistant; Unpaired t-test and ordinary one-way ANOVA were used to analyze the data; ns, not significant; **, $p < 0.01$; ****, $p < 0.001$.

A
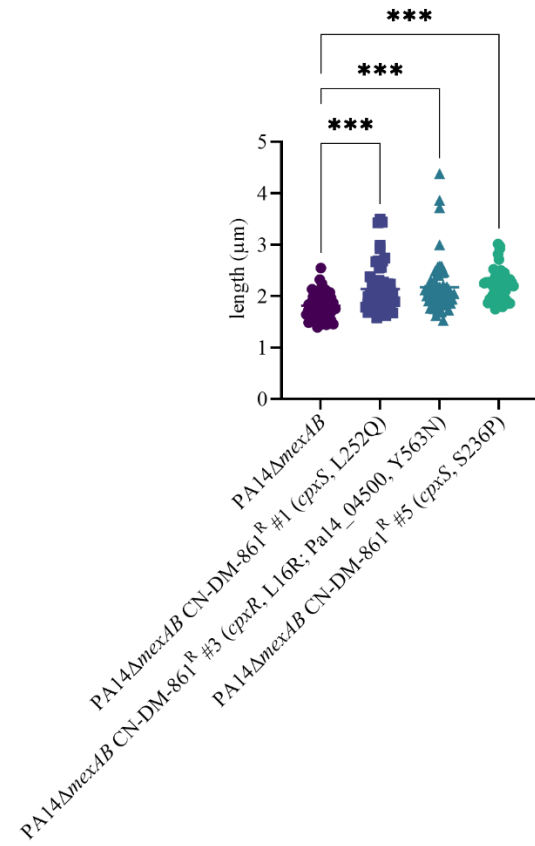
B
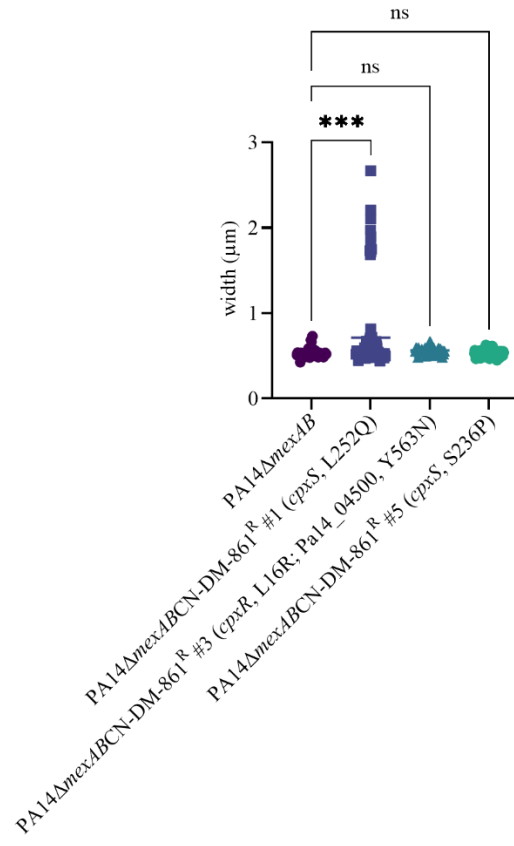
C
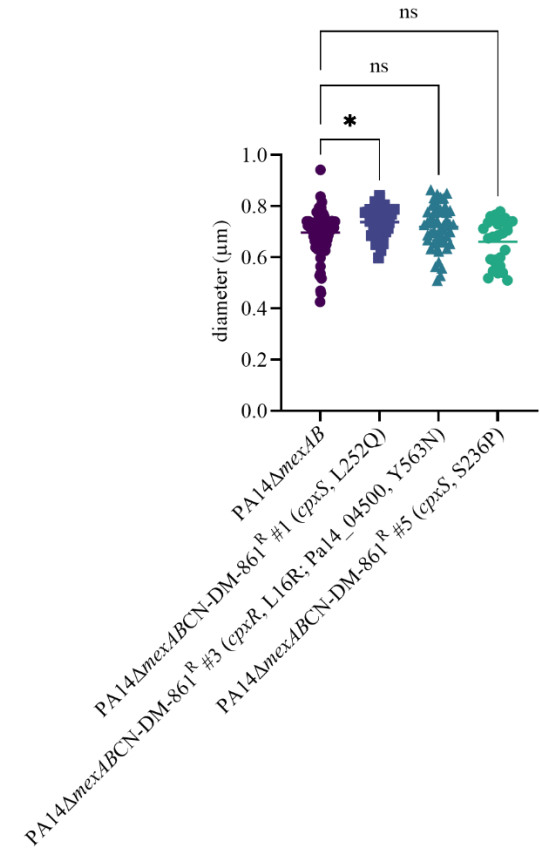
S5 Fig. Bacterial cell dimensions of *P. aeruginosa* PA14Δ*mexAB* wildtype and CN-DM-861^R mutants.
(A) Length of bacterial cells. (B) Width of bacterial cells. (C) Diameter of bacterial cells. Ordinary one-way ANOVA was used to analyze the data; ns, not significant; *, $p < 0.05$; ***, $p < 0.005$.
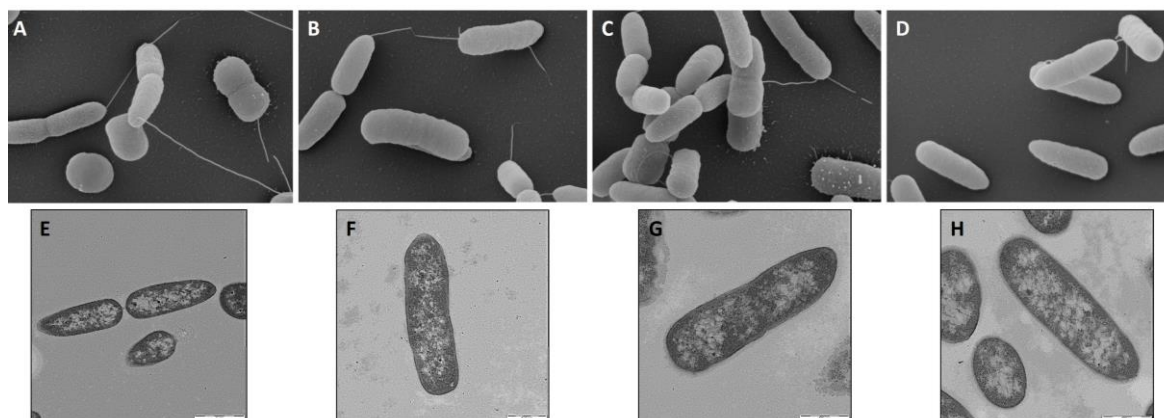
S6 Fig. Electron microscopy of *P. aeruginosa* PA14Δ*mexAB* wildtype and CN-DM-861^R mutants.
(A-D) Scanning electron microscopy. (E-H) Transmission electron microscopy. (A, E) *P. aeruginosa* PA14Δ*mexAB*, wildtype. (B, F) *P. aeruginosa* PA14Δ*mexAB* CN-DM-861^R #1 (*cpxS*, L252Q). (C, G) *P. aeruginosa* PA14Δ*mexAB* CN-DM-861^R #3 (*cpxR*, L16R; Pa14_04500, Y563N). (D, H) *P. aeruginosa* PA14Δ*mexAB* CN-DM-861^R #5 (*cpxS*, S236P).
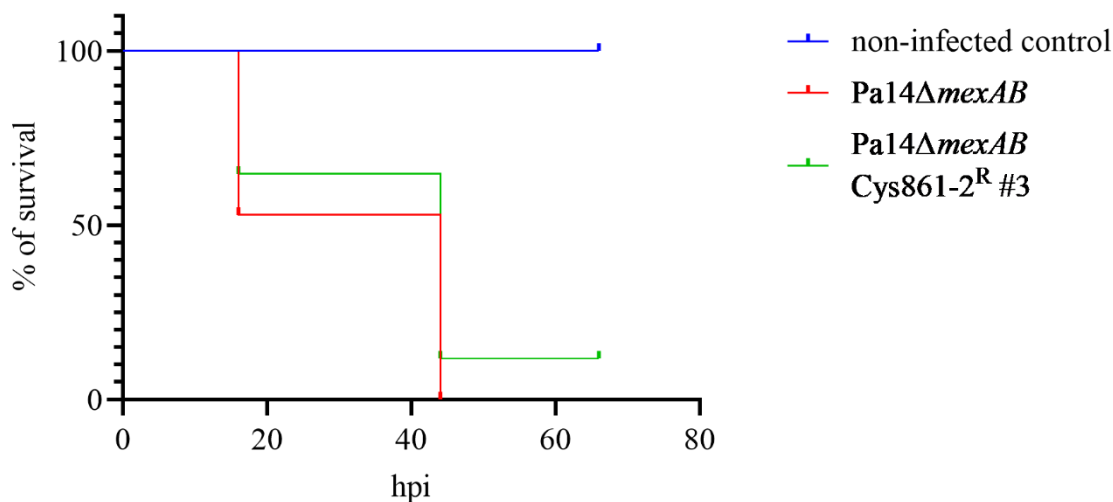
S7 Fig. *In vivo* virulence.
Brass larvae, infected at 28 hpf into yolk sack with 50 CFU/larvae.
hpf, hours post fertilization; hpi, hours post infection. Kaplan-Meier survival analysis was used to analyze the data.

S1 Table. MIC shift determined for Cys861-2, CN-DM-861 and ciprofloxacin on *P. aeruginosa* cystobactamid resistant mutants.

	MIC [µg/mL]			MIC shift		
strain	Cys861-2	CN-DM-861	CIP	Cys861-2	CN-DM-861	CIP

PA14Δ*mexAB*	0.25	0.25	0.01	na	na	na
PA14Δ*mexAB* Cys861-2[R] #1	> 64	nd	0.0125	> 256	nd	1
PA14Δ*mexAB* Cys861-2[R] #2	> 64	nd	0.0125	> 256	nd	1
PA14Δ*mexAB* Cys861-2[R] #3	> 64	nd	0.0125	> 256	nd	1
PA14Δ*mexAB* Cys861-2[R] #4	> 64	nd	0.0125	> 256	nd	1
PA14Δ*mexAB* Cys861-2[R] #5	> 64	nd	0.0125	> 256	nd	1
PA14Δ*mexAB* CN-DM-861[R] #1	nd	> 64	0.8	nd	> 256	80
PA14Δ*mexAB* CN-DM-861[R] #2	nd	> 64	0.4	nd	> 256	40
PA14Δ*mexAB* CN-DM-861[R] #3	nd	> 64	0.4	nd	> 256	40
PA14Δ*mexAB* CN-DM-861[R] #4	nd	> 64	0.8	nd	> 256	80
PA14Δ*mexAB* CN-DM-861[R] #5	nd	> 64	0.8	nd	> 256	80
PA14Δ*mexAB* CN-DM-861[R] #6	nd	> 64	0.8	nd	> 256	80
PA14Δ*mexAB* CN-DM-861[R] #7	nd	> 64	0.8	nd	> 256	80
PA14Δ*mexAB* CN-DM-861[R] #8	nd	> 64	0.8	nd	> 256	80
PA14Δ*mexAB* CN-DM-861[R] #9	nd	> 64	0.4	nd	> 256	40
PAO750	nd	2	0.005	nd	na	na
PAO750 CN-DM-861[R] #1	nd	32	0.005	nd	16	1
PAO750 CN-DM-861[R] #2	nd	16	0.005	nd	8	1
PAO750 CN-DM-861[R] #3	nd	16	0.0025	nd	8	0.5
PAO750 CN-DM-861[R] #4	nd	16	0.0025	nd	8	0.5
PAO750 CN-DM-861[R] #5	nd	16	0.0025	nd	8	0.5
PAO750 CN-DM-861[R] #6	nd	32	0.08	nd	16	16
PAO750 CN-DM-861[R] #7	nd	> 64	0.04	nd	> 32	8
PAO750 CN-DM-861[R] #8	nd	> 64	0.005	nd	> 32	1
PAO750 CN-DM-861[R] #9	nd	> 64	0.04	nd	> 32	8

CIP, ciprofloxacin; na, not applicable; nd, not determined.
[R] resistant.

S2 Table. Co-/cross-resistance of PA14Δ*mexAB* and PAO750 resistant to CN-DM-861 with relevant clinical antibiotics.

strain	antibiotic	ceftazidime	aztreonam	gentamicin	colistin	meropenem
				diameter [mm]		
	disc potency (µg)	30	30	10	10	10
PA14Δ*mexAB*	wt	28	32	24	12	40
	CN-DM-861[R] #1	27	29	22	12	39
	CN-DM-861[R] #2	30	32	24	12	40
	CN-DM-861[R] #3	26	31	22	12	40
	CN-DM-861[R] #4	30	32	25	12	40
	CN-DM-861[R] #5	28	33	24	12	40
	CN-DM-861[R] #6	29	34	22	12	42
	CN-DM-861[R] #7	30	32	22	12	40
	CN-DM-861[R] #8	28	31	22	12	40
	CN-DM-861[R] #9	29	35	22	12	40
PAO750	wt	27	30	23	11	32
	CN-DM-861[R] #1	20	34	24	11	35
	CN-DM-861[R] #2	27	30	23	11	31
	CN-DM-861[R] #3	30	34	25	11	34
	CN-DM-861[R] #4	30	35	24	12	34
	CN-DM-861[R] #5	28	32	22	11	32
	CN-DM-861[R] #6	28	32	24	12	32
	CN-DM-861[R] #7	28	32	22	12	31
	CN-DM-861[R] #8	27	31	24	11	31
	CN-DM-861[R] #9	29	31	24	11	31

In green sensitive phenotype.

S3 Table. Reversibility of resistance determined for selected *P. aeruginosa* clones obtained in resistance development to CN-DM-861.

MIC [µg/mL]

strain	starting point		passage 3		passage 10	
	CN-DM-861	CIP	CN-DM-861	CIP	CN-DM-861	CIP
PA14Δ*mexAB*	0.25	0.01	0.25	0.01	0.25	0.01
PA14Δ*mexAB* CN-DM-861[R] #4	> 64	0.8	> 64	0.4	> 64	0.4
PAO750	2	0.005	2	0.005	2	0.005
PAO750 CN-DM-861[R] #5	16	0.0025	32	0.005	32	0.005
PAO750 CN-DM-861[R] #7	> 64	0.04	> 64	0.02	> 64	0.005

CIP, ciprofloxacin.
[R] resistant.

Table S4. Different motility types assessed for *P. aeruginosa* (cystobactamid resistant mutants, *cpxS* and *cpxR* transposon mutants and their respective wildtype).

strain	mutant	Motility		
		Swimming	swarming	twitching
PA14Δ*mexAB*	WT			
	CN-DM-861[R] #1	+	+	≈
	CN-DM-861[R] #3	+	+	+
	CN-DM-861[R] #5	+	+	+
PAO750	WT			
	CN-DM-861[R] #1	-	-	-
	CN-DM-861[R] #6	-	-	-
PAO1	WT			
	3204	-	+	-
	3206-1	≈	+	-
	3206-2	-	-	-
PA14	WT			
	22730	≈	≈	-

[R], resistant; WT, wildtype; +, increase; -, decrease, ≈, no change.

Table S5. Full list of differentially expressed genes found in transcriptome analysis of PA14Δ*mexAB* Cys861-2^R mutant #3 compared to its respective wildtype.

locus tag	product	2log fold change
PA14_RS28950	YeiH family protein	12.17
PA14_RS28955	alpha/beta hydrolase	11.37
PA14_RS09225	Spy/CpxP family protein refolding chaperone	8.64
PA14_RS05075	hypothetical protein	8.37
PA14_RS01705	YgiW/YdeI family stress tolerance OB fold protein	7.58
PA14_RS05080	CDF family cation-efflux transporter FieF	7.37
PA14_RS00850	purine permease	6.94
PA14_RS09220	HAMP domain-containing histidine kinase	6.7
PA14_RS15410	TonB-dependent receptor	6.28
PA14_RS13040	multidrug efflux RND transporter periplasmic adaptor subunit MuxA	5.93
PA14_RS15065	molecular chaperone	5.67
PA14_RS13045	multidrug efflux RND transporter permease subunit MuxB	5.37
PA14_RS03745	isochorismate lyase PchB	5.07
PA14_RS05085	hypothetical protein	5.02
PA14_RS13050	multidrug efflux RND transporter permease subunit MuxC	4.98
PA14_RS13055	multidrug efflux RND transporter outer membrane subunit OpmB	4.86
PA14_RS23880	PepSY domain-containing protein	4.86
PA14_RS03755	pyochelin biosynthesis salicyl-AMP ligase PchD	4.78
PA14_RS01740	YjiK family protein	4.68
PA14_RS12125	PepSY domain-containing protein	4.55
PA14_RS07145	bifunctional transcriptional activator/DNA repair protein Ada	4.53
PA14_RS13060	hypothetical protein	4.35
PA14_RS03765	pyochelin non-ribosomal peptide synthetase PchE	4.34
PA14_RS22270	LysR family transcriptional regulator	4.13

PA14_RS03770	pyochelin non-ribosomal peptide synthetase PchF	4.12
PA14_RS03775	pyochelin biosynthesis thiazoline reductase PchG	4.07
PA14_RS07250	cytochrome b	4.04
PA14_RS12130	PepSY domain-containing protein	4.03
PA14_RS04205	hypothetical protein	3.94
PA14_RS22275	hypothetical protein	3.94
PA14_RS09205	YkgJ family cysteine cluster protein	3.91
PA14_RS18830	hypothetical protein	3.88
PA14_RS07150	MHS family MFS transporter	3.87
PA14_RS09210	nitroreductase family protein	3.86
PA14_RS01710	histone deacetylase family protein	3.85
PA14_RS09215	hypothetical protein	3.82
PA14_RS03740	isochorismate synthase PchA	3.76
PA14_RS03780	ABC transporter ATP-binding protein PchH	3.7
PA14_RS03785	ABC transporter ATP-binding protein PchI	3.67
PA14_RS03795	hypothetical protein	3.64
PA14_RS02485	RNA polymerase sigma factor	3.61
PA14_RS03790	Fe(3+)-pyochelin receptor FptA	3.43
PA14_RS12135	response regulator transcription factor	3.37
PA14_RS13065	sensor histidine kinase	3.16
PA14_RS04200	FAD-binding protein	3.15
PA14_RS05970	aldo/keto reductase	2.96
PA14_RS21270	response regulator transcription factor	2.94
PA14_RS02255	multidrug efflux RND transporter permease subunit MexB	2.87
PA14_RS05090	ATP-dependent helicase HrpB	2.74
PA14_RS03760	pyochelin biosynthesis transcriptional regulatorPchR	2.7
PA14_RS07485	bacterioferritin-associated ferredoxin	2.43
PA14_RS00520	carbonic anhydrase	2.42

PA14_RS14195	chitinase	2.39
PA14_RS13795	transcriptional repressor	2.38
PA14_RS04195	hypothetical protein	2.36
PA14_RS02250	multidrug efflux RND transporter periplasmic adaptor subunit MexA	2.35
PA14_RS04190	HlyD family efflux transporter periplasmic adaptor subunit	2.29
PA14_RS07245	hypothetical protein	2.27
PA14_RS16190	phenazine biosynthesis protein phzB 2	2.25
PA14_RS02260	multidrug efflux RND transporter outer membrane channel subunit OprM	2.21
PA14_RS18960	RNA polymerase sigma factor	2.14
PA14_RS16160	HIT family protein	2.11
PA14_RS12140	sensor histidine kinase	2.09
PA14_RS08425	putative isomerase	-2.05
PA14_RS08415	putative acyl carrier protein	-2.06
PA14_RS08410	uncharacterized protein	-2.07
PA14_RS26440	putative transcriptional regulator	-2.37
PA14_RS14505	possible glycosyl transferase	-2.41
PA14_RS10810	putative enoyl-CoA hydratase	-2.72
PA14_RS20330	uncharacterized protein	-3.17
PA14_RS26930	putative transcriptional regulator, GntR family	-3.82
PA14_RS29190	aminotransferase	-4.13
PA14_RS16835	nitrate/nitrite transporter	-4.32
PA14_RS13565	PvdL	-4.55
PA14_RS14005	xylulose kinase (Xylulokinase) (EC 2.7.1.17)	-4.74
PA14_RS13320	probable MFS transporter	-5.11
PA14_RS08045	putative membrane protein	-5.24
PA14_RS00395	uncharacterized protein	-5.31
PA14_RS22000	urease accessory protein	-5.35

PA14_RS04850	possible hydrolase	-5.4
PA14_RS04405	putative transcriptional regulator, AraC family	-7.02
PA14_RS11815	putative protease	-9.35

Chapter 4

4 AlbA-mediated mode of resistance in *Klebsiella pneumoniae*

4.1 Introduction

K. pneumoniae is a rod-shaped, Gram-negative [285] microorganism commonly found in the gastrointestinal and respiratory tract, and on the skin of humans and animals. It can also be found in the environment, *e.g.* in soil or surface water [286]. Two pathotypes of *K. pneumoniae* exist; classical *K. pneumoniae* (cKp), an opportunistic pathogen associated with hospital-acquired infections of immunocompromised individuals, and hypervirulent *K. pneumoniae* (hvKp), a community-acquired pathogen infecting healthy individuals, which can cause *e.g.* necrotizing fasciitis and meningitis. cKp causes UTIs, cystitis, pneumonia, surgical wound infections, septicemia, endocarditis, and device-associated infections, accounting for a third of all Gram-negative infections [287]. *K. pneumoniae* infections are highly problematic, not only because of its intrinsic resistance to antibiotics, but also because of its ability to readily accept and disseminate mobile genetic elements carrying antibiotic resistance determinants [288]. The most problematic are ESBL- and carbapenemase-producing *K. pneumoniae*, producing TEM, CTX-M, NDM-1, VIM, OXA enzymes, as they confer resistance to third-generation cephalosporins, some but not all fourth-generation cephalosporins, aztreonam and all β-lactams [287]. Plasmid-mediated resistance against quinolones (*qnr* genes and *aac(6´)-lb-cr*) and aminoglycosides (*aac*, *ant* and *aph* gene families), coupled with chromosomally encoded determinants (target protecting enzymes and antibiotic modifying enzymes) and acquired resistance (target mutations, decreased drug uptake, and increase in MDR efflux pump expression), are the main cause of non-susceptible phenotypes [289]. Common intrinsic resistance is caused by chromosomally encoded SHV β-lactamase [19], and multidrug efflux pumps such as OqxAB [21], AcrAB, EefAB KmrA, CepA and KexD [290, 291], resulting in

resistance to β-lactams, fluoroquinolones and aminoglycosides. Moreover, overproduction of the extracellular capsule, LPS modifications, secretion of LPS-containing vesicles and expression of peptidoglycan-associated lipoproteins, additionally hamper antibiotic efficacy [292]. Currently, carbapenems serve as a first line of defense against ESBL-producing *K. pneumoniae*, high-dose carbapenem therapy used in combination with second line antibiotics, such as tigecycline, gentamicin and fosfomycin is the recommended treatment for carbapenem-producing *K. pneumoniae*, with polymyxins, namely colistin, being the last line of defense [293].

According to the European Center for Disease Control and Prevention report on antimicrobial resistance surveillance the in EU/EEA between 2015-2019, carbapenem and fluoroquinolone resistance in *K. pneumoniae* was on the rise, third-generation cephalosporin resistance was stagnating, resistance to aminoglycosides and combined resistance to fluoroquinolones, aminoglycosides and third-generation cephalosporins had a minor negative trend. Over a third of isolates were resistant to more than one antibiotic under surveillance. Third-generation cephalosporin resistance was the most prevalent (31.3%), followed by fluoroquinolone resistance (31.2%), resistance to aminoglycosides (22.3%) and carbapenems (7.9%) [294]. Due to increasing difficulties in finding effective treatment options, the WHO is calling for accelerating and increasing research and development efforts to develop antibiotics targeting third-generation cephalosporin resistant Enterobacteriaceae, including *E. coli* and *K. pneumoniae* [115].

Albicidin, produced by the plant pathogen *Xanthomonas albilineans* [295], is structurally similar to cystobactamids (Fig. 1), and both compound classes exert their antibacterial activity through inhibition of type IIa topoisomerases. Due to the similarities between cystobactamids and albicidins, one could assume that resistance mechanisms that confer resistance to albicidin could also hinder the activity of cystobactamids. Three major albicidin resistance proteins are

described: AlbA (sequestering of albicidin without and with further chemical modification) from *Klebisella* spp. [99, 100], AlbD (endopeptidase that degrades albicidin) from *P. dispersa* [145], and AlbB (reversible binding of albicidins) from *A. denitrificans* [144]. Mutations in *E. coli* Tsx have also been described to confer resistance to albicidin, and are described and discussed in Chapter 2. We have previously shown that cystobactamids display moderate activity against AlbD-expressing *P. dispersa*, whereas albicidin was inactive. Additionally, amide-triazole replacement prevented cystobactamid degradation via AlbD and further enhanced the activity of cystobactamids against *P. dispersa* [105]. AlbA is the most relevant of the above mentioned enzymes as it commonly occurs in *K. pneumonia* and *K. oxytoca*, whereas AlbB and AlbD are found in bacteria not commonly known to cause human diseases.

TipA belongs to the superfamily of mercuric ion resistance (MerR)-like transcriptional regulators containing two alternative start codons, resulting in TipA-L and TipA-S protein isoforms identical in their C-terminal domains. TipA-S binds the antibiotic in the cytoplasm, and is the predominant form consisting only of an effector binding domain. This domain is able to covalently bind a wide variety of thiopeptide antibiotics and permanently sequester these compounds. TipA-L dimerizes after ligand binding and induces the transcription of multiple genes, including *tipA*. We have previously shown AlbA to be a member of the TipA family of multi-drug resistance autoregulatory systems, and found an alternative upstream start codon giving rise to AlbA-L and AlbA-S. AlbA was unable to covalently bind albicidin, unlike TipA binds its substrates, but formed a stable complex from which albicidin dissociates very slowly. In addition, we discovered that AlbA promotes the cyclization of albicidin, which leads to a loss of activity and decreased affinity. The mechanism of very tight binding combined with slow chemical modification may also be beneficial for for its role as a transcriptional regulator. Which transcriptional events may be controlled by AlbA-L requires further study. It is unclear if AlbA itself is a multi-drug resistance protein or merely evolved from such a system, since the

AlbA system is not induced by the related cystobactamid. Furthermore, we investigated the affinity of AlbA to albicidin and cystobactamid and could show that the affinity of AlbA towards albicidin is in the single-digit nanomolar range (K_D 2 nM), whereas the affinity towards cystobactamid was much lower (K_D 1.6 μM). This indicated that cystobactamid binding to AlbA does not cause dimerization of AlbA needed for it to exhibit its function as a transcriptional regulator [99]. These results prompted us to further investigate the possible mode of cystobactamid resistance in *K. pneumoniae*.
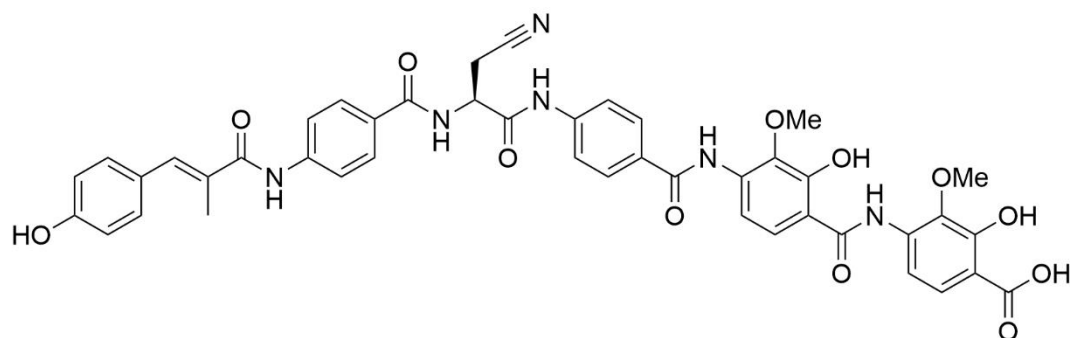
A
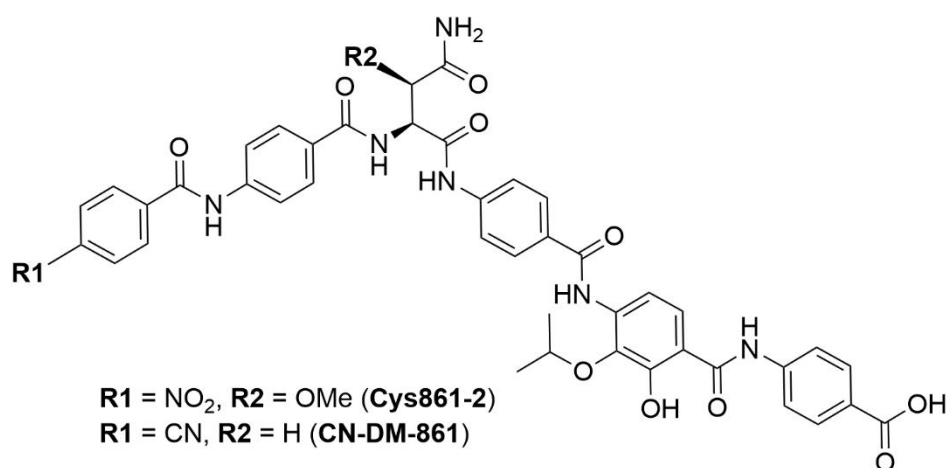
R1 = NO$_2$, R2 = OMe (**Cys861-2**)
R1 = CN, R2 = H (**CN-DM-861**)

B

Fig. 1. Chemical structures of cystobactamids and albicidin.
(A) Cystobactamids Cys861-2 and CN-DM-861. (B) Albicidin.

4.2 Results

4.2.1   Activity of cystobactamids against *K. pneumoniae* strains

We assessed the activity of Cys861-2 and CN-DM-861 using several *K. pneumoniae* and *K. oxytoca strains* (Table 1). Both, Cys861-2 and CN-DM-861, were highly active against *K. oxytoca*, with the synthetic derivative CN-DM-861 being on average more potent than natural derivative Cys861-2. Moreover, both derivatives were active on CTX-M producing *K. oxytoca* strains that were fully resistant to CIP. However, Cys861-2 and CN-DM-861 were inactive on most tested *K. pneumoniae* strains, with *K. pneumoniae* ATCC-43816 and DSM-30104 being the most sensitive wildtype strains. *K. pneumoniae* ATCC-43816 had a MIC of 0.06 µg/mL for CN-DM-861, whereas the MICs of Cys861-2 and CN-DM-861 on *K. pneumonia* DSM-30104 were 16 µg/mL and 1 µg/mL, respectively. The CIP resistant (MIC $\geq$ 0.2 µg/mL) strains of *K. pneumoniae* were all resistant to cystobactamids, however, it is not clear if there is a direct correlation between CIP and cystobactamid resistance due to general insufficient activity of the latter against *K. pneumoniae*. The QnrA1-expressing strain *K. pneumoniae* R1525 displayed weak susceptibility to Cys861-2 (MIC 16 µg/mL), but it was not susceptible to CN-DM-861. Similarly, *K. pneumoniae* 1161486 carrying *gyrA* (S83I) and *parC* (S80I) mutations was non-susceptible to both Cys861-2 and CN-DM-861, whereas moderate activity was observed for Cys861-2 (MIC 4 µg/mL) but not for CN-DM-861 on its isogenic parent strain. This led us conclude that FQ resistance mechanisms (target protection and target mutations) play a role in resistance towards cystobactamids but other factors might additionally hamper their activity against *K. pneumoniae*. The wildtype strain *K. pneumoniae* MKP103 was resistant towards cystobactamids, and the respective *ramA* (a transcriptional regulator of *lpx* genes involved in lipid A biosynthesis [296]) and *acrR* (a transcriptional regulator of the AcrAB-TolC efflux pump [291]) transposon mutants remained resistant. Interestingly, a *waaC* transposon mutant of *K. pneumoniae* MKP103, a heptose-less LPS mutant [297], was susceptible to both

cystobactamids. Interestingly, in *E. coli*, we found *waaH* significantly upregulated in a cystobactamid-resistant mutants bearing mutations in QseBC, resulting in addition of glucuronic acid to LPS core therefore increasing the positive charge of the OM. Taken together, our results suggest that the rather weak and inconsistent activity of cystobactamids against *K. pneumoniae* is mainly caused by insufficient drug penetration and it is not due to efflux. Uptake into K. *pneumoniae* seems to be hindered due to interactions of cystobactamids with sugar moieties of LPS (*waaC* mutant) and not due to lipid A modifications (*ramA* mutant). Finally, both *K. pneumoniae* and *K. oxytoca* express AlbA, however, *K. oxytoca* was sensitive to cystobactamids, indicating that the MoR of cystobactamids in *Klebsiella* spp. differs from the MoR of albicidin.

Table 1. MIC profile of Cys861-2, CN-DM-861 and CIP on selected *K. pneumoniae* and *K. oxytoca* strains.

Strain	MIC [µg/mL]		
	Cys861-2	CN-DM-861	CIP
K. pneumoniae DSM-30104	16	1	0.02
K. pneumoniae ATCC-43816	nd	0.06	0.06
K. pneumoniae CIP-104298	> 64	> 64	0.05
K. pneumoniae CIP-105705	> 64	2	0.2
K. pneumoniae CIP-106685	> 64	> 64	0.1
K. pneumoniae G306	> 64	> 64	> 6.4
K. pneumoniae G199	> 64	> 64	0.05
K. pneumoniae R1242	> 64	> 64	0.1
K. pneumoniae R1525 (QnrA1)	16	> 64	> 6.4
K. pneumoniae 1161486	4	> 64	0.1
K. pneumoniae 1161486 [*parC*(S80I) *gyrA*(S83I)]	> 64	> 64	> 6.4
K. pneumoniae MKP103 WT	> 64	> 64	> 6.4
K. pneumoniae KP02746 (*acrR*::Tn30)	> 64	> 64	> 6.4

Strain			
K. pneumoniae KP03197 (*ramA*::Tn30)	> 64	> 64	> 6.4
K. pneumoniae KP10581 (*waaC*::Tn30)	0.1	2	> 6.4
K. oxytoca ATCC-13182	1	0.125	0.025
K. oxytoca R1052 (CTX-M-3)	1	0.5	6.4
K. oxytoca R1053 (CTX-M-14)	4	2	> 6.4

WT, wildtype; nd, not determined.

Next, we assessed the activity of cystobactamids on a small panel of *K. pneumoniae* clinical isolates, including ESBL- and carbapenemase-producing isolates (Table 2). The median MIC and median MBC of Cys861-2 on *K. pneumoniae* clinical isolates were 16 µg/mL and 32-> 64 µg/mL, respectively. In contrast, the median MIC and median MBC of Cys861-2 on *K. oxytoca* were significantly lower than that of *K. pneumoniae* isolates and there was no shift between the inhibiting and bactericidal concentrations (2 µg/mL and 2 µg/mL, respectively). The four ESBL- or r carbapenemase-producing *K. pneumoniae* clinical isolates were resistant or displayed low susceptibility towards Cys861-2 .

Table 2. MIC and MBC determination on selected *K. pneumoniae* and *K. oxytoca* clinical isolates.

Strain	MIC [µg/mL]		MBC [µg/mL]	
	Cys861-2	MEMP	Cys861-2	MEMP
K. pneumoniae 3	16	> 64	16	> 64
K. pneumoniae 11	8	2	> 64	2
K. pneumoniae 13	1	≤ 0.06	2	≤ 0.06
K. pneumoniae 30[a]	> 64	32	> 64	64
K. pneumoniae 39[a]	> 64	64	> 64	16
K. pneumoniae 40	4	≤ 0.06	16	≤ 0.06
K. pneumoniae sc16203574[b]	> 64	> 64	> 64	> 64
K. pneumoniae UR17032073[b]	16	64	32	64
K. oxytoca 42	2	≤ 0.06	4	≤ 0.06

K. oxytoca 55	1	≤ 0.06	2	≤ 0.06
K. oxytoca 58	2	8	2	≤ 0.06
median *K. pneumonia*	16	32-64	32-> 64	16-64
median *K. oxytoca*	2	≤ 0.06	2	≤ 0.06

MEMP, meropenem.
[a], ESBL-producing.
[b], carbapenemase-producing.

Additionally, we testes a large panel of recent clinical isolates, collected in 2020 at Medical School Hannover, isolated from tracheal and bronchial sputum, bronchoalveolar lavage, midstream urine samples, urine catheters and renal pelvic aspirations (Table 3). Encouragingly, cystobactamid CN-DM-861 was active on CIP- and ceftazidime-resistant *K. pneumoniae* clinical isolates with MIC_{50} of 8 µg/mL and 4 µg/mL, respectively. However, the MIC_{90} of CN-DM-861 was > 32 µg/mL for both, ciprofloxacin- and ceftazidime-resistant *K. pneumoniae* clinical isolates. Antibiograms provided by Medical School Hannover stated that all 88 clinical isolates were fully resistant to amikacin and intermediately resistant to gentamicin. In general, CN-DM-861 showed a large MIC distribution but we could confirm the lack of cross-resistance between CIP and cystobactamids (Fig. 2).

Table 3. MIC_{50} and MIC_{90} determination of CN-DM-861, ciprofloxacin and cefotaxim on a large panel of *K. pneumoniae* clinical isolates.

strain	n	MIC_{50} [µg/mL]			MIC_{90} [µg/mL]		
		CN-DM-861	CIP	CTX	CN-DM-861	CIP	CTX
K. pneumoniae[a]	88	4	0.05	0.13	> 32	3.2	> 64
Kp CIP[R]	19	8	> 6.4	> 64	> 32	> 6.4	> 64
Kp CAZ[R]	14	4	1.6	> 64	> 32	> 6.4	> 64

CTX, cefotaxim; CAZ, ceftazidime; Kp, *K. pneumoniae*.
[a] recent clinical isolates.
[R] resistant.
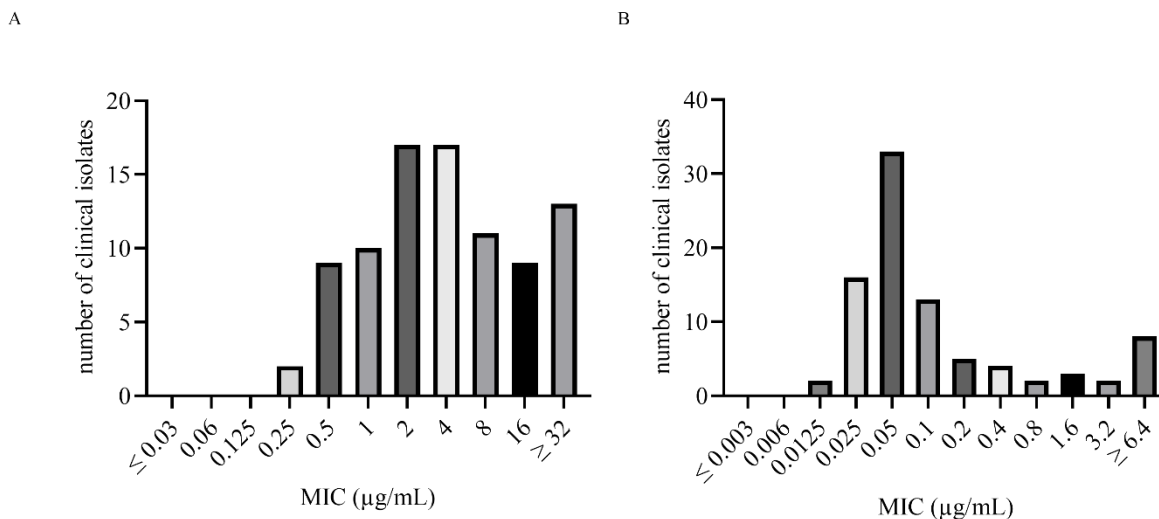
Fig. 2. MIC distribution for CN-DM-861 and CIP on recent of *K. pneumoniae* clinical isolates.
(A) CN-DM-861. (B) CIP.

4.2.2   Bactericidal mode of action

Using isothermal microcalorimetry, we assessed whether cystobactamid CN-DM-861 acts bactericidal or bacteriostatic on *K. pneumoniae* DSM-30104 (Fig. 3). For samples treated at 2x and 4x MIC, no metabolic activity was observed throughout the duration of the experiment, which let us to conclude that cystobactamid CN-DM-861 acts rapidly bactericidal. Most importantly, we did not observe any increase of emitted heat at any point for both tested concentrations, which would indicate regrowth due to either spontaneous resistance development or persistence.
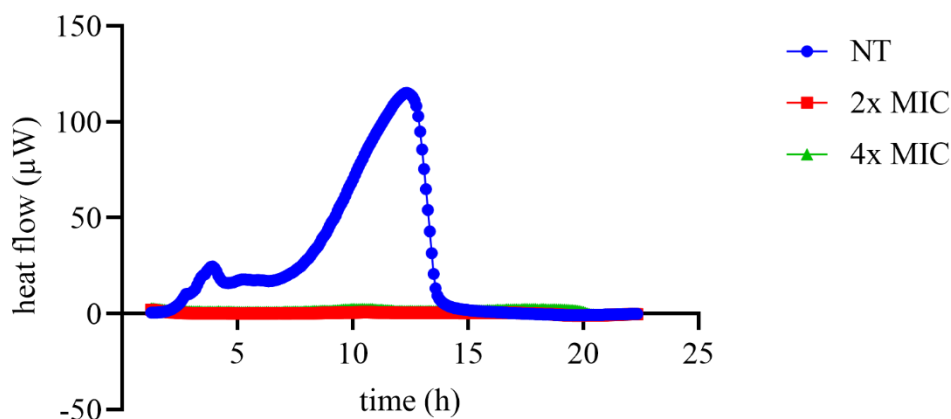
Fig. 3. Heat flow curves recorded for *K. pneumoniae* DSM-30104 exposed to 2x and 4x MIC cystobactamid CN-DM-861 and the non-treated control.
NT, non-treated.

4.2.3 Frequency of resistance and mutant characterization

Based on our previous findings [99] indicating that AlbA might not be involved in conferring resistance to cystobactamids, we decided to generate spontaneous cystobactamid-resistant mutants, which were initially analyze on the genome level (Table 4). We could not determine the frequency of resistance for *K. pneumoniae* ATCC-43816, despite its high susceptibility towards CN-DM-861. *K. pneumoniae* CIP-105705 displayed a high frequency of resistance for both CN-DM-861 and CIP. Only *K. pneumoniae* DSM-30104 exhibited an acceptable frequency of resistance in the range of 10^{-8} for CN-DM-861 and 10^{-10} for CIP. Increasing the compound concentration from 4x to 8x MIC for mutant selection did not significantly lower the frequency of resistance. Several *K. pneumoniae* DSM-30104 CN-DM-861 resistant mutants were selected for further characterization. All tested resistant mutants displayed a high level of resistance against CN-DM-861 with an MIC shift > 64-fold. However, no co-/cross-resistance with CIP was detected. Moreover, the resistant phenotype was not reversible even after ten subcultivations in non-selective medium. Interestingly, WGS revealed that all mutants harbored mutations in AlbA, and one mutant (#5) had an additional mutation in *trmJ*, encoding a tRNA methyltransferase. However, none of the observed mutations were at positions we previously

154

described as problematic, where we observed clashes with I95, T97, W110, F166 and Y169 residues and Cys919-2 (Fig. 4) [99].The cystobactamid-resistant mutants also did not exhibit any fitness changes on account of the mutations (Fig. 5). However, isothermal microcalorimetry revealed complete obliteration of metabolism in all resistant mutants in the stationary phase compared to the wildtype. This effect was directly linked to the mutant genotypes.

Table 4. Frequency of resistance, detailed characterization of resistant mutants and whole genome sequencing results.

	Frequency of Resistance			
	CN-DM-861		CIP	
Strain	4x MIC	8 x MIC	4x MIC	8 x MIC
K. pneumoniae DSM-30104	2.4×10^{-8}	9.7×10^{-8}	$\leq 1 \times 10^{-10}$	$\leq 1 \times 10^{-10}$
K. pneumoniae ATCC-43816	bacterial lawn	bacterial lawn	8×10^{-9}	$\leq 1 \times 10^{-9}$
K. pneumoniae CIP-105705	6.7×10^{-7}	nd	4.1×10^{-7}	nd
	CN-DM-861[R] mutant characterization			
	mutation in	MIC shift (CN-DM-861, parent vs. Cys[R] mutant)[a]	co-/cross-resistance with CIP[a] (CIP, parent vs. Cys[R] mutant)	reversibility of resistance[b]
K. pneumoniae DSM-30104	AlbA	> 64	2	no
	WGS results			
	mutant	MIC CN-DM-861 [µg/mL]	*alba*	*trmJ*
K. pneumoniae DSM-30104	WT	1	-	-
	#1	> 64	L97R	
	#2	> 64	L97V	
K. pneumoniae DSM-30104	#3	> 64	T122R	
	#4	> 64	N42K	
	#5	> 64	T122K	Fs

Fig. 4. Model of AlbA[wt] in complex with cystobactamid Cys919-2 [99].
Cystobactamid is shown as sticks (carbon atoms grey, oxygen atoms red, nitrogen atoms blue, hydrogen atoms white) and clashes with the protein as red discs. Protein residues responsible for the clashes are shown as cyan sticks and labeled, the protein is shown as a pale yellow cartoon. We used the AlbAwt-albicidin complex structure as a template to model an AlbA-cystobactamid Cys919-2 complex.
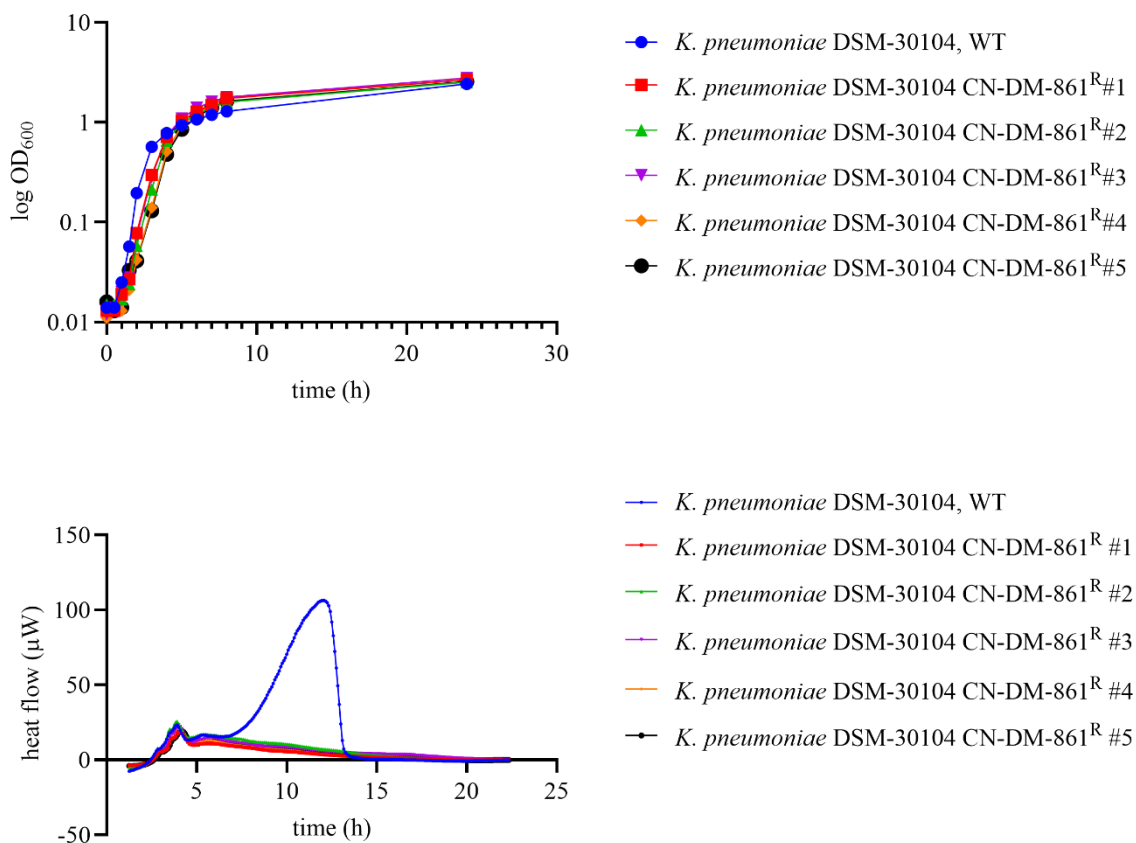
Fig. 5. Fitness assessment of *K. pneumoniae* CN-DM-861 resistant mutants in comparison to the sensitive wildtype.
(A) OD_{600} over time. (B) Heat flow (μW) over time.

4.2.4 *albA* expression levels in resistant mutants

Due to the unexpected WGS results, and the fact that we have previously shown that cystobactamid does not induce the expression of AlbA [99], we decided to determine the transcript levels of *albA* in resistant mutants using RT-qPCR. Surprisingly, both *albA-L* and *albA-S* transcript levels were significantly increased by 1800-fold and ~ 1700-fold,

respectively (Fig. 6), indicating that the obtained mutation allows dimerization of AlbA, which then, in turn, can act as a transcriptional regulator, primarily as an autoregulator.
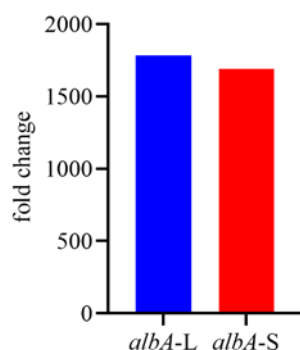
Fig. 6. Difference in transcription levels of *albA*-L and *albA*-S between a CN-DM-861 resistant mutant #1 (*albA*, L97R) compared to the wildtype.

4.3 Discussion

In contrast to *E. coli* and *P. aeruginosa*, where efflux hampered the activity of cystobactamids in the indicator strain panel (AcrAB-TolC and MexAB-Oprm mediated efflux), the outer membrane barrier appears to be the major (intrinsic) resistance factor in *K. pneumonia*. This finding was demonstrated by an > 640-fold increase of activity in the *waaC* disruption mutant of *K. pneumoniae* KP10581. Upon disruption of *waaC*, gene encoding a LPS heptosyl transferase I, core LPS lacks heptose, leading to architectural changes of the OM such as reduced protein content and ability to bind divalent cations, and increased sensitivity towards CAMP, detergents and salts [298, 299]. Due to substantial increase in sensitivity of *K. pneumonia waaC* mutant, we speculate that close interplay between LPS heptose and cystobactamids takes place in the wildtype background, presumably due to charge changes of the OM as was observed in *E. coli* cystobactamid-resistant mutants. Intracellular accumulation data are needed to guide the design and synthesis of new synthetic derivatives with optimized penetration traits and retained on-target activity in *K. pneumoniae*. Surprisingly, *K. oxytoca*

was generally sensitive towards cystobactamid treatment, including ESBL-producing (CTX-M) *K. oxytoca*. The same trends were observed in clinical isolates testing, with *K. oxytoca* being sensitive (MIC and MBC both 2 µg/mL) and *K. pneumonie* isolates displaying variable MIC and MBC distributions. Since both *K. pneumoniae* and *K. oxytoca* express AlbA, with the former being cystobactamid non-sensitive due to hindered influx and the latter cystobactamid sensitive, we speculate that the differences in the outer membrane composition, not just LPS, could be responsible for the observed efficacy differences between the two close Klebsiella relatives. One such difference is the presence of the outer membrane ion permeable channel CymA, uniquely described in *K. oxytoca* and is responsible for uptake of cyclodextrin, ~ 1000 Da in size [300]. Passage thorough the outer membrane happens in one of two ways, through passive diffusion channels with cut-off size of ~ 600 Da, and active transport of large, bulky molecules [301]. We have shown in *E. coli* that porins negligibly contribute to import of cystobactamids due to theirs size (~ 850 Da), but that their "longish" structure could compensate for this. Presence of CymA in *K. oxytoca*, able to passively import larger bulky compounds, could explain the observed activity on *K. oxytoca* that was not observed in *K. pneumoniae*. We speculate that cystobactamids could be imported via CymA and essentially bypass the negative charge of outer membrane. MIC determination on recently isolated clinical isolates showed that cystobactamid CN-DM-861 effectively kills FQR and 3GCR, with MIC_{50} of 8 µg/mL and 2 µ/mL, respectively. Due to the broad MIC distribution in clinical isolates, and a high number of isolates with CN-DM-861 MIC $\geq$ 32 µg/mL, MIC_{90} is > 32 µg/mL on both FQR and 3GCR. We previously observed that exposure of *K. pneumoniae* to cystobactamids does not induce *albA* transcription, assumingly due to different binding affinities of AlbA to albicidin and cystobactamid (K_D 2 nM and 1.6 µM, respectively). Furthermore, both *K. pneumoniae* and *K. oxytoca* express AlbA, with the former being resistant to cystobactamids and the latter susceptible, we hypothesized that high-level cystobactamid resistance in *K. pneumoniae* relies on an AlbA-independent mechanism. Surprisingly, cystobactamid resistant mutants carry

159

mutations in *albA*, and the mutants display significantly increased transcript levels of *albA*. In our previous work, we have shown that although cystobactamid fits relatively well in the substrate binding tunel of AlbA, certain amino acid residues clash with cystobactamid-specific functional groups: the terminal isopropoxy group of terminal PABA group of cystobactamid 919-2 clashes with W110, F166, and Y169 of AlbA, and the β-methoxy group in the central linker clashes with I95 and T99 amino acid residues. The compounds used in the current study do not have an isopropoxy group on ring D (both Cys861-2 and CN-DM-861), and CN-DM-861, but not Cys861-2, has a desmethoxy central linker. The introduced modifications should therefore result in less clashes with relevant amino acid residues in the binding tunel of AlbA and stronger binding of Cys861-2 and CN-DM-861 to AlbA. However, this needs to be proven by determining the K_D values of AlbA for Cys861-2 and CN-DM-861 using MST or SPR. Interestingly, in cystobactamid-resistant mutants of *K. pneumoniae* DSM-30104, other amino acid residues than the ones mentioned above were found mutated; Leucine at position 97 was replaced by either valine (shorter hydrophobic side chain), or arginine (long, positively charged side chain), asparagine at position 42 mutated into lysine (long, positively charged side chain), and threonine at position 122 was replaced by lysine or arginine. The used cystobactamids derivatives might per se fit better into the binding site of AlbA compared to the natural product Cys919-2 leading to sequestration with possible chemical modification (although this was not observed for cystobactamid Cys919-2), or the observed mutations could affect the role of AlbA as a transcriptional regulator resulting in differential expression of genes under its control leading to resistance. Several questions remain that could not be answered as part of this thesis but which should be picked up in future studies. The role of amino acid residues of AlbA that we found exchanged in the CN-DM-861 resistant mutants needs further investigation based on structural models and K_D determination. However, the question remains, if we would have found mutations at positions I95, T97, W110, F166 and Y169, had we used cystobactamid 919-2 for resistance development, resulting in higher affinity of AlbA for Cys919-2? Do structural

differences between Cys919-2 and CN-DM-861 result in *K. pneumoniae* needing to mutate positions N42, L97 and T122 to ensure efficient binding and sequestration of CN-DM-861? To answer these questions we need to express the mutant variant and determine the K_D of AlbA^{mut} for CN-DM-861 and Cys861-2 using SPR or MST. The role of AlbA as a transcriptional regulator also needs to be investigated, as we currently do not know which genes are under its regulation, whether observed mutations lead to upregulation or downregulations of gene under its control, and ultimately lead to cystobactamid resistance.

4.4 Materials and Methods

4.4.1 Minimal Inhibitory Concentration (MIC) and Minimal Bactericidal Concentration (MBC) determination

MIC [215] and MBC [216] values were determined as previously described. Assessment in artificial urine was performed as stated in Chapter 2.

4.4.2 Isothermal microcalorimetry

Sample preparation, assay execution and analysis was performed as previously described [219]. Strains were grown overnight in MHB at 180 rpm and 37 °C. Starting OD_{600} was adjusted to 0.001. To assess fitness of mutants vs. wildtype, no compound was added. To assess the time-kill kinetics, compound dissolved in DMSO was added equaling 2x MIC, and 4x MIC in caMHB. DMSO concentration did not exceed 1%. Controls samples were ran in presence of DMSO.

4.4.3 *In vitro* resistance development

Assay was performed as described in Chapter 2.

4.4.4 Fitness cost

Assay was performed as described in Chapter 2.

4.4.5 Reversibility of resistant phenotype

Assay was performed as described in Chapter 2.

4.4.6 RNA isolation and RT-qPCR

All steps were performed as previously described, including the primers used [99].

4.4.7 Whole genome sequencing

WGS was performed as described before in Chapter 2. Samples yielded 0.25-0.4 Gbp of data, which resulted in an estimated 45x-74x mean genome coverage. The raw data was then mapped to a reference sequence of *K. pneumonia* DSM-30104, GenBank accession number AJJI00000000.

4.5 Supporting information

S1 Table. MIC and MIC shift values of *K. pneumoniae* DSM-30104 mutants resistant to CN-DM-861.

strain	MIC [µg/mL]		MIC shift	
	CN-DM-861	CIP	CN-DM-861	CIP
K. pneumoniae DSM-30104	1	0.01	na	na
K. pneumoniae DSM-30104 CN-DM-861^R #1	> 64	0.02	> 64	2
K. pneumoniae DSM-30104 CN-DM-861^R #2	> 64	0.02	> 64	2
K. pneumoniae DSM-30104 CN-DM-861^R #3	> 64	0.02	> 64	2
K. pneumoniae DSM-30104 CN-DM-861^R #4	> 64	0.02	> 64	2
K. pneumoniae DSM-30104 CN-DM-861^R #5	> 64	0.02	> 64	2

CIP, ciprofloxacin.
na, not applicable.

S2 Table. Reversibility of resistance determined for *K. pneumoniae* DSM-30104 mutants resistant to CN-DM-861.

strain	MIC [µg/mL]					
	starting point		passage 3		passage 10	
	CN-DM-861	CIP	CN-DM-861	CIP	CN-DM-861	CIP
K. pneumoniae DSM-30104	1	0.02	1	0.02	1	0.02
K. pneumoniae DSM-30104 CN-DM-861^R #1	> 64	0.02	> 64	0.05	> 64	0.05
K. pneumoniae DSM-30104 CN-DM-861^R #2	> 64	0.02	> 64	0.05	> 64	0.05
K. pneumoniae DSM-30104 CN-DM-861^R #3	> 64	0.02	> 64	0.05	> 64	0.05
K. pneumoniae DSM-30104 CN-DM-861^R #4	> 64	0.02	> 64	0.05	> 64	0.05
K. pneumoniae DSM-30104 CN-DM-861^R #5	> 64	0.02	> 64	0.05	> 64	0.05

CIP, ciprofloxacin.

Chapter 5

5 Cystobactamid resistance in *Staphylococcus aureus* and *Acinetobacter baumannii* relies on target mutations

5.1 Introduction

Due to the diversity and complexity of observed modes of resistance in *E. coli*, *P. aeruginosa* and *K. pneumoniae*, the mechanisms of cystobactamid resistance were studied in additional bacterial species, namely *S. aureus* and *A. baumannii*.

A. baumannii is the most virulent species among the *Acinetobacter* genus, mainly due to its broad-spectrum resistance to antibiotics, compared to the non-*baumannii* species [302]. It is predominantly associated with nosocomial infections, mainly affecting immunocompromised patients [303, 304] and ICU patients [305, 306]. Although *A. baumannii* can cause a variety of diseases, it is most commonly associated with infections of the respiratory tract, namely ventilator-associated pneumonia [307]. *A. baumannii* is intrinsically resistant to various antibiotics due to its ability to prevent antibiotics to pass through the outer membrane by modifying lipid A [210, 308], producing capsular polysaccharides [309], decreased membrane permeability [310], its ability to form biofilms [311], and by employing other mechanisms such as target modifications, enzymatic modification of antibiotics, and upregulation of efflux pumps [312, 313]. According to the annual ECDC epidemiological report for 2019, *Acinetobacter* species accounted for only 1.7% of all reported infections in the EU/EEA; however, approx. 55% of all isolates were resistant to at least one antibiotic under surveillance. Although a negative trend of resistance to fluoroquinolones was observed between 2015-2019, combined resistance to fluoroquinolones, aminoglycosides and carbapenems increased significantly and multi-drug resistance is currently found in 43.6% of isolates [251]. Due to this, the WHO has

assigned carbapenem-resistant *A. baumannii* as priority 1 on the pathogen list for the research and development of new antibiotics [115].

S. aureus, the only Gram-positive pathogen under evaluation in this work, has a great capacity to asymptotically infect healthy individuals [314]. It also causes hospital-acquired and community-acquired infectious diseases, local and systemic infections, such as skin and tissue infections, bacteremia and fatal pneumonia [315]. Intrinsic resistance is achieved via decreased outer membrane permeability (resistance to aminoglycosides), upregulation of efflux systems (resistance to methicillin), production of β-lactamase (resistance to β-lactams and methicillin), biofilm formation and persistence. Several instances of methicillin-resistant *S. aureus* (MRSA) have been found to be resistant to penicillins, cephalosporins, chloramphenicol, aminoglycosides, tetracyclines, macrolides, rifampicin and sulfonamides. Currently, vancomycin, daptomycin and linezolid are used in the clinics to treat MRSA infections [101, 316, 317]. Although rare, daptomycin- [318, 319], and linezolid-resistant isolates have been reported globally, and their incidence is rising [320, 321], emphasizing the need for new antibiotics.

5.2 Results

5.2.1 Activity of cystobactamids against *S. aureus* and *A. baumannii* strains

The activity of cystobactamids against selected *S. aureus* and *A. baumannii* strains was assessed in microbroth dilution assays (Table 1). Cystobactamids Cys861-2 and CN-DM-861 were active on the two wildtype *S. aureus* strains with MICs in the low µg/mL range, whereas the natural Cys861-2 was 2-fold more potent than synthetic CN-DM-861. Both derivatives were also active on a CIP-resistant MRSA isolate (*S. aureus* NRS643), with MICs of 8 µg/mL for Cys861-2 and 16 µ/mL for CN-DM-861. The mutations M121K and Y87F in gyrase A did not impact the activity of cystobactamids. However, in the double mutant [*gyrA* (D83N) and *parC* (D79N)] an 8-fold reduction in activity for Cys861-2 and a complete loss of activity for CN-

DM-861 was observed. This suggests that there is partial overlap of the cystobactamid binding sites on GyrA and ParC with that of fluoroquinolones. However, the activity of the natural derivative Cys861-2 was much less affected than that of the synthetic derivative CN-DM-861. Based on the structures of both cystobactamids, the absence of the β-methoxy moiety in the linker and the presence of the *N*-terminal cyano group in CN-DM-861 appears to be detrimental for activity in the *gyrA* and *parC* double mutant. Both cystobactamids were active against the *A. baumannii* wildtype strains DSM-30008 and CIP-105742, whereas CN-DM-861 was by tendency more potent than the natural derivative Cys861-2. However, both cystobactamids were inactive on the MDR *A. baumannii* strains CIP107292 and R835. Encouragingly, Cys861-2 displayed retained activity on the XDR *A. baumannii* strain ATCC BAA-1710 (MIC 4 µg/mL) whereas CN-DM-861 was inactive.

Table 1. Cys861-2 and CN-DM-861 MIC determination on selected *S. aureus* and *A. baumannii* strains.

	MIC [µg/mL]		
Strain	Cys861-2	CN-DM-861	CIP
S. aureus ATCC-29213	2	1	0.8
S. aureus NRS643[a]	8	16	> 6.4
S. aureus RN4220	0.25	0.5	0.4
S. aureus RN4220 [*gyrA*(D83N), *parC*(D79N)]	2	> 64	3.2
S. aureus RN4220 [*gyrA*(M121K)]	0.5	1	0.8
S. aureus RN4220 [*gyrA*(Y87F)]	0.5	0.5	0.8
A. baumannii DSM-30008	1	0.5	0.1
A. baumannii CIP-105742	0.25	0.06	0.1
A. baumannii CIP107292	> 64	> 64	> 6.4
A. baumannii R835	> 64	> 64	> 6.4
A. baumannii ATCC BAA-1710[b]	4	> 64	> 6.4

[a], MRSA, resistant to erythromycin, levofloxacin, oxacillin and penicillin.
[b], isolated from blood, resistant to ampicillin, amoxicillin/clavulanic acid, ticarcillin, cefalotin, cefazolin, cefuroxime, cefoxitine, ceftazidime,ceftriaxone, gentamicin, nalidixic acid, ciprofloxacin, norfloxacin, tetracycline, nitrofurantoin and trimetroprim/sufamethoxazole.

Next, we assessed the activity of cystobactamids on a selection of *S. aureus* and *A. baumannii* clinical isolates (Table 2). Cystobactamids Cys861-2 and CN-DM-861 displayed comparable activities on clinical isolates of *S. aureus*, with a median MIC of 0.06-0.13 µg/mL and 0.25 µg/mL, respectively. CN-DM-861 also showed medium activity, MIC of 16 µg/mL, on a vancomycin-resistant *S. aureus* (VRSA) clinical isolate (*S. aureus* HOM7). It should be noted that the median MIC of Cys861-2 and CN-DM-861 was comparable to the median MIC of CIP (0.25-0.4 µg/mL), and both cystobactamids were active on *S. aureus* CIP-resistant isolates (MIC $\geq$ 0.1 mg/mL). Additionally, both cystobactamids were active on *A. baumannii* clinical isolates, with the exception of the isolate A6, with median MICs of 1 µg/mL and 2 µg/mL, respectively. The median MIC of CIP was only 2.5-fold lower (0.4 µg/mL). Both cystobactamids retained activity on CIP-resistant *A. baumannii* clinical isolates (MIC $\geq$ 1 µg/mL).

Table 2. Activity of Cys861-2 and CN-DM-861 on *S. aureus* and *A. baumannii* clinical isolates.

Strain	MIC [µg/mL]		
	Cys861-2	CN-DM-861	CIP
S. aureus 1457	0.25	$\leq$ 0.03	0.1
S. aureus 62A	$\leq$ 0.03	$\leq$ 0.03	0.05
S. aureus 3269	$\leq$ 0.03	$\leq$ 0.03	0.05
S. aureus AGC	0.06	$\leq$ 0.03	0.05
S. aureus S26	0.5	0.25	> 6.4
S. aureus S27	0.13	0.25	0.4
S. aureus S28	0.13	0.25	0.4
S. aureus S29	$\leq$ 0.03	$\leq$ 0.03	0.2
S. aureus S38	2	4	> 6.4
S. aureus S39	2	4	> 6.4

S. aureus HOM5[a]	nd	1	0.25
S. aureus HOM7 [b]	nd	16	32
median MIC *S. aureus* (with VRSA)	0.06-0.13	0.25	0.25-0.4
median MIC *S. aureus* (without VRSA)	na	≤ 0.03-0.25	0.2-0.4
A. baumannii A1	2	2	0.4
A. baumannii A3	1	16	0.8
A. baumannii A5	1	2	0.2
A. baumannii A6	> 64	> 64	1.6
A. baumannii A7	0.5	1	0.1
A. baumannii A8	0.25	1	0.4
A. baumannii A9	0.5	8	> 6.4
A. baumannii A10	1	4	3.2
A. baumannii AT1	1	2	0.2
median MIC *A. baumannii*	1	2	0.4

[a], vancomycin-sensitive S. aureus (VSSA).
[b], VRSA.
nd, not determined.
na, not applicable.

5.2.2 On-target activity in *S. aureus*

Cystobactamids Cys861-2 and CN-DM-861-2 were equipotent and inhibited the supercoiling activity of both, *S. aureus* gyrase and topoisomerase IV, with IC_{50} values in the one-digit µM range (Table 3). In contrast to Gram-negative *E. coli*, topoisomerase IV seems to be the preferred target over gyrase in *S. aureus*. The same trend was observed for CIP, where IC_{50} values of 1.84 µM and 7.85 µM were determined in supercoiling assays with gyrase and topoisomerase IV, respectively.

Table 3. IC$_{50}$ values of Cys861-2 and CN-DM-861 determined on *S. aureus* gyrase and topoisomerase IV.

	Supercoiling assay IC$_{50}$ [µM]		
S. aureus	Cys861-2	CN-DM-861	CIP
gyrase	3.34	3.55	7.85
topoisomerase IV	1.82	1.50	1.84

5.2.3 Frequency of resistance and mutant characterization

5.2.3.1 *S. aureus*

Resistance development experiments revealed a low frequency of resistance of CN-DM-861 on *S. aureus* Newman (Table 4). The obtained resistant mutants exhibited a variable level of resistance to CN-DM-861, with a MIC shift of 20- to 1280-fold compared to the parent strain, and minimal co-/cross-resistance with CIP (2.5- to 10-fold shift in MIC). WGS revealed that 4 out of 5 sequenced CN-DM-861 resistant *S. aureus* mutants carried A64S, D79G, R570C mutations, and a deletion of 4 amino acids (516-519) in topoisomerase IV (*parC*), and one mutant had a C to A transvertion mutation upstream of drug resistance transporter EmrB/QacA. After 10 passages in non-selective growth medium, the resistance phenotype was mostly abolished and the mutants only retained low-level resistance (10-fold shift in MIC compared to initial parent strain). Interestingly, this was not due to the loss of obtained mutations in *parC*, but rather due to acquisition of new mutations, namely in the two-component system SaeRS, the *pur* operon repressor (*purR*), and adenine phosphoribosyltransferase (*apt*). In general, resistance to cystobactamids in *S. aureus* did not result in a fitness loss, although some differences between the mutants and their parent strain were observed as assessed by isothermal microcalorimetry (Fig. S1-S3). The resistant mutants displayed significantly reduced time to peak and time to activity compared to the sensitive wildtype; the metabolic rate and total heat emitted were not affected (Fig. S2).

Table 4. *S. aureus* frequency of resistance, detailed characterization of resistant mutants and whole genome sequencing results.

		Frequency of resistance			
		CN-DM-861		CIP	
strain		4x MIC	8x MIC	4x MIC	8x MIC
S. aureus Newman		4×10^{-8}	$< 10^{-9}$	$< 10^{-9}$	$< 10^{-9}$

		Resistant mutant characterization			
strain		MIC shift[a] (CN-DM-861, parent vs. Cys^R mutant)	co-/cross-resistance with CIP[a] (CIP, parent vs. Cys^R mutant)	fitness/metabolic changes[b]	reversibility of resistance[c]
S. aureus Newman CN-DM-861^R		20-1280	2.5-10	no/yes	yes

		WGS results of CN-DM-861^R mutants			
		MIC [µg/mL] (CN-DM-861)	*parC*	intragenic	
S. aureus Newman	WT	0.05			
	#1	32	A64S		
	#2	64	del516-519 aa		
S. aureus Newman CN-DM-861^R	#3	32	R570C		
	#4	0.5		C to A transversion upstream of drug resistance transporter EmrB/QacA	

	#5		4			D79G		

WGS results of resensitized mutants								
	MIC [µg/mL] (CN-DM-861)	*parC*	intragenic	hypothetical potein	*saeS*	*saeR*	*purR*	*apt*
	WT	0.05						
	#1	1	A64S			fs		E221D
	#2	0.06	del516-519 aa		E147K				H104Y
S. aureus Newman	#3	0.5	R570C				Fs	
	#4	0.5		C to A transversion upstream of drug resistance transporter EmrB/QacA			Fs		Del25-28 aa
	#5	0.5	D79G			fs			fs

WT, wildtype; fs, frameshift; del, deletion, aa, amino acid.
[R], resistant.
[a], results can be found in Table S1.
[b], results can be found in Fig. S1-S3.
[c], results can be found in Table S2.

5.2.3.2 *A. baumannii*

Spontaneous resistance development with cystobactamid CN-DM-861 revealed a wide range of frequency of resistance (approx. 10^{-6}-10^{-10}) for both *A. baumannii* strains and was higher than that of CIP (approx. 10^{-9}-10^{-10}), although most FoR values for CIP are undetermined (FoR reported as < 1 x 10^{-9} and < 5 x 10^{-10}) (Table 5). First round of resistance development with *A. baumannii* DSM-30008 resulted in a high frequency of resistance, 10^{-6}-10^{-7}, 2-3 orders of magnitude higher than the second round of resistance development, 10^{-8}-10^{-10}. It is difficult to explain what led to the observed FoR discrepancy when the same strain (*A. baumannii* DSM-30008) and compound (CN-DM-861) were used. We speculate that some experimental differences must have occurred, i.e. growth phase at the time of exposure. We observed variable levels of resistance to CN-DM-861, with MIC shifts ranging from 4- to > 128-fold. However, resistance to cystobactamids did not result in co-/cross-resistance with ciprofloxacin, as we only observed a 1-4-fold increase in CIP MIC. Furthermore, resistance to cystobactamids presented a fitness cost for the mutants and their metabolic activity was significantly lower than for the parent wildtype strain (Fig. S4-S6). The resistant mutants displayed changes in time to activity, metabolic rate and time to peak, but not in total heat emitted. Only the resistant mutants obtained during the first round of resistance development did not show any fitness loss due to resistance. These cystobactamid-resistant mutants that developed at a high frequency had mutations in aconitate hydratase (*acnB*), LysR family transcriptional regulator, alkyl hydroperoxide reductase subunit F (*ahpF*), and insertion of transposase upstream of gyrase, mechanosensitive ion channel protein (*mscS*), and a DNA-binding protein gene. These results differed significantly from the results obtained in the second round of resistance development. In the first set of *A. baumannii* DSM-30008 CN-DM-861 resistant mutants, only one clone displayed a mutation upstream of the target gene *gyrA*. Surprisingly, when the resistance development was repeated the FoR dropped significantly and almost all mutants (8 out of 9) displayed target mutations in either *gyrA* or *gyrB*. The same was true for *A. baumannii* CIP-105742 strain where

mutants developed at a frequency of 5-8 $\times 10^{-9}$ and most independent mutants (4 out of 9) carried mutations in *gyrA* and *gyrB*. The target mutations were partly accompanied by several other mutations; mutations in *yhbW* (putative luciferase-like monooxygenase of unknown function) were associated with *gyrA* mutations, whereas mutations in *ybdL* (aminotransferase), *gcvA* (transcriptional regulator), *rhaR* (rhamnose catabolism regulatory protein), *carB* (carbamoylphospahte synthesis), *pyrC* (dihydroorotase), *pepA* (aminopeptidase) and *gltA* (citrate synthase) were associated with *gyrB* mutations. Only 4 (out of 8) *A. baumannii* DSM-30008 cystobactamid-resistant mutants had only mutations in either *gyrA* (3 out of 4) or *gyrB* (1 out of 4). Four mutants had mutations in *gyrA* and *yhbW*. Only one mutant did not have target mutations, but did have a mutation in *yhbW*. In *A. baumannii* CIP-105742, only one mutant had a mutation in *gyrA*, however, it was also carrying mutations in *ybdL*, *gcvA* and *rhaR*. Furthermore, 3 mutants had mutations in *gyrB* in combination with a mutation in *pepA*. There were also 5 mutants that did not have target mutations; one had a combination of mutations in *ybdL* and *gltA*, one in *ybdL*, *carB* and *pyrC*, and 3 mutants only had mutations in *ybdL*. Target mutations were frequent (12 out of 18 mutants) with *gyrA* (8 out of 12) being the preferred target not *gyrB* (4 out of 12).

Table 5. *A. baumannii* frequency of resistance, detailed characterization of resistant mutants and whole genome sequencing results.

	Frequency of resistance			
	CN-DM-861		CIP	
Strain	4x MIC	8x MIC	4x MIC	8x MIC
A. baumannii DSM-30008[*]	4×10^{-6}	2×10^{-7}	8×10^{-10}	8×10^{-10}
A. baumannii DSM-30008[**]	2×10^{-8}	9×10^{-10}	$< 5 \times 10^{-10}$	$< 5 \times 10^{-10}$
A. baumannii CIP-105742	8×10^{-9}	5×10^{-9}	$< 1 \times 10^{-9}$	$< 1 \times 10^{-9}$

Resistant mutant characterization				
	MIC shift[a] (CN-DM-861, parent vs. Cys[R] mutant)	co-/cross-resistance with CIP[a] (CIP, parent vs. Cys[R] mutant)	fitness/metabolic changes[b]	Reversibility of resistance[c]
A. baumannii DSM-30008[*]	4-> 64	1-2	no/nd	yes
A. baumannii DSM-30008[**]	> 128	1-4	yes/yes	no
A. baumannii CIP-105742	4-8	1-2	yes/nd	no

WGS results of CN-DM-861[R] mutants								
		gyrA	*acnB*	*mscS*	LysR FTP	TR	*ahpF*	DNA-binding protein gene
A. baumannii DSM-30008[*] CN-DM-861[R]	#1	Insertion of transposase upstream of start codon		Insertion of transposase upstream of start codon				

	#	gyrA	gyrB	yhbW	ybdL	gcvA	rhaR	carB	pyrC	pepA	gltA
	#2						Insertion of transposase upstream of start codon		T63N		Insertion of transposase
	#3					M649R				G181A	
	#4					T750I		H299Q			
	#5										Insertion of transposase

	#	gyrA	gyrB	yhbW	ybdL	gcvA	rhaR	carB	pyrC	pepA	gltA
A. baumannii DSM-30008** CN-DM-861R	#1	R719C									
	#2	In									
	#3	In		D105E							
	#4			D105E							
	#5	In		D105E							
	#6	In									
	#7	R786C		D105E							
	#8	R786G									
	#9		K460E								
	#1	R615C			Q357P	D139E	G140D				

A. baumannii CIP-105742							
	#2	R399S				V297D	
	#3	K400I				V297D	
	#4		Q357P				del12bp
	#5		Q357P				
	#6		Q357P				
	#7	K400I				V297D	
	#8		Q357P				
	#9		Q357P	C793Y	G296S		

FTR, family transcriptional regulator; TR, transcriptional regulator; in, insertion; del, deletion; bp, base pair.

[R], resistant.

[*], first round of FoR.

[**], second round of FoR.

[a], results can be found in Table S3.

[b], results can be found in Fig. S4-S6.

[c], results can be found in Table S4.

5.3 Discussion

Resistance to cystobactamids in *S. aureus* was due to target mutations in topoisomerase IV (*parC*/*grlA*). We observed three mutations (A64S, D79G, and R570C), and a four amino acid deletion in topoisomerase IV. Mutations S80F, S80Y, S81P, and E84K in ParC of *S. aureus* are reported as the most frequent target mutations, conferring resistance to fluoroquinolones, which are all located in the quinolone-resistance determining region (QRDR), which spans amino acid residues 67-116 [187, 322]. Each single mutations leads to FQ resistance to an extent that laboratory breakpoints for susceptibility are not reached anymore [91]. Although we did not observe these specific mutations in cystobactamid-resistant *S. aureus*, the mutated amino acids A64S and D79G are relatively close or within the QRDR in ParC of *S. aureus*, whereas R570C mutation in ParC is not, and literature reports for this mutation do not exist. This would suggest that on-target binding site of cystobactamids and CIP is similar, but not identical. Our findings of minimal loss of activity for Cys861-2, and complete loss of activity for CN-DM-861 on fluoroquinolone-resistant *gyrA* (D83N), *parC* (D79N) double mutant *S. aureus* strain further support this. We do not have access to *S. aureus* strains with only *gyrA* (D83N) or only *parC* (D79N) mutation to discern contributions of each of the two mutations to decreased susceptibility to cystobactamid. Furthermore, based on the structures of both cystobactamids, the absence of the β-methoxy moiety in the linker and the presence of the *N*-terminal cyano group in CN-DM-861 appears to be detrimental for activity in the *gyrA* and *parC* double mutant. Cystobactamids, as FQ [323], seem to preferentially target topoisomerase IV in Gram-positive bacteria, this was further supported by on-target activity assessment as both cystobactamids exhibited 2-3-fold lower IC_{50} values on topoisomerase IV compared to gyrase.

One resistant mutant (out of five) without target mutations carried mutations in the promoter region of the multidrug efflux pump EmrB/QacA. This pump is described to confer resistance to tetracyclines and nalidixic acid in *E. coli* [324], trimethoprim in *Bulkholderia* spp. [325], and

to antiseptic agents (such as chlorhexidine) in *S. aureus* [326, 327], we therefore concluded that cystobactamid is effluxed through this pump. Deletion of *emrB*/*qacA* in the resistant mutant background should therefore result in cystobactamid-sensitive phenotype. Cystobactamid-resistant mutants in *E. coli*, *P. aeruginosa*, and *K. pneumoniae* were non-reversible, i.e. their resistance level towards cystobactamids remained unchanged after serial passaging in non-selective medium. Surprisingly, we found that the high-level cystobactamid- resistant *S. aureus* mutants can be resensitized by serial passaging. These revertants displayed only low-level resistance to cystobactamids (approx. 10-fold MIC shift of revertants vs. wildtype) and genome analyses revealed that this was due to additional mutations in *saeRS*, *purD* and *apt*, whereas mutations in *parC* were maintained. The main role of the SaeRS two-component system is the regulation of expression of virulence genes, such as α-hemolysin, β-hemolysin, nuclease, and coagulase [328]. Frameshift mutations observed in our resensitized mutants lead to a production of nonsense proteins, leading us to believe that regulation of virulence is disrupted and results in avirulent *S. aureus* clones. Moreover, SaeR is presumed to be involved in regulation of genes responsible for production of capsule polysaccharides, lipoproteins and 2-oxoglutarat [329], all involved in hindering uptake of compounds. We presume that *S. aureus* SaeRS TCS works similarly as QseBC in *E. coli*, where mutations in QseBC led to a less virulent phenotype *in vitro* and resistance to cystobactamids, although it is worth to remember that *E. coli* cystobactamid-resistant mutants remained sensitive in sub- to low micromolar range and mutations in QseBC were gain-in-function. In order to regain sensitivity to cystobactamids mutations in SaeSR TCS need to be a loss-of function mutations and impact production of capsule, polysaccharides and lipoproteins, allowing for easier entry of cystobactamids, however more work needs to be done to prove this theory. Additionally, PurR is a transcriptional regulator and regulates both genes involved in metabolism (purine biosynthesis) and genes involved in virulence, playing a major role in pathogenesis of *S. aureus* [329]. Moreover, exposure to stress induces can lead to *purR* mutations, and inactivation of *purR* results in growth

defects and diminished virulence [330, 331]. Furthermore, Apt is a protein involved in AMP biosynthesis and is a part of the purine biosynthesis pathway. It was found mutated when *S. aureus* was passaged *in vitro* in presence of vancomycin [332]. Deletion of the gene led to decrease in eDNA release, an integral part of biofilm [333]. Purine biosynthesis was directly linked to increased growth and survival rates of *S. aureus* persistent bacteremia, and disruption of purine biosynthesis resulted in decreased growth rates and an attenuated phenotype *in vivo* [334, 335]. Whether PurR is also a regulator of Apt is unclear. However, given their roles in purine biosynthesis and regulation of virulence, we speculate that mutations in these genes must somehow affect cell wall architecture and capsule formation. Similarly, to SaeSR mutations, mutations in PurR and Apt are probably loss-of-function mutations. Taken together, mutations in SaeRS, PurR and Apt weaken the outer barrier protecting *S. aureus* against antibiotics, making it more susceptible to treatment with antibiotics, and reduce its virulence.

Similar observations were made for *A. baumannii* cystobactamid-resistant clones, where the main mode of resistance is target modification. Contrary to *S. aureus*, where only mutations in *parC* were observed, in *A. baumannii* both *gyrA* and *gyrB* genes were mutated, although not simultaneously. In *A. baumannii* DSM-30008 background mutations solely present in *gyrA* (R719C, R786G, In) or *gyrB* (K460E) were already enough to achieve full resistance without a fitness cost. This is unusual considering these mutations developed in a single step, are not found in the QDRD, are not literature described and furthermore, literature described FQ mutants needed to accumulate several target mutations in multiple steps in order to achieve full resistance [186]. Mutants harboring only *yhbW* mutations were also fully resistant at no fitness cost. Mutations in *gyrA* were associated with mutations in *yhbW*. *yhbW* is a gene of unknown function and it was shown to enable *rpoE* deletion in *E. coli*; RpoE is a cell envelope stress-response sigma factor responsible for outer membrane maintenance, and it is activated by misfolded and/or mis-translocated outer membrane proteins or LPS [336-338]. We speculate

that YhbW is involved in the maintenance of cell envelope integrity possibly as a transcriptional regulator.

In *A. baumannii* CIP-105742 background mutation in *gyrA* (R615C) was in combination with mutations in *ybdL*, *gcvA*, and *rhaR*, and resulted in merely 4-fold increase in MIC with no fitness cost; similar MIC shift (2-4-fold) was observed for *gyrB* mutations (R399S, K400I) that occurred exclusively together with *pepA* (V297D) mutation, and decreased mutant fitness during the exponential growth phase. Standalone *ybdL* mutations, or in combination with mutations in other genes (*carB*, *pyrC*, and *gltA*), resulted in the same level of resistance as target mutations. However, *ybdL* mutations were predominantly associated with *gyrB* mutations. *ybdL* encodes a methionine aminotransferase in *E. coli*, although its function is unknown it has a moderate sequence homology with vitamin B(6) dependent enzymes suggesting it can bind pyridoxal-5'-phosphate, the active form of vitamin B6 [339] essential for glucose, lipid and amino acid metabolism [340]. Citrate synthase (*gltA*) and aconitate hydratase (*acnB*) are both part of the TCA cycle and they play a role in the formation of 2-oxoglutarate, a master regulatory metabolite, connecting carbon and nitrogen metabolism [341]. Accumulation of 2-oxoglutarate is linked to resistance to cationic antimicrobial peptides in *E. coli* via outer membrane modifications [213, 342] in a manner similar to what we observed in cystobactamid resistant *E. coli* carrying *qseB* and *qseC* mutations. PyrC and CarB are both involved in arginine biosynthesis and pyrimidine metabolism [343]. Changing the arginine content was shown to affect the activity of cationic antimicrobial peptides, which are attracted to the anionic bacterial membrane [344]. RhaR is a positive regulator of the *rhaSR* operon, encoding two AraC family transcription activator proteins, involved in regulation of rhamnose catabolism [345] and overexpression of *rhaR* gene was reported to confer resistance towards metronidazole in *B. thetaiontaomicron* [346]. Rhamnose is essential for virulence and viability [347], and is used for the biosynthesis of O-antigens, the sugar part of lipopolysaccharides in the outer membrane

of Gram-negative bacteria [348]. Standalone mutations in these genes (excluding target mutations) hint toward OM modifications, however they are not enough to confer full resistance. We conclude that Cystobactamid resistance in *A. baumannii* is a result of target mutations and/or outer membrane modifications.

5.4 Materials and Methods

5.4.1 Minimal Inhibitory Concentration (MIC) and Minimal Bactericidal Concentration (MBC) determination

MIC [215] and MBC [216] values were determined as previously described.

5.4.2 Supercoiling assay

Assay was performed as described in Chapter 2.

5.4.3 Isothermal microcalorimetry

Sample preparation, assay execution and analysis was performed as previously described [219]. Strains were grown overnight in MHB at 180 rpm and 37 °C. Starting OD_{600} was adjusted to 0.001. To assess fitness of mutants vs. wildtype, no compound was added. To assess the time-kill kinetics, compound dissolved in DMSO was added equaling 2x MIC, and 4x MIC in caMHB. DMSO concentration did not exceed 1%. Controls samples were ran in presence of DMSO.

5.4.4 *In vitro* resistance development

Assay was performed as described in Chapter 2.

5.4.5 Fitness cost

Assay was performed as described in Chapter 2.

5.4.6 Reversibility of resistant phenotype

Assay was performed as described in Chapter 2.

5.4.7 Whole genome sequencing

WGS was performed as described before in Chapter 2.

S. aureus Newman: Samples yielded 0.14-0.19 Gbp of data, which resulted in an estimated 51x-69x mean genome coverage. The raw data was then mapped to a reference sequence of *S. aureus* Newman, GenBank accession number NC_009641.

A. baumannii DSM-30008: Samples yielded 0.2-0.29 Gbp of data, which resulted in an estimated 51x-74x mean genome coverage. The raw data was then mapped to a reference sequence of *A. baumannii* ab736, GenBank accession number CP015121.

5.5 Supporting information

A
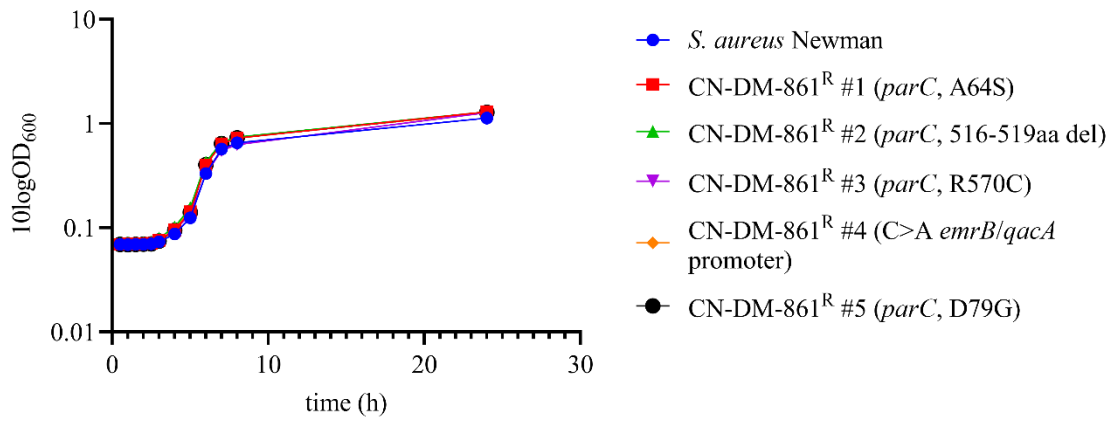
B
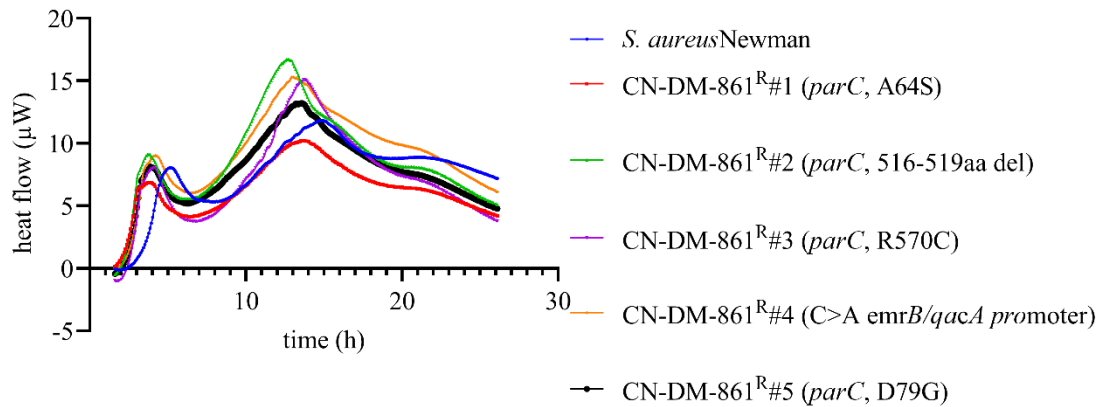
S1 Fig. Fitness and metabolic assessment of *S. aureus* CN-DM-861 resistant mutants.
(A) OD600 over time. (B) Heat flow over time.
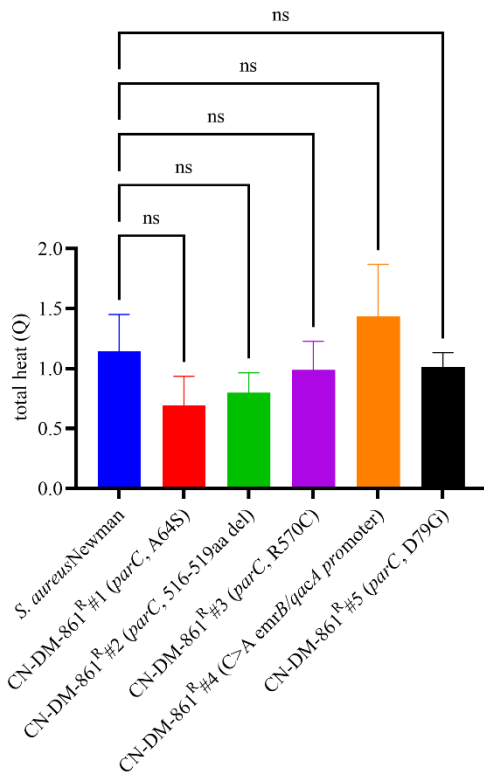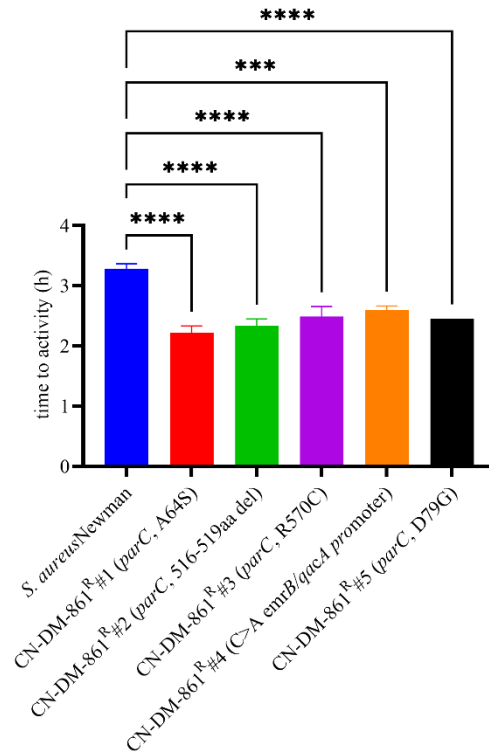
S2 Fig. Total heat and time to activity assessed for *S. aureus* CN-DM-861 resistant mutants.
(A) Total heat. (B) Time to activity. Ordinary one-way ANOVA was used to analyze the data; ns, not significant; ***, $p < 0.005$; ****, $p < 0.001$.
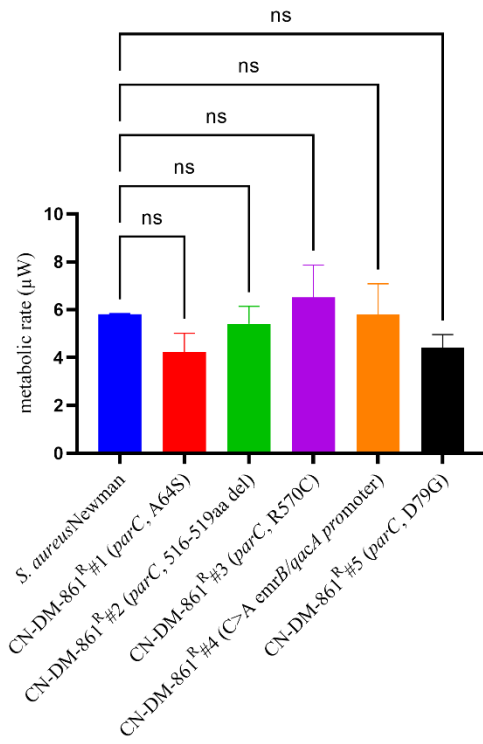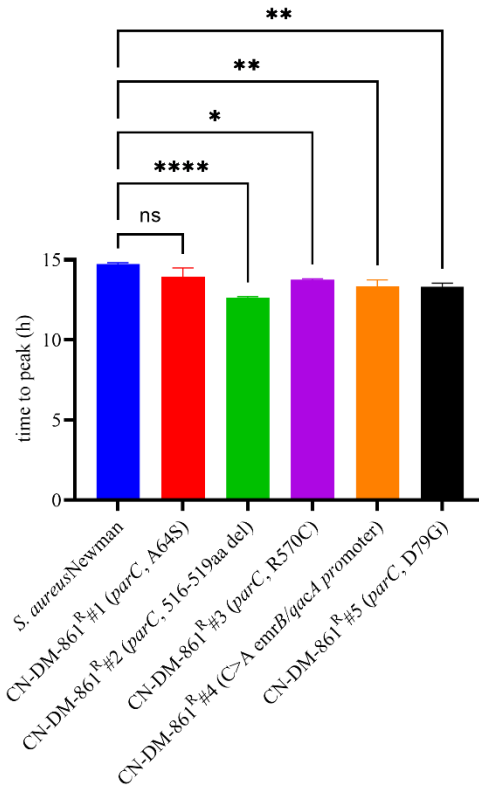
S3 Fig. Metabolic rate and time to peak assessed for *S. aureus* CN-DM-861 resistant mutants.
(A) Metabolic rate. (B) Time to peak. Ordinary one-way ANOVA was used to analyze the data; ns, not significant; *, $p < 0.05$; **, $p < 0.01$; ****, $p < 0.001$.

A

- A. baumannii DSM-30008
- CN-DM-861^R #1 (*gyrA*, R719C)
- CN-DM-861^R #2 (*gyrA*, In)
- CN-DM-861^R #3 (*gyrA*, In; *yhbW*, D105E)
- CN-DM-861^R #4 (*yhbW*, D105E)
- CN-DM-861^R #5 (*gyrA*, In; *yhbW*, D105E)
- CN-DM-861^R #6 (*gyrA*, In)
- CN-DM-861^R #7 (*gyrA*, R786C; *yhbW*, D105E)
- CN-DM-861^R #8 (*gyrA*, R786G; *yhbW*, D105E)
- CN-DM-861^R #9 (*gyrB*, K460E)

B

- A. baumannii DSM-30008
- CN-DM-861^R #1 (*gyrA*, R719C)
- CN-DM-861^R #2 (*gyrA*, In)
- CN-DM-861^R #3 (*gyrA*, In;*yhbW*, D105E)
- CN-DM-861^R #4 (*yhbW*, D105E)
- CN-DM-861^R #5 (*gyrA*, In;*yhbW*, D105E)
- CN-DM-861^R #6 (*gyrA*, In)
- CN-DM-861^R #7 (*gyrA*, R786C; *yhbW*, D105E)
- CN-DM-861^R #8 (*gyrA*, R786G; *yhbW*, D105E)
- CN-DM-861^R #9 (*gyrB*, K460E)

C

- A. baumannii CIP-105742
- CN-DM-861^R #1 (*gyrA*, R615C; *ybdL*, Q357P; *gcvA*, D139E; *rhaR*, G140D)
- CN-DM-861^R #2 (*gyrB*, R399S; *pepA*, V297D)
- CN-DM-861^R #3 (*gyrB*,K400I; *pepA*, V297D)
- CN-DM-861^R #4 (*ybdL*, Q357P; *gltA*, 12aa del)
- CN-DM-861^R #5 (*ybdL*, Q357P)
- CN-DM-861^R #6 (*ybdL*, Q357P)
- CN-DM-861^R #7 (*gyrB*,K400I; *pepA*, V297D)
- CN-DM-861^R #8 (*ybdL*, Q357P)
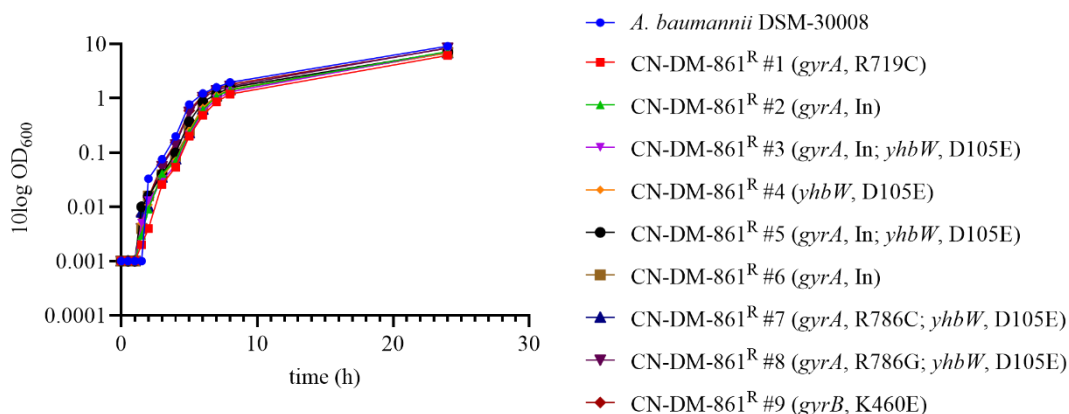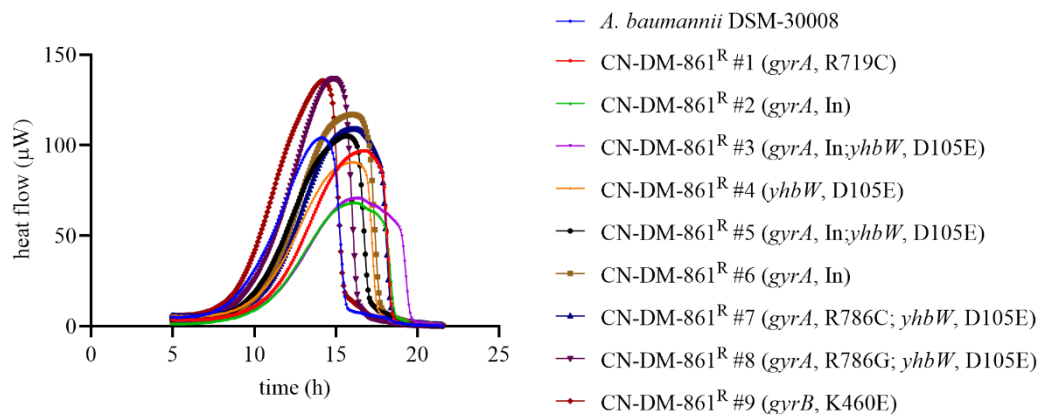- CN-DM-861^R #9 (*ybdL*, Q375P; *carB*, C793Y; *pyrC*, G296S)

S4 Fig. Fitness and metabolic assessment of *A. baumannii* CN-DM-861 resistant mutants.
(A) OD600 over time *A. baumannii* DSM-30008, from 2nd round of FoR. (B) Heat flow over time *A. baumannii* DSM-30008, from 2nd round of FoR. (C) OD600 over time *A. baumannii* CIP-105742.
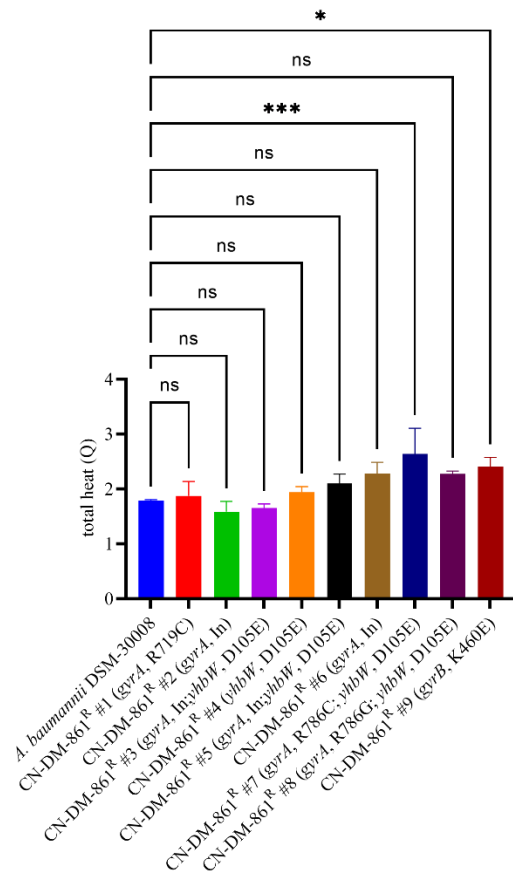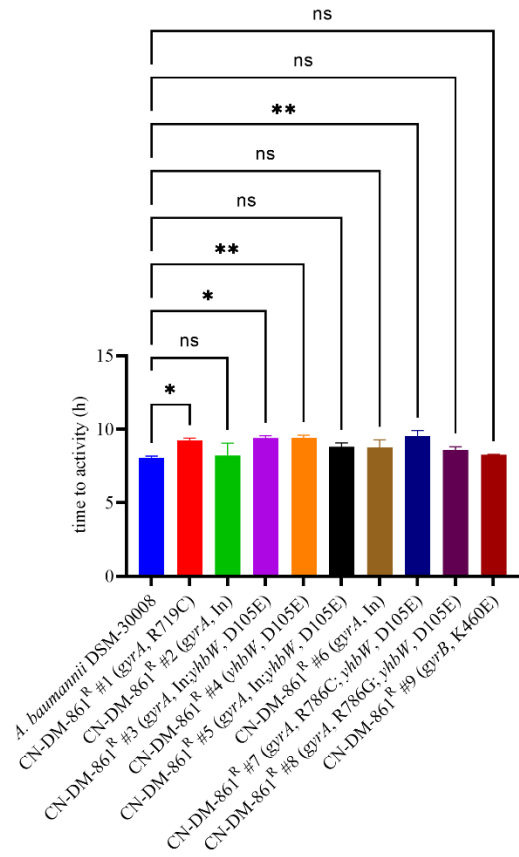
S5 Fig. Total heat and time to activity assessed for *A. baumanni* CN-DM-861 resistant mutants from 2ⁿᵈ round of FoR.

(A) Total heat. (B) Time to activity. Ordinary one-way ANOVA was used to analyze the data; ns, not significant; *, $p < 0.05$; **, $p < 0.01$; ***, $p < 0.005$.
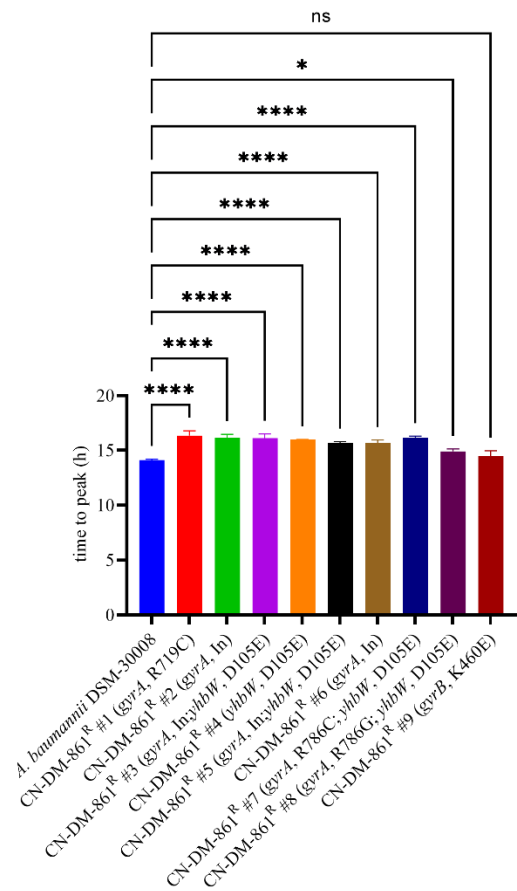
S6 Fig. Metabolic rate and time to peak assessed for *A. baumanni* CN-DM-861 resistant mutants from 2nd round of FoR.
(A) Metabolic rate. (B) Time to peak. Ordinary one-way ANOVA was used to analyze the data; ns, not significant; *, $p < 0.05$; **, $p < 0.01$; ***, $p < 0.005$; ****, $p < 0.001$.
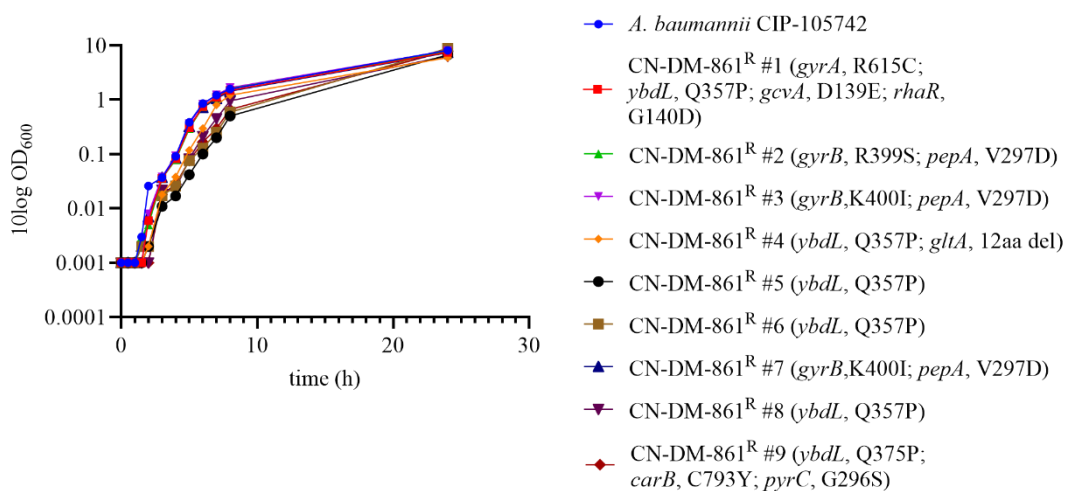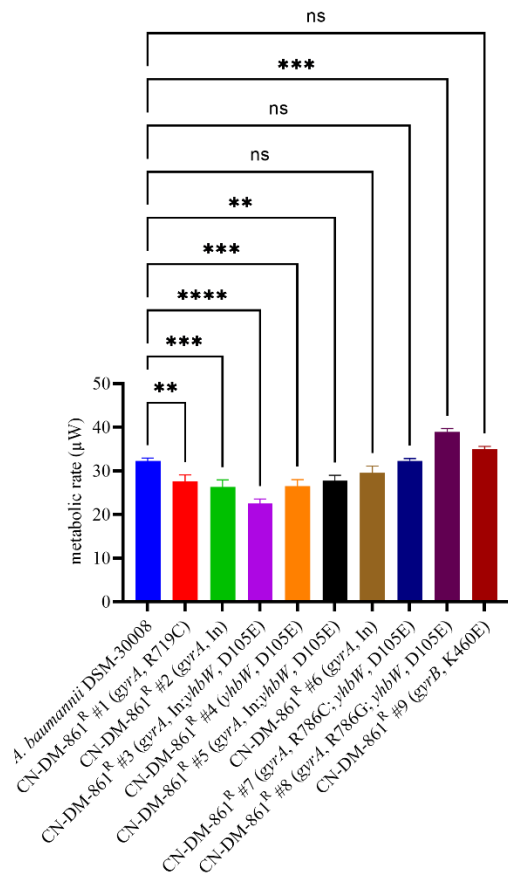
S1 Table. MIC and MIC shift determination of *S. aureus* Newman CN-DM-861 resistant clones.

	MIC [μg/mL]		MIC shift	
strain	CN-DM-861	CIP	CN-DM-861	CIP
S. aureus Newman	0.05	0.08	na	na
S. aureus Newman CN-DM-861[R] #1	32	0.4	640	5
S. aureus Newman CN-DM-861[R] #2	64	0.8	1280	10
S. aureus Newman CN-DM-861[R] #3	32	0.4	640	5
S. aureus Newman CN-DM-861[R] #4	0.5	0.1	10	1.25
S. aureus Newman CN-DM-861[R] #5	4	0.2	80	2.5
S. aureus Newman CN-DM-861[R] #6	1	0.4	20	5

strain				
S. aureus Newman CN-DM-861^R #7	4	0.2	80	2.5
S. aureus Newman CN-DM-861^R #8	4	0.4	80	5
S. aureus Newman CN-DM-861^R #9	8	0.4	160	5
S. aureus Newman CN-DM-861^R #10	4	0.4	80	5

CIP, ciprofloxacin.
na, not applicable.

S2 Table. Reversibility of resistance assessed on *S. aureus* Newman CN-DM-861 resistant mutants.

	MIC [μg/mL]					
	starting point		passage 3		passage 10	
strain	CN-DM-861	CIP	CN-DM-861	CIP	CN-DM-861	CIP
S. aureus Newman	0.05	0.08	0.05	0.08	0.05	0.08
S. aureus Newman CN-DM-861^R #1	32	0.4	1	0.1	1	0.05
S. aureus Newman CN-DM-861^R #2	64	0.8	0.06	0.1	0.06	0.1
S. aureus Newman CN-DM-861^R #3	32	0.4	0.25	0.1	0.5	0.1
S. aureus Newman CN-DM-861^R #4	0.5	0.1	0.5	0.1	0.5	0.05
S. aureus Newman CN-DM-861^R #5	4	0.2	0.5	0.1	0.5	0.05

CIP, ciprofloxacin.

S3 Table. MIC and MIC shift determination of *A. baumannii* CN-DM-861 resistant clones.

	MIC [μg/mL]		MIC shift	
strain	CN-DM-861	CIP	CN-DM-861	CIP
A. baumanii DSM-30008[*]	1	0.1	na	na
A. baumanii DSM-30008[*] CN-DM-861^R #1	8	0.4	8	4
A. baumanii DSM-30008[*] CN-DM-861^R #2	64	0.4	64	4
A. baumanii DSM-30008[*] CN-DM-861^R #3	4	0.2	4	2
A. baumanii DSM-30008[*] CN-DM-861^R #4	64	0.4	64	4
A. baumanii DSM-30008[*] CN-DM-861^R #5	64	0.8	64	8
A. baumannii DSM-30008[**]	0.5	0.4	na	na
A. baumannii DSM-30008[**] CN-DM-861^R #1	> 64	0.4	>128	1

A. baumannii DSM-30008[**] CN-DM-861[R] #2	> 64	0.4	>128	1
A. baumannii DSM-30008[**] CN-DM-861[R] #3	> 64	1.6	>128	4
A. baumannii DSM-30008[**] CN-DM-861[R] #4	> 64	0.8	>128	2
A. baumannii DSM-30008[**] CN-DM-861[R] #5	> 64	0.4	>128	1
A. baumannii DSM-30008[**] CN-DM-861[R] #6	> 64	0.4	>128	1
A. baumannii DSM-30008[**] CN-DM-861[R] #7	> 64	0.4	>128	1
A. baumannii DSM-30008[**] CN-DM-861[R] #8	> 64	0.4	>128	1
A. baumannii DSM-30008[**] CN-DM-861[R] #9	> 64	0.4	>128	1
A. baumannii CIP-105742	0.125	0.1	na	na
A. baumannii CIP-105742 CN-DM-861[R] #1	1	0.2	8	2
A. baumannii CIP-105742 CN-DM-861[R] #2	1	0.2	8	2
A. baumannii CIP-105742 CN-DM-861[R] #3	1	0.2	8	2
A. baumannii CIP-105742 CN-DM-861[R] #4	1	0.2	8	2
A. baumannii CIP-105742 CN-DM-861[R] #5	0.5	0.2	4	2
A. baumannii CIP-105742 CN-DM-861[R] #6	0.5	0.2	4	2
A. baumannii CIP-105742 CN-DM-861[R] #7	0.5	0.2	4	2
A. baumannii CIP-105742 CN-DM-861[R] #8	0.5	0.1	4	1
A. baumannii CIP-105742 CN-DM-861[R] #9	0.5	0.1	4	1

CIP, ciprofloxacin; na, not aplicable.
[*], first round of FoR.
[**], second round of FoR.

S4 Table. Reversibility of resistance assessed on *A. baumannii* CN-DM-861 resistant mutants.

strain	MIC [µg/mL]					
	starting point		passage 5		passage 10	
	CN-DM-861	CIP	CN-DM-861	CIP	CN-DM-861	CIP
A. baumanii DSM-30008[*]	1	0.1	1	0.1	1	0.1
A. baumanii DSM-30008[*] CN-DM-861[R] #1	8	0.4	1	0.4	1	0.4
A. baumanii DSM-30008[*] CN-DM-861[R] #2	64	0.4	1	0.4	1	0.4

A. baumanii DSM-30008[*] CN-DM-861[R] #3	4	0.2	1	0.2	1	0.2
A. baumanii DSM-30008[*] CN-DM-861[R] #4	64	0.4	1	0.4	1	0.4
A. baumanii DSM-30008[*] CN-DM-861[R] #5	64	0.8	1	0.4	1	0.4
A. baumannii DSM-30008[**]	0.5	0.4	0.5	0.4	0.5	0.4
A. baumannii DSM-30008[**] CN-DM-861[R] #5	> 64	0.4	> 64	0.4	> 64	0.4
A. baumannii CIP-105742	0.125	0.1	0.125	0.1	0.125	0.1
A. baumannii CIP-105742 CN-DM-861[R] #3	1	0.2	1	0.2	1	0.2

CIP, ciprofloxacin.
[*], first round of FoR.
[**], second round of FoR.

Chapter 6

6 Summary and Perspectives

Cystobactamids, representing a novel chemical scaffold first isolated from myxobacteria, and fluoroquinolones share the same target, bacterial topoisomerase IIa, and exert their effect by stabilizing DNA cleavage complex, leading to cell death. Due to the shared target and similar mode-of-action, we expected to observe a substantial cross-resistance with fluoroquinolones. However, cystobactamids remained highly active on *E. coli* indicator strains overexpressing AcrAB-TolC and on strains with deficient AcrAb-TolC efflux pump. Additionally, cystobactamids remained active on strains harboring target mutations (*gyrA*, *parC*), plasmid-mediated FQ resistance determinants (Qnr proteins, aminoglycoside acetyltransferase), and Qnr efflux proteins. In *S. aureus* only *gyrA*, *parC* double mutant exhibited a partial cross-resistance, whereas other tested *gyrA* mutations showed no effect on cystobactamid activity. This was further substantiated by on-target assessment, where cystobactamids and CIP showed equipotent activity on wildtype *E. coli* gyrase, however, when tested on gyrase containing major *gyrA* (S83L) and *gyrB* (D426N) mutations, CIP lost activity whereas cystobactamids remained very active. Furthermore, lack of FQ cross-resistance is also supported by FoR data. FQ resistance due to target mutations is rare (FoR in the 10^{-10} range) and cystobactamid FoR was by tendency, albeit variable, higher and on average in the 10^{-8} range. No cross-resistance with CIP was observed for cystobactamid-resistant *E. coli*, *K. pneumoniae* and *A. baumannii*, whereas *S. aureus* mutants displayed a medium cross-resistance with CIP (up to 10-fold). Cystobactamid-resistant *P. aeruginosa* PA14Δ*mexAB* displayed a high level of cross-resistance with FQ; however, this was only observed with the synthetic derivative CN-DM-861 and not with the natural derivative Cys861. Furthermore, only in some cystobactamid-resistant mutants of *S. aureus* and *A. baumannii* did we find exclusively target mutations (topoisomerase IV or

gyrase, respectively) conferring different levels of resistance to cystobactamids, i.e. variable level of resistance in *S. aureus* (MIC 0.5-32 µg/mL), full resistance in *A. baumannii* DSM-30008 (MIC > 64 µg/mL), and low resistance in *A. baumannii* CIP-105742 (MIC 0.5-1 µg/mL). Cystobactamids can therefore overcome FQ resistance mechanisms. Despite their resistance-breaking properties, activity of cystobactamids is often hindered. This is mainly due to efflux in *P. aeruginsa*, and efflux (AcrAB-TolC) and hindered penetration in *E. coli* (*hldE* mutant) and *K. pneumoniae* (*waaC* mutant), due to inteactions with LPS of the OM. We could show that cystobactamids do not enter the bacterial cells via porins, however, at this point it remains unclear how they reach their cytoplasmic target. Some hints about this are given in *K. oxytoca* background. *K. oxytoca*, like *K. pneumoniae* expresses AlbA, albicidin high-affinity binding protein, and both are consequently resistant to albicidin. Albicidin, also a topoisomerase IIa poison, and cystobactamids do not only share the same target, but are also structurally very similar. Consequently, it was expected that cystobactamids would not be active on *K. oxytoca* and *K. pneumoniae*. Surprisingly, cystobactamids were active on *K. oxytoca* strains but not on *K. pneumoniae*. We already know that inactivity on *K. pneumoniae* is due to LPS modifications (*waaC* mutant – a heptose-less LPS mutant is cystobactamid-sensitive), but since both express AlbA, the discrepancy could not be explained. However, *K. oxytoca* has in its OM an ion permeable channel CymA, able to passively import larger bulky compounds, like cyclodextrin and potentially cystobactamids, and this could explain the observed activity on *K. oxytoca* that was not observed in *K. pneumoniae*.

Resistance development revealed unusual modes of resistance. Not target mutations but rather mutations in QseBC and CpxSR two-component systems in *E. coli* and in *P. aeruginosa*, respectively. Mutations in both TCS are gain-in-function mutations, and initiate a complex regulatory cascade. In *E. coli* this results in QseBC-PmrAB cross-talk, upregulation of genes encoding LPS modifying enzymes (addition of L-Ara4N and pEtN) under the control of both

QseBC and PmrAB, and upregulation of 2-oxoglutarat production (for synthesis of L-Ara4N) by upregulating expression of genes feeding glutamate, succinat and fumarate back in the TCA cycle to sustain production of modified LPS molecules. Addition of L-Ara4 and pEtN to LPS results in reduced negative charge of the outer membrane. How exactly this hinders translocation of cystobactamids accros outer membrane is unclear, especially since the terminal carboxylic acid would be negatively charged at physiological pH, therefore cystobactamids would be attracted to the now more positive outer membrane. It is possible that outer membrane charge changes cause cystobactamids to be stuck in the membrane. Although QseBC-PmrAB cross-talk resulting in increased survival to CAMP due to LPS modifications has been described, cystobactamids are the first compound class directly implicating QseBC TCS in antibiotic resistance in a manner similar to CAMP resistance. Similarly, in *P. aeruginosa*, mutations in the novel CpxSR TCS resulted in upregulation of mutidrug efflux pump (MuxABC), OB-fold proteins interacting with porins (YdeI-OmpD, YgiW-OmpF), and proteins involed in maintenance of cell envelope architecture (Sky/CpxP protein). CpxSR mutations therefore confer resistance to cystobactamids by limiting the uptake of cystobactamid, changing the cell envelope and upregulating efflux. In *A. baumannii* we found that resistance to cystobactamid relies on target modifications and occasionaly on outer membrane modifications. In *S. aureus* target mutations are the main cause of cystobactamid resistance. The least understood mode of resistance is the AlbA-mediated cystobactamid resistance in *K. pneumoniae*.

Cystobactamid resistance is achieved by employing several resistance mechanisms. Although we are aware that several modes-of-resistance to every antibiotic class exist, there is no literature reported data on it. Whether this means a study as extensive as ours was not done or simply not reported, due to the obvious diversity and complexitiy of bacterial responses upon application of selective pressure, is unclear. One could speculate that species-specific mode-of-

resistance arises due to diverse intrinsic resistance of the species under investigation. There is a clear difference in how Gram-positive species protect themselves versus the Gram-negative species. Whereas Gram-positive *S. aureus* achieved resistance by only modifying the target (*parC/grlA*), Gram-negatives, *E. coli*, *P. aeruginosa*, and *A. baumannii* predominantly utilized active efflux and limit the drug uptake occasionally in combination with target mutations. These findings additionally emphasize the role of the outer membrane as the entry checkpoint for compounds, and why R&D of antibiotics targeting Gram-negative pathogens is challenging. It additionally demonstrates the enormous plasticity of bacterial genomes and the complexity and adaptability of microbial responses to selective pressure. Although challenging to elucidate, understanding the underlying mechanisms of resistance will help us in design and synthesis of improved cystobactamid derivatives.

7   References

1.   WHO.   Antibiotic   resistance   https://www.who.int/news-room/fact-sheets/detail/antibiotic-resistance: WHO;   2020   [cited   2020].   Available   from: https://www.who.int/news-room/fact-sheets/detail/antibiotic-resistance.

2.   Perry J, Waglechner N, Wright G. The Prehistory of Antibiotic Resistance. Cold Spring Harb Perspect Med. 2016;6(6). Epub 2016/06/03. doi: 10.1101/cshperspect.a025197. PubMed PMID: 27252395; PubMed Central PMCID: PMCPMC4888810.

3.   Holmes B. Antibiotic resistance predates drugs – by 30,000 years. New Scientist. 2011;211(2828):14. doi: https://doi.org/10.1016/S0262-4079(11)62130-1.

4.   Kraemer SA, Ramachandran A, Perron GG. Antibiotic Pollution in the Environment: From   Microbial   Ecology   to   Public   Policy.   Microorganisms.   2019;7(6):180.   doi: 10.3390/microorganisms7060180. PubMed PMID: 31234491.

5.   D'Costa VM, King CE, Kalan L, Morar M, Sung WWL, Schwarz C, et al. Antibiotic resistance is ancient. Nature. 2011;477(7365):457-61. doi: 10.1038/nature10388.

6.   Petrova M, Gorlenko Z, Mindlin S. Molecular structure and translocation of a multiple antibiotic resistance region of a Psychrobacter psychrophilus permafrost strain. FEMS Microbiol Lett. 2009;296(2):190-7. Epub 2009/05/23. doi: 10.1111/j.1574-6968.2009.01635.x. PubMed PMID: 19459955.

7.   Santiago-Rodriguez TM, Fornaciari G, Luciani S, Dowd SE, Toranzos GA, Marota I, et al. Gut Microbiome of an 11th Century A.D. Pre-Columbian Andean Mummy. PLoS One. 2015;10(9):e0138135. doi: 10.1371/journal.pone.0138135.

8.   Warinner C, Rodrigues JF, Vyas R, Trachsel C, Shved N, Grossmann J, et al. Pathogens and host immunity in the ancient human oral cavity. Nat Genet. 2014;46(4):336-44. Epub 2014/02/25. doi: 10.1038/ng.2906. PubMed PMID: 24562188; PubMed Central PMCID: PMCPMC3969750.

9.   Aslam B, Wang W, Arshad MI, Khurshid M, Muzammil S, Rasool MH, et al. Antibiotic resistance: a rundown of a global crisis. Infect Drug Resist. 2018;11:1645-58. doi: 10.2147/IDR.S173867. PubMed PMID: 30349322.

10.   Munita JM, Arias CA. Mechanisms of Antibiotic Resistance. Microbiol Spectr. 2016;4(2):10.1128/microbiolspec.VMBF-0016-2015.   doi: 10.1128/microbiolspec.VMBF-0016-2015. PubMed PMID: 27227291.

11.   Peterson E, Kaur P. Antibiotic Resistance Mechanisms in Bacteria: Relationships Between Resistance Determinants of Antibiotic Producers, Environmental Bacteria, and Clinical Pathogens. Frontiers in Microbiology. 2018;9(2928). doi: 10.3389/fmicb.2018.02928.

12.   Prevention CfDCa. Antibiotic/Antimicrobial Resistance (AR/AMR) 2020 [updated 13.03.2020;   cited   2021   26.04.].   Available   from: https://www.cdc.gov/drugresistance/about.html.

13.   Zaman SB, Hussain MA, Nye R, Mehta V, Mamun KT, Hossain N. A Review on Antibiotic Resistance: Alarm Bells are Ringing. Cureus. 2017;9(6):e1403. Epub 2017/08/31. doi: 10.7759/cureus.1403.   PubMed   PMID: 28852600;   PubMed   Central   PMCID: PMCPMC5573035.

14.   Dadgostar P. Antimicrobial Resistance: Implications and Costs. Infect Drug Resist. 2019;12:3903-10. doi: 10.2147/IDR.S234610. PubMed PMID: 31908502.

15.   OECD W, FAO, OIE. Tackling Antimicrobial Resistance Ensuring Sustainable R&D. 2017.

16.   Olga B. Jonas AI, Berthe Franck, Cesar Jean Le Gall, Francois G. Marquez, Patricio V. Drug-resistant infections: a threat to our economic future (Vol.2): final report (English). The World Bank, 2017 01.03.2017. Report No.: 114679.

17.   Reygaert WC. An overview of the antimicrobial resistance mechanisms of bacteria. AIMS Microbiol. 2018;4(3):482-501. doi: 10.3934/microbiol.2018.3.482. PubMed PMID: 31294229.

18.   Fyfe C, Grossman TH, Kerstein K, Sutcliffe J. Resistance to Macrolide Antibiotics in Public Health Pathogens. Cold Spring Harb Perspect Med. 2016;6(10):a025395. doi: 10.1101/cshperspect.a025395. PubMed PMID: 27527699.

19.   Babini GS, Livermore DM. Are SHV beta-lactamases universal in Klebsiella pneumoniae? Antimicrobial agents and chemotherapy. 2000;44(8):2230-. doi: 10.1128/aac.44.8.2230-2230.2000. PubMed PMID: 11023444.

20.   Guo Q, Tomich AD, McElheny CL, Cooper VS, Stoesser N, Wang M, et al. Glutathione-S-transferase FosA6 of Klebsiella pneumoniae origin conferring fosfomycin resistance in ESBL-producing Escherichia coli. J Antimicrob Chemother. 2016;71(9):2460-5. Epub 2016/06/05. doi: 10.1093/jac/dkw177. PubMed PMID: 27261267; PubMed Central PMCID: PMCPMC4992852.

21.   Yuan J, Xu X, Guo Q, Zhao X, Ye X, Guo Y, et al. Prevalence of the oqxAB gene complex in Klebsiella pneumoniae and Escherichia coli clinical isolates. J Antimicrob Chemother. 2012;67(7):1655-9. Epub 2012/03/23. doi: 10.1093/jac/dks086. PubMed PMID: 22438434.

22.   Seitz P, Blokesch M. Cues and regulatory pathways involved in natural competence and transformation in pathogenic and environmental Gram-negative bacteria. FEMS Microbiol Rev. 2013;37(3):336-63. Epub 2012/08/30. doi: 10.1111/j.1574-6976.2012.00353.x. PubMed PMID: 22928673.

23.   Blokesch M. Natural competence for transformation. Current Biology. 2016;26(21):R1126-R30. doi: https://doi.org/10.1016/j.cub.2016.08.058.

24.   Burmeister AR. Horizontal Gene Transfer. Evol Med Public Health. 2015;2015(1):193-4. doi: 10.1093/emph/eov018. PubMed PMID: 26224621.

25.   Lerminiaux NA, Cameron ADS. Horizontal transfer of antibiotic resistance genes in clinical environments. Canadian Journal of Microbiology. 2018;65(1):34-44. doi: 10.1139/cjm-2018-0275.

26.   Brandis G, Wrande M, Liljas L, Hughes D. Fitness-compensatory mutations in rifampicin-resistant RNA polymerase. Molecular Microbiology. 2012;85(1):142-51. doi: https://doi.org/10.1111/j.1365-2958.2012.08099.x.

27.   Brandis G, Hughes D. Mechanisms of fitness cost reduction for rifampicin-resistant strains with deletion or duplication mutations in rpoB. Scientific Reports. 2018;8(1):17488. doi: 10.1038/s41598-018-36005-y.

28.   Wood TK, Knabel SJ, Kwan BW. Bacterial persister cell formation and dormancy. Appl Environ Microbiol. 2013;79(23):7116-21. Epub 2013/09/13. doi: 10.1128/AEM.02636-13. PubMed PMID: 24038684.

29.   Vogwill T, Comfort AC, Furió V, MacLean RC. Persistence and resistance as complementary bacterial adaptations to antibiotics. Journal of Evolutionary Biology. 2016;29(6):1223-33. doi: https://doi.org/10.1111/jeb.12864.

30.   Brauner A, Fridman O, Gefen O, Balaban NQ. Distinguishing between resistance, tolerance and persistence to antibiotic treatment. Nature Reviews Microbiology. 2016;14(5):320-30. doi: 10.1038/nrmicro.2016.34.

31.   Levin-Reisman I, Brauner A, Ronin I, Balaban NQ. Epistasis between antibiotic tolerance, persistence, and resistance mutations. Proceedings of the National Academy of Sciences. 2019;116(29):14734. doi: 10.1073/pnas.1906169116.

32.   Handwerger S, Tomasz A. Antibiotic tolerance among clinical isolates of bacteria. Annu Rev Pharmacol Toxicol. 1985;25:349-80. Epub 1985/01/01. doi: 10.1146/annurev.pa.25.040185.002025. PubMed PMID: 3890707.

33. Bates DM, Eiff Cv, McNamara PJ, Peters G, Yeaman MR, Bayer AS, et al. Staphylococcus aureus menD and hemB Mutants Are as Infective as the Parent Strains, but the Menadione Biosynthetic Mutant Persists within the Kidney. The Journal of Infectious Diseases. 2003;187(10):1654-61. doi: 10.1086/374642.

34. Bhattacharyya S, Roy S, Mukhopadhyay P, Rit K, Dey J, Ganguly U, et al. Small Colony variants of Staphylococcus aureus isolated from a patient with infective endocarditis: a case report and review of the literature. Iran J Microbiol. 2012;4(2):98-9. Epub 2012/09/14. PubMed PMID: 22973477; PubMed Central PMCID: PMCPMC3434649.

35. Huemer M, Mairpady Shambat S, Brugger SD, Zinkernagel AS. Antibiotic resistance and persistence—Implications for human health and treatment perspectives. EMBO reports. 2020;21(12):e51034. doi: https://doi.org/10.15252/embr.202051034.

36. Chaw PS, Schlinkmann MKM, Raupach-Rosin H, Karch A, Pletz MW, Huebner J, et al. Knowledge, attitude and practice of Gambian health practitioners towards antibiotic prescribing and microbiological testing: a cross-sectional survey. Trans R Soc Trop Med Hyg. 2017;111(3):117-24. Epub 2017/06/22. doi: 10.1093/trstmh/trx027. PubMed PMID: 28633334.

37. Adorka M, Dikokole M, Mitonga KH, Allen K. Healthcare providers' attitudes and perceptions in infection diagnosis and antibiotic prescribing in public health institutions in Lesotho: a cross sectional survey. Afr Health Sci. 2013;13(2):344-50. doi: 10.4314/ahs.v13i2.21. PubMed PMID: 24235934.

38. Shakoor O, Taylor RB, Behrens RH. Assessment of the incidence of substandard drugs in developing countries. Trop Med Int Health. 1997;2(9):839-45. Epub 1997/10/07. doi: 10.1046/j.1365-3156.1997.d01-403.x. PubMed PMID: 9315042.

39. Ogunshe A, Adinmonyema P. Evaluation of bacteriostatic potency of expired oral paediatric antibiotics and implications on infant health. Pan Afr Med J. 2014;19:378-. doi: 10.11604/pamj.2014.19.378.2156. PubMed PMID: 25977741.

40. Okuonghae HO, Ighogboja IS, Lawson JO, Nwana EJ. Diethylene glycol poisoning in Nigerian children. Ann Trop Paediatr. 1992;12(3):235-8. Epub 1992/01/01. doi: 10.1080/02724936.1992.11747577. PubMed PMID: 1280035.

41. Pandya SK. Letter from Bombay. An unmitigated tragedy. Bmj. 1988;297(6641):117-9. Epub 1988/07/09. doi: 10.1136/bmj.297.6641.117. PubMed PMID: 3408933; PubMed Central PMCID: PMCPMC1833772.

42. Sammons HM, Choonara I. Substandard medicines: a greater problem than counterfeit medicines? BMJ Paediatr Open. 2017;1(1):e000007-e. doi: 10.1136/bmjpo-2017-000007. PubMed PMID: 29637090.

43. Chokshi A, Sifri Z, Cennimo D, Horng H. Global Contributors to Antibiotic Resistance. J Glob Infect Dis. 2019;11(1):36-42. Epub 2019/03/01. doi: 10.4103/jgid.jgid_110_18. PubMed PMID: 30814834; PubMed Central PMCID: PMCPMC6380099.

44. Okeke IN, Lamikanra A, Edelman R. Socioeconomic and behavioral factors leading to acquired bacterial resistance to antibiotics in developing countries. Emerg Infect Dis. 1999;5(1):18-27. Epub 1999/03/19. doi: 10.3201/eid0501.990103. PubMed PMID: 10081668; PubMed Central PMCID: PMCPMC2627681.

45. Enzler MJ, Berbari E, Osmon DR. Antimicrobial prophylaxis in adults. Mayo Clin Proc. 2011;86(7):686-701. doi: 10.4065/mcp.2011.0012. PubMed PMID: 21719623.

46. Nordahl Petersen T, Rasmussen S, Hasman H, Carøe C, Bælum J, Schultz AC, et al. Meta-genomic analysis of toilet waste from long distance flights; a step towards global surveillance of infectious diseases and antimicrobial resistance. Sci Rep. 2015;5:11444. Epub 2015/07/15. doi: 10.1038/srep11444. PubMed PMID: 26161690; PubMed Central PMCID: PMCPMC4498435.

47. Börjesson S, Guillard T, Landén A, Bengtsson B, Nilsson O. Introduction of quinolone resistant Escherichia coli to Swedish broiler population by imported breeding animals. Veterinary Microbiology. 2016;194:74-8. doi: https://doi.org/10.1016/j.vetmic.2015.11.004.

48.   Abdallah HM, Reuland EA, Wintermans BB, Al Naiemi N, Koek A, Abdelwahab AM, et al. Extended-Spectrum β-Lactamases and/or Carbapenemases-Producing Enterobacteriaceae Isolated from Retail Chicken Meat in Zagazig, Egypt. PLoS One. 2015;10(8):e0136052. Epub 2015/08/19. doi: 10.1371/journal.pone.0136052. PubMed PMID: 26284654; PubMed Central PMCID: PMCPMC4540287.

49.   He T, Wang Y, Sun L, Pang M, Zhang L, Wang R. Occurrence and characterization of blaNDM-5-positive Klebsiella pneumoniae isolates from dairy cows in Jiangsu, China. J Antimicrob Chemother. 2017;72(1):90-4. Epub 2016/09/14. doi: 10.1093/jac/dkw357. PubMed PMID: 27621177.

50.   Yaici L, Haenni M, Saras E, Boudehouche W, Touati A, Madec JY. blaNDM-5-carrying IncX3 plasmid in Escherichia coli ST1284 isolated from raw milk collected in a dairy farm in Algeria. J Antimicrob Chemother. 2016;71(9):2671-2. Epub 2016/05/12. doi: 10.1093/jac/dkw160. PubMed PMID: 27165785.

51.   Bogaerts P, Huang TD, Bouchahrouf W, Bauraing C, Berhin C, El Garch F, et al. Characterization of ESBL- and AmpC-Producing Enterobacteriaceae from Diseased Companion Animals in Europe. Microb Drug Resist. 2015;21(6):643-50. Epub 2015/06/23. doi: 10.1089/mdr.2014.0284. PubMed PMID: 26098354.

52.   Richman PB, Garra G, Eskin B, Nashed AH, Cody R. Oral antibiotic use without consulting a physician: a survey of ED patients. Am J Emerg Med. 2001;19(1):57-60. Epub 2001/01/09. doi: 10.1053/ajem.2001.20035. PubMed PMID: 11146021.

53.   Grigoryan L, Haaijer-Ruskamp F, Burgerhof JGM, Mechtler R, Deschepper R, Tambic-Andrasevic A, et al. Self-medication with Antimicrobial Drugs in Europe. Emerging Infectious Disease journal. 2006;12(3):452. doi: 10.3201/eid1203.050992.

54.   Lescure D, Paget J, Schellevis F, van Dijk L. Determinants of Self-Medication With Antibiotics in European and Anglo-Saxon Countries: A Systematic Review of the Literature. Frontiers in Public Health. 2018;6(370). doi: 10.3389/fpubh.2018.00370.

55.   Van Lunen TA. Growth performance of pigs fed diets with and without tylosin phosphate supplementation and reared in a biosecure all-in all-out housing system. Can Vet J. 2003;44(7):571-6. Epub 2003/08/02. PubMed PMID: 12892287; PubMed Central PMCID: PMCPMC340208.

56.   He S, Zhou Z, Meng K, Zhao H, Yao B, Ringø E, et al. Effects of dietary antibiotic growth promoter and Saccharomyces cerevisiae fermentation product on production, intestinal bacterial community, and nonspecific immunity of hybrid tilapia (Oreochromis niloticus female x Oreochromis aureus male). J Anim Sci. 2011;89(1):84-92. Epub 2010/09/21. doi: 10.2527/jas.2010-3032. PubMed PMID: 20852079.

57.   Soma JA, Speer VC. Effects of pregnant mare serum and chlortetracycline on the reproductive efficiency of sows. J Anim Sci. 1975;41(1):100-5. Epub 1975/07/01. doi: 10.2527/jas1975.411100x. PubMed PMID: 1158786.

58.   Lindemann MD, Kornegay ET, Stahly TS, Cromwell GL, Easter RA, Kerr BJ, et al. The efficacy of salinomycin as a growth promotant for swine from 9 to 97 kg. J Anim Sci. 1985;61(4):782-8. Epub 1985/10/01. doi: 10.2527/jas1985.614782x. PubMed PMID: 4066536.

59.   Hao H, Cheng G, Iqbal Z, Ai X, Hussain HI, Huang L, et al. Benefits and risks of antimicrobial use in food-producing animals. Front Microbiol. 2014;5:288. Epub 2014/06/28. doi: 10.3389/fmicb.2014.00288. PubMed PMID: 24971079; PubMed Central PMCID: PMCPMC4054498.

60.   Manyi-Loh C, Mamphweli S, Meyer E, Okoh A. Antibiotic Use in Agriculture and Its Consequential Resistance in Environmental Sources: Potential Public Health Implications. Molecules (Basel, Switzerland). 2018;23(4):795. doi: 10.3390/molecules23040795. PubMed PMID: 29601469.

61.   Muriuki FK, Ogara WO, Njeruh FM, Mitema ES. Tetracycline residue levels in cattle meat from Nairobi salughter house in Kenya. J Vet Sci. 2001;2(2):97-101. Epub 2003/11/14. PubMed PMID: 14614278.

62.   Er B, Onurdag FK, Demirhan B, Ozgacar S, Oktem AB, Abbasoglu U. Screening of quinolone antibiotic residues in chicken meat and beef sold in the markets of Ankara, Turkey. Poult Sci. 2013;92(8):2212-5. Epub 2013/07/23. doi: 10.3382/ps.2013-03072. PubMed PMID: 23873571.

63.   Billah MM, Rana SMM, Hossain MS, Ahamed SK, Banik S, Hasan M. Ciprofloxacin residue and their impact on biomolecules in eggs of laying hens following oral administration. International Journal of Food Contamination. 2015;2(1):13. doi: 10.1186/s40550-015-0019-x.

64.   Olatoye O, Agboola E. Oxytetracycline Residues in Edible Tissues of Cattle Slaughtered in Akure, Nigeria. Nigerian Vet J. 2011;31. doi: 10.4314/nvj.v31i2.68952.

65.   You Y, Silbergeld EK. Learning from agriculture: understanding low-dose antimicrobials as drivers of resistome expansion. Front Microbiol. 2014;5:284. Epub 2014/06/25. doi: 10.3389/fmicb.2014.00284. PubMed PMID: 24959164; PubMed Central PMCID: PMCPMC4050735.

66.   Osei Sekyere J. Antibiotic Types and Handling Practices in Disease Management among Pig Farms in Ashanti Region, Ghana. Journal of Veterinary Medicine. 2014;2014:1-8. doi: 10.1155/2014/531952.

67.   Executive HaS. Veterinary medicines: Safe use by farmers and other animal handlers. The Health and Safety Executive; 2012. p. 8.

68.   Kempf I, Fleury MA, Drider D, Bruneau M, Sanders P, Chauvin C, et al. What do we know about resistance to colistin in Enterobacteriaceae in avian and pig production in Europe? International Journal of Antimicrobial Agents. 2013;42(5):379-83. doi: https://doi.org/10.1016/j.ijantimicag.2013.06.012.

69.   Martins AF, Rabinowitz P. The impact of antimicrobial resistance in the environment on public health. Future Microbiology. 2020;15(9):699-702. doi: 10.2217/fmb-2019-0331.

70.   Biswas DK, Bhunia R, Maji D, Das P. Contaminated pond water favors cholera outbreak at haibatpur village, purba medinipur district, west bengal, India. J Trop Med. 2014;2014:764530. Epub 2014/06/06. doi: 10.1155/2014/764530. PubMed PMID: 24899903; PubMed Central PMCID: PMCPMC4036642.

71.   He F, Han K, Liu L, Sun W, Zhang L, Zhu B, et al. Shigellosis outbreak associated with contaminated well water in a rural elementary school: Sichuan Province, China, June 7-16, 2009. PLoS One. 2012;7(10):e47239. Epub 2012/10/17. doi: 10.1371/journal.pone.0047239. PubMed PMID: 23071767; PubMed Central PMCID: PMCPMC3468462.

72.   OO Soge MG, IC Ivanova, AL Pearson, JS Meschke, C Roberts. Low-prevalence of antibiotic-resistant gram-negative bacteria isolated from rural south-western Ugandan groundwater. AJOL. 2009;35(3):6. doi: 10.4314/wsa.v35i3.76779.

73.   Pieper U, von Hildebrand A, Tisocki K. Call for a Sound Management of Pharmaceutical Waste and Wastewater to Curb Antimicrobial Resistance. 2020.

74.   Nathan C. Resisting antimicrobial resistance. Nature Reviews Microbiology. 2020;18(5):259-60. doi: 10.1038/s41579-020-0348-5.

75.   WHO. Global Action Plan on Antimicrobial Resistance. Geneva, Switzerland: WHO, 2015.

76.   Lorencatto F, Charani E, Sevdalis N, Tarrant C, Davey P. Driving sustainable change in antimicrobial prescribing practice: how can social and behavioural sciences help? Journal of Antimicrobial Chemotherapy. 2018;73(10):2613-24. doi: 10.1093/jac/dky222.

77.   Haenssgen MJ, Charoenboon N, Khine Zaw Y. It is time to give social research a voice to tackle antimicrobial resistance? Journal of Antimicrobial Chemotherapy. 2018;73(4):1112-3. doi: 10.1093/jac/dkx533.

78.   Donisi V, Sibani M, Carrara E, Del Piccolo L, Rimondini M, Mazzaferri F, et al. Emotional, cognitive and social factors of antimicrobial prescribing: can antimicrobial stewardship intervention be effective without addressing psycho-social factors? Journal of Antimicrobial Chemotherapy. 2019;74(10):2844-7. doi: 10.1093/jac/dkz308.

79.   Luepke KH, Suda KJ, Boucher H, Russo RL, Bonney MW, Hunt TD, et al. Past, Present, and Future of Antibacterial Economics: Increasing Bacterial Resistance, Limited Antibiotic Pipeline, and Societal Implications. Pharmacotherapy: The Journal of Human Pharmacology and Drug Therapy. 2017;37(1):71-84. doi: https://doi.org/10.1002/phar.1868.

80.   Spellberg B. The future of antibiotics. Critical Care. 2014;18(3):228. doi: 10.1186/cc13948.

81.   WHO. Antibacterial agents in clinical development. An analysis of the antibacterial clinical development pipeline, including tuberculosis. Geneva, Switzerland: WHO, 2017 09.2017. Report No.: Contract No.: WHO/EMP/IAU/2017.11.

82.   Terreni M, Taccani M, Pregnolato M. New Antibiotics for Multidrug-Resistant Bacterial Strains: Latest Research Developments and Future Perspectives. Molecules (Basel, Switzerland). 2021;26(9):2671. doi: 10.3390/molecules26092671. PubMed PMID: 34063264.

83.   WHO. 2019 Antibacterial agents in clinical development: an analysis of the antibacterial clinical development pipeline. WHO, 2019.

84.   WHO. Antibacterial agents in preclinical development: an open access database. Geneva, Switzerland: WHO, 2019 2019. Report No.

85.   Blair JMA, Webber MA, Baylay AJ, Ogbolu DO, Piddock LJV. Molecular mechanisms of antibiotic resistance. Nature Reviews Microbiology. 2015;13(1):42-51. doi: 10.1038/nrmicro3380.

86.   Okuda K-I, Nagahori R, Yamada S, Sugimoto S, Sato C, Sato M, et al. The Composition and Structure of Biofilms Developed by Propionibacterium acnes Isolated from Cardiac Pacemaker Devices. Frontiers in microbiology. 2018;9:182-. doi: 10.3389/fmicb.2018.00182. PubMed PMID: 29491850.

87.   Cornaglia G, Mazzariol A, Fontana R, Satta G. Diffusion of carbapenems through the outer membrane of enterobacteriaceae and correlation of their activities with their periplasmic concentrations. Microb Drug Resist. 1996;2(2):273-6. Epub 1996/07/01. doi: 10.1089/mdr.1996.2.273. PubMed PMID: 9158772.

88.   Chow JW, Shlaes DM. Imipenem resistance associated with the loss of a 40 kDa outer membrane protein in Enterobacter aerogenes. J Antimicrob Chemother. 1991;28(4):499-504. Epub 1991/10/01. doi: 10.1093/jac/28.4.499. PubMed PMID: 1761444.

89.   Gill MJ, Simjee S, Al-Hattawi K, Robertson BD, Easmon CS, Ison CA. Gonococcal resistance to beta-lactams and tetracycline involves mutation in loop 3 of the porin encoded at the penB locus. Antimicrob Agents Chemother. 1998;42(11):2799-803. Epub 1998/10/31. doi: 10.1128/aac.42.11.2799. PubMed PMID: 9797206; PubMed Central PMCID: PMCPMC105946.

90.   Olaitan AO, Morand S, Rolain JM. Mechanisms of polymyxin resistance: acquired and intrinsic resistance in bacteria. Front Microbiol. 2014;5:643. Epub 2014/12/17. doi: 10.3389/fmicb.2014.00643. PubMed PMID: 25505462; PubMed Central PMCID: PMCPMC4244539.

91.   Hooper DC. Fluoroquinolone resistance among Gram-positive cocci. Lancet Infect Dis. 2002;2(9):530-8. Epub 2002/09/11. doi: 10.1016/s1473-3099(02)00369-9. PubMed PMID: 12206969.

92.   Zhu D, Zheng M, Xu J, Wang M, Jia R, Chen S, et al. Prevalence of fluoroquinolone resistance and mutations in the gyrA, parC and parE genes of Riemerella anatipestifer isolated from ducks in China. BMC Microbiology. 2019;19(1):271. doi: 10.1186/s12866-019-1659-4.

93.   Redgrave LS, Sutton SB, Webber MA, Piddock LJ. Fluoroquinolone resistance: mechanisms, impact on bacteria, and role in evolutionary success. Trends Microbiol.

2014;22(8):438-45. Epub 2014/05/21. doi: 10.1016/j.tim.2014.04.007. PubMed PMID: 24842194.

94. Cetinkaya Y, Falk P, Mayhall CG. Vancomycin-resistant enterococci. Clinical microbiology reviews. 2000;13(4):686-707. doi: 10.1128/cmr.13.4.686-707.2000. PubMed PMID: 11023964.

95. Cai X-C, Xi H, Liang L, Liu J-D, Liu C-H, Xue Y-R, et al. Rifampicin-Resistance Mutations in the rpoB Gene in Bacillus velezensis CC09 have Pleiotropic Effects. Frontiers in Microbiology. 2017;8(178). doi: 10.3389/fmicb.2017.00178.

96. Zaw MT, Emran NA, Lin Z. Mutations inside rifampicin-resistance determining region of rpoB gene associated with rifampicin-resistance in Mycobacterium tuberculosis. J Infect Public Health. 2018;11(5):605-10. Epub 2018/05/01. doi: 10.1016/j.jiph.2018.04.005. PubMed PMID: 29706316.

97. Ramirez MS, Tolmasky ME. Aminoglycoside modifying enzymes. Drug Resist Updat. 2010;13(6):151-71. Epub 2010/09/14. doi: 10.1016/j.drup.2010.08.003. PubMed PMID: 20833577; PubMed Central PMCID: PMCPMC2992599.

98. Bush K, Jacoby GA. Updated functional classification of beta-lactamases. Antimicrob Agents Chemother. 2010;54(3):969-76. Epub 2009/12/10. doi: 10.1128/aac.01009-09. PubMed PMID: 19995920; PubMed Central PMCID: PMCPMC2825993.

99. Sikandar A, Cirnski K, Testolin G, Volz C, Brönstrup M, Kalinina OV, et al. Adaptation of a Bacterial Multidrug Resistance System Revealed by the Structure and Function of AlbA. Journal of the American Chemical Society. 2018;140(48):16641-9. doi: 10.1021/jacs.8b08895.

100. Rostock L, Driller R, Grätz S, Kerwat D, von Eckardstein L, Petras D, et al. Molecular insights into antibiotic resistance - how a binding protein traps albicidin. Nat Commun. 2018;9(1):3095. Epub 2018/08/08. doi: 10.1038/s41467-018-05551-4. PubMed PMID: 30082794; PubMed Central PMCID: PMCPMC6078987.

101. Foster TJ. Antibiotic resistance in Staphylococcus aureus. Current status and future prospects. FEMS Microbiology Reviews. 2017;41(3):430-49. doi: 10.1093/femsre/fux007.

102. Colclough AL, Alav I, Whittle EE, Pugh HL, Darby EM, Legood SW, et al. RND efflux pumps in Gram-negative bacteria; regulation, structure and role in antibiotic resistance. Future Microbiol. 2020;15:143-57. Epub 2020/02/20. doi: 10.2217/fmb-2019-0235. PubMed PMID: 32073314.

103. Baumann S, Herrmann J, Raju R, Steinmetz H, Mohr KI, Hüttel S, et al. Cystobactamids: myxobacterial topoisomerase inhibitors exhibiting potent antibacterial activity. Angew Chem Int Ed Engl. 2014;53(52):14605-9. Epub 2014/12/17. doi: 10.1002/anie.201409964. PubMed PMID: 25510965.

104. Hüttel S, Testolin G, Herrmann J, Planke T, Gille F, Moreno M, et al. Discovery and Total Synthesis of Natural Cystobactamid Derivatives with Superior Activity against Gram-Negative Pathogens. Angew Chem Int Ed Engl. 2017;56(41):12760-4. Epub 2017/07/22. doi: 10.1002/anie.201705913. PubMed PMID: 28730677.

105. Testolin G, Cirnski K, Rox K, Prochnow H, Fetz V, Grandclaudon C, et al. Synthetic studies of cystobactamids as antibiotics and bacterial imaging carriers lead to compounds with high in vivo efficacy. Chemical Science. 2020;11(5):1316-34. doi: 10.1039/C9SC04769G.

106. Groß S, Schnell B, Haack PA, Auerbach D, Müller R. In vivo and in vitro reconstitution of unique key steps in cystobactamid antibiotic biosynthesis. Nature Communications. 2021;12(1):1696. doi: 10.1038/s41467-021-21848-3.

107. Planke T, Cirnski K, Herrmann J, Müller R, Kirschning A. Synthetic and Biological Studies on New Urea and Triazole Containing Cystobactamid Derivatives. Chemistry. 2020;26(19):4289-96. Epub 2019/12/14. doi: 10.1002/chem.201904073. PubMed PMID: 31834653; PubMed Central PMCID: PMCPMC7186842.

108. Elgaher WAM, Hamed MM, Baumann S, Herrmann J, Siebenbürger L, Krull J, et al. Cystobactamid 507: Concise Synthesis, Mode of Action, and Optimization toward More Potent

Antibiotics. Chemistry – A European Journal. 2020;26(32):7219-25. doi: https://doi.org/10.1002/chem.202000117.

109.   Moeller M, Norris MD, Planke T, Cirnski K, Herrmann J, Müller R, et al. Scalable Syntheses of Methoxyaspartate and Preparation of the Antibiotic Cystobactamid 861-2 and Highly Potent Derivatives. Org Lett. 2019;21(20):8369-72. Epub 2019/10/11. doi: 10.1021/acs.orglett.9b03143. PubMed PMID: 31599597.

110.   Planke T, Moreno M, Hüttel S, Fohrer J, Gille F, Norris MD, et al. Cystobactamids 920-1 and 920-2: Assignment of the Constitution and Relative Configuration by Total Synthesis. Organic Letters. 2019;21(5):1359-63. doi: 10.1021/acs.orglett.9b00058.

111.   Hutchings MI, Truman AW, Wilkinson B. Antibiotics: past, present and future. Current Opinion in Microbiology. 2019;51:72-80. doi: https://doi.org/10.1016/j.mib.2019.10.008.

112.   Davies J. Where have All the Antibiotics Gone? Can J Infect Dis Med Microbiol. 2006;17(5):287-90. doi: 10.1155/2006/707296. PubMed PMID: 18382641.

113.   Theuretzbacher U, Outterson K, Engel A, Karlén A. The global preclinical antibacterial pipeline. Nature Reviews Microbiology. 2020;18(5):275-85. doi: 10.1038/s41579-019-0288-0.

114.   Theuretzbacher U, Bush K, Harbarth S, Paul M, Rex JH, Tacconelli E, et al. Critical analysis of antibacterial agents in clinical development. Nature Reviews Microbiology. 2020;18(5):286-98. doi: 10.1038/s41579-020-0340-0.

115.   WHO. Global priority list of antibiotic-resistant bacteria to guide research, discovery, and development of new antibiotics. Geneva, Switzerland: WHO, 2017 27.02.2017. Report No.

116.   Kelly BG, Vespermann A, Bolton DJ. Gene transfer events and their occurrence in selected environments. Food and Chemical Toxicology. 2009;47(5):978-83. doi: https://doi.org/10.1016/j.fct.2008.06.012.

117.   Keese P. Risks from GMOs due to Horizontal Gene Transfer. Environmental Biosafety Research. 2008;7(3):123-49. Epub 2008/09/20. doi: 10.1051/ebr:2008014.

118.   Hasegawa H, Suzuki E, Maeda S. Horizontal Plasmid Transfer by Transformation in Escherichia coli: Environmental Factors and Possible Mechanisms. Frontiers in Microbiology. 2018;9(2365). doi: 10.3389/fmicb.2018.02365.

119.   Gordillo Altamirano FL, Barr JJ. Phage Therapy in the Postantibiotic Era. Clinical Microbiology Reviews. 2019;32(2):e00066-18. doi: 10.1128/cmr.00066-18.

120.   Allen HK, Trachsel J, Looft T, Casey TA. Finding alternatives to antibiotics. Ann N Y Acad Sci. 2014;1323:91-100. Epub 2014/06/24. doi: 10.1111/nyas.12468. PubMed PMID: 24953233.

121.   Khan HA, Ahmad A, Mehboob R. Nosocomial infections and their control strategies. Asian Pacific Journal of Tropical Biomedicine. 2015;5(7):509-14. doi: https://doi.org/10.1016/j.apjtb.2015.05.001.

122.   Nagarjuna D, Mittal G, Dhanda RS, Verma PK, Gaind R, Yadav M. Faecal Escherichia coli isolates show potential to cause endogenous infection in patients admitted to the ICU in a tertiary care hospital. New Microbes New Infect. 2015;7:57-66. doi: 10.1016/j.nmni.2015.05.006. PubMed PMID: 26257914.

123.   Camins BC, Marschall J, DeVader SR, Maker DE, Hoffman MW, Fraser VJ. The clinical impact of fluoroquinolone resistance in patients with E coli bacteremia. J Hosp Med. 2011;6(6):344-9. doi: 10.1002/jhm.877. PubMed PMID: 21834116.

124.   Abdelwahab R, Yasir M, Godfrey RE, Christie GS, Element SJ, Saville F, et al. Antimicrobial resistance and gene regulation in Enteroaggregative Escherichia coli from Egyptian children with diarrhoea: Similarities and differences. Virulence. 2021;12(1):57-74. doi: 10.1080/21505594.2020.1859852.

125.   Taggar G, Attiq Rheman M, Boerlin P, Diarra MS. Molecular Epidemiology of Carbapenemases in Enterobacteriales from Humans, Animals, Food and the Environment. Antibiotics (Basel). 2020;9(10):693. doi: 10.3390/antibiotics9100693. PubMed PMID: 33066205.

126. Poole K. Efflux-mediated resistance to fluoroquinolones in gram-negative bacteria. Antimicrobial agents and chemotherapy. 2000;44(9):2233-41. doi: 10.1128/aac.44.9.2233-2241.2000. PubMed PMID: 10952561.

127. Bidell MR, Palchak M, Mohr J, Lodise TP. Fluoroquinolone and Third-Generation-Cephalosporin Resistance among Hospitalized Patients with Urinary Tract Infections Due to Escherichia coli: Do Rates Vary by Hospital Characteristics and Geographic Region? Antimicrobial Agents and Chemotherapy. 2016;60(5):3170-3. doi: 10.1128/aac.02505-15.

128. Pallett A, Hand K. Complicated urinary tract infections: practical solutions for the treatment of multiresistant Gram-negative bacteria. Journal of Antimicrobial Chemotherapy. 2010;65(suppl_3):iii25-iii33. doi: 10.1093/jac/dkq298.

129. Partridge SR. Resistance mechanisms in Enterobacteriaceae. Pathology. 2015;47(3):276-84. doi: https://doi.org/10.1097/PAT.0000000000000237.

130. Liu Y-Y, Wang Y, Walsh TR, Yi L-X, Zhang R, Spencer J, et al. Emergence of plasmid-mediated colistin resistance mechanism MCR-1 in animals and human beings in China: a microbiological and molecular biological study. The Lancet Infectious Diseases. 2016;16(2):161-8. doi: https://doi.org/10.1016/S1473-3099(15)00424-7.

131. El-Mokhtar MA, Daef E, Mohamed Hussein AAR, Hashem MK, Hassan HM. Emergence of Nosocomial Pneumonia Caused by Colistin-Resistant Escherichia coli in Patients Admitted to Chest Intensive Care Unit. Antibiotics. 2021;10(3):226. PubMed PMID: doi:10.3390/antibiotics10030226.

132. Nguyen F, Starosta AL, Arenz S, Sohmen D, Dönhöfer A, Wilson DN. Tetracycline antibiotics and resistance mechanisms. Biol Chem. 2014;395(5):559-75. Epub 2014/02/06. doi: 10.1515/hsz-2013-0292. PubMed PMID: 24497223.

133. Moore IF, Hughes DW, Wright GD. Tigecycline is modified by the flavin-dependent monooxygenase TetX. Biochemistry. 2005;44(35):11829-35. Epub 2005/09/01. doi: 10.1021/bi0506066. PubMed PMID: 16128584.

134. Li W, Atkinson GC, Thakor NS, Allas U, Lu CC, Chan KY, et al. Mechanism of tetracycline resistance by ribosomal protection protein Tet(O). Nat Commun. 2013;4:1477. Epub 2013/02/14. doi: 10.1038/ncomms2470. PubMed PMID: 23403578; PubMed Central PMCID: PMCPMC3576927.

135. Thaker M, Spanogiannopoulos P, Wright GD. The tetracycline resistome. Cell Mol Life Sci. 2010;67(3):419-31. Epub 2009/10/29. doi: 10.1007/s00018-009-0172-6. PubMed PMID: 19862477.

136. Xu Y, Liu L, Zhang H, Feng Y. Co-production of Tet(X) and MCR-1, two resistance enzymes by a single plasmid. Environmental Microbiology. n/a(n/a). doi: https://doi.org/10.1111/1462-2920.15425.

137. Yan WJ, Jing N, Wang SM, Xu JH, Yuan YH, Zhang Q, et al. Molecular characterization of carbapenem-resistant Enterobacteriaceae and emergence of tigecycline non-susceptible strains in the Henan province in China: a multicentrer study. Journal of Medical Microbiology. 2021. doi: https://doi.org/10.1099/jmm.0.001325.

138. CDC. Biggest threats and data 2019 [updated 28.10.2020; cited 2021]. Available from: https://www.cdc.gov/drugresistance/biggest-threats.html.

139. Hashimi SM, Wall MK, Smith AB, Maxwell A, Birch RG. The Phytotoxin Albicidin is a Novel Inhibitor of DNA Gyrase. Antimicrobial Agents and Chemotherapy. 2007;51(1):181. doi: 10.1128/AAC.00918-06.

140. EMA. Disabling and potentially permanent side effects lead to suspension or restriction of quinolone and gluoroquinolone antibiotics. Amsterdam: European Medicines Agency, 2018 16.11.2018. Report No.

141. Maigaard Hermansen GM, Boysen A, Krogh TJ, Nawrocki A, Jelsbak L, Møller-Jensen J. HldE Is Important for Virulence Phenotypes in Enterotoxigenic Escherichia coli. Frontiers in

cellular and infection microbiology. 2018;8:253-. doi: 10.3389/fcimb.2018.00253. PubMed PMID: 30131942.

142. Bush NG, Diez-Santos I, Abbott LR, Maxwell A. Quinolones: Mechanism, Lethality and Their Contributions to Antibiotic Resistance. Molecules. 2020;25(23). Epub 2020/12/05. doi: 10.3390/molecules25235662. PubMed PMID: 33271787; PubMed Central PMCID: PMCPMC7730664.

143. Walker MJ, Birch RG, Pemberton JM. Cloning and characterization of an albicidin resistance gene from Klebsiella oxytoca. Mol Microbiol. 1988;2(4):443-54. Epub 1988/07/01. doi: 10.1111/j.1365-2958.1988.tb00050.x. PubMed PMID: 2845223.

144. Basnayake WV, Birch RG. A gene from Alcaligenes denitrificans that confers albicidin resistance by reversible antibiotic binding. Microbiology (Reading). 1995;141 (Pt 3):551-60. Epub 1995/03/01. doi: 10.1099/13500872-141-3-551. PubMed PMID: 7711894.

145. Vieweg L, Kretz J, Pesic A, Kerwat D, Grätz S, Royer M, et al. The Albicidin Resistance Factor AlbD Is a Serine Endopeptidase That Hydrolyzes Unusual Oligoaromatic-Type Peptides. J Am Chem Soc. 2015;137(24):7608-11. Epub 2015/06/10. doi: 10.1021/jacs.5b04099. PubMed PMID: 26057615.

146. Nieweg A, Bremer E. The nucleoside-specific Tsx channel from the outer membrane of Salmonella typhimurium, Klebsiella pneumoniae and Enterobacter aerogenes: functional characterization and DNA sequence analysis of the tsx genes. Microbiology (Reading). 1997;143 (Pt 2):603-15. Epub 1997/02/01. doi: 10.1099/00221287-143-2-603. PubMed PMID: 9043137.

147. Birch RG, Pemberton JM, Basnayake WV. Stable albicidin resistance in Escherichia coli involves an altered outer-membrane nucleoside uptake system. J Gen Microbiol. 1990;136(1):51-8. Epub 1990/01/01. doi: 10.1099/00221287-136-1-51. PubMed PMID: 2191080.

148. Choi U, Lee C-R. Distinct Roles of Outer Membrane Porins in Antibiotic Resistance and Membrane Integrity in Escherichia coli. Frontiers in Microbiology. 2019;10(953). doi: 10.3389/fmicb.2019.00953.

149. Liu Y-F, Yan J-J, Lei H-Y, Teng C-H, Wang M-C, Tseng C-C, et al. Loss of outer membrane protein C in Escherichia coli contributes to both antibiotic resistance and escaping antibody-dependent bactericidal activity. Infect Immun. 2012;80(5):1815-22. Epub 2012/02/21. doi: 10.1128/IAI.06395-11. PubMed PMID: 22354022.

150. Lou H, Chen M, Black SS, Bushell SR, Ceccarelli M, Mach T, et al. Altered antibiotic transport in OmpC mutants isolated from a series of clinical strains of multi-drug resistant E. coli. PLoS One. 2011;6(10):e25825-e. Epub 2011/10/28. doi: 10.1371/journal.pone.0025825. PubMed PMID: 22053181.

151. Kirschning A, Seedorf T, Solga D. Natural and Synthetic Oligoarylamides - priviledged structures for medical applications. Chemistry. 2021. Epub 2021/01/23. doi: 10.1002/chem.202005086. PubMed PMID: 33481284.

152. Deng J-H, Luo J, Mao Y-L, Lai S, Gong Y-N, Zhong D-C, et al. π-π stacking interactions: Non-negligible forces for stabilizing porous supramolecular frameworks. Science Advances. 2020;6(2):eaax9976. doi: 10.1126/sciadv.aax9976.

153. Zhuang W-R, Wang Y, Cui P-F, Xing L, Lee J, Kim D, et al. Applications of π-π stacking interactions in the design of drug-delivery systems. Journal of Controlled Release. 2019;294:311-26. doi: https://doi.org/10.1016/j.jconrel.2018.12.014.

154. Wang H, Bian X, Xia L, Ding X, Müller R, Zhang Y, et al. Improved seamless mutagenesis by recombineering using ccdB for counterselection. Nucleic Acids Res. 2014;42(5):e37. Epub 2013/12/27. doi: 10.1093/nar/gkt1339. PubMed PMID: 24369425; PubMed Central PMCID: PMCPMC3950717.

155. Clarke MB, Sperandio V. Transcriptional autoregulation by quorum sensing Escherichia coli regulators B and C (QseBC) in enterohaemorrhagic E. coli (EHEC). Mol Microbiol.

2005;58(2):441-55. Epub 2005/10/01. doi: 10.1111/j.1365-2958.2005.04819.x. PubMed PMID: 16194231.

156. Juárez-Rodríguez MD, Torres-Escobar A, Demuth DR. Transcriptional regulation of the Aggregatibacter actinomycetemcomitans ygiW-qseBC operon by QseB and integration host factor proteins. Microbiology (Reading, England). 2014;160(Pt 12):2583-94. Epub 2014/09/15. doi: 10.1099/mic.0.083501-0. PubMed PMID: 25223341.

157. Sperandio V, Torres AG, Kaper JB. Quorum sensing Escherichia coli regulators B and C (QseBC): a novel two-component regulatory system involved in the regulation of flagella and motility by quorum sensing in E. coli. Mol Microbiol. 2002;43(3):809-21. Epub 2002/04/04. doi: 10.1046/j.1365-2958.2002.02803.x. PubMed PMID: 11929534.

158. Hadjifrangiskou M, Kostakioti M, Chen SL, Henderson JP, Greene SE, Hultgren SJ. A central metabolic circuit controlled by QseC in pathogenic Escherichia coli. Mol Microbiol. 2011;80(6):1516-29. Epub 2011/05/06. doi: 10.1111/j.1365-2958.2011.07660.x. PubMed PMID: 21542868; PubMed Central PMCID: PMCPMC3643513.

159. Naves P, Del Prado G, Huelves L, Gracia M, Ruiz V, Blanco J, et al. Measurement of biofilm formation by clinical isolates of Escherichia coli is method-dependent. Journal of Applied Microbiology. 2008;105(2):585-90. doi: https://doi.org/10.1111/j.1365-2672.2008.03791.x.

160. Guckes KR, Kostakioti M, Breland EJ, Gu AP, Shaffer CL, Martinez CR, et al. Strong cross-system interactions drive the activation of the QseB response regulator in the absence of its cognate sensor. Proceedings of the National Academy of Sciences. 2013;110(41):16592. doi: 10.1073/pnas.1315320110.

161. Li W, Xue M, Yu L, Qi K, Ni J, Chen X, et al. QseBC is involved in the biofilm formation and antibiotic resistance in Escherichia coli isolated from bovine mastitis. PeerJ. 2020;8:e8833. Epub 2020/04/08. doi: 10.7717/peerj.8833. PubMed PMID: 32257646; PubMed Central PMCID: PMCPMC7102498.

162. Jorgenson MA, Bryant JC. A genetic screen to identify factors affected by undecaprenyl phosphate recycling uncovers novel connections to morphogenesis in Escherichia coli. bioRxiv. 2020:2020.07.28.225441. doi: 10.1101/2020.07.28.225441.

163. Wang X, Quinn PJ, Yan A. Kdo2 -lipid A: structural diversity and impact on immunopharmacology. Biol Rev Camb Philos Soc. 2015;90(2):408-27. Epub 2014/05/16. doi: 10.1111/brv.12114. PubMed PMID: 24838025.

164. Klein G, Müller-Loennies S, Lindner B, Kobylak N, Brade H, Raina S. Molecular and structural basis of inner core lipopolysaccharide alterations in Escherichia coli: incorporation of glucuronic acid and phosphoethanolamine in the heptose region. The Journal of biological chemistry. 2013;288(12):8111-27. Epub 2013/01/31. doi: 10.1074/jbc.M112.445981. PubMed PMID: 23372159.

165. Lee J, Hiibel SR, Reardon KF, Wood TK. Identification of stress-related proteins in Escherichia coli using the pollutant cis-dichloroethylene. J Appl Microbiol. 2010;108(6):2088-102. Epub 2009/11/19. doi: 10.1111/j.1365-2672.2009.04611.x. PubMed PMID: 19919618.

166. Sinha A, Nyongesa S, Viau C, Gruenheid S, Veyrier FJ, Le Moual H. PmrC (EptA) and CptA Negatively Affect Outer Membrane Vesicle Production in Citrobacter rodentium. Journal of Bacteriology. 2019;201(7):e00454-18. doi: 10.1128/JB.00454-18.

167. Kwan BW, Lord DM, Peti W, Page R, Benedik MJ, Wood TK. The MqsR/MqsA toxin/antitoxin system protects Escherichia coli during bile acid stress. Environ Microbiol. 2015;17(9):3168-81. Epub 2014/12/24. doi: 10.1111/1462-2920.12749. PubMed PMID: 25534751.

168. Liu R, Ochman H. Stepwise formation of the bacterial flagellar system. Proceedings of the National Academy of Sciences. 2007;104(17):7116. doi: 10.1073/pnas.0700266104.

169.   Yamamoto K, Hirao K, Oshima T, Aiba H, Utsumi R, Ishihama A. Functional characterization in vitro of all two-component signal transduction systems from Escherichia coli. J Biol Chem. 2005;280(2):1448-56. Epub 2004/11/04. doi: 10.1074/jbc.M410104200. PubMed PMID: 15522865.

170.   Eguchi Y, Okada T, Minagawa S, Oshima T, Mori H, Yamamoto K, et al. Signal transduction cascade between EvgA/EvgS and PhoP/PhoQ two-component systems of Escherichia coli. Journal of bacteriology. 2004;186(10):3006-14. doi: 10.1128/jb.186.10.3006-3014.2004. PubMed PMID: 15126461.

171.   Clarke MB, Sperandio V. Transcriptional regulation of flhDC by QseBC and sigma (FliA) in enterohaemorrhagic Escherichia coli. Mol Microbiol. 2005;57(6):1734-49. Epub 2005/09/02. doi: 10.1111/j.1365-2958.2005.04792.x. PubMed PMID: 16135237.

172.   Kostakioti M, Hadjifrangiskou M, Cusumano CK, Hannan TJ, Janetka JW, Hultgren SJ. Distinguishing the contribution of type 1 pili from that of other QseB-misregulated factors when QseC is absent during urinary tract infection. Infect Immun. 2012;80(8):2826-34. Epub 2012/06/06. doi: 10.1128/iai.00283-12. PubMed PMID: 22665375; PubMed Central PMCID: PMCPMC3434567.

173.   Wood TK, González Barrios AF, Herzberg M, Lee J. Motility influences biofilm architecture in Escherichia coli. Appl Microbiol Biotechnol. 2006;72(2):361-7. Epub 2006/01/07. doi: 10.1007/s00253-005-0263-8. PubMed PMID: 16397770.

174.   Breazeale SD, Ribeiro AA, Raetz CRH. Origin of Lipid A Species Modified with 4-Amino-4-deoxy-l-arabinose in Polymyxin-resistant Mutants of Escherichia coli: AN AMINOTRANSFERASE (ArnB) THAT GENERATES UDP-4-AMINO-4-DEOXY-l-ARABINOSE*. Journal of Biological Chemistry. 2003;278(27):24731-9. doi: https://doi.org/10.1074/jbc.M304043200.

175.   Breazeale SD, Ribeiro AA, McClerren AL, Raetz CR. A formyltransferase required for polymyxin resistance in Escherichia coli and the modification of lipid A with 4-Amino-4-deoxy-L-arabinose. Identification and function oF UDP-4-deoxy-4-formamido-L-arabinose. J Biol Chem. 2005;280(14):14154-67. Epub 2005/02/08. doi: 10.1074/jbc.M414265200. PubMed PMID: 15695810.

176.   Collin F, Maxwell A. The Microbial Toxin Microcin B17: Prospects for the Development of New Antibacterial Agents. Journal of molecular biology. 2019;431(18):3400-26. Epub 2019/06/08. doi: 10.1016/j.jmb.2019.05.050. PubMed PMID: 31181289.

177.   Michalak K, Sobolewska-Włodarczyk A, Włodarczyk M, Sobolewska J, Woźniak P, Sobolewski B. Treatment of the Fluoroquinolone-Associated Disability: The Pathobiochemical Implications. Oxidative Medicine and Cellular Longevity. 2017;2017:8023935. doi: 10.1155/2017/8023935.

178.   Priyanka, Singh V, Ekta, Katiyar D. Synthesis, antimicrobial, cytotoxic and E. coli DNA gyrase inhibitory activities of coumarinyl amino alcohols. Bioorganic Chemistry. 2017;71:120-7. doi: https://doi.org/10.1016/j.bioorg.2017.01.019.

179.   Nakada N, Shimada H, Hirata T, Aoki Y, Kamiyama T, Watanabe J, et al. Biological characterization of cyclothialidine, a new DNA gyrase inhibitor. Antimicrob Agents Chemother. 1993;37(12):2656-61. Epub 1993/12/01. doi: 10.1128/aac.37.12.2656. PubMed PMID: 8109932; PubMed Central PMCID: PMCPMC192769.

180.   Angehrn P, Goetschi E, Gmuender H, Hebeisen P, Hennig M, Kuhn B, et al. A new DNA gyrase inhibitor subclass of the cyclothialidine family based on a bicyclic dilactam-lactone scaffold. Synthesis and antibacterial properties. J Med Chem. 2011;54(7):2207-24. Epub 2011/03/11. doi: 10.1021/jm1014023. PubMed PMID: 21388139.

181.   Gibson EG, Bax B, Chan PF, Osheroff N. Mechanistic and Structural Basis for the Actions of the Antibacterial Gepotidacin against Staphylococcus aureus Gyrase. ACS infectious diseases. 2019;5(4):570-81. Epub 2019/02/28. doi: 10.1021/acsinfecdis.8b00315. PubMed PMID: 30757898.

182. Bradford PA, Miller AA, O'Donnell J, Mueller JP. Zoliflodacin: An Oral Spiropyrimidinetrione Antibiotic for the Treatment of Neisseria gonorrheae, Including Multi-Drug-Resistant Isolates. ACS Infectious Diseases. 2020;6(6):1332-45. doi: 10.1021/acsinfecdis.0c00021.

183. Higuchi S, Onodera Y, Chiba M, Hoshino K, Gotoh N. Potent In Vitro Antibacterial Activity of DS-8587, a Novel Broad-Spectrum Quinolone, against Acinetobacter baumannii. Antimicrobial Agents and Chemotherapy. 2013;57(4):1978. doi: 10.1128/AAC.02374-12.

184. Chopra I. New developments in tetracycline antibiotics: glycylcyclines and tetracycline efflux pump inhibitors. Drug Resist Updat. 2002;5(3-4):119-25. Epub 2002/09/19. doi: 10.1016/s1368-7646(02)00051-1. PubMed PMID: 12237079.

185. Hirai K, Aoyama H, Suzue S, Irikura T, Iyobe S, Mitsuhashi S. Isolation and characterization of norfloxacin-resistant mutants of Escherichia coli K-12. Antimicrob Agents Chemother. 1986;30(2):248-53. Epub 1986/08/01. doi: 10.1128/aac.30.2.248. PubMed PMID: 3532944; PubMed Central PMCID: PMCPMC180528.

186. Jacoby GA. Mechanisms of Resistance to Quinolones. Clinical Infectious Diseases. 2005;41(Supplement_2):S120-S6. doi: 10.1086/428052.

187. Sanfilippo CM, Hesje CK, Haas W, Morris TW. Topoisomerase Mutations That Are Associated with High-Level Resistance to Earlier Fluoroquinolones in <i>Staphylococcus aureus</i> Have Less Effect on the Antibacterial Activity of Besifloxacin. Chemotherapy. 2011;57(5):363-71. doi: 10.1159/000330858.

188. Alm RA, Lahiri SD, Kutschke A, Otterson LG, McLaughlin RE, Whiteaker JD, et al. Characterization of the Novel DNA Gyrase Inhibitor AZD0914: Low Resistance Potential and Lack of Cross-Resistance in Neisseria gonorrhoeae. Antimicrobial Agents and Chemotherapy. 2015;59(3):1478. doi: 10.1128/AAC.04456-14.

189. Quesada A, Porrero MC, Téllez S, Palomo G, García M, Domínguez L. Polymorphism of genes encoding PmrAB in colistin-resistant strains of Escherichia coli and Salmonella enterica isolated from poultry and swine. J Antimicrob Chemother. 2015;70(1):71-4. Epub 2014/08/26. doi: 10.1093/jac/dku320. PubMed PMID: 25150146.

190. Sato T, Shiraishi T, Hiyama Y, Honda H, Shinagawa M, Usui M, et al. Contribution of Novel Amino Acid Alterations in PmrA or PmrB to Colistin Resistance in mcr-Negative Escherichia coli Clinical Isolates, Including Major Multidrug-Resistant Lineages O25b:H4-ST131-H30Rx and Non-x. Antimicrobial agents and chemotherapy. 2018;62(9):e00864-18. doi: 10.1128/AAC.00864-18. PubMed PMID: 29914952.

191. Cannatelli A, Giani T, Aiezza N, Di Pilato V, Principe L, Luzzaro F, et al. An allelic variant of the PmrB sensor kinase responsible for colistin resistance in an Escherichia coli strain of clinical origin. Scientific Reports. 2017;7(1):5071. doi: 10.1038/s41598-017-05167-6.

192. Phan M-D, Nhu NTK, Achard MES, Forde BM, Hong KW, Chong TM, et al. Modifications in the pmrB gene are the primary mechanism for the development of chromosomally encoded resistance to polymyxins in uropathogenic Escherichia coli. Journal of Antimicrobial Chemotherapy. 2017;72(10):2729-36. doi: 10.1093/jac/dkx204.

193. Nirwan PK, Chatterjee N, Panwar R, Dudeja M, Jaggi N. Mutations in two component system (PhoPQ and PmrAB) in colistin resistant Klebsiella pneumoniae from North Indian tertiary care hospital. The Journal of Antibiotics. 2021;74(7):450-7. doi: 10.1038/s41429-021-00417-2.

194. Huang J, Li C, Song J, Velkov T, Wang L, Zhu Y, et al. Regulating polymyxin resistance in Gram-negative bacteria: roles of two-component systems PhoPQ and PmrAB. Future Microbiol. 2020;15(6):445-59. Epub 2020/04/07. doi: 10.2217/fmb-2019-0322. PubMed PMID: 32250173; PubMed Central PMCID: PMCPMC7236789.

195.   Breland EJ, Zhang EW, Bermudez T, Martinez CR, 3rd, Hadjifrangiskou M. The Histidine Residue of QseC Is Required for Canonical Signaling between QseB and PmrB in Uropathogenic Escherichia coli. J Bacteriol. 2017;199(18). Epub 2017/04/12. doi: 10.1128/jb.00060-17. PubMed PMID: 28396353; PubMed Central PMCID: PMCPMC5573081.

196.   Xie W, Dickson C, Kwiatkowski W, Choe S. Structure of the cytoplasmic segment of histidine kinase receptor QseC, a key player in bacterial virulence. Protein Pept Lett. 2010;17(11):1383-91. doi: 10.2174/092986651100901383. PubMed PMID: 20594156.

197.   Bhate MP, Molnar KS, Goulian M, DeGrado WF. Signal transduction in histidine kinases: insights from new structures. Structure. 2015;23(6):981-94. Epub 2015/05/14. doi: 10.1016/j.str.2015.04.002. PubMed PMID: 25982528.

198.   Kostakioti M, Hadjifrangiskou M, Pinkner JS, Hultgren SJ. QseC-mediated dephosphorylation of QseB is required for expression of genes associated with virulence in uropathogenic Escherichia coli. Molecular microbiology. 2009;73(6):1020-31. Epub 2009/08/23. doi: 10.1111/j.1365-2958.2009.06826.x. PubMed PMID: 19703104.

199.   Guckes KR, Breland EJ, Zhang EW, Hanks SC, Gill NK, Algood HMS, et al. Signaling by two-component system noncognate partners promotes intrinsic tolerance to polymyxin B in uropathogenic Escherichia coli. Sci Signal. 2017;10(461):eaag1775. doi: 10.1126/scisignal.aag1775. PubMed PMID: 28074004.

200.   Park YK, Lee JY, Ko KS. Transcriptomic analysis of colistin-susceptible and colistin-resistant isolates identifies genes associated with colistin resistance in Acinetobacter baumannii. Clin Microbiol Infect. 2015;21(8):765.e1-7. Epub 2015/04/29. doi: 10.1016/j.cmi.2015.04.009. PubMed PMID: 25911992.

201.   Srinivasan VB, Rajamohan G. KpnEF, a new member of the Klebsiella pneumoniae cell envelope stress response regulon, is an SMR-type efflux pump involved in broad-spectrum antimicrobial resistance. Antimicrob Agents Chemother. 2013;57(9):4449-62. Epub 2013/07/10. doi: 10.1128/aac.02284-12. PubMed PMID: 23836167; PubMed Central PMCID: PMCPMC3754300.

202.   Aghapour Z, Gholizadeh P, Ganbarov K, Bialvaei AZ, Mahmood SS, Tanomand A, et al. Molecular mechanisms related to colistin resistance in Enterobacteriaceae. Infect Drug Resist. 2019;12:965-75. doi: 10.2147/IDR.S199844. PubMed PMID: 31190901.

203.   Ito-Kagawa M, Koyama Y. Selective cleavage of a peptide antibiotic, colistin by colistinase. J Antibiot (Tokyo). 1980;33(12):1551-5. Epub 1980/12/01. doi: 10.7164/antibiotics.33.1551. PubMed PMID: 7019177.

204.   Ahmed ZS, Elshafiee EA, Khalefa HS, Kadry M, Hamza DA. Evidence of colistin resistance genes (mcr-1 and mcr-2) in wild birds and its public health implication in Egypt. Antimicrobial Resistance & Infection Control. 2019;8(1):197. doi: 10.1186/s13756-019-0657-5.

205.   Maciuca IE, Cummins ML, Cozma AP, Rimbu CM, Guguianu E, Panzaru C, et al. Genetic Features of mcr-1 Mediated Colistin Resistance in CMY-2-Producing Escherichia coli From Romanian Poultry. Frontiers in Microbiology. 2019;10(2267). doi: 10.3389/fmicb.2019.02267.

206.   Kieffer N, Royer G, Decousser JW, Bourrel AS, Palmieri M, Ortiz De La Rosa JM, et al. mcr-9, an Inducible Gene Encoding an Acquired Phosphoethanolamine Transferase in Escherichia coli, and Its Origin. Antimicrob Agents Chemother. 2019;63(9). Epub 2019/06/19. doi: 10.1128/aac.00965-19. PubMed PMID: 31209009; PubMed Central PMCID: PMCPMC6709461.

207.   Faccone D, Martino F, Albornoz E, Gomez S, Corso A, Petroni A. Plasmid carrying mcr-9 from an extensively drug-resistant NDM-1-producing Klebsiella quasipneumoniae subsp. quasipneumoniae clinical isolate. Infect Genet Evol. 2020;81:104273. Epub 2020/03/08. doi: 10.1016/j.meegid.2020.104273. PubMed PMID: 32145334.

208.   Samantha A, Vrielink A. Lipid A Phosphoethanolamine Transferase: Regulation, Structure and Immune Response. J Mol Biol. 2020;432(18):5184-96. Epub 2020/05/01. doi: 10.1016/j.jmb.2020.04.022. PubMed PMID: 32353363.

209.   Thomanek N, Arends J, Lindemann C, Barkovits K, Meyer HE, Marcus K, et al. Intricate Crosstalk Between Lipopolysaccharide, Phospholipid and Fatty Acid Metabolism in Escherichia coli Modulates Proteolysis of LpxC. Front Microbiol. 2018;9:3285. Epub 2019/01/30. doi: 10.3389/fmicb.2018.03285. PubMed PMID: 30692974; PubMed Central PMCID: PMCPMC6339880.

210.   Beceiro A, Llobet E, Aranda J, Bengoechea JA, Doumith M, Hornsey M, et al. Phosphoethanolamine modification of lipid A in colistin-resistant variants of Acinetobacter baumannii mediated by the pmrAB two-component regulatory system. Antimicrobial agents and chemotherapy. 2011;55(7):3370-9. Epub 2011/05/16. doi: 10.1128/AAC.00079-11. PubMed PMID: 21576434.

211.   Pesavento C, Becker G, Sommerfeldt N, Possling A, Tschowri N, Mehlis A, et al. Inverse regulatory coordination of motility and curli-mediated adhesion in Escherichia coli. Genes Dev. 2008;22(17):2434-46. doi: 10.1101/gad.475808. PubMed PMID: 18765794.

212.   Si H-M, Zhang F, Wu A-N, Han R-Z, Xu G-C, Ni Y. DNA microarray of global transcription factor mutant reveals membrane-related proteins involved in n-butanol tolerance in Escherichia coli. Biotechnol Biofuels. 2016;9:114-. doi: 10.1186/s13068-016-0527-9. PubMed PMID: 27252779.

213.   Hurst MN, Beebout CJ, Mersfelder R, Hollingsworth A, Guckes KR, Bermudez T, et al. A Bacterial Signaling Network Controls Antibiotic Resistance by Regulating Anaplerosis of 2-oxoglutarate. bioRxiv. 2020:2020.10.22.351270. doi: 10.1101/2020.10.22.351270.

214.   Sharma P, Haycocks JRJ, Middlemiss AD, Kettles RA, Sellars LE, Ricci V, et al. The multiple antibiotic resistance operon of enteric bacteria controls DNA repair and outer membrane integrity. Nature communications. 2017;8(1):1444-. doi: 10.1038/s41467-017-01405-7. PubMed PMID: 29133912.

215.   Wiegand I, Hilpert K, Hancock REW. Agar and broth dilution methods to determine the minimal inhibitory concentration (MIC) of antimicrobial substances. Nature Protocols. 2008;3(2):163-75. doi: 10.1038/nprot.2007.521.

216.   Hennessen F, Miethke M, Zaburannyi N, Loose M, Lukežič T, Bernecker S, et al. Amidochelocardin Overcomes Resistance Mechanisms Exerted on Tetracyclines and Natural Chelocardin. Antibiotics. 2020;9(9):619. PubMed PMID: doi:10.3390/antibiotics9090619.

217.   Stickler DJ, Morris NS, Winters C. Simple physical model to study formation and physiology of biofilms on urethral catheters. Methods Enzymol. 1999;310:494-501. Epub 1999/11/05. doi: 10.1016/s0076-6879(99)10037-5. PubMed PMID: 10547813.

218.   Bafna JA, Sans-Serramitjana E, Acosta-Gutiérrez S, Bodrenko IV, Hörömpöli D, Berscheid A, et al. Kanamycin Uptake into Escherichia coli Is Facilitated by OmpF and OmpC Porin Channels Located in the Outer Membrane. ACS Infectious Diseases. 2020;6(7):1855-65. doi: 10.1021/acsinfecdis.0c00102.

219.   Cirnski K, Coetzee J, Herrmann J, Müller R. Metabolic Profiling to Determine Bactericidal or Bacteriostatic Effects of New Natural Products using Isothermal Microcalorimetry. J Vis Exp. 2020;(164). Epub 2020/11/17. doi: 10.3791/61703. PubMed PMID: 33191927.

220.   Schmittgen TD, Livak KJ. Analyzing real-time PCR data by the comparative CT method. Nature Protocols. 2008;3(6):1101-8. doi: 10.1038/nprot.2008.73.

221.   Perrin S, Firmo C, Lemoine S, Le Crom S, Jourdren L. Aozan: an automated post-sequencing data-processing pipeline. Bioinformatics. 2017;33(14):2212-3. Epub 2017/04/04. doi: 10.1093/bioinformatics/btx154. PubMed PMID: 28369225.

222. Wingett S, Andrews S. FastQ Screen: A tool for multi-genome mapping and quality control [version 2; peer review: 4 approved]. F1000Research. 2018;7(1338). doi: 10.12688/f1000research.15931.2.

223. Langmead B, Trapnell C, Pop M, Salzberg SL. Ultrafast and memory-efficient alignment of short DNA sequences to the human genome. Genome Biology. 2009;10(3):R25. doi: 10.1186/gb-2009-10-3-r25.

224. Rosinski-Chupin I, Sauvage E, Sismeiro O, Villain A, Da Cunha V, Caliot ME, et al. Single nucleotide resolution RNA-seq uncovers new regulatory mechanisms in the opportunistic pathogen Streptococcus agalactiae. BMC Genomics. 2015;16(1):419. Epub 2015/05/31. doi: 10.1186/s12864-015-1583-4. PubMed PMID: 26024923; PubMed Central PMCID: PMCPMC4448216.

225. Varet H, Brillet-Guéguen L, Coppée J-Y, Dillies M-A. SARTools: A DESeq2- and EdgeR-Based R Pipeline for Comprehensive Differential Analysis of RNA-Seq Data. PLoS One. 2016;11(6):e0157022. doi: 10.1371/journal.pone.0157022.

226. Benjamini Y, Hochberg Y. Controlling the False Discovery Rate: A Practical and Powerful Approach to Multiple Testing. Journal of the Royal Statistical Society Series B (Methodological). 1995;57(1):289-300.

227. Carver T, Berriman M, Tivey A, Patel C, Böhme U, Barrell BG, et al. Artemis and ACT: viewing, annotating and comparing sequences stored in a relational database. Bioinformatics. 2008;24(23):2672-6. Epub 2008/10/11. doi: 10.1093/bioinformatics/btn529. PubMed PMID: 18845581; PubMed Central PMCID: PMCPMC2606163.

228. Heberle H, Meirelles GV, da Silva FR, Telles GP, Minghim R. InteractiVenn: a web-based tool for the analysis of sets through Venn diagrams. BMC Bioinformatics. 2015;16(1):169. doi: 10.1186/s12859-015-0611-3.

229. Yi EC, Hackett M. Rapid isolation method for lipopolysaccharide and lipid A from Gram-negative bacteria. Analyst. 2000;125(4):651-6. doi: 10.1039/B000368I.

230. Bhagirath AY, Li Y, Somayajula D, Dadashi M, Badr S, Duan K. Cystic fibrosis lung environment and Pseudomonas aeruginosa infection. BMC Pulm Med. 2016;16(1):174-. doi: 10.1186/s12890-016-0339-5. PubMed PMID: 27919253.

231. Lamas Ferreiro JL, Álvarez Otero J, González González L, Novoa Lamazares L, Arca Blanco A, Bermúdez Sanjurjo JR, et al. Pseudomonas aeruginosa urinary tract infections in hospitalized patients: Mortality and prognostic factors. PLoS One. 2017;12(5):e0178178-e. doi: 10.1371/journal.pone.0178178. PubMed PMID: 28552972.

232. Fujii A, Seki M, Higashiguchi M, Tachibana I, Kumanogoh A, Tomono K. Community-acquired, hospital-acquired, and healthcare-associated pneumonia caused by Pseudomonas aeruginosa. Respir Med Case Rep. 2014;12:30-3. doi: 10.1016/j.rmcr.2014.03.002. PubMed PMID: 26029534.

233. Rahdar HA, Kazemian H, Bimanand L, Shahraki-Zahedani S, Feyisa SG, Taki E, et al. Community Acquired Pseudomonas Aeruginosa Pneumonia in a Young Athlete Man: A Case Report and Literature Review. Infect Disord Drug Targets. 2018;18(3):249-54. Epub 2018/04/12. doi: 10.2174/1871526518666180410122531. PubMed PMID: 29637871.

234. Wang T, Hou Y, Wang R. A case report of community-acquired Pseudomonas aeruginosa pneumonia complicated with MODS in a previously healthy patient and related literature review. BMC Infectious Diseases. 2019;19(1):130. doi: 10.1186/s12879-019-3765-1.

235. Kang CI, Kim SH, Park WB, Lee KD, Kim HB, Kim EC, et al. Clinical features and outcome of patients with community-acquired Pseudomonas aeruginosa bacteraemia. Clinical Microbiology and Infection. 2005;11(5):415-8. doi: https://doi.org/10.1111/j.1469-0691.2005.01102.x.

236. Nathwani D, Raman G, Sulham K, Gavaghan M, Menon V. Clinical and economic consequences of hospital-acquired resistant and multidrug-resistant Pseudomonas aeruginosa

infections: a systematic review and meta-analysis. Antimicrobial resistance and infection control. 2014;3(1):32-. doi: 10.1186/2047-2994-3-32. PubMed PMID: 25371812.

237. Venier AG, Lavigne T, Jarno P, L'Heriteau F, Coignard B, Savey A, et al. Nosocomial urinary tract infection in the intensive care unit: when should Pseudomonas aeruginosa be suspected? Experience of the French national surveillance of nosocomial infections in the intensive care unit, Rea-Raisin. Clinical Microbiology and Infection. 2012;18(1):E13-E5. doi: https://doi.org/10.1111/j.1469-0691.2011.03686.x.

238. Mittal R, Aggarwal S, Sharma S, Chhibber S, Harjai K. Urinary tract infections caused by Pseudomonas aeruginosa: A minireview. Journal of Infection and Public Health. 2009;2(3):101-11. doi: https://doi.org/10.1016/j.jiph.2009.08.003.

239. Micek ST, Lloyd AE, Ritchie DJ, Reichley RM, Fraser VJ, Kollef MH. Pseudomonas aeruginosa bloodstream infection: importance of appropriate initial antimicrobial treatment. Antimicrobial agents and chemotherapy. 2005;49(4):1306-11. doi: 10.1128/AAC.49.4.1306-1311.2005. PubMed PMID: 15793102.

240. Hattemer A, Hauser A, Diaz M, Scheetz M, Shah N, Allen JP, et al. Bacterial and Clinical Characteristics of Health Care- and Community-Acquired Bloodstream Infections Due to <span class="named-content genus-species" id="named-content-1">Pseudomonas aeruginosa</span&gt. Antimicrobial Agents and Chemotherapy. 2013;57(8):3969. doi: 10.1128/AAC.02467-12.

241. Zorgani A, Abofayed A, Glia A, Albarbar A, Hanish S. Prevalence of Device-associated Nosocomial Infections Caused By Gram-negative Bacteria in a Trauma Intensive Care Unit in Libya. Oman Med J. 2015;30(4):270-5. doi: 10.5001/omj.2015.54. PubMed PMID: 26366261.

242. Litwin A, Rojek S, Gozdzik W, Duszynska W. Pseudomonas aeruginosa device associated – healthcare associated infections and its multidrug resistance at intensive care unit of University Hospital: polish, 8.5-year, prospective, single-centre study. BMC Infectious Diseases. 2021;21(1):180. doi: 10.1186/s12879-021-05883-5.

243. Domingo P, Ferré A, Baraldès MA, Ris J, Sánchez F. Pseudomonas aeruginosa bronchopulmonary infection in patients with AIDS, with emphasis on relapsing infection. Eur Respir J. 1998;12(1):107-12. Epub 1998/08/13. doi: 10.1183/09031936.98.12010107. PubMed PMID: 9701423.

244. Shepp DH, Tang IT, Ramundo MB, Kaplan MK. Serious Pseudomonas aeruginosa infection in AIDS. J Acquir Immune Defic Syndr (1988). 1994;7(8):823-31. Epub 1994/08/01. PubMed PMID: 8021816.

245. Gomes MZR, Machado CR, de Souza da Conceição M, Ortega JA, Neves SMFM, da Silva Lourenço MC, et al. Outbreaks, persistence, and high mortality rates of multiresistant Pseudomonas aeruginosa infections in a hospital with AIDS-predominant admissions. The Brazilian Journal of Infectious Diseases. 2011;15(4):312-22. doi: https://doi.org/10.1016/S1413-8670(11)70198-2.

246. Oliver A, Cantón R, Campo P, Baquero F, Blázquez J. High Frequency of Hypermutable Pseudomonas aeruginosa in Cystic Fibrosis Lung Infection. Science. 2000;288(5469):1251. doi: 10.1126/science.288.5469.1251.

247. Høiby N, Ciofu O, Bjarnsholt T. Pseudomonas aeruginosa biofilms in cystic fibrosis. Future Microbiology. 2010;5(11):1663-74. doi: 10.2217/fmb.10.125.

248. Ahmed S, Rudden M, Elias SM, Smyth TJ, Marchant R, Banat IM, et al. Pseudomonas aeruginosa PA80 is a cystic fibrosis isolate deficient in RhlRI quorum sensing. Sci Rep. 2021;11(1):5729. Epub 2021/03/13. doi: 10.1038/s41598-021-85100-0. PubMed PMID: 33707533; PubMed Central PMCID: PMCPMC7970962.

249. Moradali MF, Ghods S, Rehm BHA. Pseudomonas aeruginosa Lifestyle: A Paradigm for Adaptation, Survival, and Persistence. Frontiers in Cellular and Infection Microbiology. 2017;7(39). doi: 10.3389/fcimb.2017.00039.

250.   Smith RS, Iglewski BH. P. aeruginosa quorum-sensing systems and virulence. Curr Opin Microbiol. 2003;6(1):56-60. Epub 2003/03/05. doi: 10.1016/s1369-5274(03)00008-0. PubMed PMID: 12615220.

251.   Control ECfDPa. Antimicrobial resistance in the EU/EEA (EARS-Net) - Annual Epidemiological Report for 2019. Stockholm: ECDC, 2020 18.11.2020. Report No.

252.   Yayan J, Ghebremedhin B, Rasche K. Antibiotic Resistance of Pseudomonas aeruginosa in Pneumonia at a Single University Hospital Center in Germany over a 10-Year Period. PLoS One. 2015;10(10):e0139836. Epub 2015/10/03. doi: 10.1371/journal.pone.0139836. PubMed PMID: 26430738; PubMed Central PMCID: PMCPMC4592231.

253.   Schäfer E, Malecki M, Tellez-Castillo CJ, Pfennigwerth N, Marlinghaus L, Higgins PG, et al. Molecular surveillance of carbapenemase-producing Pseudomonas aeruginosa at three medical centres in Cologne, Germany. Antimicrob Resist Infect Control. 2019;8:208. Epub 2020/01/02. doi: 10.1186/s13756-019-0665-5. PubMed PMID: 31893042; PubMed Central PMCID: PMCPMC6937969.

254.   Horcajada JP, Montero M, Oliver A, Sorlí L, Luque S, Gómez-Zorrilla S, et al. Epidemiology and Treatment of Multidrug-Resistant and Extensively Drug-Resistant Pseudomonas aeruginosa Infections. Clinical Microbiology Reviews. 2019;32(4):e00031-19. doi: 10.1128/CMR.00031-19.

255.   Potron A, Poirel L, Nordmann P. Emerging broad-spectrum resistance in Pseudomonas aeruginosa and Acinetobacter baumannii: Mechanisms and epidemiology. International Journal of Antimicrobial Agents. 2015;45(6):568-85. doi: https://doi.org/10.1016/j.ijantimicag.2015.03.001.

256.   Mirzaei B, Bazgir ZN, Goli HR, Iranpour F, Mohammadi F, Babaei R. Prevalence of multi-drug resistant (MDR) and extensively drug-resistant (XDR) phenotypes of Pseudomonas aeruginosa and Acinetobacter baumannii isolated in clinical samples from Northeast of Iran. BMC Research Notes. 2020;13(1):380. doi: 10.1186/s13104-020-05224-w.

257.   Ríos P, Rocha C, Castro W, Vidal M, Canal E, Bernal M, et al. Extensively drug-resistant (XDR) Pseudomonas aeruginosa identified in Lima, Peru co-expressing a VIM-2 metallo-β-lactamase, OXA-1 β-lactamase and GES-1 extended-spectrum β-lactamase. JMM Case Rep. 2018;5(7):e005154-e. doi: 10.1099/jmmcr.0.005154. PubMed PMID: 30275958.

258.   Saderi H, Owlia P. Detection of Multidrug Resistant (MDR) and Extremely Drug Resistant (XDR) P. Aeruginosa Isolated from Patients in Tehran, Iran. Iran J Pathol. 2015;10(4):265-71. Epub 2015/09/10. PubMed PMID: 26351496; PubMed Central PMCID: PMCPMC4539747.

259.   Pérez A, Gato E, Pérez-Llarena J, Fernández-Cuenca F, Gude MJ, Oviaño M, et al. High incidence of MDR and XDR Pseudomonas aeruginosa isolates obtained from patients with ventilator-associated pneumonia in Greece, Italy and Spain as part of the MagicBullet clinical trial. Journal of Antimicrobial Chemotherapy. 2019;74(5):1244-52. doi: 10.1093/jac/dkz030.

260.   Maurice NM, Bedi B, Sadikot RT. Pseudomonas aeruginosa Biofilms: Host Response and Clinical Implications in Lung Infections. Am J Respir Cell Mol Biol. 2018;58(4):428-39. doi: 10.1165/rcmb.2017-0321TR. PubMed PMID: 29372812.

261.   Schulze A, Mitterer F, Pombo JP, Schild S. Biofilms by bacterial human pathogens: Clinical relevance - development, composition and regulation - therapeutic strategies. Microb Cell. 2021;8(2):28-56. Epub 2021/02/09. doi: 10.15698/mic2021.02.741. PubMed PMID: 33553418; PubMed Central PMCID: PMCPMC7841849.

262.   Lee DG, Urbach JM, Wu G, Liberati NT, Feinbaum RL, Miyata S, et al. Genomic analysis reveals that Pseudomonas aeruginosa virulence is combinatorial. Genome Biology. 2006;7(10):R90. doi: 10.1186/gb-2006-7-10-r90.

263.   Meylan S, Porter CBM, Yang JH, Belenky P, Gutierrez A, Lobritz MA, et al. Carbon Sources Tune Antibiotic Susceptibility in Pseudomonas aeruginosa via Tricarboxylic Acid

Cycle Control. Cell Chem Biol. 2017;24(2):195-206. Epub 2017/01/19. doi: 10.1016/j.chembiol.2016.12.015. PubMed PMID: 28111098.

264.   Minandri F, Imperi F, Frangipani E, Bonchi C, Visaggio D, Facchini M, et al. Role of Iron Uptake Systems in Pseudomonas aeruginosa Virulence and Airway Infection. Infect Immun. 2016;84(8):2324-35. doi: 10.1128/IAI.00098-16. PubMed PMID: 27271740.

265.   Pang Z, Raudonis R, Glick BR, Lin T-J, Cheng Z. Antibiotic resistance in Pseudomonas aeruginosa: mechanisms and alternative therapeutic strategies. Biotechnology Advances. 2019;37(1):177-92. doi: https://doi.org/10.1016/j.biotechadv.2018.11.013.

266.   Lundgren BR, Sarwar Z, Pinto A, Ganley JG, Nomura CT. Ethanolamine Catabolism in Pseudomonas aeruginosa PAO1 Is Regulated by the Enhancer-Binding Protein EatR (PA4021) and the Alternative Sigma Factor RpoN. Journal of bacteriology. 2016;198(17):2318-29. doi: 10.1128/JB.00357-16. PubMed PMID: 27325678.

267.   Pier GB, Coleman F, Grout M, Franklin M, Ohman DE. Role of Alginate O Acetylation in Resistance of Mucoid Pseudomonas aeruginosa to Opsonic Phagocytosis. Infect Immun. 2001;69(3):1895. doi: 10.1128/IAI.69.3.1895-1901.2001.

268.   Franklin M, Nivens D, Weadge J, Howell P. Biosynthesis of the Pseudomonas aeruginosa Extracellular Polysaccharides, Alginate, Pel, and Psl. Frontiers in Microbiology. 2011;2(167). doi: 10.3389/fmicb.2011.00167.

269.   Raivio TL, Leblanc SKD, Price NL. The Escherichia coli Cpx Envelope Stress Response Regulates Genes of Diverse Function That Impact Antibiotic Resistance and Membrane Integrity. Journal of Bacteriology. 2013;195(12):2755. doi: 10.1128/JB.00105-13.

270.   Roemhild R, Gokhale CS, Dirksen P, Blake C, Rosenstiel P, Traulsen A, et al. Cellular hysteresis as a principle to maximize the efficacy of antibiotic therapy. Proc Natl Acad Sci U S A. 2018;115(39):9767-72. Epub 2018/09/12. doi: 10.1073/pnas.1810004115. PubMed PMID: 30209218.

271.   Tian Z-X, Yi X-X, Cho A, O'Gara F, Wang Y-P. CpxR Activates MexAB-OprM Efflux Pump Expression and Enhances Antibiotic Resistance in Both Laboratory and Clinical nalB-Type Isolates of Pseudomonas aeruginosa. PLoS pathogens. 2016;12(10):e1005932-e. doi: 10.1371/journal.ppat.1005932. PubMed PMID: 27736975.

272.   De Wulf P, McGuire AM, Liu X, Lin EC. Genome-wide profiling of promoter recognition by the two-component response regulator CpxR-P in Escherichia coli. J Biol Chem. 2002;277(29):26652-61. Epub 2002/04/16. doi: 10.1074/jbc.M203487200. PubMed PMID: 11953442.

273.   Danese PN, Silhavy TJ. CpxP, a stress-combative member of the Cpx regulon. J Bacteriol. 1998;180(4):831-9. Epub 1998/02/24. doi: 10.1128/jb.180.4.831-839.1998. PubMed PMID: 9473036; PubMed Central PMCID: PMCPMC106961.

274.   Baranova N, Nikaido H. The baeSR two-component regulatory system activates transcription of the yegMNOB (mdtABCD) transporter gene cluster in Escherichia coli and increases its resistance to novobiocin and deoxycholate. Journal of bacteriology. 2002;184(15):4168-76. doi: 10.1128/jb.184.15.4168-4176.2002. PubMed PMID: 12107134.

275.   Serino L, Reimmann C, Visca P, Beyeler M, Chiesa VD, Haas D. Biosynthesis of pyochelin and dihydroaeruginoic acid requires the iron-regulated pchDCBA operon in Pseudomonas aeruginosa. J Bacteriol. 1997;179(1):248-57. Epub 1997/01/01. doi: 10.1128/jb.179.1.248-257.1997. PubMed PMID: 8982005; PubMed Central PMCID: PMCPMC178686.

276.   Braud A, Hannauer M, Mislin GLA, Schalk IJ. The Pseudomonas aeruginosa Pyochelin-Iron Uptake Pathway and Its Metal Specificity. Journal of Bacteriology. 2009;191(11):3517. doi: 10.1128/JB.00010-09.

277. Salusso A, Raimunda D. Defining the Roles of the Cation Diffusion Facilitators in Fe(2+)/Zn(2+) Homeostasis and Establishment of Their Participation in Virulence in Pseudomonas aeruginosa. Frontiers in cellular and infection microbiology. 2017;7:84-. doi: 10.3389/fcimb.2017.00084. PubMed PMID: 28373967.

278. Munkelt D, Grass G, Nies DH. The Chromosomally Encoded Cation Diffusion Facilitator Proteins DmeF and FieF from Wautersia metallidurans CH34 Are Transporters of Broad Metal Specificity. Journal of Bacteriology. 2004;186(23):8036. doi: 10.1128/JB.186.23.8036-8043.2004.

279. Pilonieta MC, Erickson KD, Ernst RK, Detweiler CS. A protein important for antimicrobial peptide resistance, YdeI/OmdA, is in the periplasm and interacts with OmpD/NmpC. J Bacteriol. 2009;191(23):7243-52. Epub 2009/09/22. doi: 10.1128/jb.00688-09. PubMed PMID: 19767429; PubMed Central PMCID: PMCPMC2786563.

280. Schmidt J, Müsken M, Becker T, Magnowska Z, Bertinetti D, Möller S, et al. The Pseudomonas aeruginosa chemotaxis methyltransferase CheR1 impacts on bacterial surface sampling. PLoS One. 2011;6(3):e18184-e. doi: 10.1371/journal.pone.0018184. PubMed PMID: 21445368.

281. Martin M. Cutadapt removes adapter sequences from high-throughput sequencing reads. EMBnetjournal; Vol 17, No 1: Next Generation Sequencing Data Analysis. 2011. doi: 10.14806/ej.17.1.200.

282. Förstner KU, Vogel J, Sharma CM. READemption—a tool for the computational analysis of deep-sequencing–based transcriptome data. Bioinformatics. 2014;30(23):3421-3. doi: 10.1093/bioinformatics/btu533.

283. Hoffmann S, Otto C, Kurtz S, Sharma CM, Khaitovich P, Vogel J, et al. Fast mapping of short sequences with mismatches, insertions and deletions using index structures. PLoS Comput Biol. 2009;5(9):e1000502-e. Epub 2009/09/11. doi: 10.1371/journal.pcbi.1000502. PubMed PMID: 19750212.

284. Love MI, Huber W, Anders S. Moderated estimation of fold change and dispersion for RNA-seq data with DESeq2. Genome Biol. 2014;15(12):550. Epub 2014/12/18. doi: 10.1186/s13059-014-0550-8. PubMed PMID: 25516281; PubMed Central PMCID: PMCPMC4302049.

285. Lenchenko E, Blumenkrants D, Sachivkina N, Shadrova N, Ibragimova A. Morphological and adhesive properties of Klebsiella pneumoniae biofilms. Vet World. 2020;13(1):197-200. Epub 2020/01/28. doi: 10.14202/vetworld.2020.197-200. PubMed PMID: 32158172.

286. Bagley ST. Habitat association of Klebsiella species. Infect Control. 1985;6(2):52-8. Epub 1985/02/01. doi: 10.1017/s0195941700062603. PubMed PMID: 3882590.

287. Navon-Venezia S, Kondratyeva K, Carattoli A. Klebsiella pneumoniae: a major worldwide source and shuttle for antibiotic resistance. FEMS Microbiol Rev. 2017;41(3):252-75. Epub 2017/05/19. doi: 10.1093/femsre/fux013. PubMed PMID: 28521338.

288. Wyres KL, Holt KE. Klebsiella pneumoniae as a key trafficker of drug resistance genes from environmental to clinically important bacteria. Current Opinion in Microbiology. 2018;45:131-9. doi: https://doi.org/10.1016/j.mib.2018.04.004.

289. Santajit S, Indrawattana N. Mechanisms of Antimicrobial Resistance in ESKAPE Pathogens. Biomed Res Int. 2016;2016:2475067-. Epub 2016/05/05. doi: 10.1155/2016/2475067. PubMed PMID: 27274985.

290. Ni RT, Onishi M, Mizusawa M, Kitagawa R, Kishino T, Matsubara F, et al. The role of RND-type efflux pumps in multidrug-resistant mutants of Klebsiella pneumoniae. Scientific reports. 2020;10(1):10876-. doi: 10.1038/s41598-020-67820-x. PubMed PMID: 32616840.

291. Padilla E, Llobet E, Doménech-Sánchez A, Martínez-Martínez L, Bengoechea JA, Albertí S. Klebsiella pneumoniae AcrAB efflux pump contributes to antimicrobial resistance and virulence. Antimicrob Agents Chemother. 2010;54(1):177-83. Epub 2009/10/28. doi:

10.1128/aac.00715-09. PubMed PMID: 19858254; PubMed Central PMCID: PMCPMC2798511.

292. Doorduijn DJ, Rooijakkers SHM, van Schaik W, Bardoel BW. Complement resistance mechanisms of Klebsiella pneumoniae. Immunobiology. 2016;221(10):1102-9. doi: https://doi.org/10.1016/j.imbio.2016.06.014.

293. Chung PY. The emerging problems of Klebsiella pneumoniae infections: carbapenem resistance and biofilm formation. FEMS Microbiology Letters. 2016;363(20). doi: 10.1093/femsle/fnw219.

294. (ECDC) OfEC-oaDOaECfDPaC. Antimicrobial Resistance. Tackling the burden in the European Union. Paris: OECDC, 2019.

295. Royer M, Costet L, Vivien E, Bes M, Cousin A, Damais A, et al. Albicidin pathotoxin produced by Xanthomonas albilineans is encoded by three large PKS and NRPS genes present in a gene cluster also containing several putative modifying, regulatory, and resistance genes. Mol Plant Microbe Interact. 2004;17(4):414-27. Epub 2004/04/14. doi: 10.1094/mpmi.2004.17.4.414. PubMed PMID: 15077674.

296. De Majumdar S, Yu J, Fookes M, McAteer SP, Llobet E, Finn S, et al. Elucidation of the RamA Regulon in Klebsiella pneumoniae Reveals a Role in LPS Regulation. PLOS Pathogens. 2015;11(1):e1004627. doi: 10.1371/journal.ppat.1004627.

297. Izquierdo L, Coderch N, Piqué N, Bedini E, Corsaro MM, Merino S, et al. The Klebsiella pneumoniae wabG gene: role in biosynthesis of the core lipopolysaccharide and virulence. Journal of bacteriology. 2003;185(24):7213-21. doi: 10.1128/jb.185.24.7213-7221.2003. PubMed PMID: 14645282.

298. Gronow S, Brabetz W, Brade H. Comparative functional characterization in vitro of heptosyltransferase I (WaaC) and II (WaaF) from Escherichia coli. Eur J Biochem. 2000;267(22):6602-11. Epub 2000/10/29. doi: 10.1046/j.1432-1327.2000.01754.x. PubMed PMID: 11054112.

299. Wang Z, Wang J, Ren G, Li Y, Wang X. Deletion of the genes waaC, waaF, or waaG in Escherichia coli W3110 disables the flagella biosynthesis. Journal of Basic Microbiology. 2016;56(9):1021-35. doi: https://doi.org/10.1002/jobm.201600065.

300. van den Berg B, Prathyusha Bhamidimarri S, Dahyabhai Prajapati J, Kleinekathöfer U, Winterhalter M. Outer-membrane translocation of bulky small molecules by passive diffusion. Proceedings of the National Academy of Sciences. 2015;112(23):E2991. doi: 10.1073/pnas.1424835112.

301. Yang NJ, Hinner MJ. Getting across the cell membrane: an overview for small molecules, peptides, and proteins. Methods Mol Biol. 2015;1266:29-53. doi: 10.1007/978-1-4939-2272-7_3. PubMed PMID: 25560066.

302. Chusri S, Chongsuvivatwong V, Rivera JI, Silpapojakul K, Singkhamanan K, McNeil E, et al. Clinical outcomes of hospital-acquired infection with Acinetobacter nosocomialis and Acinetobacter pittii. Antimicrob Agents Chemother. 2014;58(7):4172-9. Epub 2014/05/14. doi: 10.1128/aac.02992-14. PubMed PMID: 24820079; PubMed Central PMCID: PMCPMC4068534.

303. Tega L, Raieta K, Ottaviani D, Russo GL, Blanco G, Carraturo A. Catheter-related bacteremia and multidrug-resistant Acinetobacter lwoffii. Emerg Infect Dis. 2007;13(2):355-6. doi: 10.3201/eid1302.060858. PubMed PMID: 17479919.

304. Yoon YK, Lee J, Ryu SY, Chang HH, Choi WS, Yoon JH, et al. Clinical significance of multidrug-resistant Acinetobacter baumannii isolated from central venous catheter tip cultures in patients without concomitant bacteremia. Scand J Infect Dis. 2013;45(12):900-6. Epub 2013/09/21. doi: 10.3109/00365548.2013.830191. PubMed PMID: 24047226.

305. Sileem AE, Said AM, Meleha MS. Acinetobacter baumannii in ICU patients: A prospective study highlighting their incidence, antibiotic sensitivity pattern and impact on ICU

stay and mortality. Egyptian Journal of Chest Diseases and Tuberculosis. 2017;66(4):693-8. doi: https://doi.org/10.1016/j.ejcdt.2017.01.003.

306.   Mo GX, She DY, Guan XZ, Cui JC, Wang R, Chen LA. [Antimicrobial resistance and genotyping of Acinetobacter baumannii in ICU]. Zhonghua Jie He He Hu Xi Za Zhi. 2010;33(9):656-9. Epub 2010/11/26. PubMed PMID: 21092631.

307.   Čiginskienė A, Dambrauskienė A, Rello J, Adukauskienė D. Ventilator-Associated Pneumonia due to Drug-Resistant Acinetobacter baumannii: Risk Factors and Mortality Relation with Resistance Profiles, and Independent Predictors of In-Hospital Mortality. Medicina (Kaunas). 2019;55(2). Epub 2019/02/20. doi: 10.3390/medicina55020049. PubMed PMID: 30781896; PubMed Central PMCID: PMCPMC6410055.

308.   Boll JM, Tucker AT, Klein DR, Beltran AM, Brodbelt JS, Davies BW, et al. Reinforcing Lipid A Acylation on the Cell Surface of Acinetobacter baumannii Promotes Cationic Antimicrobial Peptide Resistance and Desiccation Survival. mBio. 2015;6(3):e00478-15. Epub 2015/05/21. doi: 10.1128/mBio.00478-15. PubMed PMID: 25991684; PubMed Central PMCID: PMCPMC4442142.

309.   Russo TA, Luke NR, Beanan JM, Olson R, Sauberan SL, MacDonald U, et al. The K1 capsular polysaccharide of Acinetobacter baumannii strain 307-0294 is a major virulence factor. Infect Immun. 2010;78(9):3993-4000. Epub 2010/07/21. doi: 10.1128/iai.00366-10. PubMed PMID: 20643860; PubMed Central PMCID: PMCPMC2937447.

310.   Kwon SO, Gho YS, Lee JC, Kim SI. Proteome analysis of outer membrane vesicles from a clinical Acinetobacter baumannii isolate. FEMS Microbiol Lett. 2009;297(2):150-6. Epub 2009/06/25. doi: 10.1111/j.1574-6968.2009.01669.x. PubMed PMID: 19548894.

311.   Cevahir N, Demir M, Kaleli I, Gurbuz M, Tikvesli S. Evaluation of biofilm production, gelatinase activity, and mannose-resistant hemagglutination in Acinetobacter baumannii strains. J Microbiol Immunol Infect. 2008;41(6):513-8. Epub 2009/03/04. PubMed PMID: 19255696.

312.   Kyriakidis I, Vasileiou E, Pana ZD, Tragiannidis A. Acinetobacter baumannii Antibiotic Resistance Mechanisms. Pathogens. 2021;10(3). doi: 10.3390/pathogens10030373.

313.   Vrancianu CO, Gheorghe I, Czobor IB, Chifiriuc MC. Antibiotic Resistance Profiles, Molecular Mechanisms and Innovative Treatment Strategies of Acinetobacter baumannii. Microorganisms. 2020;8(6). doi: 10.3390/microorganisms8060935.

314.   Gorwitz RJ, Kruszon-Moran D, McAllister SK, McQuillan G, McDougal LK, Fosheim GE, et al. Changes in the prevalence of nasal colonization with Staphylococcus aureus in the United States, 2001-2004. J Infect Dis. 2008;197(9):1226-34. Epub 2008/04/22. doi: 10.1086/533494. PubMed PMID: 18422434.

315.   Bonesso MF, Yeh AJ, Villaruz AE, Joo H-S, McCausland J, Fortaleza CMCB, et al. Key Role of α-Toxin in Fatal Pneumonia Caused by Staphylococcus aureus Sequence Type 398. American Journal of Respiratory and Critical Care Medicine. 2016;193(2):217-20. doi: 10.1164/rccm.201506-1225LE.

316.   Chambers HF, Deleo FR. Waves of resistance: Staphylococcus aureus in the antibiotic era. Nat Rev Microbiol. 2009;7(9):629-41. doi: 10.1038/nrmicro2200. PubMed PMID: 19680247.

317.   Guo Y, Song G, Sun M, Wang J, Wang Y. Prevalence and Therapies of Antibiotic-Resistance in Staphylococcus aureus. Frontiers in Cellular and Infection Microbiology. 2020;10(107). doi: 10.3389/fcimb.2020.00107.

318.   Sabat AJ, Tinelli M, Grundmann H, Akkerboom V, Monaco M, Del Grosso M, et al. Daptomycin Resistant Staphylococcus aureus Clinical Strain With Novel Non-synonymous Mutations in the mprF and vraS Genes: A New Insight Into Daptomycin Resistance. Frontiers in microbiology. 2018;9:2705-. doi: 10.3389/fmicb.2018.02705. PubMed PMID: 30459746.

319.   Barros EM, Martin MJ, Selleck EM, Lebreton F, Sampaio JLM, Gilmore MS. Daptomycin Resistance and Tolerance Due to Loss of Function in <span

class="named-content genus-species" id="named-content-1">Staphylococcus aureus dsp1 and <em>asp23</em&gt. Antimicrobial Agents and Chemotherapy. 2019;63(1):e01542-18. doi: 10.1128/AAC.01542-18.

320.   Yoo IY, Kang OK, Shim HJ, Huh HJ, Lee NY. Linezolid Resistance in Methicillin-Resistant Staphylococcus aureus in Korea: High Rate of False Resistance to Linezolid by the VITEK 2 System. Ann Lab Med. 2020;40(1):57-62. doi: 10.3343/alm.2020.40.1.57. PubMed PMID: 31432640.

321.   Hasan R, Acharjee M, Noor R. Prevalence of vancomycin resistant Staphylococcus aureus (VRSA) in methicillin resistant S. aureus (MRSA) strains isolated from burn wound infections. Ci Ji Yi Xue Za Zhi. 2016;28(2):49-53. Epub 2016/04/23. doi: 10.1016/j.tcmj.2016.03.002. PubMed PMID: 28757721.

322.   Tanaka M, Wang T, Onodera Y, Uchida Y, Sato K. Mechanism of quinolone resistance in Staphylococcus aureus. J Infect Chemother. 2000;6(3):131-9. Epub 2002/01/26. doi: 10.1007/s101560070010. PubMed PMID: 11810552.

323.   Higgins PG, Fluit AC, Schmitz FJ. Fluoroquinolones: structure and target sites. Curr Drug Targets. 2003;4(2):181-90. Epub 2003/02/01. doi: 10.2174/1389450033346920. PubMed PMID: 12558069.

324.   Lomovskaya O, Lewis K. Emr, an Escherichia coli locus for multidrug resistance. Proc Natl Acad Sci U S A. 1992;89(19):8938-42. Epub 1992/10/01. doi: 10.1073/pnas.89.19.8938. PubMed PMID: 1409590; PubMed Central PMCID: PMCPMC50039.

325.   Sabrin A, Gioe BW, Gupta A, Grove A. An EmrB multidrug efflux pump in Burkholderia thailandensis with unexpected roles in antibiotic resistance. Journal of Biological Chemistry. 2019;294(6):1891-903. doi: https://doi.org/10.1074/jbc.RA118.006638.

326.   Ho CM, Li CY, Ho MW, Lin CY, Liu SH, Lu JJ. High rate of qacA- and qacB-positive methicillin-resistant Staphylococcus aureus isolates from chlorhexidine-impregnated catheter-related bloodstream infections. Antimicrob Agents Chemother. 2012;56(11):5693-7. Epub 2012/08/22. doi: 10.1128/aac.00761-12. PubMed PMID: 22908163; PubMed Central PMCID: PMCPMC3486537.

327.   Lu Z, Chen Y, Chen W, Liu H, Song Q, Hu X, et al. Characteristics of qacA/B-positive Staphylococcus aureus isolated from patients and a hospital environment in China. Journal of Antimicrobial Chemotherapy. 2015;70(3):653-7. doi: 10.1093/jac/dku456.

328.   Giraudo AT, Calzolari A, Cataldi AA, Bogni C, Nagel R. The sae locus of Staphylococcus aureus encodes a two-component regulatory system. FEMS Microbiol Lett. 1999;177(1):15-22. Epub 1999/08/07. doi: 10.1111/j.1574-6968.1999.tb13707.x. PubMed PMID: 10436918.

329.   Liu Q, Yeo W-S, Bae T. The SaeRS Two-Component System of Staphylococcus aureus. Genes (Basel). 2016;7(10):81. doi: 10.3390/genes7100081. PubMed PMID: 27706107.

330.   Yee R, Cui P, Shi W, Feng J, Zhang Y. Genetic Screen Reveals the Role of Purine Metabolism in Staphylococcus aureus Persistence to Rifampicin. Antibiotics. 2015;4(4). doi: 10.3390/antibiotics4040627.

331.   Goncheva MI, Flannagan RS, Sterling BE, Laakso HA, Friedrich NC, Kaiser JC, et al. Stress-induced inactivation of the Staphylococcus aureus purine biosynthesis repressor leads to hypervirulence. Nature Communications. 2019;10(1):775. doi: 10.1038/s41467-019-08724-x.

332.   Hattangady DS, Singh AK, Muthaiyan A, Jayaswal RK, Gustafson JE, Ulanov AV, et al. Genomic, Transcriptomic and Metabolomic Studies of Two Well-Characterized, Laboratory-Derived Vancomycin-Intermediate Staphylococcus aureus Strains Derived from the Same Parent Strain. Antibiotics. 2015;4(1). doi: 10.3390/antibiotics4010076.

333.	Okshevsky M, Meyer RL. The role of extracellular DNA in the establishment, maintenance and perpetuation of bacterial biofilms. Critical Reviews in Microbiology. 2015;41(3):341-52. doi: 10.3109/1040841X.2013.841639.

334.	Li L, Abdelhady W, Donegan NP, Seidl K, Cheung A, Zhou Y-F, et al. Role of Purine Biosynthesis in Persistent Methicillin-Resistant Staphylococcus aureus Infection. The Journal of infectious diseases. 2018;218(9):1367-77. doi: 10.1093/infdis/jiy340. PubMed PMID: 29868791.

335.	Samant S, Lee H, Ghassemi M, Chen J, Cook JL, Mankin AS, et al. Nucleotide biosynthesis is critical for growth of bacteria in human blood. PLoS Pathog. 2008;4(2):e37. Epub 2008/02/20. doi: 10.1371/journal.ppat.0040037. PubMed PMID: 18282099; PubMed Central PMCID: PMCPMC2242838.

336.	Hews CL, Cho T, Rowley G, Raivio TL. Maintaining Integrity Under Stress: Envelope Stress Response Regulation of Pathogenesis in Gram-Negative Bacteria. Frontiers in cellular and infection microbiology. 2019;9:313-. doi: 10.3389/fcimb.2019.00313. PubMed PMID: 31552196.

337.	Egler M, Grosse C, Grass G, Nies DH. Role of the extracytoplasmic function protein family sigma factor RpoE in metal resistance of Escherichia coli. Journal of bacteriology. 2005;187(7):2297-307. doi: 10.1128/JB.187.7.2297-2307.2005. PubMed PMID: 15774872.

338.	Korotetskiy IS, Shilov SV, Kuznetsova TV, Ilin AI, Joubert M, Taukobong S, et al. Comparison of transcriptional responses and metabolic alterations in three multidrug resistant model microorganisms, Staphylococcus aureus ATCC BAA-39, Escherichia coli ATCC BAA-196 and Acinetobacter baumannii ATCC BAA-1790, on exposure to iodine-containing nano-micelle drug FS-1. bioRxiv. 2020:2020.09.01.278945. doi: 10.1101/2020.09.01.278945.

339.	El Qaidi S, Yang J, Zhang J-R, Metzger DW, Bai G. The Vitamin B<sub>6</sub> Biosynthesis Pathway in Streptococcus pneumoniae Is Controlled by Pyridoxal 5′-Phosphate and the Transcription Factor PdxR and Has an Impact on Ear Infection. Journal of Bacteriology. 2013;195(10):2187. doi: 10.1128/JB.00041-13.

340.	Hoegl A, Nodwell MB, Kirsch VC, Bach NC, Pfanzelt M, Stahl M, et al. Mining the cellular inventory of pyridoxal phosphate-dependent enzymes with functionalized cofactor mimics. Nat Chem. 2018;10(12):1234-45. Epub 2018/10/08. doi: 10.1038/s41557-018-0144-2. PubMed PMID: 30297752.

341.	Huergo LF, Dixon R. The Emergence of 2-Oxoglutarate as a Master Regulator Metabolite. Microbiology and Molecular Biology Reviews. 2015;79(4):419. doi: 10.1128/MMBR.00038-15.

342.	Maszewska A, Moryl M, Wu J, Liu B, Feng L, Rozalski A. Amikacin and bacteriophage treatment modulates outer membrane proteins composition in Proteus mirabilis biofilm. Scientific Reports. 2021;11(1):1522. doi: 10.1038/s41598-020-80907-9.

343.	Charlier D, Nguyen Le Minh P, Roovers M. Regulation of carbamoylphosphate synthesis in Escherichia coli: an amazing metabolite at the crossroad of arginine and pyrimidine biosynthesis. Amino Acids. 2018;50(12):1647-61. doi: 10.1007/s00726-018-2654-z.

344.	Cutrona KJ, Kaufman BA, Figueroa DM, Elmore DE. Role of arginine and lysine in the antimicrobial mechanism of histone-derived antimicrobial peptides. FEBS Lett. 2015;589(24 Pt B):3915-20. Epub 2015/11/10. doi: 10.1016/j.febslet.2015.11.002. PubMed PMID: 26555191.

345.	Wickstrum JR, Santangelo TJ, Egan SM. Cyclic AMP receptor protein and RhaR synergistically activate transcription from the L-rhamnose-responsive rhaSR promoter in Escherichia coli. Journal of bacteriology. 2005;187(19):6708-18. doi: 10.1128/JB.187.19.6708-6718.2005. PubMed PMID: 16166533.

346.   Patel EH, Paul LV, Casanueva AI, Patrick S, Abratt VR. Overexpression of the rhamnose catabolism regulatory protein, RhaR: a novel mechanism for metronidazole resistance in Bacteroides thetaiotaomicron. Journal of Antimicrobial Chemotherapy. 2009;64(2):267-73. doi: 10.1093/jac/dkp203.

347.   Mistou M-Y, Sutcliffe IC, van Sorge NM. Bacterial glycobiology: rhamnose-containing cell wall polysaccharides in Gram-positive bacteria. FEMS microbiology reviews. 2016;40(4):464-79. Epub 2016/03/13. doi: 10.1093/femsre/fuw006. PubMed PMID: 26975195.

348.   Samuel G, Reeves P. Biosynthesis of O-antigens: genes and pathways involved in nucleotide sugar precursor synthesis and O-antigen assembly. Carbohydr Res. 2003;338(23):2503-19. Epub 2003/12/13. doi: 10.1016/j.carres.2003.07.009. PubMed PMID: 14670712.